Chemical and Pharmacological Analysis of *Caesalpinia volkensii* (H.), *Senna didymobotrya* (F.) and *Vitex doniana* (S.) from Kenya

By

OCHIENG CHARLES OTIENO

A thesis submitted in fulfillment of the requirements for the degree of Doctor of Philosophy (Ph.D) in Chemistry

DEPARTMENT OF CHEMISTRY

MASENO UNIVERSITY

ABSTRACT

Despite efforts to eradicate malaria, it remains a deadly disease with severe pathophysiological impacts, due to parasitic resistance to available drugs. The success of plant-based drugs motivated a study aimed at evaluating antiplasmodial and other pharmacologically active principles from the plants, *Caesalpinia volkensii* (Leguminocae) root- and stem-bark, *Senna didymobotrya* (Leguminocae) roots and *Vitex doniana* (Lamiaceae) stem-bark, which have been used to manage malaria and other ailments by different African communities. Antiplasmodial, analgesic, anti-inflammatory, antidyslipidaemic, and antioxidants bioassay guided isolation and spectroscopic characterization of compounds on the three plants were carried out by subjecting their crude extracts, fractions, and pure isolates to: *in vitro* antiplasmodial assay, *in vivo* antinociceptive and anti-inflammatory assay, *in vivo* hyperlipidaemic assays followed by *in vitro* adipocyte differentiation inhibition, and *in vitro* antioxidant assays. Two new furanoditerpenes [1α,5α-dihydroxyvoucapane (**400**) and 1α,6β-dihydroxyvoucapane-19β-methyl ester (**401**)] together with voucapan-5α-ol (**19**), caesaldekarin C (**38**), deoxycaesaldekarin C (**95**), voucapane (**398**), 5-hydroxyvinhaticoic acid (**399**), triacontanyl-(*E*)-ferrulate (**402**), triacontanyl-(*E*)-caffaete (**403**) and 30′-hydroxytriacontanyl-(*E*)-ferulate (**404**) were isolated from the root bark of *C. volkensii*. The furanoditerpenes **19, 38, 95, 401** at 100 mg/kg, showed significantly ($P \leq 0.05$) high antinociceptive activities in the two chemical models of nociception, however, the compounds showed low to moderate (25–50μM) antiplasmodial activities. Triacontanyl-*E*-cinnamoates (**402**, **403** and **404**) exhibited significant ($P \leq 0.05$) superoxide (O_2^-) scavenging, hydroxyl radical (OH^-) and lipid peroxidation inhibitions. Three new cassane diterpenes [voulkensin A, (**408**), voulkensin B, (**407**), and voulkensin A, (**406**)] and one new steroidal glycoside [3-*O*-[β-glucopyranosyl(1→2)-*O*-β-xylopyranosyl]-stigmasterol (**409**)] together with oleanolic acid (**185**), 3-β-acetoxyolean-12-en-28-methyl ester (**406**), stigmasterol (**176**) and β-sitosterol (**177**) were isolated from the stem bark of *C. volkensii*. The novel diterpenes [**406-408**] and **409** exhibited moderate (2-22μM) antiplasmodial activities. Seven anthraquinones, chrysophanol (**269**), physcion (**273**), natalo-emodin-8-methyl ether (**279**), obtusifolin (**285**), chrysophanol-10,10′-biathrone (**295**), physcion-10,10′-bianthrone (**299**), 1,6-*O*-dimethylemodin (**410**), and **176** were isolated from the roots of *S. didymobotrya*. These anthraquinones showed significant ($P \leq 0.01$) lipid lowering and significant ($P \leq 0.05$) antioxidant effects, with **299** (50μM) exhibiting potent ($P \leq 0.05$) adipocytes growth inhibition. Four new phytoecdysteroids, 2,3-acetonide-24-hydroxyecdysone (**411**), 11-hydroxy-20-deoxyshidasterone (**412**), 21-hydroxyshidasterone (**413**) 2,3-acetonide-22-*O*-β-glucosyl-20-hydroxyecdysone (**415**) together with a known 24-hydroxyecdysone (**414**) were isolated from *V. doniana* stem bark. These ecdysteroids (10mg/kg) displayed potent *in vivo* anti-inflammatory activities comparable ($P \leq 0.05$) to diclofenac (50mg/kg). Compound **415** showed appreciably dose-dependent inhibition of adipocytes maturation by 29, 31 and 42% at 0.1, 10 and 50μM. These results supported the applications of the investigated plants in management of malaria and the cited pathophysiological conditions in ethnomedicine.

CHAPTER ONE

1.0 INTRODUCTION

Malaria is an infectious disease caused by protozoan parasites in the blood system. It is currently confined to Africa, Asia and Latin America (Anon, 2010). In Sub-Saharan Africa, malaria is the most common disease and major public health problem. The malaria burden and transmission patterns vary across the region, from highly endemic to epidemic-prone (Anon, 2010). Four species of *Plasmodium: P. falciparum, P. ovale, P. vivax,* and *P. malaria* are the prevailing disease causative agents. Among the four species of human malaria *Plasmodium falciparum* is most wide spread and very dangerous, if unmanaged can lead to fatal cerebral malaria. Every year an estimated 2.7 million deaths are due to malaria and most of these deaths occur in Africa (Anon, 2008). Remarkable progress has been realized as a result of a comprehensive scale-up of malaria control and prevention measures, especially widespread distribution of insecticide-treated mosquito nets, expanding and improving the indoor residual spraying program, and increasing availability of effective antimalarial drugs. In spite of all these efforts, the problems of controlling malaria in these countries are aggravated by inadequate health structures and poor socioeconomic conditions. The situation is even more complex with the increase in resistance to the drugs normally used to combat the parasite that causes the disease (Jambuo *et al.*, 2005). Substantial efforts have been made towards the development of new active compounds especially from artemisinin (**1**) as an alternative to chloroquine (**2**). However, no single drug is available that is effective against multi-drug resistant malaria (Jambuo *et al.*, 2005; Wichmann *et al.*, 2004). Efforts towards development of antimalarial drugs alternatives from the available ethno medicinal knowledge remain imperative, since there are numerous unexplored botanical remedies.

The use of plant-derived drugs for the management of malaria and related pathophysiological conditions has a long and successful tradition, particularly plants used in popular medicine. From some of these plants, it has been possible to confirm their traditional uses and isolate new biologically active molecules such as quinine (**3**) from *Cinchona* bark and artemisinin (**1**) from *Artemisia annua* L (Klaymann, 1985). A vast majority of the existing antimalarial chemotherapeutic agents are based on natural products (Ziegler *et al.*, 2002). This fact suggests that new leads may emerge from plants since the biological chemo-diversity of

plants is vast. The uses of traditional and herbal remedies are the alternative choice of treatment in countries where malaria is endemic (Sofowora, 1982; Rosoanaivo *et al*, 1992). In Kenya, several plant species are used in the management of malaria (Muthaura *et al.*, 2007), including *Caesalpinia volkensii* (Murengi *et al.*, 2007) and *Senna didymobotrya* (Njoronge & Bussmann, 2006). However, scientific validations of ethnopharmacological claims should be based on their biological and phytochemical evidence. In majority of such medicinal plants, such evidence is lacking.

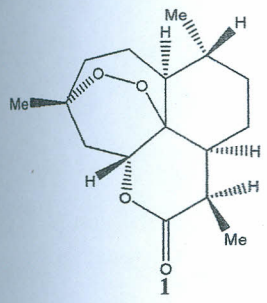

1

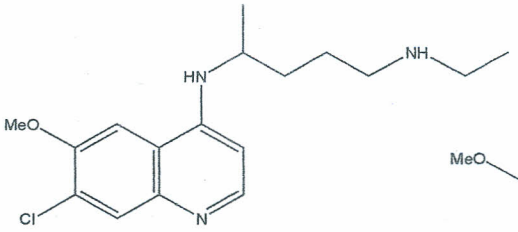

2

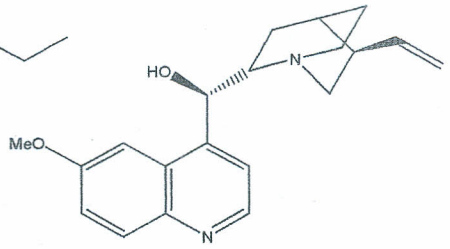

3

The manifestation of most parasitic diseases such as malaria is not only due to mechanical or chemical tissues damage but also due to the host responses to the presence of the parasites (Murray *et al.*, 1998). *Plasmodium* parasites invades the host red blood cells, thereby causing and aggravating symptoms like fever, severe joint pain, and in extreme cases, anemia (a deficiency in red blood cells) because the parasites use red blood cells to reproduce (Anon, 2008). The host's immune system may respond to such pathogenic infection by producing cytokines Tumor necrosis factor (TNF-α), interleukin-1β, and interleukin-8 subsequently increasing respiratory burst on phagocytes (Dockrell & Playfair, 1984). Production of pro-inflammatory cytokines by the resident peritoneal macrophages and mast cells are linked to nociception and inflammation (Ribeiro *et al.*, 2000). Use of synthetic analgesic or anti-inflammatory in conjunction with antimalarial irreversibly reduce nociception with high selectivity but are toxic to the hepatic cells, glomeruli, cortex of the brain and heart muscles, whereas natural inhibitors have lower selectivity with fewer side effects (Evans *et al.*, 1987).

A number of natural products including alkaloids, terpenoids and flavonoids) and plants extracts have been established to posses mild to potent antinociceptive and anti-inflammatory activities (Yunes *et al.*, 2005). Plants such as *Caesalpinia volkensii* Harms (Fabaceae) whose roots and/or fruits decoctions are used by traditional practitioners to manage general pain and stomach trouble during pregnancy (Kokwaro, 2009) although such claims have thus far not been

confirmed scientifically. Similarly, *Vitex doniana* Sweet (Lamiaceae) leaves and stem barks have traditional application against headache, fever and catarrh (Iweuke *et al.*, 2006), which have been confirmed by some pharmacological studies such as antipsychotic, antidepressant, analgesic, and anti-inflammatory (Iweuke *et al.*, 2006; Sharma *et al*, 1982; Tijjani *et al.*, 2012). However, the nature of the phytochemicals behind the claimed ethnopharmacological practice and the biological activities has not been established.

Frequent attack by malaria (cerebral) may subsequently lead to propagation of tissue injury (Ichikawa & Konishi, 2002). The genesis of reactive oxygen species (ROS) during malaria infection involves degradation of haemoglobin by intracellular malarial parasite accompanied by redox process involving Fe^{2+} to Fe^{3+} and molecular oxygen (Atamna & Ginsburg, 1993; Postna *et al.*, 1996). Reduction of the molecular oxygen to superoxide anion initiates the existing of free radicals species. Free radicals formed either on carbon-, nitrogen- or oxygen-center have been implicated in a number of clinical disorders including tissues injury (Simpson, 1987), carcinogenesis, mutagenesis, cell necrosis and lipid peroxidation (Mason, 1982; Mason & Chignell, 1982; Trush *et al.*, 1982; Halliwell & Gutteridge, 1985). Several other secondary complications of malaria such as cerebral oedema, pulmonary oedema and poor eyesight have been linked to oxidative stress (Prada *et al.*, 1996). Since free radicals and lipid peroxidation have putative role in these problems, there is need for free radical control during malaria therapy. Such roles can be achieved easily by adoption of herbal therapy against malaria ailments, since there are several plants metabolites that rank high in antioxidant capacity. Since phytochemical compositions of *C. volkensii*, *S. didymobotrya* and *V. doniana* are not documented, the antioxidant capacities of their extracts remain uncertain, though it is an important medicinal benefit of herbal remedies.

Unmanaged free radical oxidative stress coupled with elevated plasma concentration of cholesterol especially low density lipoprotein (LDL) and triglyceride are leading causes of atherosclerosis and coronary heart diseases (Deeg & Ziegenhorn, 1983). The action of these free radicals on lipid molecules in biomembrane is the most important damaging effect, which leads to changes in membrane fluidity, membranes permeability and ultimately cell necrosis (Slater, 1984) and atherosclerosis (Fogelman *et al.*, 1980). Evidence for oxidized low density lipoprotein (LDL) in the pathogenesis of atherosclerosis *in vivo* has been demonstrated from animals' studies (Parthasarathy *et al.*, 1986). The uptake of oxidized LDL increases the load of oxidized

lipid products in cells. For instance, reactive aldehydes can conjugate with cellular proteins, cholesterol oxidation products and fatty acid hydroperoxides (Yla-Herttuala, 1991). Lowering plasma LDL levels is clearly of major importance in preventing atherogenesis. The synthetic drugs can intervene by lowering cholesterol or by lowering triglyceride level in plasma. However, common side effects of the drugs such as risks of incident diabetes, mystic, arthralgia, gastrointestinal upset and elevated liver function limit their uses (Sattar *et al.*, 2010). Supplementation with exogenous therapeutics with multi-fold properties such as antioxidant, anti-diabetic and lipid lowering activities from plants sources, may manage these ailments, through protection of LDL, enzymes inhibitors or other compounds that inhibit the oxidation process itself, or combination of both. There are scarce scientific investigations of the Kenya flora against reduction of high lipid contents or reduction of LDL, but there are plants with indicative ethno medicinal application related to reduction of excess plasma lipids and/or chemotaxonomic relation to plants families have shown hypocholestrolaemic effects (hypolipidaemia). For instance, *S. didymobotrya* is used against hyperlipidaemia and hypertension (Kokwaro, 2009) while *V. doniana* from *Vitex* genus which elaborate ecdysteroids may be suspected to lower plasma cholesterol levels subject to scientific proof.

Plants are endowed with ability to make an array of structurally diverse secondary metabolites, which may impart diverse biological activities influencing their ethnopharmacological applications. The medicinal actions of plants are unique to particular plant species or groups. These facts are consistent with the concept that combination of secondary metabolites in a particular plant is taxonomically distinct. A multifold scientific investigation aimed towards validation of efficacy, safety and quality is always necessary. This study intended to investigate the antioxidant, antidyslipidaemia, and analgesic principles alongside anti-plasmodial principles found in the three medicinal plants from the family Leguminocae sub family Caesalpinioideae (*Senna didymobotrya* Fresen and *Caesalpinia volkensii* Harms) and Lamiaceae (*Vitex doniana* Sweet).

1.2. Statement of the problem

In spite of the efforts made to eradicate malaria in Sub Saharan Africa, it remains a deadly disease with adverse pathophysiological impacts, mainly due to overwhelming polymorphism of the resistant strains of *Plasmodium* parasites. The success of plant-derived drugs against resistant strains of *Plasmodium falciparum* rekindled the search for more antimalarial molecules from plants. Based on the ethnopharmacological claims that *C. volkensii* and *S. didymobotrya* are highly ranked in management of malaria, yet the presence of antimalarial molecules have not been established thus the efficacy of these plants towards management of malaria is not known. Pathophysiological impacts such as nociception and inflammation, associated with tissue damage aggravating symptoms of malaria always need urgent attention through co-administration of analgesic drugs. However, use of synthetic analgesic or anti-inflammatory drugs in conjunction with antimalarial drugs has limitations due to their contraindications. Use of natural analgesic such as *C. volkensii* and *V. doniana* extracts has been cited as alternative remedy, however, scientific justification for their efficacy are yet not established. Due to lack of proper phytochemical information about these plants, their potentials against oxidative stress, excess oxidized low-density lipoproteins (LDL) and other degenerative diseases is not certain.

1.3. Aim of the study

The aim of this study was to provide information necessary towards establishing the medicinal *in vitro* and *in vivo* efficacy in the use of *Caesalpinia volkensii* root- and stem-bark, *Senna didymobotrya* roots and *Vitex doniana* stem bark in management of malaria and other related impacts such as pain and inflammation, oxidative stress and excessive lipid accumulations.

Specific objectives were to:

1. Evaluate *in vitro* antiplasmodial activity of the crude extracts from *C. volkensii* root-and stem-bark, *S. didymobotrya* roots and *V. doniana* stem-bark against chloroquine-sensitive and chloroquine-resistant *Plasmodium falciparum* strains.
2. Evaluate *in vivo* antinociceptive and anti-inflammatory the extracts (objective 1) using laboratory animals.
3. Evaluate *in vivo* antidyslipidaemic from the extractives (objective 1) using triton-induced hyperlipidaemic rats.

4. To isolate and establish structures of the active principles from the root barks and stem barks of *Caesalpinia volkensii, Senna didymobotrya,* and *Vitex doniana.*
5. Evaluate *in vitro* antioxidant assays on the crude and pure isolates from objective 1, 2 and 3 above.
6. Evaluate *in vitro* antiadipogenesis on the active antidyslipidaemic isolates from (objective 3).

1.5. Justification

The continued malaria burden and transmission across the Sub Saharan regions outpacing the chemotherapeutic management strategies, calls for further intervention in the form of research towards development of alternative therapies. Considering the importance of the traditional medicine, the success of plant based drugs against malaria, and the fact that 80% of the rural populations in Sub Saharan Africa rely on traditional medicine (WHO, 2002), continued evaluation of traditionally confirmed antimalarial plant is imperative.

Clinical chemotherapeutic management of malaria and its secondary effects such as pyrexia, headache, nausea and anaemia may involve co-administration of analgesic to control these conditions and symptoms. It is thus a worthy course to evaluate plants with ethnopharmacological applications against malaria and its related ailments as alternative analgesic supplements. Such studies provide relevant scientific information towards the development of alternative remedies in fighting pathophysiological conditions associated with malaria.

Since degenerative diseases have been linked to malaria infection and its chemotherapy, evaluation of herbal remedies applicable against malaria and its pathophysiological impacts as primary sources of naturally occurring antioxidants is necessary. It is important to establish potential antioxidant capacities of plants claimed to have antimalarial activities, which can be remedies against the propagation of malarial oxidative stresses. The significance of plants extractives against oxidative stress is a well-established fact for plants with confirmed phytochemical components, however, for the plants with no or partial phytochemical records such as *C. volkensii, S. didymobotrya* and *V. doniana*, their potentials against such pathophysiological conditions cannot be rated. Generally, lack proper scientific investigation of the three plants validating some of the cited ethnopharmacological applications, deters proper applications and documentation of the plants among medicinal plants in Kenya.

1.6. Significance

The findings of this study serve as a preliminary phase in validating the investigated plants as antimalarial, analgesic, antioxidant and antidyslipidaemia agents, which can used as herbal remedies. The results corroborate the ethnomedicinal use of the investigated plant and contribute to the knowledge of the chemical composition of medicinal flora. This study provide biological activity data for the plants *(C. volkensii, S. didymobotrya* and *V. doniana*) and their various metabolites, which provide the use of these plants in traditional medicine attests to their economic worth besides provision of multifunctional medicinal effects.

Phytochemical and biological information about these medicinal floras are necessary towards documentations for African/ Kenyan medicinal plants database which has not been exhaustively realized as other traditional communities such as India and China (Iwu, 1993). Consequently, there is limited development of therapeutic products from Kenya. In view of the rapid loss of natural habitats due to deforestation, loss of traditional community life and cultural diversity and knowledge of medicinal plants, documentation of African medicinal plants is an urgent matter to necessitate conservation and propagation of threaten species.

CHAPTER TWO

2.0. LITERATURE REVIEW

2.1. Malaria and antimalarials

Human malaria transmitted by female *Anopheles* mosquitoes is caused by four *Plasmodium* species: *P. vivax, P. Malarae, P. falciparum* and P. *ovale* as the most common aetiological agents. The most widespread and severe malaria disease is caused by *P. falciparum*, which transiently infects the liver before invading red blood cells of the host (Fig.1). Sporozoites are injected into human dermis through the bite of infected *Anopheles* mosquito. After inoculation, sporozoites migrate to liver cells to establish the first intracellular replicative stage. Merozoites generated from this exoerythrocytic phase then invade erythrocytes, and it is during this erythrocytic stage that severe conditions of malaria occur. The life cycle is completed when a mosquito ingests sexual stages (gametocytes).

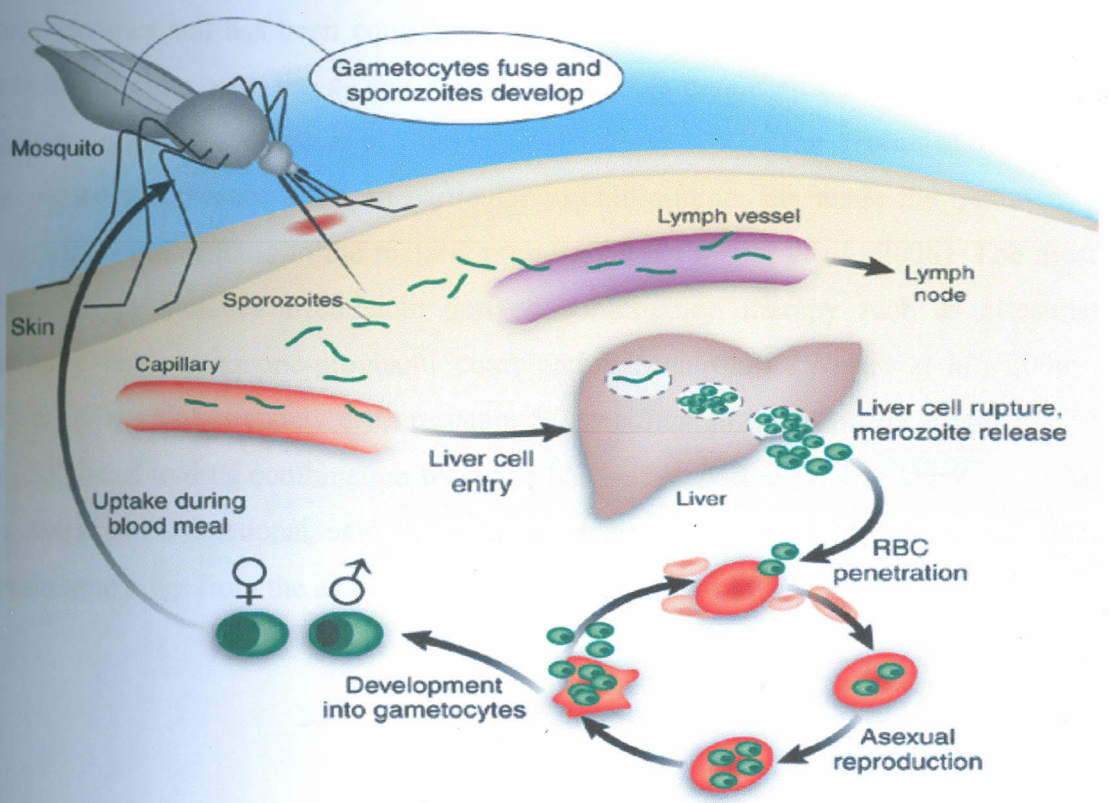

Figure 1: Schematic life cycle of malaria in humans. Adapted and reproduced by permission from Macmillan Publishers Ltd (Ziegler *et al.*, 2002).

Some sporozoites deposited in the skin eventually penetrate capillaries or lymph vessels. Those entering the lymph vessels will penetrate lymph vascular endothelial cells in lymph nodes to establish a lymph node form, which appears not to continue the life cycle - but may be significant in priming an immune response. Clinical manifestations occur at the erythrocytic stages characterized by fever, chills, prostration and anaemia, as well as delirium, metabolic acidosis, cerebral malaria and multi-organ system failure, which may be followed by coma and death (Fidock *et al.*, 2004; Jones & Good, 2006). Understanding the alternation of generation of *Plasmodium* parasite is very relevant towards development of chemotherapeutic remedy, so the bioassay models should target both the asexual and the sexual stages. As it is with the available antimalarial, some do not kill the merozoites in liver and result to relapses, necessitating development of drugs that can destroy the merozoites (Ziegler *et al.*, 2002).

Quinine (**3**), an aminoquinoline alkaloid isolated from the bark of *Cinchona* species (Rubiaceae) in 1820 is the oldest and one of the most important antimalarial drugs still in use. The alkaloid remained the sole active principle effective against malarial parasites for almost three centuries and has been considered the lead compound for the development of synthetic antimalarial drugs with the 4- and 8-aminoquinolines parent structure such as chloroquine (**2**) and primaquine (**4**) (Saxena *et al.*, 2003; Viegas *et al.*, 2007). The evolution of drug-resistant *P. falciparum* strains since 1960, in particular to chloroquine, has made the treatment of malaria increasingly problematic in the malaria prone regions (Winter *et al.*, 2006). The most effective chemotherapy includes artemisinin derived combination therapy such as artesunate (**5**), or mixtures with atovaquone-proguanil combination Malarone® (Winter *et al.*, 2006; Taylor & White, 2004). Unfortunately drug resistant *Plasmodium* strains towards artemisinin (Jambou *et al.*, 2005) and to drug combination therapies has been reported (Wichmann *et al.*, 2004). Due to the absence of a functional, safe and available malaria vaccine, efforts towards development of antimalarial drugs from the available ethno medicinal knowledge remain imperative.

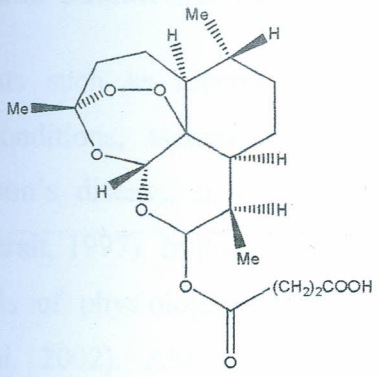

5

An array of natural products has been reported to have antiplasmodial activities. Saxena *et al.*, (2003) provided a critical account of crude extracts, essential oils and other compounds with antiplasmodial activities. A total of 127 alkaloids, 18 quassinoids, 23 sesquiternes, 27 triterpenoids, 21 flavonoids, 9 quinones and 25 miscellaneous compounds were highlighted by the year 2003 (Saxena *et al.*, 2003). Frederich *et al.*, (2008) highlighted 31 indole alkaloids isolated from plants with high antiplasmodial activity both *in vitro* and *in vivo*. Most of these indole alkaloids showed IC_{50} values under the micromolar range with good selectivity index (Frederich *et al.*, 2008; Kaur *et al.*, 2009) focused on antimalarial compounds discovered between 1998 and 2008 from both terrestrial and marine extracts. A total of 266 antiplasmodial compounds including alkaloids, terpenes, quassinoids, flavonoids, limnoids, chalcones, peptides, xanthones, quinones, coumarins and miscellaneous compounds as well as 37 promising semi synthetic antimalarials were noted (Kaur *et al.*, 2009). In spite of the vast compounds available as antiplasmodial agents, few have been subjected to structure-activity studies to establish antimalarial templates. In view of these myriad of compounds that have displayed notable antimalarial potential, however, the since compounds from *C. volkensii* and *S. didymobotrya* have not been identified, the efficacy of these plants was still unclear in spite of the ethnomedicinal claims.

The criteria for considering the *in vitro* antiplasmodial activity of crude extract as "good", "moderate", "low" or "inactive" adopted from Basco *et al* (1994) which were applicable in the course of this study consider IC_{50} < 10 µg/ml as good activity; 10-50 µg/ml as moderate; 50-100 µg/ml as low activity and >100 µg/ml as inactive for crude extracts. A criteria developed for pure compounds of known structures express IC_{50} values in µM and considers compounds showing IC_{50} > 100 µM as inactive; IC_{50} of 20-60 µM as low activity; IC_{50} 1-20 µM as of limited or moderate activity; and IC_{50} < 1 µM as excellent/potent activity (Muriithi *et al.*, 2002).

2.2. Antioxidants and Oxidative stress

Free radicals oxidants such as reactive oxygen species (ROS) are related to complex pathophysiological conditions, ischemia, anemia, asthma, arthritis, inflammation, neuro-degeneration, Parkinson's disease, mongolism, and perhaps dementias including other age related diseases (Polterait, 1997). In particular, the brain is more susceptible to oxidative insult due to the low levels of physiological antioxidants and antioxidant enzymes in the brain (Ichikawa & Konishi, 2002). Although ROS are instrumental in the initiation of lipid peroxidation, many other reactions such as Ca^{2+} release, frequent attack by disease such as malaria (cerebral), also play crucial roles in the subsequent propagation of tissue injury (Ichikawa & Konishi, 2002). The ROS are produced during malaria infection via two mechanisms. The first involves the production of ROS from the haemoglobin degradation by the intracellular parasite. In this case, the Fe^{2+} oxidizes to Fe^{3+} after the heme separates from the globin and the electron produced during this process reacts with molecular oxygen to form ROS such as superoxide anion radicals and hydrogen peroxide. Superoxide dismutase (SOD) and catalase are cellular enzymes that function to prevent oxidative stress by detoxifying the superoxide and hydrogen peroxide, respectively (Fig. 2) (Atamna & Ginsburg, 1993; Postna *et al.*, 1996). The second mechanism involves the host's immune system, which respond to pathogenic infection by producing cytokines TNF-α which increase respiratory burst (ROS) on phagocytes (Dockrell & Playfair, 1984).

High oxidative stress in patients with acute non-complicated malaria has been observed (Padon *et al.*, 2003) and it is thought to be aggravated by some antimalarial drugs like chloroquine (**3**) and artemisinin (**2**) (Oliaro *et al.*, 2001). For instance, the mode of action of artemisinin (**2**) and its derivatives involve heme-mediated decompositions of the endoperoxides-bridge to produce oxygen-centered free radicals which act against the parasite but also alkylate the heme and proteins hence damaging some intracellular targets by lipid peroxidation (Padon *et al.*, 2003). Several other secondary complication of malaria such as cerebral edema, pulmonary edema and poor eyesight has been linked to oxidative stress (Prada *et al.*, 1996). Since free radicals and lipid peroxidation have putative role in these problems, there is need for free radical control during malaria therapy using safe natural antioxidants.

The body radical scavengers or inhibitors need supplements from exogenous sources for effective tissues protection against oxidative stress. Indeed, several trials with small molecular

antioxidants have been conducted but the results are yet not satisfactory, while some results are also controversial (Dajas *et al.*, 2003; Ichikawa & Konishi, 2002). Natural antioxidants have attracted a great deal of research leading to a worldwide trend towards the use of natural phytochemicals present in berry crops, tea, herbs, fruits and vegetables as options against oxidative damages (Wolfe *et al.*, 2008). The potential of the plants *C. volkensii, S. didymobotrya* and *V. doniana* as potential remedy to the degenerative diseases by controlling oxidative insult to cells and tissues has not been established.

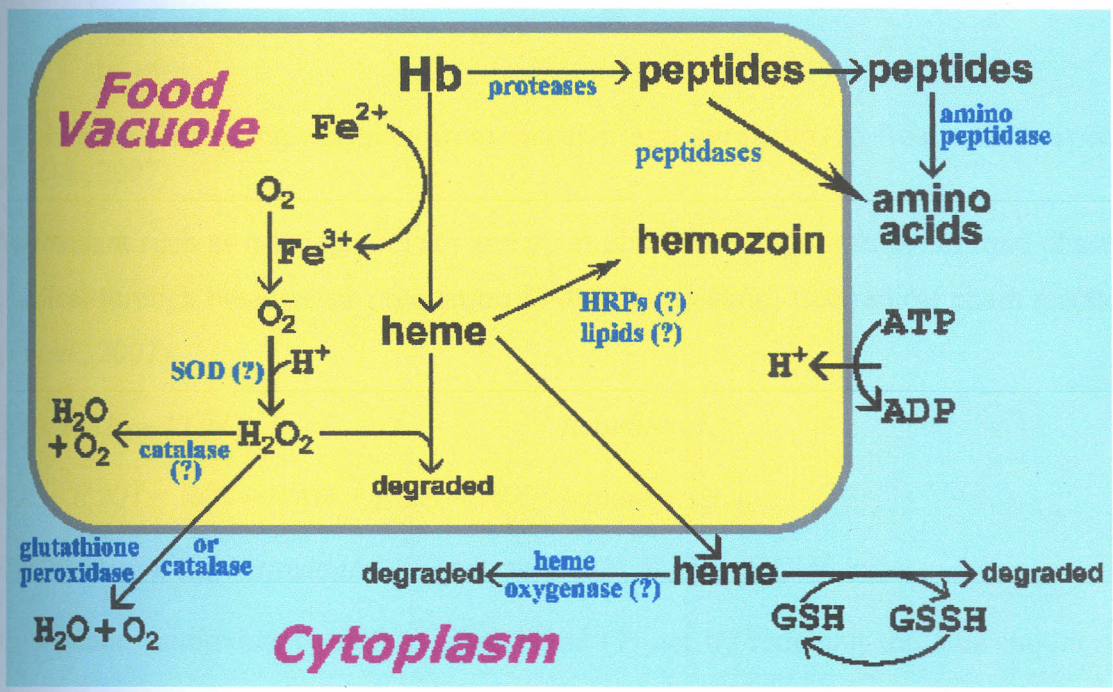

Figure 2: Oxidative electro biochemical cycle. The Ferrous (Fe^{2+}) ion bound to hemoglobin get oxidized to ferric ion (Fe^{3+}). Electrons liberated by this oxidation promote the formation of reactive oxygen species (ROS) (Atamna & Ginsburg, 1993).

Three mechanisms are most frequently involved in the radical scavenging processes: a one-step H-atom transfer mechanism (equation 1) illustrated by catechol and pyrogallol (good structural requirement for antioxidants) (Scheme 1), a proton-coupled electron transfer mechanism (equation 2) and by chelation of transition metal catalyst.

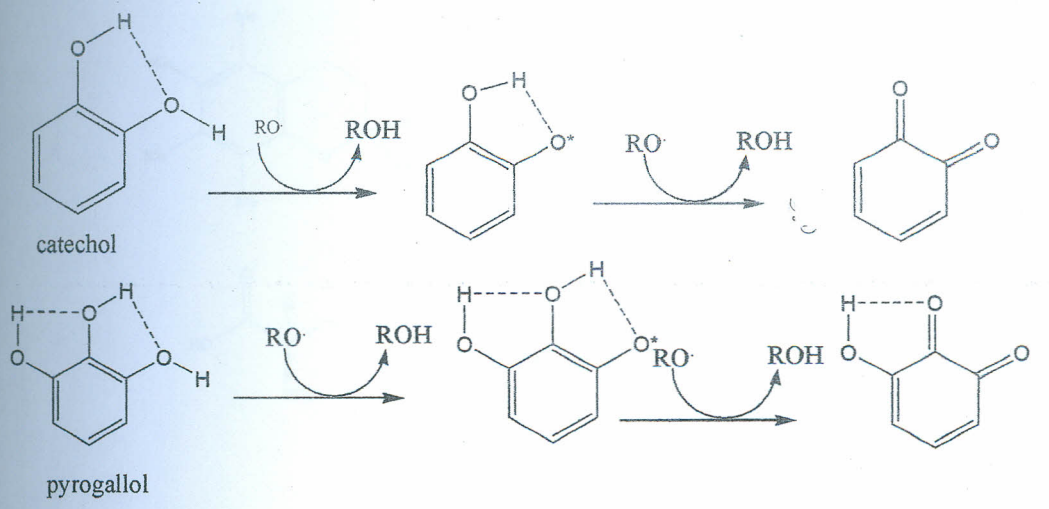

Scheme 1: H-atom abstracting reactions from catechol and pyrogallol to free radicals species (Somogyi *et al.*, 2007).

Antioxidant such as α-tocopherol (**6**) and other phenolic compounds act in lipid phase to trap free radical through mechanism I (equation 1) thereby breaking free radical chain reactions (Somogyi *et al.*, 2007).

$$RO + R'XH = ROH + R'X \qquad \textit{(equation 1)}$$

$$RO^{\cdot} + R'XH = RO^{-} + R'XH = ROH + R'X^{\cdot} \qquad \textit{(equation 2)}$$

RXH represent the antioxidant, X represent an O-, S-, N-, or C-atom.

Endogenous antioxidants such as glutathione (7) act by reducing the concentration of reactive oxygen species through donation of H^+ to form H_2O_2 which subsequently broken down to H_2O and O_2 catalyzed by glutathione peroxidase (Prior, 2003).

Some specific enzymes, for example superoxide dismutase (SOD) scavenge superoxide anion and convert it to less destructive species (Culter, 1992). A group of compounds especially with catechol or pyragollol moiety (Scheme 1) act by sequestration of transition metals that are well established proxidants (Riley, 1994). In this way, transferring, lactoferrin and ferritin functions to keep iron induced oxidative stress in check (Culter, 1992). The mechanism of antioxidant activities by the phytochemicals can thus be inferred through observation of molecular structures of their metabolites.

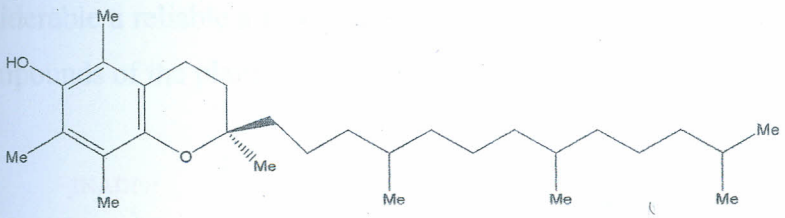

6

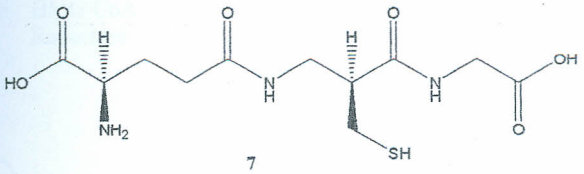

7

2.3. Hyperlipidaemia and antidyslipidaemia

Hyperlipidaemia is defined as an elevation of total cholesterol (Tc), triglyceride (Tg), low density lipoprotein cholesterol (LDL-C) and decreased level of high density lipoproteins cholesterol (HDL-C) in the blood (Chen *et al.*, 1991). The situation leads to an increased risk of coronary heart disease associated with a high serum concentration of total cholesterol, low-density lipoprotein (LDL) and triglyceride (Libby *et al.*, 1998; Martin *et al.*, 1986). Atherosclerosis, congestive heart diseases and some other diseases are strongly associated with disorders of lipid metabolism and plasma lipoproteins (Libby *et al.*, 1998; Martin *et al.*, 1986). Hyperlipidaemia has the ability to change pharmacokinetic and pharmacodynamic properties of lipoprotein bound drugs (Eliot & Jamali, 1999) such as the antimalarial drugs. This is of potential concern since the drugs can cause life threatening ventricular complications (Patel *et al.*, 2009) by raising or reducing the bioavailability of the drugs (Patel *et al.*, 2009). Therefore, a search for antimalarial alternatives should as well search for potential safe antidyslipidaemc agents.

A rational approach to the treatment and prevention of coronary heart diseases could be by decreasing any elevated levels of lipids in plasma (West *et al.*, 1983). Several studies have been conducted to evaluate the potential hypolipidaemic effects of synthetic and naturally occurring compounds. Strategies used for the management of hyperlipidaemia involve use of substances that disrupt cholesterol biosynthesis through inhibition of 3-hydroxy-3-methylglutaryl coenzyme A (HMG-CoA) reductase (Scheme 2) (Taylor *et al.*, 2011). Disruption of cholesterol

biosynthesis was considerable a reliable a model to evaluate the potential hypolipidaemic effects of the extracts and compounds of the plants *C. volkensii, S. didymobotrya* and *V. doniana.*

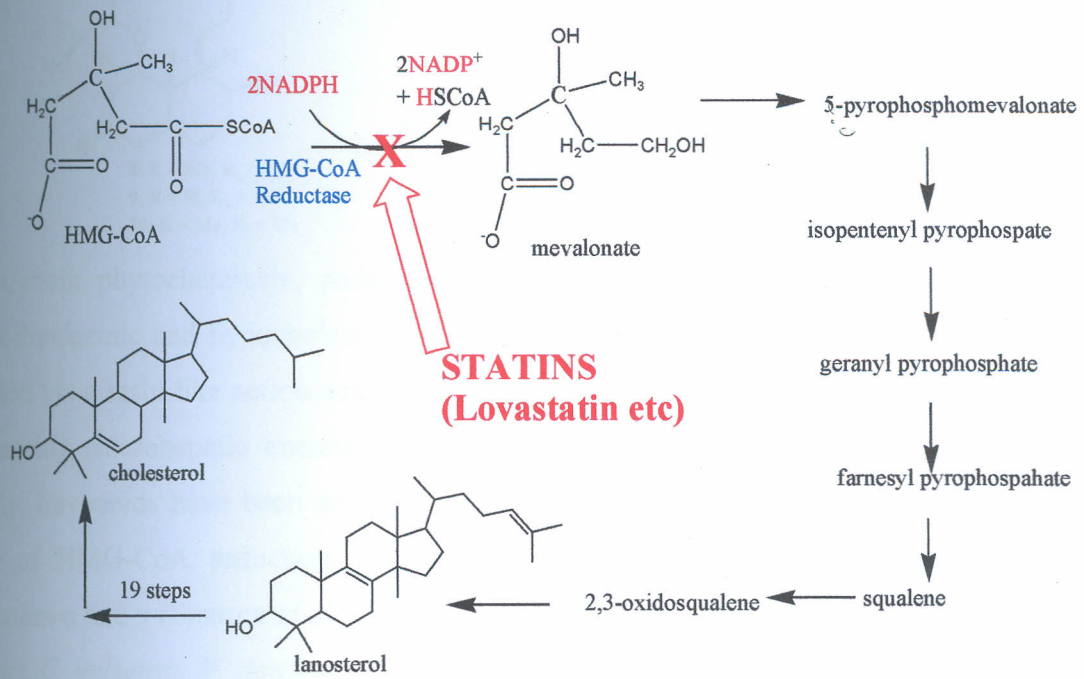

Scheme 2: Biosynthesis of cholesterol indicating statins inhibition of HMG-CoA reductase (Taylor *et al.*, 2011).

Statins are some of widely used antidyslipidaemic agents which inhibit the rate limiting step in cholesterol biosynthesis through competitive inhibition of (HMG-CoA) reductase (Scheme 2). They bind on active site of the enzyme thus preventing binding with its substrate (Taylor *et al.*, 2011). To date, there are two classes of statins: natural statins; lovastatin (**8**), compactin (**9**), simvastatin (**10**) and fluvastatin (**11**) a synthetic statins. Other antidyslipidaemic agents are the fibrates (beclofibrates, ciprofibrates, and fenofibrates) which are more effective in lowering serum LDL-cholesterol (Dierkes *et al.*, 2004). Gemfibrosil (**12**) (the second most useful antidyslipidaemic agent) is a fibrate primarily used to decrease triglyceride levels in the serum (Dierkes *et al.*, 2004). Bile acid sequestering agents are also important lipid lowering agents by reducing the enterohepatic recirculation of bile acids. This promotes up-regulation of 7α-hydroxylase and the conversion of more cholesterol in the hepatocyte into bile acids, thus reducing the cholesterol content in the hepatocytes (Wong, 2001). Reduction of cholesterol in the plasma either through inhibition of its biosynthesis or conversion to bile acids is used as one of the indicators of hypolipidaemic effects of the tested samples.

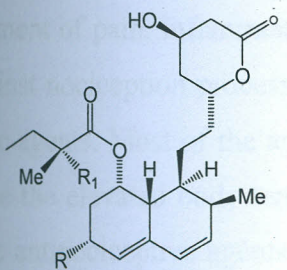

8: R = Me, R_1 = H
9: R = H, R_1 = H
10: R = Me, R_1= Me

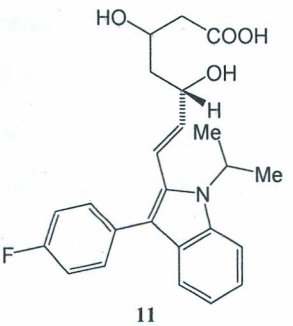

11

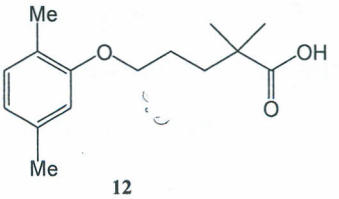

12

Certain phytochemicals, particularly saponins, have been reported to mediate their antihyperlipidaemic and hypocholesterolaemic actions by inhibiting or delaying intestinal lipid absorption via a resin-like action and inhibiting pancreatic lipase activity (Han *et al.*, 2001) and by enhancing enterohepatic excretion of cholesterol in the bile acid (Topping *et al.*, 1980). Similarly, flavonoids have been demonstrated to have lipid lowering activity by inhibiting the activity of HMG-CoA reductase and up-regulating the hepatic expression of peroxisome proliferators-α and γ (Sharma *et al.*, 2008). How diterpenoids, steroids and anthraquinones from the plants, *C. volkensii, V. doniana* and *S. didymobotrya* may mediate their antihyperlipidaemic actions is not yet established.

2.4. Nociception and antinociceptive agents

Nociception is defined as the neural processes of encoding and processing noxious stimuli (a stimulus that damages or threatens to damage tissues mechanically, thermally or chemically) (Loeser & Treede, 2008). It is initiated by nociceptors (pain receptors), that detect mechanical, thermal or chemical changes above a set threshold that triggers a variety of autonomic responses and may result in the experience of pain in sentient animals (Loeser & Treede, 2008). Technically, nociception refers to the transmission of nociceptive information to the brain without reference to the production of emotional or other types of response to the noxious stimulus (Feinstein *et al.*, 1954). Whereas pain refers to an unpleasant sensory and emotional experience associated with actual or potential tissues damage. Pain and pyrexia or fever are secondary effects of infection, tissue damage, inflammation, graft infection, malignancy or other disease states such as malaria (Debprasad *et al.*, 2005).

Normally the infected or damaged tissue initiates the enhanced formation of proinflammatory mediators (cytokines like interlenkin 1β, α, β and TNF- α), which increase the synthesis of prostaglandin E2 (PGE_2) (Scheme 3). Prostaglandins are associated with

development of pain, inflammation and headache (Browstein, 1993). Most of the analgesic thus acts against nociception process and not pain and thus known as antinociceptive agents and not analgesic agents. Most of the antinociceptive drugs inhibit cyclooxygenase (COX-2) expression to reduce the elevated body temperature by inhibiting prostaglandins (PGE_2) biosynthesis. The synthetic antinociceptive agents irreversibly inhibit COX-2 with high selectivity but are toxic to the hepatic cells, glomeruli, cortex of the brain and heart muscles, whereas natural COX-2 inhibitors have lower selectivity with fewer side effects (Evans *et al.*, 1987). Plant based herbals remedies have been indicated as effective therapy for the symptomatic management of malaria fever and relief of other painful conditions (Amos *et al.*, 2010).

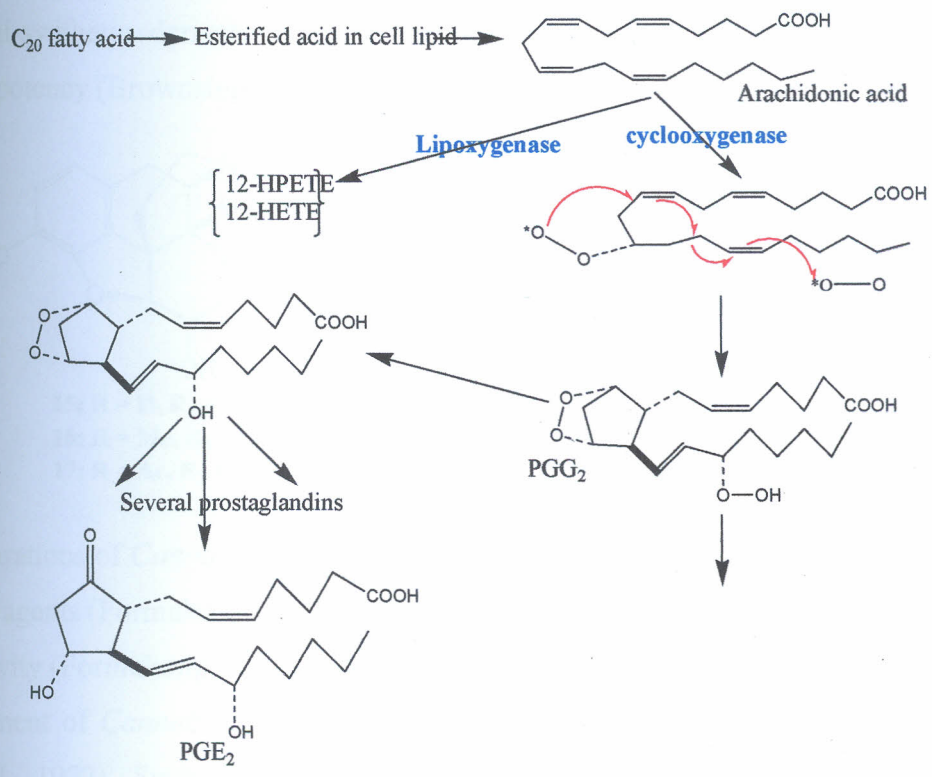

Scheme 3: Biosynthesis of prostaglandins (Browstein, 1993)

Phytochemicals have played an extremely vital role in the development of analgesic drugs and in the understanding of the complex mechanisms involved in pain transmission and pain relief (Yunes *et al.*, 2005). For instance, salicin (**13**), a glycoside obtained from the bark of *Salix* species, was the lead compound for the synthesis of aspirin (**14**) based on its activity and structure.

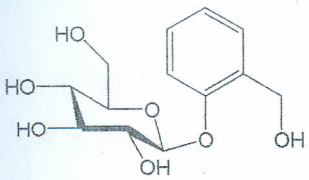

13

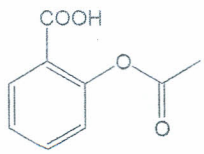

14

Morphine (**15**), the major pain-relieving agent obtained from opium poppy (*Papaver somniferum*), alongside codaine are widely used in medicine (Brownstein, 1993). Codeine (**16**) is structurally close to morphine (**15**), although it is much less potent and amounts to only 0.5% of the opium exudates while morphine amounts to about 10%. Heroin (**17**) does not occur naturally but is a semi-synthetic derivative produced by a chemical modification of morphine that increases the potency (Brownstein, 1993).

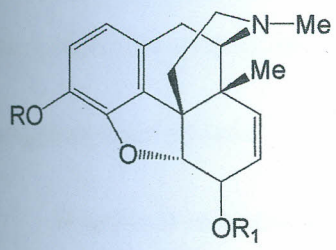

15: R = H, R_1 = H
16: R = Me, R_1 = H
17: R = Ac, R_1 = Ac

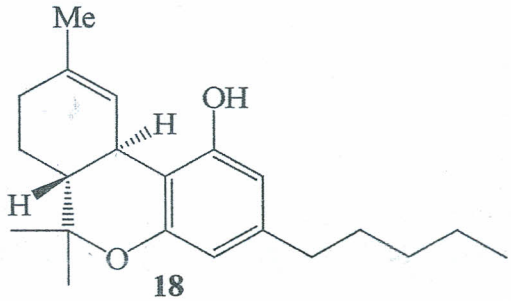

18

Various preparations of *Cannabis sativa* have also been employed as antipyretic, anti-rheumatic and analgesic agents (Formukong *et al.*, 1988). Extracts of *Cannabis* have been shown to possess analgesic activity (Formukong *et al.*, 1988); δ-1-tetrahydrocannabinol (**18**) (δ-THC), the psycho-active component of *Cannabis* has also been shown to posses this activity in various models (Dewey *et al.*, 1972). Such findings have opened new possibilities for research into new analgesic drugs based on structural similarities to δ-1-tetrahydrocannabinol. Some other metabolites including alkaloids, terpenoids and flavonoids have since been discovered with antinociceptive and anti-inflammatory properties (Calixto *et al.*, 2000). More naturally occurring analgesic and anti-inflammatory agents, though mild but effective may be elaborated by such plants as *C. volkensii* (Kokwaro, 2009) and *Vitex doniana* (Iwueke *et al*, 2006) which are reported by traditional healers as pain relievers yet the molecules responsible for such claims are not known.

2.5. The family Fabaceae

The Fabaceae families consist of herbs, vine, shrubs, trees and lianas found in both temperate and tropical areas. They comprise one of the largest families of flowering plants numbering to about 630 genera and 18,000 species (Beentje, 1994).

2.5.1 Sub-family Caesalpiniodeae

The sub-family Caesalpiniodeae consists mostly of trees or shrubs with leaves, which are pinnate, sometimes bipinnate but rarely simple. Their Flower corollas are usually showy; zygomophic, while the petals are imbricate, posterior (upper or banner) and occur inside the buds. They bear 10 or fewer stamens which are distinct and usually not showy. They produce pollens in monads and have U-shaped seeds. The two plants, *Senna didymobotrya* and *Caesalpinia volkensii* belong to this sub family of Leguminosae (Beentje, 1994)

2.5.2. The genus *Caesalpinia*

2.5.2.1. Botanical information

The genus *Caesalpinia* is mainly trees, shrubs and woody climbers. Their leaves are large and bipinnate. Their flowers are yellow or red and often showy. Racemes are paniculate in the upper leaf axils or terminal. The lowest outside petals are orbicular, clawed and imbricate. Stamens are 10 and free. Ovary are sessile and usually few ovules. Pods vary, sometimes covered with spines. The genus has about 280 species distributed in tropical and sub-tropical regions (Beentje, 1994).

2.5.2.2. Ethnopharmacological application of the genus *Caesalpinia*

Several extracts from plants of the genus *Caesalpinia* have been associated with variety of ethnopharmacological applications (Sharma *et al.*, 1997; Date *et al.*, 1998). Seed kernels *Caesalpinia bonducella* (L) and *Caesalipinia crista* (L) are extensively used by the India Ayurvedic pharmacopeia as anti-asthmatic, antidiabetic, anti-inflammatory, antibacterial, antifilarial, antitumor, and against liver, spleen and mental disorders (Sharma *et al.*, 1997; Kapoor, 1990; Date *et al.*, 1998). The heart wood of *Caesalpinia sappan* (L) has been used in folk medicine as a blood tonic, expectorant, emmenagogue and has interesting biological activities such as antioxidant (Badami *et al.*, 2003), immunomodulation (Choi *et al.*, 1997), anti-

complementary (Oh *et al.*, 1998), sedative effect (Nagai *et al.*, 1986) and vasorelaxation (Xie *et al.*, 2000) properties.

An infusion of *Caesalpinia pyramidalis* leaves are used as antidiuretic, antidispeptic, stomachache and fever in Brazil (Bahia *et al.*, 2010). Decoctions of the leaves, bark, and roots of *Caesalpinia pulcherrima* (L.), are used to manage liver disorders, ulcers of the mouth and throat, to reduce fevers, cause abortion and alleviate fungal infections (Quisumbing, 1978). *Caesalpinia mimosoides* (Lamk), soft young shoots and leaves used as fresh vegetable and appetizers (Yodsaoue *et al.*, 2010) and as a carminative to relieve dizziness and fainting (Yodsaoue *et al.*, 2010). *Caesalpinia major* (Medik) root decoction is used as a tonic, an antihelmintic, management of rheumatism and backache (Kitagawa *et al.*, 1994) while the seeds are used as expectorant and antitussive agent (Roengsumran *et al.*, 2000). *Caesalpinia benthamiana* (Baill) is reported to be used for management of topical infections and wounds (Abbiw, 1990) confirmed by *in vitro* antibacterial and antioxidant activities demonstrated by its pet ether root extract (Dickson *et al.*, 2007). A plant genus with such wide ethnopharmacological information, implies the other species as yet not investigated or lack any reported use also have potentials not yet discovered.

Caesalpinia volkensii occur in Kenya and Tanzania where it is used traditionally for a wide variety of ethnomedicinal purposes (Beentje, 1994). *C. volkensii* is common among the Kikuyu community (Kenya) where it is known as "Muchuthi", among the Swahili it is known as "Mkomwe" and the Luo community it is called "Ajua" (Kokwaro, 2009). This plant has several traditional applications, for instance its most common use is for management of malaria (Kokwaro, 2009). Herbalists prescribe a decoction of the leaves stem bark and/or root bark to cure malaria, sometimes alone, but more often mixed with other plants (Kuria *et al.*, 2001). Unspecified plant parts are used in Kenya to manage retinoblastoma (Kokwaro, 2009). The leaves, stem bark and/or root bark are boiled in soup or tea decoction administered to pregnant women to relieve pains during pregnancy and general stomach pains (Kokwaro, 2009). The Shambaa people of Tanzania uses it as an aphrodisiac while Bondei people of Tanzania cook or chew them raw or put them in sweet palm wine and drink it 2-3 times a day (Kokwaro, 2009). Despite such ethnopharmacological significance, *C. volkensii* has not received much attention regarding validation of its claimed uses.

2.5.2.3. Phytochemistry of *Caesalpinia* genus

Plants of the genus *Caesalpinia* are a rich sources of cassane-type furanoditerpenes (Jiang *et al*, 2001a; Kinoshita, 2000), triterpenoids (Bahia *et al.*, 2010), phenylpropanoids (Mendes *et al*, 2000) and flavonoids (Namikoshi & Saitoh, 1987) and aromatic phenols including phenylpropanoids. The reported chemical constituents from the genus *Caesalpinia* by the year 2010 can be estimated to 280 compounds excluding the volatile components (Wu *et al.*, 2011). Tables 1 to 4 summarize the different plants of the genus that have been investigated, the compounds isolated and the corresponding plant part. Despites extensive work done on the genus *Caesalpinia*, no phytochemical investigation has so far been reported from *C. volkensii*.

2.5.2.3.1. Cassane-type furanoditerpenes from Casealpinia species

Cassane diterpenoids isolated from the genus *Caesalpinia* (Table 1) can be classified into five basic skeleton types (Jiang *et al.*, 2002): tricyclic derivatives fused with a furan ring [**19-103**] (Pranithanchai *et al.*, 2009); tricyclic derivatives fused with an α,β-butanolide [**104-124**] (Pranithanchai *et al.*, 2009; Roach *et al.*, 2003; Yadav *et al.*, 2009); tricyclic derivatives with cleavage of the furan ring [**125-130**] (Lyder *et al.*, 1998; Peter *et al.*, 1998; Kalauni *et al.*, 2004; Cheenpracha *et al.*, 2005; Kiem *et al.*, 2005); rearranged furanoditerpenoids with migration of the methyl group at C-4 to C-3, [**131-133**] (Peter *et al.*, 1997; Kalauni *et al.*, 2005b); and a furanoditerpenoid lactones formed from the ring closure involving the *O*-atoms bridging C-7 and C-17 [**134-144**] (Kitagawa *et al.*, 1996; Peter *et al.*, 1997; Awale *et al.*, 2006; Jiang *et al.*, 2001a; Jiang *et al.*, 2001b; Jiang *et al.*, 2002). Compound **127** was reported to have rare structure of a cleaved furan ring and a lactone bridge from C-7 to C-17 along with other five novel cassane diterpene from *C. crista* seed kernels (Kalauni *et al.*, 2005a). Some eleven cassane diterpenes were also isolated from the seeds of *C. sappan* as new natural products with unusual molecular skeleton; compound **145-150** had additional oxa bridge between C-9 and C-20 while compound **151** and **152** exhibited an oxa bridge between C_{11} and C_{20} (Yodsaoue *et al.*, 2010). Dimmers of cassane diterpenes [**155** and **156**] have been encountered from the seeds of *C. minax* (Cheenpracha *et al.*, 2006) and roots of *C. mimosoides* (Yodsaoue *et al.*, 2010). Such molecular diversity is indicative of the need for continued phytochemical study on other *Caesalpinia* species not yet studied such as *C. volkensii*.

Table 1: Cassane diterpenoids isolated from the plants species of the genus *Caesalpinia*

Name of compound	Plant species	Part	Reference
Voucapen-5α-ol (**19**)	*C. pulcherrima*	Root	McPherson *et al.*, 1986
6β-cinnamoyl-7β-hydroxyvoucapen-5α-ol (**20**)	*C. pulcherrima*	Root	Roach *et al.*, 2003
8,9,11,14-Didehydrovoucapen-5α-ol (**21**)	*C. pulcherrima*	Root	McPherson *et al.*, 1986
Caesalpin F (**22**)	*C. bonducella*	Seed	Pascoe *et al.*, 1986
	C. crista	Seed kernel	Linn *et al.*, 2005
ε-caesalpin (**23**)	*C. minax*	Seed	Jiang *et al.*, 2001a
	C. bonducella		Pascoe *et al.*, 1986
Caesaljapin (**24**)	*C. decapetala*	root	Ogawa *et al.*, 1992
Caesaldekarin B (**25**)	*C. major*	root	Kitagawa *et al.*, 1996
Caesaldekarin D (**26**)	*C. major*		Kitagawa *et al.*, 1996
Caesaldekarin E (**27**)	*C. major*	Root	Kitagawa *et al.*, 1996
	C.crista	Seed kernel	Kalauni *et al.*, 2005a
Bonducellpin A (**28**)	*C. bonduc*	root	Peter & Tinto, 1997
Bonducellpin B (**29**)	*C. bonduc*	root	Peter & Tinto, 1997
Bonduccellpin C (**30**)	*C. bonduc*	Root	Peter & Tinto, 1997
	C. crista	Seed kernel	Awale *et al.*, 2006
Pulcherrimin C (**31**)	*C. pulcherrima*	Root	Patil *et al.*, 1997
		stem	McPherson *et al.*, 1983
Pulcherrimin D (**32**)	*C. pulcherrima*	Root	Patil *et al.*, 1997
Pulcherrimin B (**33**)	*C. pulcherrima*	Root	Patil *et al.*, 1997
Caesaldekarin A (**34**)	*C. bonduc*	Root	Lyder *et al.*, 1998
	C. pulcherrima	Leaves	Ragasa *et al.*, 2003
Caesaldekarin H (**35**)	*C. bonduc*	root	Lyder *et al.*, 1998
Demethylcaesaldekarin C (**36**)	*C. bonduc*	Root	Lyder *et al.*, 1998
Caesaldekarin I (**37**)	*C. bonduc*	Root	Lyder *et al.*, 1998
Caesaldekarin C (**38**)	*C. bonduc*	Root	Peter *et al.*, 1998
Caesaldekarin F (**39**)	*C. bonduc*	Root	Peter *et al.*, 1998
	C. sappan	Heartwood	Shu *et al.*, 2007
Caesaldekarin J (**40**)	*C. bonduc*	Root	Lyder *et al.*, 1998
		Bark	Udenigwe *et al.*, 2007
Caesaldekarin K (**41**)	*C. bonduc*	Root	Lyder *et al.*, 1998
14-Deoxy-ε-caesalpin (**42**)	*C. major*	Seed kernel	Roengsumran *et al.*, 2000
Caesalmin C (**43**)	*C. minax*	Seed	Kalauni *et al.*, 2004
	C. crista	Seed kernel	Peter & Tinto, 1997
Caesalmin D (**44**)	*C. minax*	Seeds	Jiang *et al.*, 2002
Caesalmin F (**45**)	*C. minax*	Seeds	Jiang *et al.*, 2002
Caesalmin H (**46**)	*C. minax*	Seeds	Jiang *et al.*, 2002
Isovoucapenol A (**47**)	*C. pulcherrima*	Leaves	Ragasa *et al.*, 2003
Isovoucapenol B (**48**)	*C. pulcherrima*	Leaves	Ragasa *et al.*, 2003
Isovoucapenol C (**49**)	*C. pulcherrima*	Leaves	Ragasa *et al.*, 2003
		Roots	Roach *et al.*, 2003
		Stem	Pranithanchai *et al.*, 2009
Isovoucapenol D (**50**)	*C. pulcherrima*	Leaves	Ragasa *et al.*, 2003
Isovoucapenol E (**51**)	*C. pulcherrima*	Leaves	Ragasa *et al.*, 2003
Pulcherrimin A (**52**)	*C. pulcherrima*	Root	Roach *et al.*, 2003

Table 1 cont'd...

Pulcherrimin E (**53**)	*C. pulcherrima*	Root	Roach *et al.*, 2003
		Stem	Pranithanchai *et al.*, 2009
Pulcherrimin F (**54**)	*C. pulcherrima*	Root	Roach *et al.*, 2003
Caesalpinin MA (**55**)	*C. crista*	Seed kernels	Kalauni *et al.*, 2004
Caesalpinin MB (**56**)	*C. crista*	Seed kernels	Kalauni *et al.*, 2004
Caesalpinin MC (**57**)	*C. crista*	Seed kernels	Kalauni *et al.*, 2004
Caesalpinin MD (**58**)	*C. crista*	Seed kernels	Kalauni *et al.*, 2004
2-acetoxycaesaldekarin E (**59**)	*C. crista*	Seed kernels	Kalauni *et al.*, 2005a
Caesalpinin C (**60**)	*C. crista*	Seed kernels	Linn *et al.*, 2005; Awale et al., 2006
14(17)-dehydrocaesallpin F (**61**)	*C. crista*	Seed kernels	Kalauni *et al.*, 2004; Linn *et al.*, 2005
Caesalpinin E (**62**)	*C. crista*	Seed kernels	Kalauni *et al.*, 2004; Yadav *et al.*, 2009
7-Acetoxybonducellpin C (**63**)	*C. crista*	Seed kernel	Kalauni *et al.*, 2004; Kalauni *et al.*, 2005a; Linn *et al.*, 2005; Awale *et al.*,2006
2-Acetoxy-3-deacetoxycaesaldekarin E (**64**)	*C. crista*	Seed kernels	Kalauni *et al.*, 2005b
1-Deacetylcaesalmin C (**65**)	*C. crista*	Seed kernels	Kalauni *et al.*, 2005c
1-Deacetoxy-1-oxocaesalmin C (**66**)	*C. crista*	Seed kernels	Kalauni *et al.*, 2005b
Caesalpinin MF (**67**)	*C. crista*	Seed kernels	Kalauni *et al.*, 2005a
Caesalpinin MG (**68**)	*C. crista*	Seed kernels	Kalauni *et al.*, 2005a
Caesalpinin MH (**69**)	*C. crista*	Seed kernels	Kalauni *et al.*, 2005a
Caesalpinin MI (**70**)	*C. crista*	Seed kernels	Kalauni *et al.*, 2005a
Caesalpinin MJ (**71**)	*C. crista*	Seed kernels	Kalauni *et al.*, 2005a
Caesalpinin MK (**72**)	*C. crista*	Seed kernels	Kalauni *et al.*, 2005a
Caesalpinin MO (**73**)	*C. crista*	Seed kernels	Kalauni *et al.*, 2005a
Caesalpinin MP (**74**)	*C. crista*	Seed kernels	Kalauni *et al.*, 2005a
Caesalpinin F (**75**)	*C. crista*	Seed kernels	Linn *et al.*, 2005
Nontaepeenin A (**76**)	*C. crista*	Stem root	Cheenpracha *et al.*, 2005
	C. mimosoides	Roots	Yodsaoue *et al.*, 2010
Nontaepeenin B (**77**)	*C. crista*	Stem root	Cheenpracha *et al.*, 2005
Taepeenin A (**78**)	*C. crista*	Stem root	Cheenpracha *et al.*, 2005
	C. mimosoides	Roots	Yodsaoue *et al.*, 2010
Taepeenin B (**79**)	*C. crista*	Stem root	Cheenpracha *et al.*, 2005
Taepeenin C (**80**)	*C. crista*	Stem root	Cheenpracha *et al.*, 2005
Taepeenin D (**81**)	*C. crista*	Stem/root	Cheenpracha *et al.*, 2005
	C. mimosoides	Roots	Yodsaoue *et al.*, 2010
Taepeenin E (**82**)	*C. crista*	Stem root	Cheenpracha *et al.*, 2005
Taepeenin H (**83**)	*C. crista*	Stem root	Cheenpracha *et al.*, 2005
Taepeenin I (**84**)	*C. crista*	Stem root	Cheenpracha *et al.*, 2005
Vinhaticoic acid (**85**)	*C. crista*	Stem root	Cheenpracha *et al.*, 2005
Methyl vinhaticoate (**86**)	*C. crista*	Stem root	Cheenpracha *et al.* ,2005
Caesalpinin J (**87**)	*C. crista*	Seed kernels	Awale *et al.*, 2006
Caesalpinin K (**88**)	*C. crista*	Seed kernels	Awale *et al.*, 2006
Caesalpinin L (**89**)	*C. crista*	Seed kernels	Awale *et al.*, 2006
Caesalpinin N (**90**)	*C. crista*	Seed kernels	Awale *et al.*, 2006
Caesalpinin M (**91**)	*C. crista*	Seed kernels	Awale *et al.*, 2006
Caesalpinin P (**92**)	*C. crista*	Seed kernels	Awale *et al.*, 2006
Benthaminin 1 (**93**)	*C. benthamiana*	Root bark	Dickson *et al.*, 2007
Benthaminin 2 (**94**)	*C. benthamiana*	Root bark	Dickson *et al.*, 2007
Deoxycaesaldekarin C (**95**)	*C. benthamiana*	Root bark	Dickson *et al.*, 2007

Table 1 cont'd....

ζ- caesalpin (**96**)		*C. sappan*	Heartwood	Shu *et al.*, 2007
Phanginin I (**97**)		*C. sappan*	Seed	Yodsaoue *et al.*, 2008
Phanginin J (**98**)		*C. sappan*	Seed	Yodsaoue *et al.*, 2008
Phanginin K (**99**)		*C. sappan*	Seed	Yodsaoue *et al.*, 2008
6β-Acetoxy-17-methylvoucapa-8(14),9(11)-diene (**100**)		*C. bonduc*	Whole plant	Yadav *et al.*, 2009
Pulcherrin A (**101**)		*C. pulcherrima*	Stem	Pranithanchai *et al.*, 2009
Pulcherrin B (**102**)		*C. pulcherrima*	Stem	Pranithanchai *et al.*, 2009
Pulcherrin C (**103**)		*C. pulcherrima*	Stem	Pranithanchai *et al.*, 2009
Neocaesalpin B (**104**)		*C. bonduc*	Seed	Kinoshita, 2000
Neocaesalpin C (**105**)		*C. bonduc*	Seed	Kinoshita, 2000
Neocaesalpin D (**106**)		*C. bonduc*	Seed	Kinoshita, 2000
Spirocaesalmin (**107**)		*C. minax*	seed	Jiang *et al.*, 2001b
Neocaesalpin E (**108**)		*C. pulcherrima*	Root	Roach *et al.*, 2003
Neocaesalpin F (**109**)		*C. pulcherrima*	Root	Roach *et al.*, 2003
Neocaesalpin G (**110**)		*C. pulcherrima*	Root	Roach *et al.*, 2003
Neocaesalpin H (**111**)		*C. crista*	Leaves	Kinoshita *et al.*, 2005
Neocaesalpin I (**112**)		*C. crista*	Leaves	Kinoshita *et al.*, 2005
Taepeenin F (**113**)		*C. crista*	Stem root	Cheenpracha *et al.*, 2006
Caesalpinolide A (**114**)		*C. bonduc*	Marine creeper	Yadav *et al.*, 2009
Caesalpinolide B (**115**)		*C. bonduc*	Marine creeper	Yadav *et al.*, 2009
Neocaesalpin W (**116**)		*C. minax*	Seed	Wu *et al.*, 2010
Neocaesalpin L1 (**117**)		*C. minax*	Seeds	Wu et al., 2010
Caesalpinolide C (**118**)		*C. bonduc*	Whole plant	Yadav *et al.*, 2009
Caesalpinolide E (**119**)		*C. bonduc*	Whole plant	Yadav *et al.*, 2009
Caesalpinolide D (**120**)		*C. bonduc*	Whole plant	Yadav *et al.*, 2009
1α,6α,7β-Triacetoxy-14β-hydroxy-12α-methoxycass-13(15)-en-16,12-olide (**121**)		*C. minax*	Seed	Jiang *et al.*, 2002
Neocaesalpin P (**122**)	*C. pulcherrima*	Stem	Pranithanchai *et al.*, 2009	
Neocaesalpin Q (**123**)	*C. pulcherrima*	Stem	Pranithanchai *et al.*, 2009	
Neocaesalpin R (**124**)	*C. pulcherrima*	Stem	Pranithanchai *et al.*, 2009	
Caesaldekarin G (**125**)	*C. bonduc*	Root	Peter *et al.*, 1998	
Caesaldekarin L (**126**)	*C. bonduc*	Root	Lyder *et al.*, 1998	
Caesalpinin ME (**127**)	*C. crista*	Seed kernel	Kalauni *et al.*, 2004	
Caesalpinin ML (**128**)	*C. crista*	Seed kernel	Kalauni *et al.*, 2004	
Caesaldecan (**129**)	*C. decapetala*	Leaves	Kiem *et al.*, 2005	
Taepeenin G (**130**)	*C. crista*	Stem root	Cheenpracha *et al.*, 2005	
Caesalpinin (**131**)	*C. bonduc*	Root	Peter *et al.*, 1997	
Caesalpinin MM (**132**)	*C. crista*	Seed kernels	Kalauni *et al.*, 2005a	
Caesalpinin MN (**133**)	*C. crista*	Seed kernels	Kalauni *et al.*, 2005a	
Bonducellpin D (**134**)	*C. minax*	Seed	Jiang *et al.*, 2002	
	C. bonduc	Root	Peter & Tinto, 1997	
Caesalmin A (**135**)	*C. minax*	Seed	Jiang *et al.*, 2001a	
Caesalmin B (**136**)	*C. minax*	Seed	Jiang *et al.*, 2002	
	C. crista	Seed kernel	Linn *et al.*, 2005	
		Seed	Kalauni *et al.*, 2004	
Caesalmin G (**137**)	*C. minax*	Seed	Jiang *et al.*, 2002	
Macrocaesalmin (**138**)	*C. minax*	Seed	McPherson *et al.*, 1986	
Caesalpinin D (**139**)	*C. crista*	Seed kernels	Linn *et al.*, 2005; Awale *et al.*, 2006	
Caesalpinin G (**140**)	*C. crista*	Seed kernels	Awale *et al.*, 2006	
Caesalpinin H (**141**)	*C. crista*	Seed kernels	Awale *et al.*, 2006	

Table 1 cont'd.....

Caesalpinin O (142)	*C. crista*	Seed kernels	Awale *et al.*, 2006
Caesalpinin I (143)	*C. crista*	Seed kernels	Awale *et al.*, 2006
Minaxin A (144)	*C. minax*	Fruit	Wu *et al.*, 2010
Phanginin A (145)	*C. sappan*	Seed	Yodsaoue *et al.*, 2008
Phanginin B (146)	*C. sappan*	Seed	Yodsaoue *et al.*, 2008
Phanginin C (147)	*C. sappan*	Seed	Yodsaoue *et al.*, 2008
Phanginin D (148)	*C. sappan*	Seed	Yodsaoue *et al.*, 2008
Phanginin E (149)	*C. sappan*	Seed	Yodsaoue *et al.*, 2008
Phanginin F (150)	*C. sappan*	Seed	Yodsaoue *et al.*, 2008
Phanginin G (151)	*C. sappan*	Seed	Yodsaoue *et al.*, 2008
Phanginin H (152)	*C. sappan*	Seed	Yodsaoue *et al.*, 2008
Mimosol A (153)	*C. mimosoides*	Roots	Yodsaoue *et al.*, 2010
Mimosol B (154)	*C. mimosoides*	Roots	Yodsaoue *et al.*, 2010
Mimosol C (155)	*C. mimosoides*	Roots	Yodsaoue *et al.*, 2010
Mimosol D (156)	*C. mimosoides*	Roots	Yodsaoue *et al.*, 2010
Mimosol E (157)	*C. mimosoides*	Roots	Yodsaoue *et al.*, 2010
Taepeenin J (158)	*C. crista*	Roots	Cheenpracha *et al.*, 2006
Norcassane Diterpenoids			
Norcaesalnin E (159)	*C. minax*	Seed	Jiang *et al.*, 2002
Norcaesalpinin A (160)	*C. crista*	Seed kernel	Linn *et al.*, 2005; Banskota *et al.*, 2003
Norcaesalpinin B (161)	*C. crista*	Seed kernel	Linn *et al.*, 2005; Banskota *et al.*, 2003
Norcaesalpinin D (162)	*C. crista*	Seed kernel	Linn *et al.*, 2005
Norcaesalpinin E (163)	*C. crista*	Seed kernel	Linn *et al.*, 2005; Kalauni et al., 2005a
Norcaesalpinin C (164)	*C. crista*	Seed kernel	Linn *et al.*, 2005; Banskota *et al.*, 2003
Norcaesalpinin F (165)	*C. crista*	Seed kernel	Awale *et al.*, 2006
Norcaesalpinin MA (166)	*C. crista*	Seed kernel	Kalauni *et al.*, 2004
Norcaesalpinin MB (167)	*C. crista*	Seed kernel	Kalauni *et al.*, 2004
Norcaesalpinin MC (168)	*C. crista*	Seed kernel	Kalauni *et al.*, 2004
Norcaesalpinin MD (169)	*C. crista*	Seed kernel	Kalauni *et al.*, 2005a
Nortaepeenin A (170)	*C. crista*	Stem root	Cheenpracha *et al.*, 2005
Nortaepeenin B (171)	*C. crista*	Stem root	Cheenpracha *et al.*, 2005

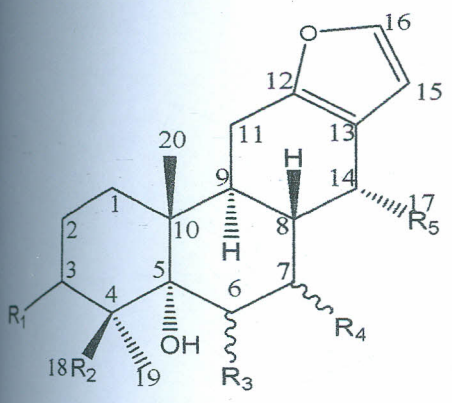

	R_1	R_2	R_3	R_4	R_5
31	H	COOH	OBz	OBz	Me
32	OAc	COOH	OBz	OBz	Me
35	H	CH_2OAc	H	H	Me
36	H	COOH	H	H	Me
37	H	CH_2OH	H	OH	Me
38	H	CO_2Me	H	H	Me
41	H	CO_2Me	H	H	OEt_β/Me_α
52	OH	COOH	OBz	OBz	Me
53	OBz	COOH	OBz	OAc	Me
54	H	COOH	OBz	OAc	Me

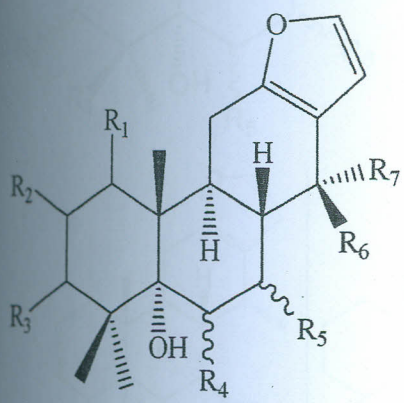

	R_1	R_2	R_3	R_4	R_5	R_6	R_7
19	H	H	H	H	H	H	H
20	H	H	H	CinnO	OH	H	Me
22	OAc	OAc	OAc	H	H	OH	Me
23	OAc	OAc	H	H	H	OH	Me
25	H	H	H	OH	H	H	Me
26	OH	H	H	OAc	H	H	Me
27	OAc	H	H	OAc	H	H	Me
28	OAc	H	H	OAc	OH	H	CO_2Me
29	=O	H	H	OAc	OH	H	CO_2Me
30	OAc	H	H	H	OH	H	CO_2Me
34	H	H	H	OAc	H	H	Me
42	OAc	OAc	H	H	H	H	Me
44	OAc	H	H	OAc	OAc	OH	Me
45	OAc	H	H	OAc	OAc	OMe	Me
46	OAc	H	H	H	OH	H	Me
48	H	H	H	OBz	H	OH	Me
49	H	H	H	OBz	OH	H	Me
55	OAc	H	OAc	H	H	H	Me
56	OAc	H	H	H	H	H	CO_2Me
62	OAc	H	H	OAc	H	H	CO_2Me
63	OAc	H	H	H	OAc	H	CO_2Me
67	OAc	H	OAc	H	H	H	CO_2Me
68	OAc	H	H	OAc	OAc	H	CO_2Me
69	OAc	H	H	OAc	OH	H	CO_2Me
70	H	H	H	OH	OH	H	Me
75	=O	H	H	OAc	H	H	CO_2Me
87	=O	H	H	OAc	OAc	H	CO_2Me
88	OAc	H	H	H	OH	H	Me
89	OAc	H	H	H	OAc	OH	Me
90	OAc	H	H	H	OH	CHO	H
96	OAc	H	H	OH	OAc	H	CO_2Me
101	H	H	H	OH	CinnO	H	Me
102	H	H	OBz	H	OH	H	Me
103	H	H	OBz	OH	OAc	H	CO_2Me

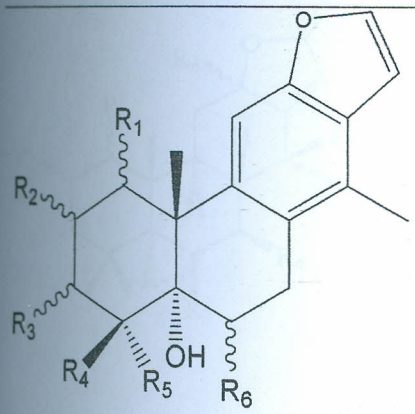

	R_1	R_2	R_3	R_4	R_5	R_6
21	H	H	H	Me	Me	H
40	H	H	H	CO_2Me	Me	H
50	H	H	H	Me	Me	OBz
57	OAc	H	OAc	Me	Me	OAc
58	OAc	OAc	H	Me	Me	H
59	OAc	OAc	OAc	Me	Me	H
64	OAc	OAc	H	Me	Me	H
74	OAc	H	H	Me	Me	H
78	H	H	H	Me	CO_2Me	CO_2Me
79	H	H	H	Me	CO_2Me	H
80	H	H	H	Me	CO_2Me	CO_2Me
81	H	H	H	Me	CO_2Me	OH
82	H	H	H	CHO	CO_2Me	H
$93_{5\text{-deoxy}}$	H	H	H	CO_2Me	Me	H
$100_{5\text{-deoxy}}$	H	H	H	Me	Me	OAc_β

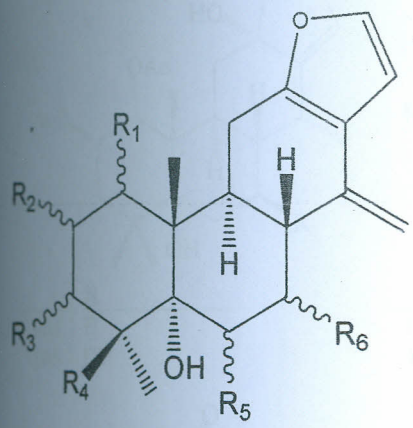

	R_1	R_2	R_3	R_4	R_5	R_6
39	H	H	H	CO_2Me	H	H
43	OAc_α	H	H	Me	OAc	OAc
47	H	H	H	Me	OBz	H
51	H	H	H	CH_2OBz	OBz	H
60	OAc_α	H	OAc_α	Me	H	H
61	OAc_α	OAc	OAc_α	Me	H	H
65	OH_α	H	H	Me	OAc_α	OAc_α
66	=O	H	H	Me	OAc_α	OAc_α
71	OAc_α	H	H	Me	H	H
72	OAc_α	H	H	Me	OAc_α	H
92	OAc_α	OAc	H	Me	H	H
$94_{5\text{-deoxy}}$	H	H	H	CO_2Me	H	H
96	OAc_α	H	H	Me	OH_α	OAc_β

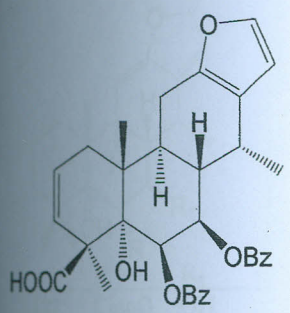

33

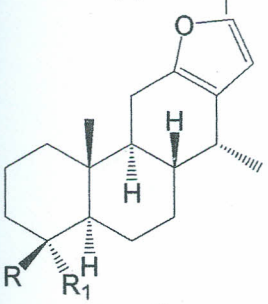

	R	R_1
83	CO_2Me	CHO
84	CO_2Me	CH_2OH
85	COOH	Me
86	CO_2Me	Me

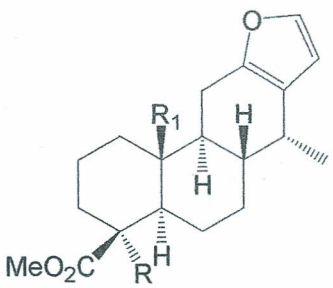

	R	R_1
95	Me	Me
97	Me	CHO
98	CHO	CHO
99	CO_2Me	CHO

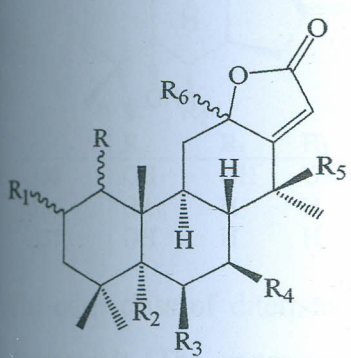

	R	R_1	R_2	R_3	R_4	R_5	R_6
114	H	H	H	OAc	H	OH	OH_α
115	H	H	H	OAc	H	OH	OH_β
116	OAc	OAc	OH	OAc	H	OH	OMe_α
117	OAc	H	OH	OAc	OAc	OH	OMe_α
118	H	H	H	H	OH	H	OH_α
119	H	H	H	OAc	H	H	OH_α
120	H	H	H	H	H	OH	OH_α
121	OAc	H	OH	OAc	OAc	OH	OMe_α

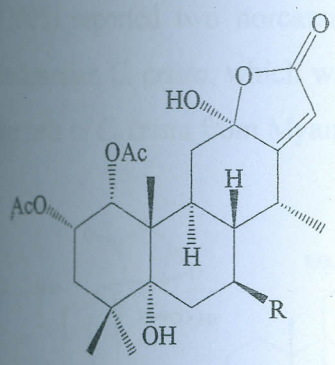

	R
104	H
105	OH

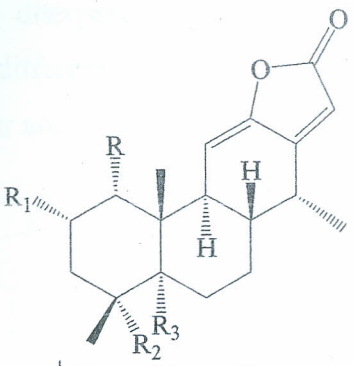

	R	R_1	R_2
106	OAc	OAc	H
107	H	H	COOH

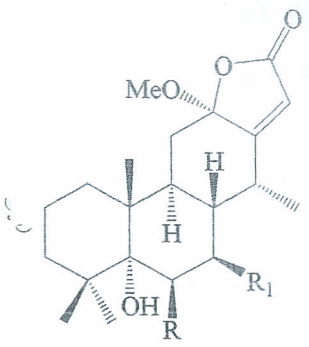

	R	R1
108	H	H
109	OBz	OH
110	CinnO	OH

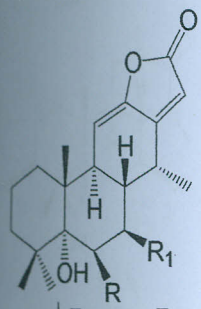

	R	R_1
122	CinnO	OH
123	OBz	H
124	OBz	OH

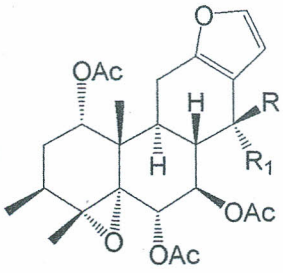

	R	R_1
132	Me	OH
133	OH	Me

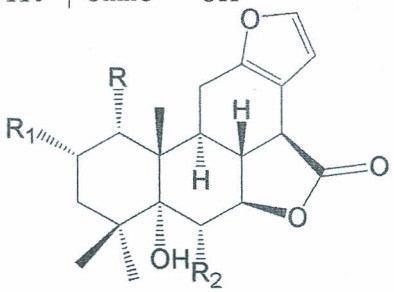

	R	R_1	R_2
135	OH	OH	OAc
136	OAc	H	H
137	OH	H	H

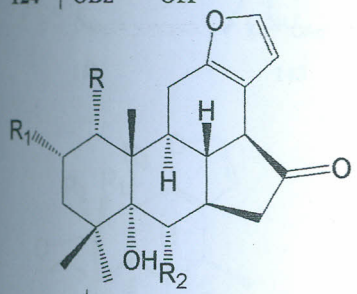

	R	R_1	R_2
135	OH	OH	OAc
136	OAc	H	H
137	OH	H	H

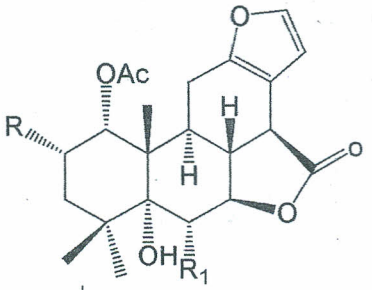

	R	R_2
139	H	OAc
140	OAc	H

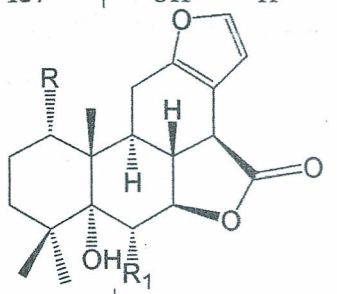

	R	R_1
141	OH	OAc
142	OAc	OH

The other class of diterpenoids elaborated by the *Caesalpinia* genus is the norcassane-type diterpenoids. The unprecedented norcaesalpinin [**160-163**] with a 17-keto norcassane and norcaesalpinin C (**164**) with 16 keto-norcassane skeletons were first examples reported from *C. crista* seed kernels (Banskota *et al.*, 2003). Norcaesalpinin F (**165**) was isolated from the same source as a 17-norcassane skeleton with a unique C-1 carbonyl group (Linn *et al.*, 2005). Investigation of *C. crista* from Myanmar resulted into isolation of three other norcassane type diterpenes, norcaesalpinins MA-MC [**166** and **167**] (Awale *et al.*, 2006). Cheenpracha *et al.*,

(2005) reported two norcassane diterpenes **170** and **171**, from the stem and root bark of Indonesian *C. crista*, which was different from the previously isolated diterpenes from the seed kernels of *C. crista* from Myanmar and Thailand.

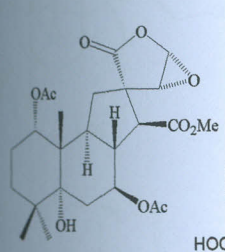

107

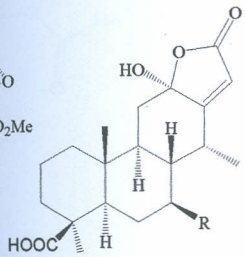

111

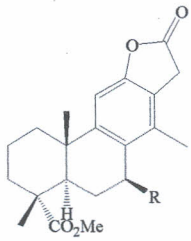

113

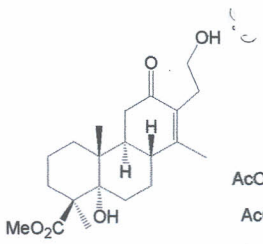

125

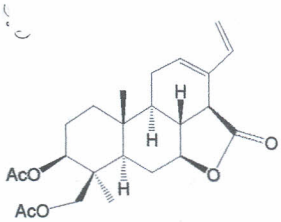

127

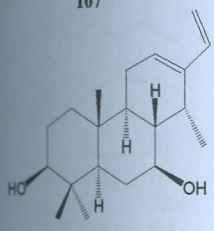

128

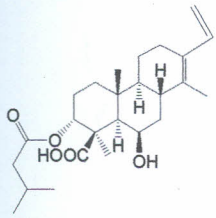

129

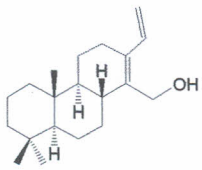

130

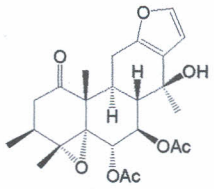

131

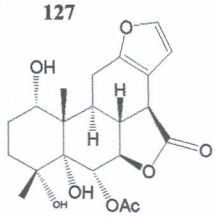

134

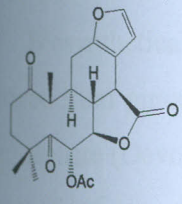

138

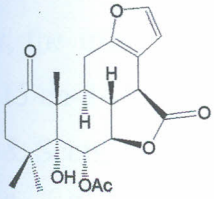

143

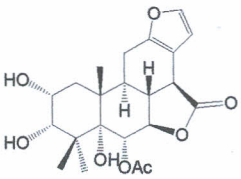

144

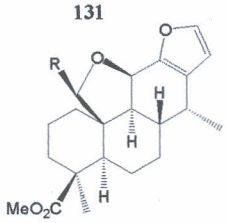

151: R = OH
152: R = H

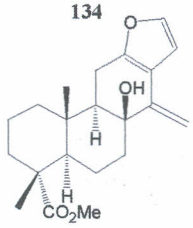

153

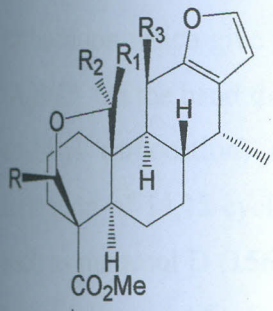

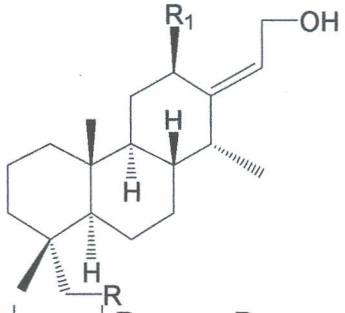

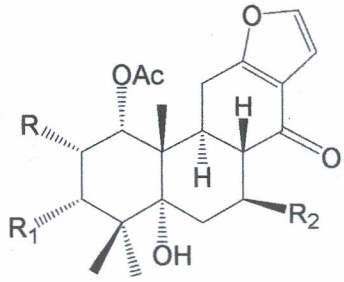

	R	R_1	R_2	R_3		R	R_2		R	R_1	R_2
145	H	OH	H	H	**154**	OH	H	**160**	OAc	H	H
146	OH	H	H	H	**155**	H	OH	**161**	H	OAc	H
147	H	H	OMe	H				**162**	OAc	OAc	H
148	OMe	H	H	H				**163**	H	H	OH
149	=O	H	H	H							
150	H	H	OH	OH							

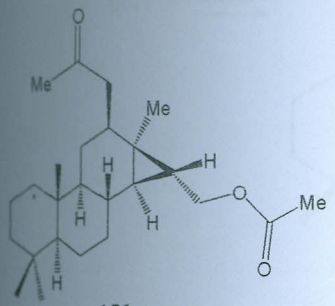

156

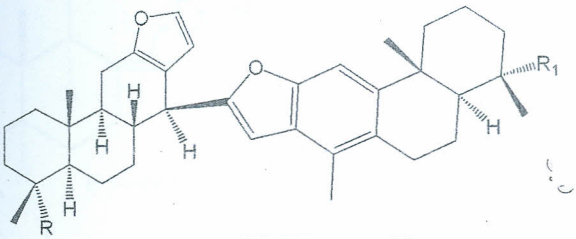

157: R = CO_2Me; R_1 = CO_2Me
158: R = H; R_1 = H

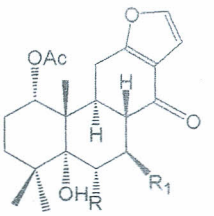

R	R_1
159: H	OH
168: OAc	OAc

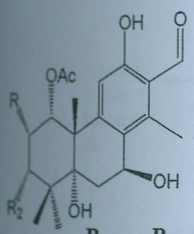

R	R_1
164: OAc	H
166: H	OAc
167: OAc	OAc

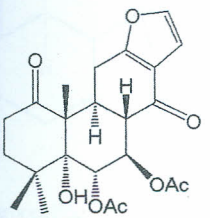

169

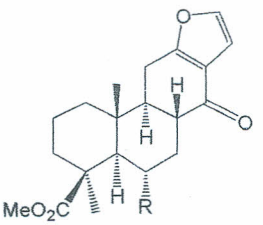

170: R = H
171: R = OH

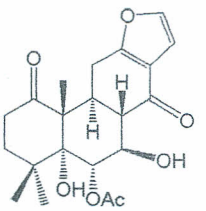

165

Biosynthetically, the tricyclic diterpenes structures common to *Caesalpinia* are plausibly derived from pimar-15-en-8-yl carbocation intermediate generated by cyclization of (+)-copayl diphosphate (Devon & Scott, 1972; Ravn *et al.*, 2002) shown in Scheme 4. A hydride shift from C_{14} to C_8 of pimar-15-en-8-yl carbocation to form a pimar-15-en-14-yl carbocation followed by methyl shift from C_{13} to C_{14} (Scheme 4-pathways I) result in formation of cass-15-en-13-yl carbocation which give rise to a cassane-type diterpenes with the *trans/anti/trans* ring junctions (A/B/C). On the hand the addition of water to C_{16} double bond of a homoallylic cation (pimar-1-en-14-yl carbocation) concomitant with ring closure (Scheme 4-pathway II) resulting in formation of 14,15-cyclopimaran-16-ol, a precursor of tricyclic derivatives with no furan ring such as mimosol D (**156**) (Yodsaoue *et al.*, 2010) and spirocaesalmin (**107**) (Jiang *et al.*, 2001b). Variation or modifications of the basic skeleton occur depending on the environmental stress (Devon & Scott, 1972). This can be explained by the fact that same species from different countries elaborated different diterpenoids. Although scientific study correlating different environmental stresses to the compounds types have not been carried out, it is highly expected to cause the marked variation among different species, and such speculation are worthy of scientific validation.

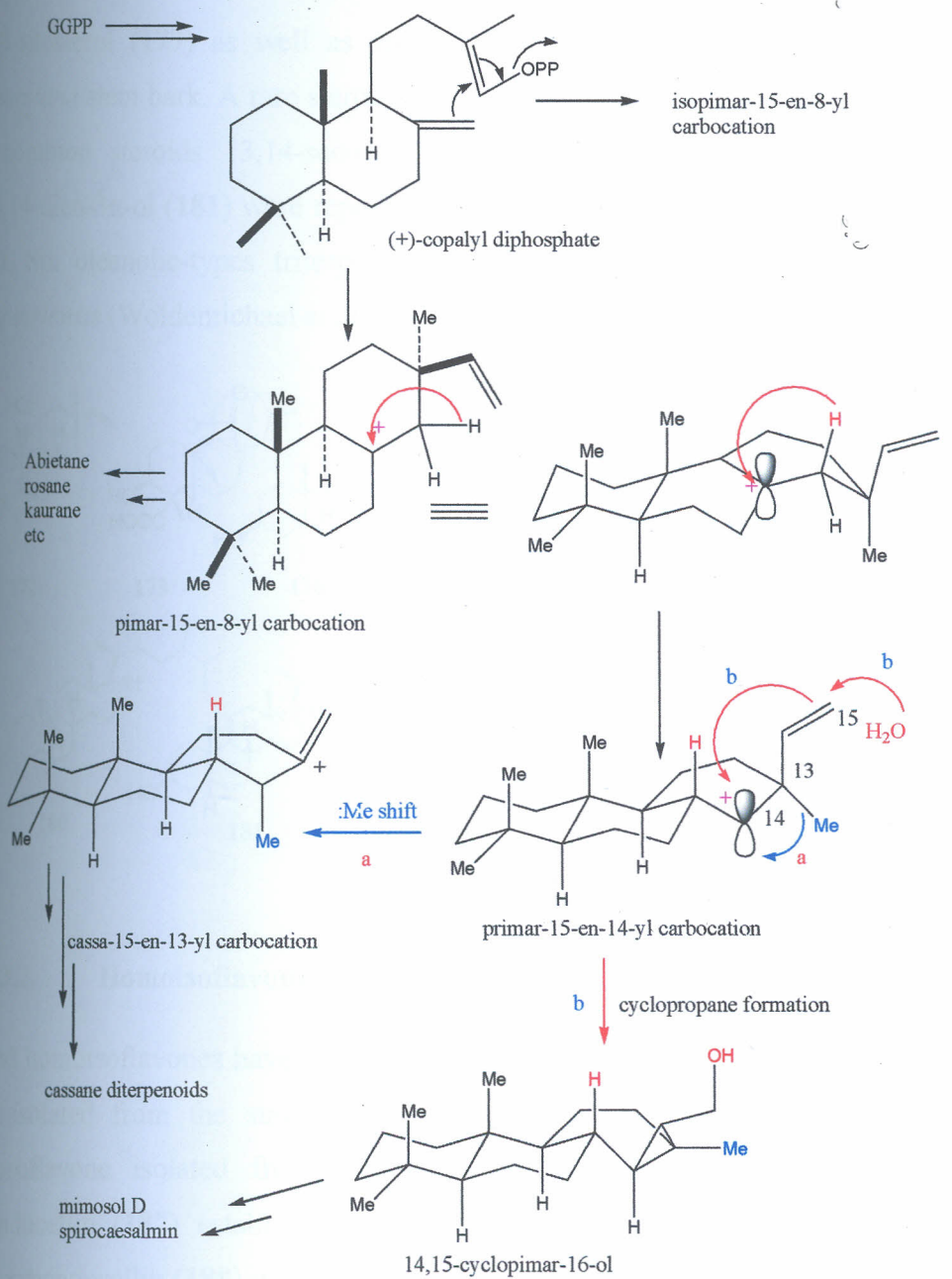

Scheme 4: Possible biosynthetic pathways to cassane diterpenoids (Yodsaoue *et al.*, 2010).

Other novel diterpenoids encountered include the sole rosane-type diterpene ent-11α-hydroxyrosa-5,15-diene (**172**) (Cheenpracha *et al.*, 2005) reported from the stems and roots of *C. crista*. Minaxin B (**173**) (Wu *et al.*, 2010) isolated from the seeds of *C. minax*, have a unique structure that differ from all cassane diterpenes and norcassane diterpenes hirtheto. Two friedolane triterpenoids **174** and **175**, isolated from stem of the *C. minax* are notable triterpenoids of the genus *Caesalpinia* (Jiang *et al.*, 2002). Dickson *et al.*, (2007) isolated stigmasterol (**176**)

and β-sitosterol (**177**) as well as stigmastenone (**178**) from petroleum ether extract of *C. benthamiana* stem bark. A rare steroid, 17-hydroxycampesta-4,6-dien-3-one (**179**), together with two common steroids 13,14-secostigmasta-5,14-dien-3α-ol (**180**) and 13,14-secostigmasta-9(11),14-dien-3α-ol (**181**) were reported from the stem bark of *C. bunducella* (Udenigwe *et al.*, 2007). Six oleanolic-types triterpenes **182-186** have been reported from stem bark of *C. paraguariensis* (Woldemichael *et al.*, 2003).

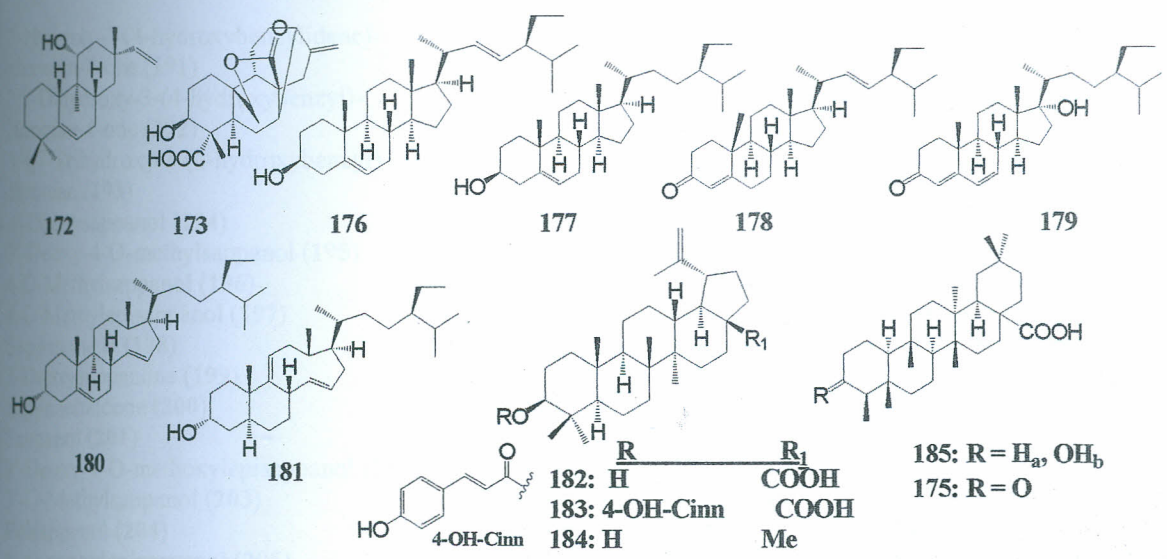

2.5.2.3.2. Homoisoflavones of Caesalpinia species

Several homoisoflavones have been isolated from the genus *Caesalpinia* (Table 2). Bonducellin (**186**) isolated from the stem bark of *C. pulcherrima* is the most common, since many homoisoflavone isolated from the genus are its derivatives (McPherson *et al.*, 1983). Isobonducellin (**187**) established to exhibit a (Z)-C_3=C_9 bond different from **186** and 8-methoxybonducellin (**188**) were isolated from the aerial parts of the same plant (Srinivas *et al.*, 2003). Tissue culture of *C. pulcherrima* cells with cork tissues afforded 2′-methoxybonducellin (**189**) (Zhao *et al.*, 2004). A couple of investigations have reported a series of homoisoflavonoids from *C. sappan*, including **[191-204]** (Peter *et al.*, 1998; Namikoshi & Saitoh., 1987; Namikoshi *et al.*, 1987; Nguyen *et al.*, 2005; Jeong *et al.*, 2009; Fu *et al.*, 2008). A part from the homoisoflavonoids, other flavonoids such as chalcones (McPherson *et al.*, 1983; Srinivas *et al.*, 2003), flavonols (Namikoshi *et al.*, 1987), and isoflavavones (Zhao *et al.*, 2004) have been reported from different *Caesalpinia* species as listed in table 2.

Table 2: Homoisoflavones, flavonoids, chalcones and isoflavonoids reported from *Caesalpinia* species

Name of compound	Plant species	Part	Reference
Isoflavonoids			
Bonducellin (**186**)	*C. pulcherrima*	Stem	Pranithanchai *et al.*, 2009
	C. mimosoides	Roots	Yodsaoue *et al.*, 2010
Isobonducellin (**187**)	*C. pulcherrima*	Aerial part	Srinivas *et al*, 2003
8-hydroxybonducellin (**188**)	*C. pulcherrima*	Cell culture	Zhao *et al.*, 2004
2′-methoxybonducellin (**189**)	*C. mimosoides*	Roots	Yodsaoue *et al.*, 2010
8-methoxyisobonducellin (**190**)	*C. milletti*	Aerial part	Yodsaoue *et al.*, 2010
	C. mimosoides	Root	Chen, 2007
7-Hydroxy-3-(4-hydroxybenzylidene)-chroman-4-one (**191**)	*C. sappan*	Heartwood	Namikoshi *et al.*, 1987
3,7-Dihydroxy-3-(4-hydroxybenzyl)-chroman-4-one (**192**)	*C. sappan*	Heartwood	Namikoshi *et al.*, 1987
3,4,7-Trihydroxy-3-(4-hydroxybenzyl)-chroman (**193**)	*C. sappan*	Heartwood	Namikoshi *et al.*, 1987
3′-Deoxysappanol (**194**)	*C. sappan*	Heartwood	Namikoshi *et al.*, 1987
3′-Deoxy-4-O-methylsappanol (**195**)	*C. sappan*	Heartwood	Namikoshi *et al.*, 1987
4-O-Methylsappanol (**196**)	*C. sappan*	Heartwood	Jeong *et al.*, 2009
4-O-Methylepisappanol (**197**)	*C. sappan*	Heartwood	Jeong *et al.*, 2009
Sappanone B (**198**)	*C. sappan*	Heartwood	Namikoshi & Saitoh, 1987
3-Deoxysappanone (**199**)	*C. sappan*	Heartwood	Namikoshi & Saitoh, 1987
Sappanchalcone (**200**)	*C. sappan*	Heartwood	Washiyama *et al.*, 2009
Sappanol (**201**)	*C. sappan*	Heartwood	Namikoshi *et al.*, 1987
3′-Deoxy-4-O-methoxylepisappanol (**202**)	*C. sappan*	Heartwood	Fu *et al.*, 2008
3′-*O*-Methylsappanol (**203**)	*C. sappan*	Heartwood	Namikoshi & Saitoh, 1987
Episappanol (**204**)	*C. sappan*	Heartwood	Namikoshi & Saitoh, 1987
3′-*O*-methylepisappanol (**205**)	*C. sappan*	Heartwood	Namikoshi & Saitoh, 1987
3′-Deoxysappanone B (**206**)	*C. sappan*	Heartwood	Namikoshi *et al.*,1987
Eucomin (**207**)	*C. milletti*	Aerial part	Chen, 2007
Intricatinol (**208**)	*C. milletti*	Aerial part	Chen, 2007
Caesalpinianone (**209**)	*C. bonduc*	Bark	Ata *et al.*, 2009
6-O-Methylcaesalpinianone (**210**)	*C. bonduc*	Bark	Ata *et al.*, 2009
Chalcones			
4′-methylisoliquiritigenin (**211**)	*C. pulcherrima*	Stem	McPherson *et al.*, 1986
4,4′-Dihydroxy-2′-methoxychalcone (**212**)	*C. sappan*	Heartwood	Namikoshi *et al.*, 1987
2′-Hydroxy-2,3,4′,6′-tetramethoxychalcone (**213**)	*C. pulcherrima*	Aerial part	Srinivas *et al.*, 2003
Isoliquiritigenin (**214**)	*C. milletti*	Aerial part	Chen, 2007
3-Deoxysappanchalcone (**215**)	*C. sappan*	Heartwood	Fu *et al.*, 2008
Flavonols			
Quercetin (**216**)	*C. decapetala*	Leaves	Kiem *et al.*, 2005
Ombuin (**217**)	*C. sappan*	Heartwood	Namikoshi *et al.*, 1987
3,8-Dihydroxy-4,10-dimethoxy-7-oxo[2]benzo[4,3-b]benzopyran (**218**)	*C. sappan*	Heartwood	Shu *et al.*, 2007
Flavanones			
5,7-Dimethoxyflavanone (**219**)	*C. pulcherrima*	Aerial part	Srinivas *et al.*, 2003
5,7-Dimethoxy-3′,4′-(methylenedioxy)-flavanone (**220**)	*C. pulcherrima*	Aerial part	Srinivas *et al.*, 2003
Liquiritigenin (**221**)	*C. milletti*	Aerial part	Chen, 2007
Isoflavanones			
Dihydrobonducellin (**222**)	*C. pulcherrima*	Cells culture	Zhao *et al.*, 2004
2′-Methoxydihydrobonducellin (**223**)	*C. pulherrima*	Cell culture	Zhao *et al.*, 2004

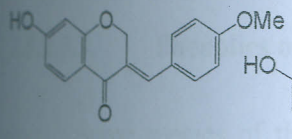

186

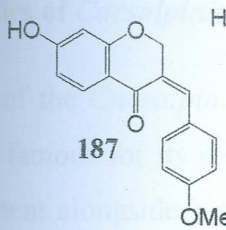

187

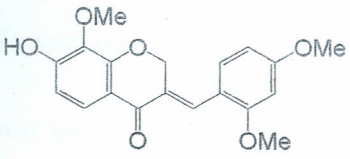

188

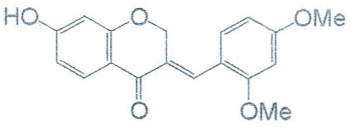

189

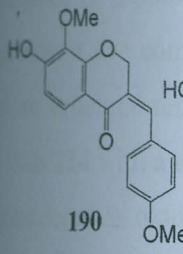

190

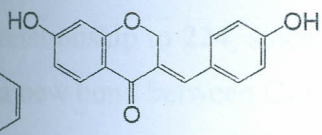

191

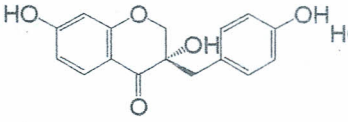

192

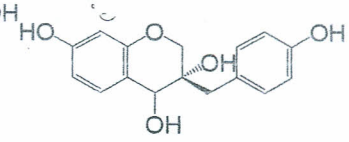

193

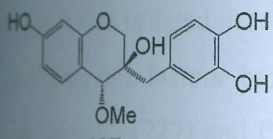

197

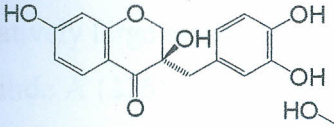

198

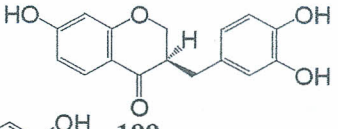

199

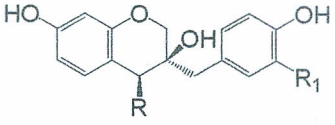

R	R1
194: OH	H
195: MeO	H
196: MeO	OH
201: OH	OH

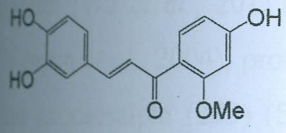

200

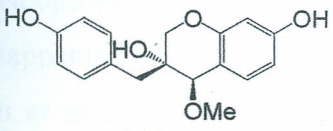

202

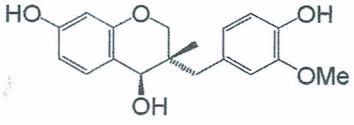

203

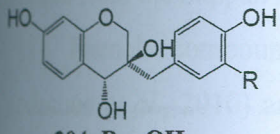

204: R = OH
205: R = MeO

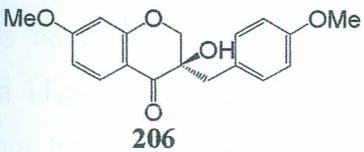

206

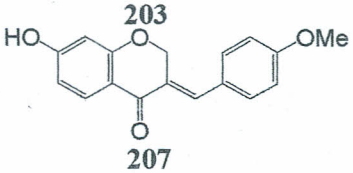

207

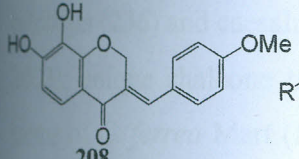

208

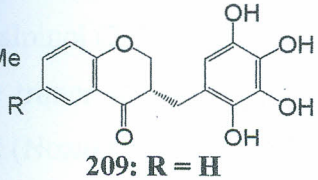

209: R = H
210: R =Me

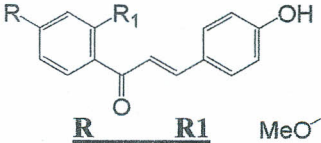

R	R1
211: OMe	OH
212: OH	OMe

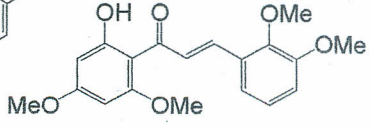

213

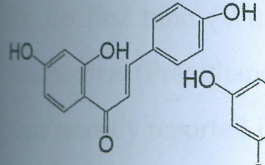

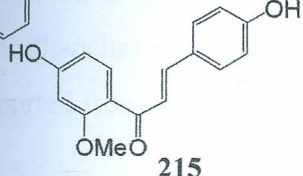

214

215

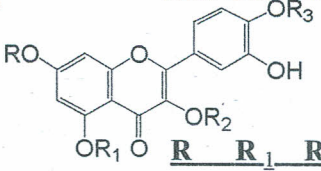

R	R1	R2	R3
216: H	H	H	H
217: Me	H	H	Me

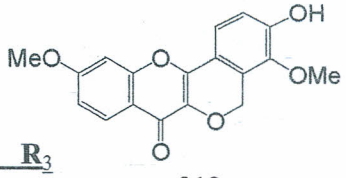

218

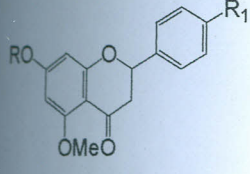

R	R1
219: Me	H
221: H	OH

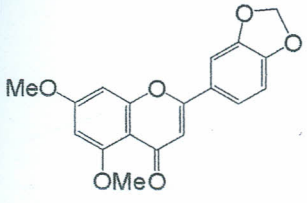

220

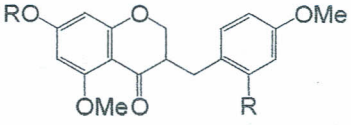

222: R = H
223: R = OMe

2.5.2.3.3. Phenolics of *Caesalpinia* species

Some species of the *Caesalpinia* genus are known for their characteristic phenols, for instance *C. sappan* is famous for its red dyestuff produced from the heartwood, brazilin (**224**), used as a dye component alongside a pair of enantiomers **201** and **204**. The enantiomers have close structural relationship to **224**, since treatment of any with a catalytic amount of acid, both yields **224** with a new bond between C_4-C_6 (Namikoshi *et al.*, 1987). Brazilein (**225**) is however considered as oxidation product of **224**, since when the organic extract was exposed to air and light it was isolated in relatively large amounts (Ye *et al.*, 2006). Yang *et al.*, (2002) reported the isolation of a lactone bazilide A (**226**) with a new skeleton derived from **224**. Two compounds, caesalpins J (**227**) and P (**228**), also offer a rare framework for the aromatic phenols of sappan lignum (Wu *et al.*, 2011). Neoprotosappanin (**229**) dimmers of **224**, neosappanone A (**230**) (Nguyen *et al.*, 2004), protosappanin D, (**231**) (Washiyama *et al.*, 2009), neocaesalpin A (**232**), and neocaesalpin (**233**) (Shu *et al.*, 2007) are some of the other compounds that have been isolated from the Sappan Lignum.

Phenolic compounds have been isolated from other species, bergenin (**234**) (Chen, 2007; Yodsaoue *et al.*, 2010) and 11-*O*-galloybergenin (**235**) (Chen, 2007) were isolated from aerial parts of *C. milletti* and root bark of *C. digyna* and *C. mimosoides;* benzoxecin derivatives, bilobetin (**236**) and caesalpinol (**237**) were isolated from *C. paraguariensis* (Woldemichael *et al.*, 2003); unique chalcone trimer linked by cyclobutane ring pauferrol (**238**) was isolated from stems of *C. ferrea* Mart (Nozaki *et al.*, 2007); compound **239** was isolated from *C. decapatala* for the first time (Wu *et al.*, 2011) and compound **240** was obtained from the stem of *C. pulcherrima* (Pranithanchai *et al.*, 2009). Two dibenzo[b,d]furans, mimosol F (**241**) and G (**242**) were recently reported from root bark of *C. mimosoides* (Yodsaoue *et al.*, 2010).

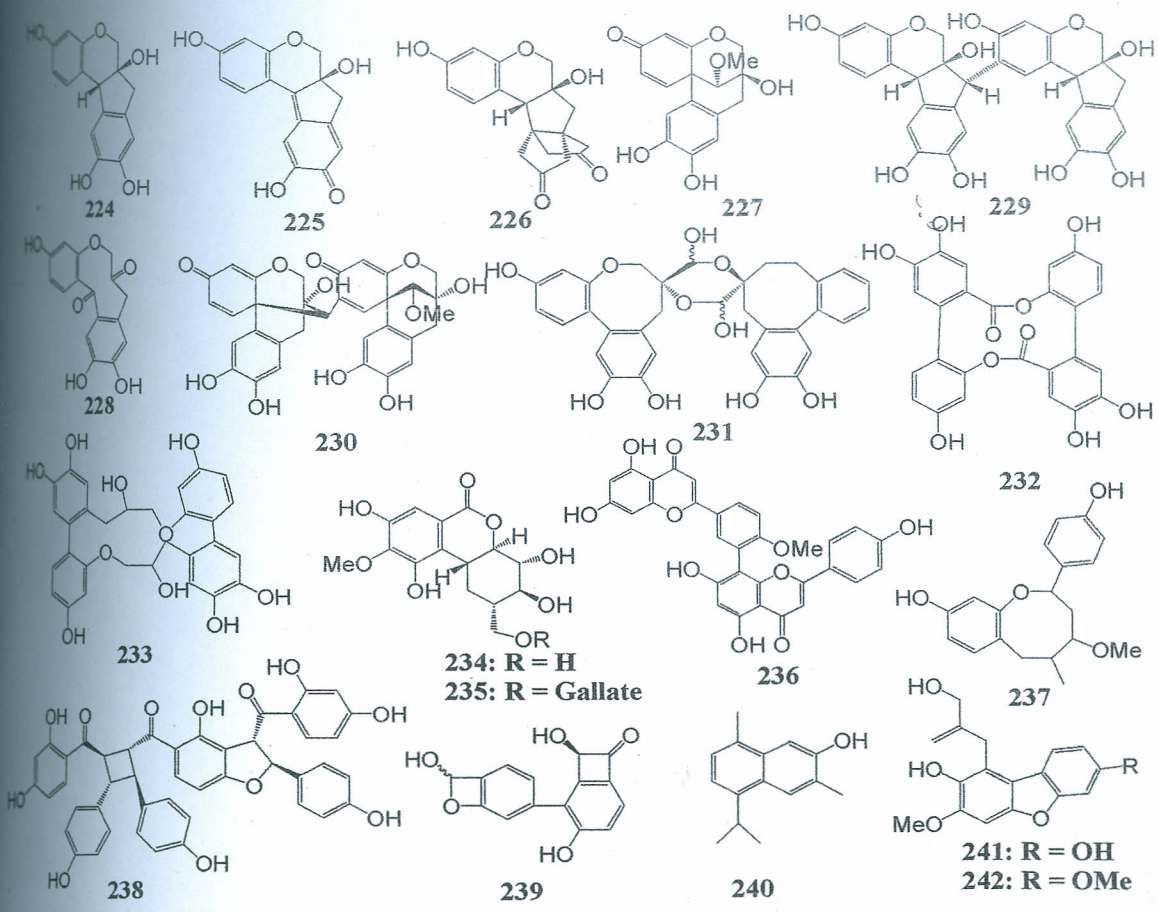

Minor compounds reported from the genus *Caesalpinia* include: organic acids and esters; antifungal benzyl-2,6-dimethoxybenzoate (**243**) from the leaves of *C. pulcherrima* (Ragasa *et al.*, 2003), compounds [**244-246**] from dried pods of *C. spinosa* (Kondo *et al.*, 2007), and compounds [**247-252**] from *C. millettii* aerial parts (Chen, 2007; Nakamura *et al.*, 2002). Phenylpropanoids: two coumarins [**253-254**] and two lignanoids [**255** and **256**] isolated from *C. ferrea* fruits and *C. sappan* heartwood (Ueda *et al.*, 2001; Shu *et al.*, 2007). Kiem *et al.*, (2005) reported a long chain phenylpropanoid (**258**) from the seeds of *C. decapetala*. Glycosides reported from some few species include daucosterol (**257**) and hyperoside (**258**) isolated from *C. milletti* aerial part (Chen, 2007); three β-sitosterol glucopyranosides with fatty acid ester [**259** and **260**] isolated from the leaf extract of *C. paraguariensis* (Woldemichael *et al.*, 2003); two glycosylphenylpropenoid acids, (*Z*)-4-(β-glucopyranosyloxy)-7-hydrocinnamic acid (**261**) and (*Z*)-4-(β-glucopyranosyloxy)-8-hydroxycinnamic acid (**262**) were isolated from leaves of *C. pyramidalis* with a common styrene skeleton (Mendes *et al.*, 2000). Only few quinines, two anthraquinones, a benzoquinone (**263**) and a naphthoquinone (**264**) from the leaves of *C.*

pulcherrima and *C. sappan* heartwood have been reported (McPherson *et al.*, 1986; Lim *et al.*, 2007) and one alkaloid, caffeine (**265**) reported from the fruits of *C. minax* (Safitri *et al.*, 2003). A peltogynoids, pulcherrimin (**266**), was isolated from stem bark of *C. pulcherrima* (McPherson *et al.*, 1986). Presence of phenolics compounds in *Caesalpinia* plants are indicators of potential antipathophysiological agents such as antioxidative stress.

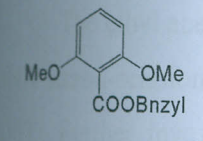

243

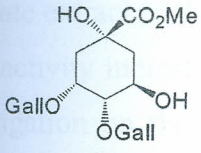

244

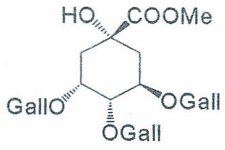

245

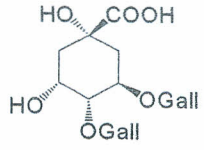

246

247

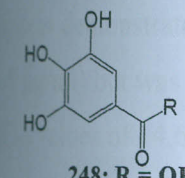

248: R = OH
249: R = MeO

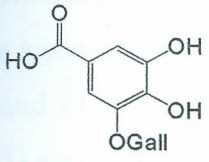

250

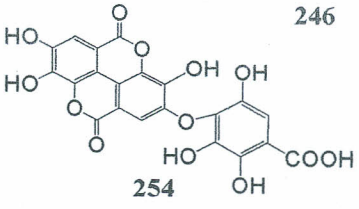

254

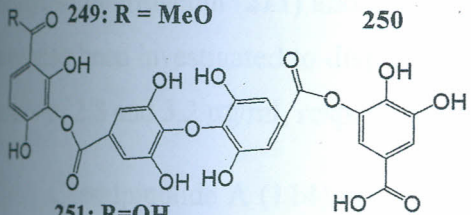

251: R=OH
252: R=OMe

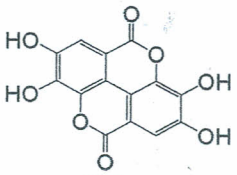

253

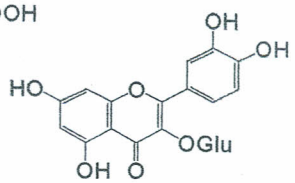

258

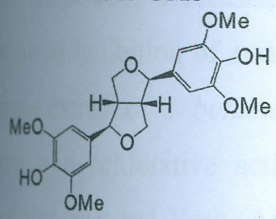

255

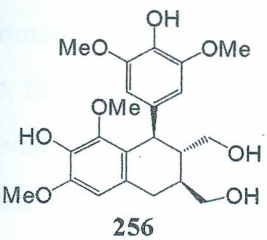

256

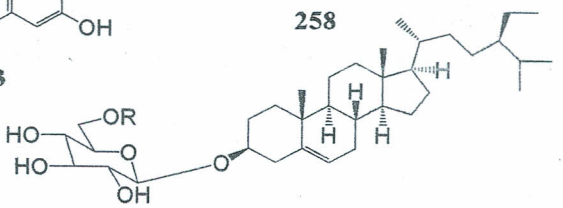

257: R = H
259: R = Me(CH$_2$)$_{14}$C(O)
260: R = Me(CH$_2$)$_{16}$C(O)

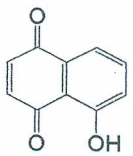

264

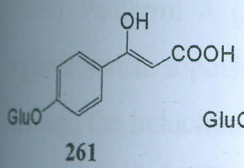

261

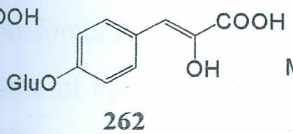

262

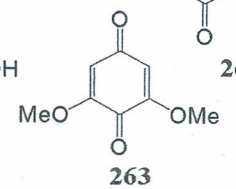

263

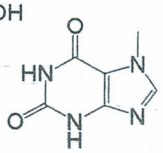

265

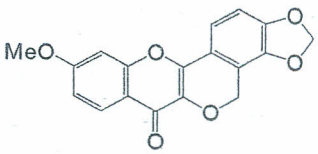

266

2.5.2.4. Biological activities of the extractives from *Caesalpinia* plants

The plants of the genus *Caesalpinia* have proven to be rich source of furanoditerpenoids and other compounds such as norcassane diterpenoids, aromatic phenols, flavonoids and triterpenes. Some of these compounds have been reported in recent years to have interesting biological activities.

The ethyl acetate extract of the heartwood of *C. sappan* has been reported to have potent DNA strand-scission activity indicating the presence of potential anticancer agents (Mar *et al.*, 2003). Further investigation on the cytotoxicity of the phytochemicals from the seeds of *C. sappan* demonstrated moderate inhibitory activity of phanginin I (**97**) against KB cell line (IC_{50} 4.4 µg/ml) but was inactive against MCF-7 (breast adenocarcinoma), HeLa, and HT-29 cell lines (IC_{50} values of 14.6, 19.0, and 14. 0 µg/ml, respectively) (Yodsaoue *et al.*, 2008). Compound 4'-methylisoliquiritigenin (**211**) and 2,6-dimethoxypulcherrimin (**267**) from stem of *C. pulcherrima* have also been investigated to display *in vitro* cytotoxicity effects against KB cell line with ED_{50} values of 2.8 and 3.2 µg/ml, respectively (Roengsumran *et al.*, 2000).

Caesalpinolide A (**114**) and caesalpinolide B (**115**) isolated from *C. bonduc* were found to inhibit MCF-7 breast cancer cell lines with IC_{50} values of 12.8 and 6.1 µM, respectively and showed inhibition of endometrial and cervical cancer cell lines (Yadav *et al.*, 2009). From the same extract of *C. bonduc*, three other compounds **118-120** were reported to exhibit moderate to low antiproliferative activity against MCF-7, DU145 (prostate carcinoma), C33A (cervical carcinoma), and Vero (African green monkey kidney fibroblast) cancer cell lines (Yadav *et al.*, 2009). Pauferrol A (**248**) isolated from stems of *C. ferrea* showed potent inhibitory activity against human topoisomerase II (IC_{50} value of 2.1 µM) and cell proliferation inhibitory activity through the induction of apoptosis in human leukemia HL_{60} cells, with an IC_{50} value of 5.2 µM (Nozaki *et al.*, 2007).

Antimicrobial activity have been demonstrated from several *Caesalpinia* plants' extracts and pure compounds, notably oleanolic acid (**185**) from *C. paraguariensis* was found active against *Bacillus subtilis* and both methicilin-sentisitive and resistant *Staphylococcus aureus* with MIC values of (17.5 µM), and (140 µM), respectively (Woldemichael *et al.*, 2003). Quinic acid gallate esters **244-247** isolated from pod of *C. spinosa* were reported intensify the susceptibility of methicilin-resistant *Staphylococcus* to oxacillin at a dose of 25 µg/ml in 22 strains. The most

active compound was 3,4,5-tri-*O*-galloylquinic acid methyl ester (**245**) compared with the MIC of oxacillin at 4 µg/ml (Kondo *et al.*, 2007). The naphthoquinone (**264**) isolated from *C. sappan* heartwood exhibited a strong inhibition at 5 and 2 µg/disk and moderate inhibition at 1, 0.5 and 0.25 µg/disk against *Clostridium perfringens*, and a weak growth inhibition against *Lactobacillus casei* at 5 and 2 µg/disk (Mendes *et al.*, 2000). Structure-activity relationship study for naphthoquinone derivatives indicated that **264** had selective growth inhibitory activity against *Clostridium perfringens* and was considered a potent drug against diseases caused by *Clostridium perfringens* (Mendes *et al.*, 2000).

The CH_2Cl_2 extract of the seed kernels of *C. crista* from Indonesia was reported to exhibit *in vivo* antimalarial activities against *Plasmodium berghei* in mice (Linn *et al.*, 2005). An activity attributed to the cassane and norcassane-type diterpenoids isolated from the same seed kernels (Linn *et al.*, 2005). The compounds **22**, **59-64**, **75**, **136**, **139**, **140** and **160-163** exhibited significant dose-dependent inhibitory effects on *Plasmodium falciparium* FCR-3/A2 growth *in vitro*. The IC_{50} values ranged from 90 nM to 6.5 µM with norcaesalpinin E **[163]** showing the most potent activity (IC_{50} 90 nM) (Linn *et al.*, 2005). Kalauni *et al.*, (2005) investigated 44 cassane and norcassane-type diterpenes isolated form *C. crista* of Myanmar and Indonesia against *Plasmodium falciparum* FCR-3/A2 clone *in vitro* and noted that **163** was the most potent with an IC_{50} value of 0.90 µM above the clinically used drug chloroquine (IC_{50} 0.29 µM). Such results are important gestures towards investigating the antimalarial principles from *C. volkensii* claimed against management of malaria (Kuria *et al.*, 2001; Kokwaro, 2009) and some crude extracts have demonstrated antimalarial (Muregi *et al.*, 2007).

In section 2.5.2.2 several *Caesalpinia* plants extractives display immunomodulatory (Choi *et al.*, 1997) and anti-inflammatory activities (Yodsaoue *et al.*, 2010; Kiem *et al.*, 2005) from folklore information backed with relevant biological assays. Pure compounds have also been investigated by some workers against immunosuppressive and anti-inflammatory activity. The CH_2Cl_2 and acetone extracts of the root bark *Caesalpinia mimosoides* exhibited potent inhibitory activity against LPS-induced NO production in RAW264.7 cell lines and two metabolites, mimosol D **(156)** and (E)-7-hydroxy-3-(4-methoxybenzyl) chroman-4-one **(191)** were established to possess the most potent activity against TNF-α release and NO production (Yodsaoue *et al.*, 2010). A Similar study on chalcones **186**, **187**, **213**, **219** and **220** from aerial part of the *C. pulcherrima* was performed against lipopolysaccharide (LPS) and (IFN)-γ

activated murine peritoneal macrophages previously (Yodsaoue *et al.*, 2008). All the compounds showed significant and dose-dependent inhibition against inflammatory mediators, nitric oxide (NO) and cytokines {tumor necrosis factor (TNF)-α and interleukin (IL)-12} (Yodsaoue *et al.*, 2008). The study supported the use of *C. pulcherrima* for the treatment of inflammatory diseases in traditional medicine. Compounds **200**, **224**, and **231**, isolated from the *C. sappan* heartwood were evaluated for their inhibitory effects on several inflammatory mediators. Brazilin (**224**) inhibited NO production and demonstrated an almost no inhibition in PGE_2, while sappanchalcone (**200**) and protosappanin D (**231**) inhibited both NO and PGE_2 production as well as suppressing TNF-α, IL-6, COX-2 and iNOS mRNA expression (Washiyama *et al.*, 2009). Brazilein (**225**) has also been demonstrated to inhibit proliferation of T lymphocyte stimulated by concanavalin A (Con A) and proliferation of B lymphocyte stimulated by lipopolysaccharides (LPS). The compound **235** also suppressed mice humoral immune response by plaque forming cell (PFC) test (Ye *et al.*, 2006). Caesaldecan (**129**) isolated from *C. decapatala*, exhibited anti-inflammatory activities (Kiem *et al.*, 2005). It is worth noting the significant biological activities displayed by the compounds isolated various *Caesalpinia* plants, especially analgesic, anti-inflammatory and towards pain receptors and enzymes. These activities are important indicators that there are undiscovered potential from the *Caesalpinia* plants as yet not been investigated such as *C. volkensii*.

Some compounds isolated from seed of *C. minax* have been investigated for antiviral activity. Furanoditerpenoid lactones **[44-45]** and **137** showed significant antiproliferation activities against the Para3 virus with IC_{50} in the range 7.8 – 14.8 μg/ml (Kalauni *et al.*, 2004). However, caesalmin G (**137**) was found to be highly toxic with a toxicity index (TI) of 3.0 (Kalauni *et al.*, 2004). Stigmasterol (**176**) also showed moderate activity against Para3 virus (Kalauni *et al.*, 2004). In the same bioassay, macrocaesalmin (**138**) was active against the RSV with IC_{50} of 24.2 μg/ml, TC_{50} of 138.3 μg/ml and a selectivity index (SI) of 5.7 in cell culture, relative to SI > 4 for natural products which is considered significant (Jiang *et al.*, 2002). However, it was inactive against the para-3 and the Flu-A virus (Jiang *et al.*, 2002). In spite of such intensive biological activities, *C. volkensii* has only been reported for *in vitro* antiplasmodial activity of the crude leaf extracts (Muregi *et al.*, 2007).

2.5.3. The genus *Senna*

2.5.3.1. Botanical information

Senna plants are usually a several-stemmed shrub of 0.5-5 m tall with terete or striate branches. The leaves are simple paripinnate, narrowly oblong to elliptical in outline about 10-15 cm long. They have erect inflorescence axillary flowers which are around 20-30 cm long, having spike-like receme, 10-50 cm long. The peduncle are terete about 5-8 cm long with pubescent bracts which are broadly ovate 8-27 mm by 5-15 mm which are black green in colour and enclosing the flowers buds. The fruits pods containing about 9-16 seeds, linear –oblong, 7-12 cm by 1.5-2.5 cm, glabrescent, short beaked, dehiscent or indehiscent when dry, depressed between the seeds (Sunarno, 1997).

2.5.3.2. Ethnopharmacological application of *Senna* species

Senna extracts have a wide range of application, which have been commercialized in some parts of the world as medicine and for cosmetic purposes and the extracts are popularly referred to as "senna" which basically mean the active ingredients from the plant (ILDIS, 2005). Sennas have for millennia played a major role in herbalism and folk medicine. Alexandria senna (*Senna alexandria*) was and still is a significant item of trans-national trade by the Ababdeh people of Egypt (ILDIS, 2005).

The leaves and flowers of *Senna siamese* in either fresh or pickled in brine (cooking salt) are used in cooking particularly in *gaeng khi-lek* curry in Thailand (ILDIS, 2005). This particular application (as food additives) can be attributed to its purgative properties and possible antihelmithic activity thus suitable for those with indigestion problems and those who consume uninspected foods (ILDIS, 2005). *Senna alata* is predominantly used for digestive and skin ailments and in the last case; an infectious etiology is athlete's foot cited by over 20% of the informants (Hennebelle *et al.*, 2009). *Cassia tora* L, a small shrub growing as common weed in Asian countries, is reported to constitute an Ayurvedic preparation in antifungal formulations (Patil *et al.*, 2004) and is claimed to be effective against jaundice (Patil *et al.*, 2004). In Chinese medicine, it is highly valued for the treatment of hyperlipidaemia and prevention of atherosclerosis plaque (Kee, 1997). *Cassia obtusifolia* is traditionally used to improve visual

acuity and to remove "heat" from the liver (Li *et al.*, 2004). *Cassia occidentalis* is used in Chinese medicine as a mild purgative and a stomachic (Kitanaka *et al.*, 1985).

S. didymobotrya is widely used as a medicinal plant, especially in East Africa, where a decoction or infusion from the leaves, stem and root bark is drunk as a laxative and purgative (Kokwaro, 2009). The plant extractives are also used in the management of hypertension, atherosclerosis, microbial infections, hemorrhoids, sickle cell anemia, inflammation of the fallopian tubes, fibroids, backache and to induce uterine contractions and abortion (Kamatenesi-Mugisha, 2004; Geissler *et al.*, 2002). Despite well spelt ethno medicinal applications, very little bioassay guided studies have been conducted on the extractives from this plant.

2.5.3.3. Phytochemistry of the genus *Senna*

Majority of the *Senna* species have been used as a laxative or as cathartics medication based on their known content of the sennocides. Sennocides A and/or (**267**/**268**) are bianthraquinone glucosides mainly of chrysophanol (**269**) and emodin (**270**) from *Senna* species appears in a considerable number of published phytochemical studies. A selection of non-volatile metabolites mainly anthraquinones and flavonoids are summarized in Table 3 with the plant part studied. *Senna didymobotrya* is not an exception among the citations, since an array of compounds has been isolated from the naturally growing plant pods (Alemayehu *et al*, 1996) and its tissues culture (Delle-Monache *et al.*, 1991). Although the presence of sennosides and others anthraquinone glycosides is likely, formal characterization of specific compounds in this species is lacking. Besides the naturally growing plant, only the metabolites from the pods have been reported and no investigation has been carried out on the roots and the stem.

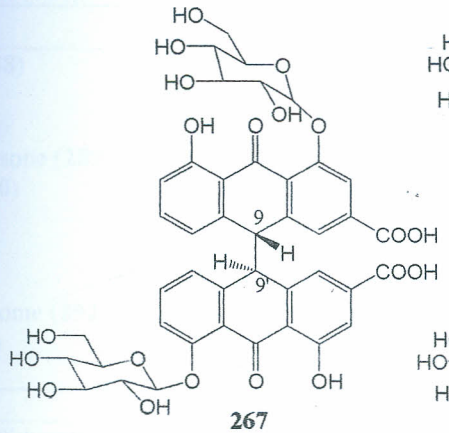

267

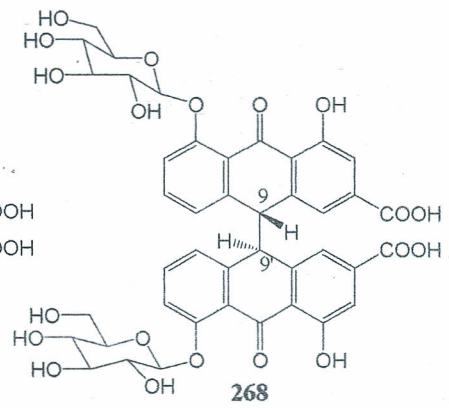

268

Table 3: Compounds reported from some *Senna* species

Compound	Plant	Part	Reference
Anthraquinones			
Chyrsophanol (**269**)	*S. alata*	Roots	Hennebelle *et al.*, 2009
	S. didymobotrya	Pods	Alemayehu *et al.*, 1996
	S. longiracemosa	Roots, leaves	Alemayehu *et al.*, 1993
	S. occidentalis	Tissue culture	Kitanaka *et al.*, 1985
	S. racemosa	Leaves	Mena-Rajon *et al.*, 2002
	S. rugusa	Leaves	Barbosa *et al.*, 2004
Isochrysophanol (**271**)	*S. alata*	Leaves	Hennebelle *et al.*, 2009
7-acetylchrysophanol (**272**)	*S. didymobotrya*	Tissue culture	Delle-Monache *et al.*, 1991
Emodin (**270**)	*S.alata*	Roots, stem	Hennebelle *et al.*, 2009
	S. didymobotrya	Pods	Alemayehu *et al.*, 1996
	S. occidentalis	Tissue culture	Kitanaka *et al.*, 1985
	S. tora	Seeds	Hatano *et al.*, 1999
Physcion (**273**)	*S. alata*	Roots	Hennebelle *et al.*, 2009
	S. didymobotrya	Pods	Alemayehu *et al.*, 1996
	S. longiracemosa	Leaves, roots	Alemayehu *et al.*, 1993
	S. occidentalis	Tissues	Kitanaka *et al.*, 1985
	S. racemosa	culture	Mena-Rajon *et al.*, 2002
	S. rugusa	Leaves	Barbosa *et al.*, 2004
Aloe-emodin (**274**)	*S. alata*	Leaves	Hennebelle *et al.*, 2009
	S. tora	Seeds	Hatano *et al.*, 1999
Emodin-6,8-dimethyl ether (**275**)	*S. didymobotrya*	Tissue culture	Delle-Monache *et al.*, 1991
Chrysophanol-8-methyl ether (**276**)	*S. didympbotrya*	Tissue culture	Delle-Monache *et al.*, 1991
Emodin-1,6-dimethyl ether (**277**)	*S. didymobotrya*	Tissue culture	Delle-Monache *et al.*, 1991
Nataloe-emodin (**278**)	*S. longirasemosa*	Leaves, roots	Alemayehu *et al.*, 1993
Nataloe-emodin-8-methyl ether (**279**)	*S. didymobotrya*	Tissue culture	Delle-Monache *et al.*, 1991
Questin (**280**)	*S. didymobotrya*	Tissue culture	Delle-Monache *et al.*, 1991
	S. occidentalis	Tissue culture	Kitanaka *et al.*, 1985
Rhein (**281**)	*S. tora*	seeds	Hatano *et al.*, 1999
Alquinone (**282**)	*S. alata*	roots	Yadav & Kalidhar, 1994
Alarone (**283**)	*S. alata*	stem	Hennebelle *et al.*, 2009
Alatonal (**284**)	*S. alata*	stem	Hennebelle *et al.*, 2009
Obtusifolin (**285**)	*C. obtusifolia*	seeds	Li *et al.*, 2004
Racemosa (**286**)	*S. racemosa*	Leaves	Mena-Rajon *et al.*, 2002
1,8-dicarboxylic-3-methylanthraquinone (**287**)	*S. italica*	Leaves	Magano *et al.*, 2007
Anthracenes			
Torosachrysone (**288**)	*S. didymobotrya*	Tissue culture	Delle-Monache *et al.*, 1991
	S. longiracemosa	Leaves, roots	Alemayehu *et al.*, 1993
	S. tora	Seeds	Hatano *et al.*, 1999
7-methyltorosachrysone (**289**)	*S. occidentalis*	Tissue culture	Kitanaka *et al.*, 1985
Germichrysone (**290**)	*S. didymobotrya*	Tissue culture	Delle-Monache *et al.*, 1991
	S. occidentalis	Tissue culture	Kitanaka *et al.*, 1985
Rubrofusarin (**291**)	*S. longiracemosa*	Leaves, roots	Alemayehu *et al.*, 1993
	S. rugusa	Leaves	Barbosa *et al.*, 2004
2-methoxystypandrome (**292**)	*S. longiracemosa*	Leaves, root	Alemayehu *et al.*, 1993
Torachrysone (**293**)	*S. tora*	Seeds	Hatano *et al.*, 1999
Toralactone (**294**)	*S. longitacemosa*	Leaves	Alemayehu *et al.*, 1993
Bianthrones			
Chrysophanol-10,10′-bianthrone (**295**)	*S. didymobotrya*	Tisues culture	Delle-Monache *et al.*, 1991

Table 3 contd...'

Chrysophanol-physcion-10,10′-bianthrone (**296**)	*S. longiracemosa*	Leaves, roots	Alemayehu *et al.*, 1993
Chrysophanol-isophyscion-10,10′-bianthrone (**297**)	*S. didymobotrya*	Tissue culture	Delle-Monache *et al.*, 1991
	S. longiracemosa	Leaves, roots	Alemayehu *et al.*, 1993
IsePhyscion-10,10′-bianthrone (**298**)	*S. longiracemosa*	Leaves, roots	Alemayehu *et al.*, 1993
Physcion-10,10′-bianthrone (**299**)	*S. didymobotrya*	Tissue culture	Delle-Monache *et al.*, 1991
	S. longiracemosa	Leaves, roots	Alemayehu *et al.*, 1993
10-(chrysophanol-7′-yl)-10-hydroxychrysophanol-9-anthrone (**300**)	*S. longiracemosa*	Leaves, roots	Alemayehu *et al.*, 1993
10-hydroxy-10- (physcion-7-yl) chrysophanol athrone (**301**)	*S. didymobotrya*	pods	Alemayehu *et al.*, 1996;
5, 10-dihydroxy-2-methyl-9- (physcion-7'-yl)-1, 4-anthraquinone (**302**)	*S. didymobotrya*	pods	Alemayehu *et al.*, 1996;
Anthraquinone Glycosides			
Rubrofusarin triglucoside (**303**)	*S. tora*	Seeds	Hatano *et al.*, 1999
Nor-rubrofusarin gentiobioside (**304**)	*S. tora*	Seeds	Hatano *et al.*, 1999
Torachrysone gentiobioside (**305**)	*S. tora*	Seeds	Hatano *et al.*, 1999
Torachrysone tetraglucoside (**306**)	*S. tora*	Seeds	Hatano *et al.*, 1999
Torachrysone apioglucoside (**307**)	*S. tora*	Seeds	Hatano *et al.*, 1999
Demethylflavasperone gentiobioside (**308**)	*S. tora*	Seeds	Hatano *et al.*, 1999
Emodin-1-*O*-β-gentiobioside (**309**)	*C. obtusifolia*	Seeds	Li *et al.*, 2004
Physcion-8-O-β-gentiobioside (**310**)	*C. obtusifolia*	Seeds	Li *et al.*, 2004
Chrysophanol-1-O-β-gentiobioside (**311**)	*C. obtusifolia*	Seeds	Li *et al.*, 2004
Chrysophanol-1-*O*-β-D-glucopyranosyl-(1-3)-β-D-glucopyranosyl-(1-6)-β-D-glucopyranside (**312**)	*C. obtusifolia*	Seeds	Li *et al.*, 2004
Physcion-1-*O*-β-glucoside (**313**)	*S. alata*	leaves	Hennebelle *et al.*, 2009
1,5-dihyroxy-8-methoxy-2-methylanthraquinone-3-*O*-β-D-glucospyranoside (**314**)	*S. alata*	roots	Hennebelle *et al.*, 2009
Martianine, 10,10′-il-chrysophanol-10-oxi-10,10′-biglycosyl (**315**)	*S. martiana*	Stalks	Macedo *et al.*, 2009
Flavonoids			
Kampferol (**316**)	*S. alata*	Leaves	Hennebelle *et al.*, 2009
	S. didymobotrya	Tissue culture	Delle-Monache *et al.*, 1991
Luteolin (**317**)	*S. alata*	Leaves	Kelly *et al.*, 1994
	S. didymobotrya	Tissue culture	Delle-Monache *et al.*, 1991
Apigenin (**318**)	*S. didymobotrya*	Tissue culture	Delle-Monache *et al.*, 1991
Quercetin (**216**)	*S. didymobotrya*	Tissue culture	Delle-Monache *et al.*, 1991
Quercetin-3-methyl ether (**319**)	*S. didymobotrya*	Tissue culture	Delle-Monache *et al.*, 1991
7,4′-dihydroxy-5,3′-dimethoxyflavone (**320**)	*S. didymobotrya*	Tissue culture	Delle-Monache *et al.*, 1991
7,4′-dihydroxy-3,5,3′-trimethoxyflavone (**321**)	*S. didymobotrya*	Tissue culture	Delle-Monache *et al.*, 1991
Santal-7-O-methylorobol (**322**)	*S. alata*	stem	Hennebelle *et al.*, 2009
Kampferol-3-O-gentiobioside (**323**)	*S. alata*	Leaves	Gupta & Singh, 1991
Chrysoeriol-7-O-(2″-O-β-D-manopyranosyl)-β)-D-allopyranoside (**324**)	*S. alata*	Leaves	Gupta & Singh, 1991

Table 3 cont'd.....

Other compounds			
Knipholone (**325**)	*S. didymobotrya*	Pods	Alemayehu *et al.*, 1996
(E)- and (Z)-3′-hydroxy-3,4,5′-trimethoxystilbene (**326**)	*S. didymobotrya*	Tissue culture	Delle-Monache *et al.*, 1991
(E)-4,3′-dihydroxy-3,5′-dimethoxystilbene (**327**)	*S. didymobotrya*	Tissue culture	Delle-Monache *et al.*, 1991
Cassiaxanthanine (**328**)	*S. alata*	Leaves	Hennebelle *et al.*, 2009
2,3,7-tri-O-methylellagic acid (**329**)	*S. alata*	Leaves	Hennebelle *et al.*, 2009
2,6-dimethoxybenzoquinone (**330**)	*S. alata*	Leaves	Hennebelle *et al.*, 2009
Hexitol (pinitol) (**331**)	*S. racemosa*	Leaves	Mena-Rajon *et al.*, 2002
Piperidine alkaloid (Cassine) (**332**)	*S. racemosa*	Leaves	Mena-Rajon *et al.*, 2002
Coumarin (Dalbergin) (**333**)	*S. alata*	Stem	Hennebelle *et al.*, 2009

2.5.3.4. Biological activities of extractives from *Senna* species

For a long period, the therapeutic uses of anthraquinones have been limited to laxatives properties (Mohammed *et al.*, 2008). The biological activities investigated so far included laxative activities, inhibition of enzymes, antimicrobial activity, antiulcerogenic/spasmolytic activity, anti-inflammatory, anti-arthritic, anti-rheumatic and antioxidant activity (Mohammed *et al.*, 2008). Ethanol extract and the ether and water-soluble fractions of the ethanol extracts of the seeds of *Cassia tora* have been reported to have hypolipidaemic activity on triton induced hyperlipidemic profile (Patil *et al.*, 2004).

Cassia obtusifolia is reported to be used for management of hypercholesterolemia and hypertension (Li *et al.*, 2004). Martianine (**315**), an anthraquinone glycoside from *Senna martiniana* was reported to have inhibitory action against *Trypanosome cruzi* glyceradehyde-3-phosphate dehydrogenase (GAPDH) enzymes and was noted as lead molecule towards development of a drug for management of Chagas disease (Macedo *et al.*, 2009). Emodin (**270**), physcion (**273**), aloe-emodin (**274**), and rhein (**281**) have been reported to possess inhibitory actions against certain enzymatic activity (protein tyrosine kinase, arylamine N-acetyltransferase, pincillase, reverse transcriptase) (Mohammed *et al.*, 2008). The moderate antiplasmodial activities of various plants parts of *S. didymobotrya* against *Plasmodium falciparum* have been reported (Muregi *et al.*, 2007), though no further evaluation was performed to determine the phytochemical responsible for the activities.

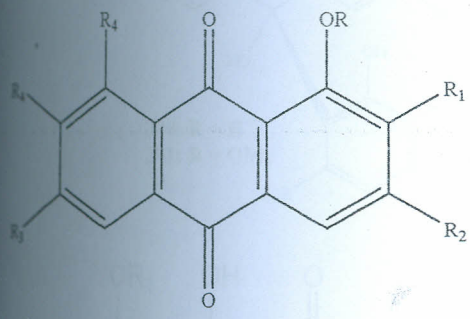

	R	R_1	R_2	R_3	R_4	R_5
269	H	H	Me	H	H	H
270	H	H	Me	OH	H	H
271	H	Me	H	H	H	H
272	H	H	Me	H	Ac	H
273	H	H	Me	OMe	H	H
274	H	H	CH_2OH	H	H	H
275	H	H	Me	OMe	H	Me
276	H	H	Me	H	H	Me
277	Me	H	Me	OMe	H	H
278	H	H	Me	H	OH	OH
279	H	H	Me	H	OH	Me
280	H	H	Me	OH	H	Me
281	H	H	COOH	H	H	H
282	H	OH	CHO	H	H	H
283	H	CHO	OH	H	H	H
284	H	H	CHO	OH	H	H
285	H	H	Me	OMe	Me	H
287	COOH	H	Me	H	H	COOH

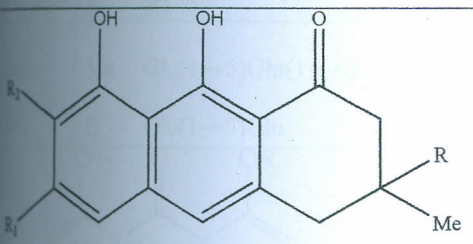

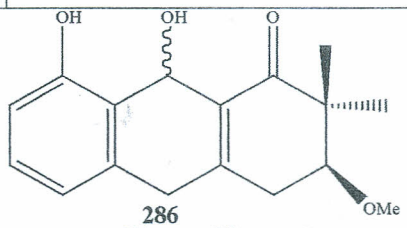

286

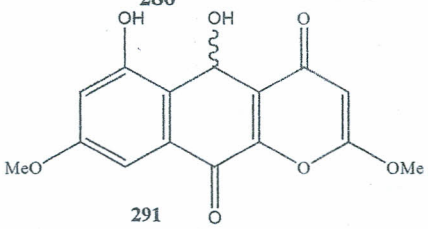

291

	R	R_1	R_2
288	Me	OMe	H
289	Me	OMe	Me
290	H	Me	H

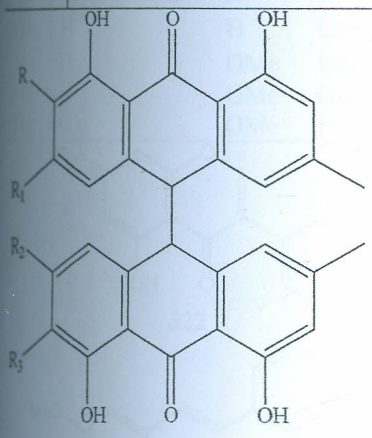

	R	R_1	R_2	R_3
295	H	H	H	H
296	H	H	OMe	H
297	H	H	H	OMe
298	OMe	H	H	OMe
299	H	OMe	OMe	H

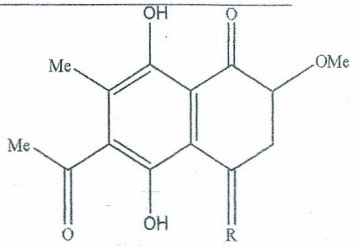

292: R = O
293: R = OH, H

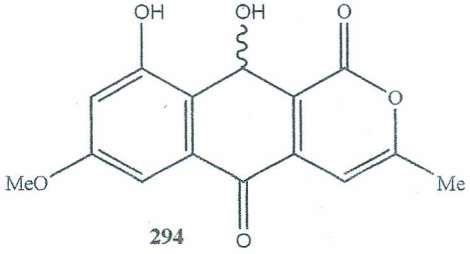

294

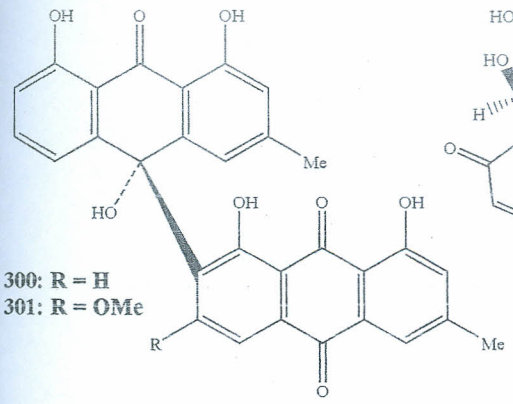

300: R = H
301: R = OMe

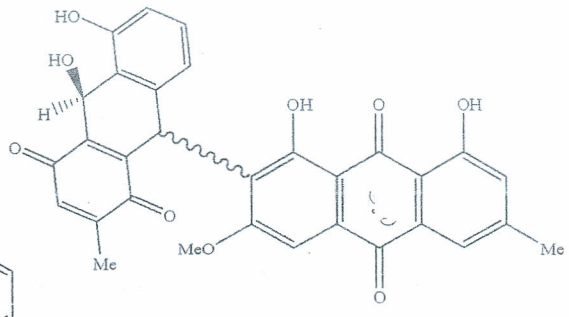

302

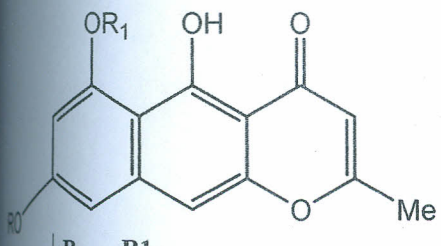

	R	R1
303	Me	Glu(1→6)Glu(1→6)Glu
304	H	Glu(1→6)Glu

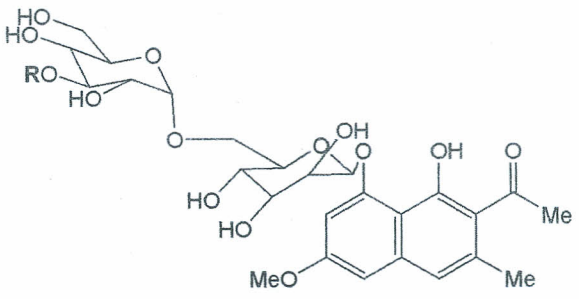

305: R = H
306: R = GB

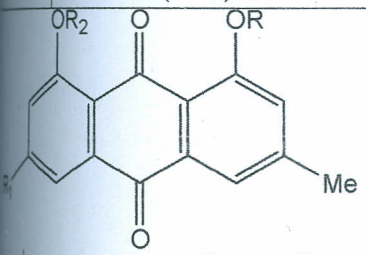

	R	R_1	R_2
309	Glu(1→6)Glu	H	H
310	H	H	Glu(1→6)Glu
311	H	OMe	Glu(1→6)Glu
312	H	OMe	Glu(1→6)Glu
313	Glu	OMe	H

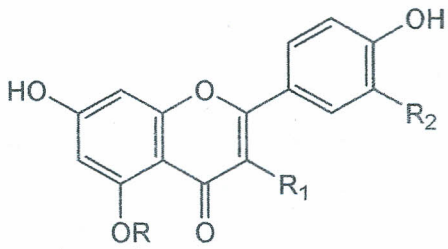

	R	R_1	R_2
316	H	OH	H
317	H	H	OH
318	H	H	H
319	H	OMe	OH
320	Me	H	OMe
321	Me	OMe	OMe

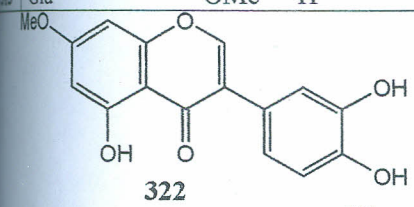

322

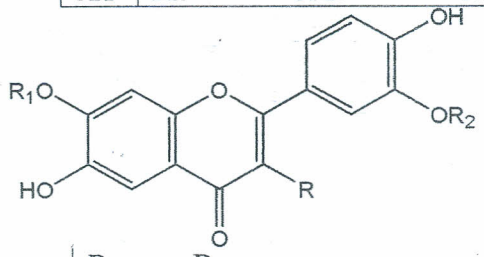

	R	R_1	R_2
323	*O*-Glu	Me	H
324	H	*O*-Glu(1→6)Allopyranoside	OMe

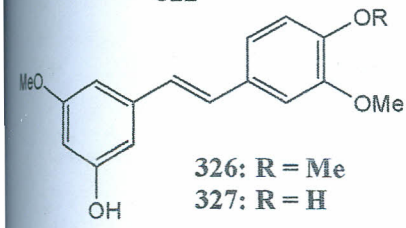

326: R = Me
327: R = H

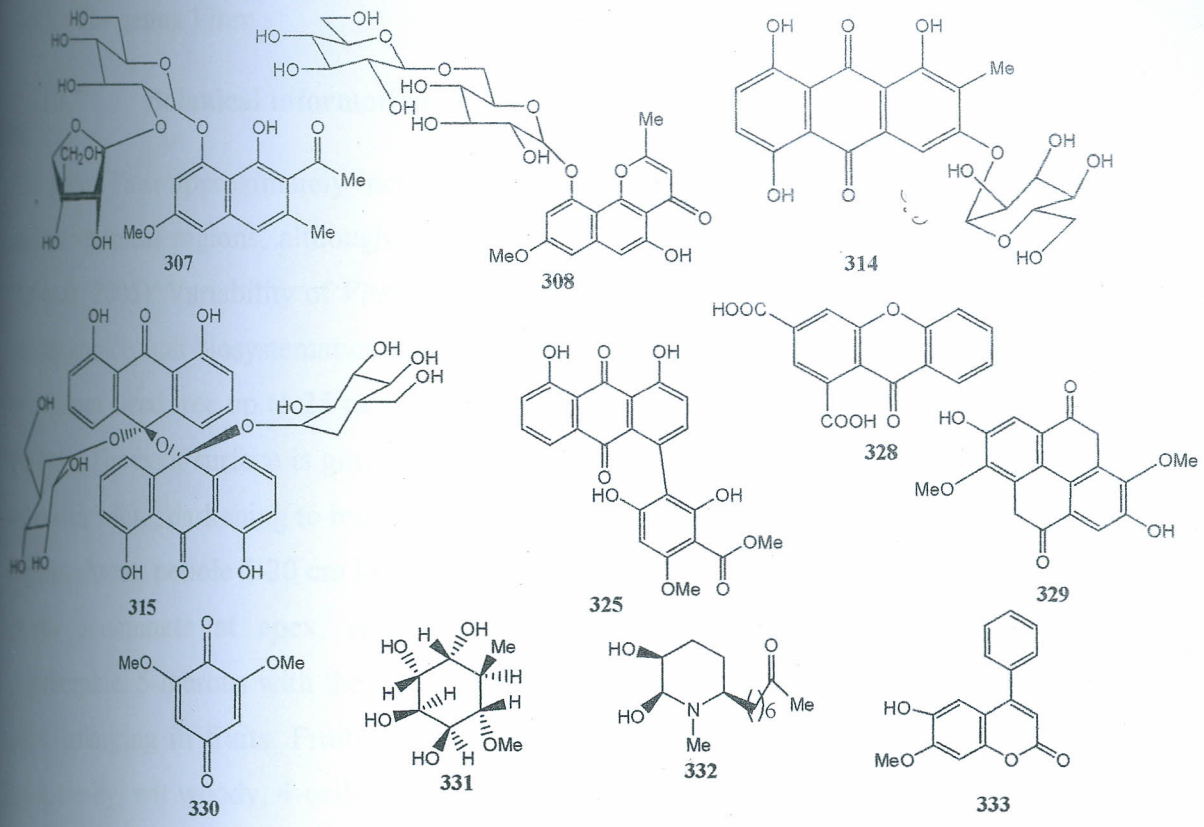

2.6. The Family Lamiaceae

The family Lamiaceae or Labiatae consist of flowering plants which have traditionally been considered to be related to Verbenaceae (Raymond *et al.*, 2004), but in the 1990s, phylogenetic studies suggested that many genera classified in Verbenaceae belong instead to Lamiaceae (Cantino *et al.*, 1992). The currently accepted version of Verbenaceae may not be more closely related to Lamiaceae than some of the other families in the Lamiales (Stevens *et al.*, 2001).

The family Lamiaceae has a cosmopolitan distribution consisting of about 236 genera (Raymond *et al.*, 2004) and 6,900 to 7,200 species. The largest genera are *Salvia* (900), *Scutellaria* (360), *Stachys* (300), *Plectranthus* (300), *Hyptis* (280), *Teucrium* (250), *Vitex* (250) *Thymus* (220) and *Nepeta* (200).

2.6.1. The genus *Vitex*

2.6.1.1. Botanical information on the genus *Vitex*

The genus *Vitex* approximately includes 270 known species of trees and shrubs within tropical and sub-tropical regions, although few species may be found in temperate zones (Maundu & Tengnas, 2005). Variability of *Vitex doniana* is remarkable; regarding its morphology as well as habitat choice, and biosystematics research is warranted (Maundu & Tengnas, 2005). It is a small to medium sized tree up to 25 m tall with bole branches for up to 11 m, often slightly fluted at the base. The bark surface is grayish white to pale grayish brown, fissured and scaly, inner bark yellowish white, darkening to brown. Leaves are opposite, digitately compound with 3-7 leaflets, stipules absent, petiole 5-20 cm long. The leaflets are obovate to elliptical, notched to rounded or shortly acumunate at apex, entire, leathery and nearly glabrous. Flowers are bisexual, zygomorphic, 5-merous with the pedicel up to 2 mm long, calyx conical, 3-5 mm long, stamens are 4, enlarging in fruits. Fruits are obovoid to oblong-ellipsoid drupe 2-3 cm long, purplish black, fleshy, wit woody, 4-celled stone, up to 4 seeded. Seeds are without endosperm (Maundu & Tengnas, 2005).

2.6.1.2. Ethnopharmacological uses of *Vitex* plants

Several other *Vitex* species are used as folk remedies in different countries against several human and animal diseases. *Vitex negundo* (Lamiaceae) is an important medicinal plant found throughout India, with all its parts used in Ayurvedic and Unani systems of medicine. Its leaves (Dharmasiri *et al.*, 2003) and seeds (Chawla *et al.*, 1992a) are widely used externally for rheumatism and inflammation of joints and reported to have insecticidal properties. Decoction of its leaves are consumed as diuretic, expectorant, vermifuge, tonic and febrifuge (Chawla *et al.*, 1992a). The essential oil obtained from *V. negundo* and *V. gaumeri* is used to treat colds and coughing spells (Ekundayo *et al.*, 1990). *Vitex mollis* is reported as a remedy to alleviate dysentery, as well as an analgesic and anti-inflammatory medicine; other folk uses include the treatment of scorpion stings, diarrhea and stomach ache (Argueta *et al.*, 1994). Antimalarial, antimicrobial and antifungal properties have been reported for *V. gaumeri, V. agnus-castus* and *V. negundo*, respectively (Meena *et al.*, 2010). The genus *Vitex* is not an exception among plants with insecticidal activities. *V. negundo* has been reported to possess larvicidal activity against the

mosquito species *Culex quiquefasciatus* and *Anopheles stephensi* (Pushpalatha & Muthukrishnan, 1995), and acts as a deterrent to the mosquito *Aedes aegypti* (Hebbalkar *et al.*, 1992).

Cooked young leaves of *V. doniana* are eaten as vegetables (Neuwinger, 2000). The blackish pulp of the fruits is edible and sweet, and eaten raw. It is often used to make jam (Alobo, 2000). Leaf sap is used as an eye drop to treat conjunctivitis and other eye complaints (Neuwinger, 2000). Leaf decoction is applied externally as a galactagogue and against headache, stiffness, measles, rash, fever, chickenpox and hemiplegic, and internally as tonic, anodyne, febrifige and to treat respiratory diseases (Neuwinger, 2000). Powdered stem bark added to water is taken to treat colic and a bark extract is used to treat stomach complaints and kidney troubles (Agunu *et al*, 2005). Dried and fresh fruits are eaten against diarrhea and as remedy against lack of vitamin A and B (Agunu *et al*, 2005). Sections 2.6.1.3 and 2.6.1.4 highlight some of the phytochemicals and biological activities that reported from these ethno medicinally important plants of family Lamiaceae, which can confirm their applications. There is no phytochemical information for the claimed ethnopharmacological applications, although few biological reports about *V. doniana* are available.

2.6.1.3. Phytochemistry of *Vitex* species

Plants from the genus *Vitex* contain several types of ecdysteroids that may be utilized as taxonomic markers. For instance, 20-hydroxyecdysone (**334**) has been reported in many *Vitex* species (Filho *et al*, 2008).

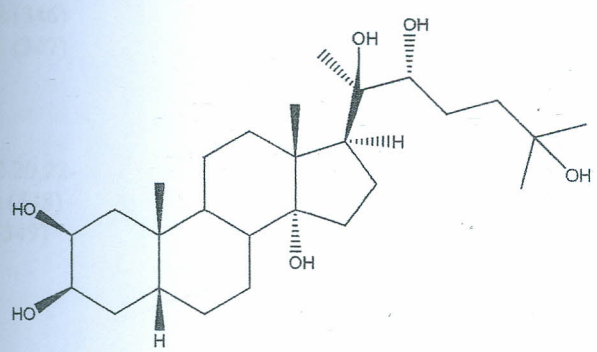

334

Some species such as *Vitex garderiana* and *Vitex agnus-castus* contain also iridoids (Filho *et al*, 2008). The apparent associations of iridoids and ecdysteroids with *Vitex* species require further

chemotaxonomic studies. Table 4 provides a summarized review of the phytochemical isolated from different species of *Vitex*. *Vitex doniana* is small to medium sized tree up to 25 m tall tropical tree with no phytochemical report in spite of some biological activities reported (section 2.6.1-4).

Table 4: Some Important Compounds reported from *Vitex* species

Compound	Plant	Part	Reference
20-Hydroxyecdysone (**334**)	*V. canescens*	Stem bark	Suksamrarn *et al.*, 2000
	V. cooperi	Stem	Filho *et al.*, 2008
	V. cymosa	Stem bark	Leit *et al.*, 2001
	V. fischeri	Root bark	Filho *et al.*, 2008
	V. polygama	Root bark	Filho *et al.*, 2008
	V. stickeri	Stem	Zhang *et al.*, 1992
	V. pinnata	Root bark	Suksamrarn & Sommechai, 1993
11α-Hydroxyecdysone (**335**)	*V. scabra*	Roots	Suksamrarn *et al.*, 2002
	V. strickeri	Stem bark	Zhang *et al.*, 1992
(24R)-11α,20,24-trihydroxyecdysone (**336**)	*V. canescens*	Root bark	Suksamrarn *et al.*, 2000
11α,20,26-trihydroxyecdysone (**337**)	*V. canescens*	Root bark	Suksamrarn *et al.*, 2000
Abutasterone (**338**)	*V. stickeri*	Stem bark	Zhang *et al.*, 1992
24-epi-abustasterone (**339**)	*V. canescens*	Stem bark	Suksmararn *et al.*, 2000
	V. scabra	Root bark	Suksmararn *et al.*, 2002
Makisterone A (**340**)	*V. canescens*	Root bark	Suksmararn *et al.*, 1997
	V. leptobotrys	Stem bark	Filho *et al.*, 2008
24-epi-makisterone A (**341**)	*V. canescens*	Root bark	Suksmararn *et al.*, 1997
	V. leptobotrys	Stem bark	Filho *et al.*, 2008
	V. scabra	Root bark	Suksmararn *et al.*, 2002
24(28)-dehydromakisterone A (**342**)	*V. leptobotrys*	Stem bark	Filho *et al.*, 2008
Pinnatasterone (**343**)	*V. agnus-castus*	Roots	Filho *et al.*, 2008
	V. canscens	Stem bark	Suksamrarn *et al.*, 2000
	V. leptobotrys	Stem bark	Filho *et al.*, 2008
	V. scabra	Stem bark	Suksmararn *et al.*, 2002
	V. pinnata	Stem bark	Suksmararn & Sommechai, 1993
26-hydroxypinnastasterone (**344**)	*V. cymosa*	Stem bark	Leit *et al.*, 2001
24-epipinnatasterone (**345**)	*V. scabra*	Root bark	Suksmararn *et al.*, 2002
Viticosterone E (**346**)	*V. agnus-castus*	Root bark	Filho *et al.*, 2008
Ajugasterone C (**347**)	*V. fischeri*	Root bark	Filho *et al.*, 2008
	V. leptobotrys	Stem bark	Filfo *et al.*, 2008
	V. polygama	Root bark	Filho *et al.*, 2008
	V. stickeri	Stem bark	Zhang *et al.*, 1992
Ajugasterone C 20,22-monoacetonide (**348**)	*V. polygama*	Root bark	Filho *et al.*, 2008
	V. stickeri	Stem bark	Zhang *et al.*, 1992
Turkesterone (**349**)	*V. canescens*	Root bark	Suksmararn *et al.*, 2000
	V. fischeri	Root bark	Filho *et al.*, 2008
	V. polygama	Root bark	Filho *et al.*, 2008
	V. scabra	Stem bark	Suksmararn *et al.*, 2002
	V. pinnata	Stem bark	Suksmararn & Sommechai, 1993
Vitexirone (**350**)	*V. fischeri*	Root bark	Filho *et al.*, 2008
Canescensterone (**351**)	*V. canescens*	Stem bark	Suksamrarn *et al.*, 2000

Table 4 cont'd...

Calonysterone (352)	*V. scabra*	Stem bark	Suksamrarn *et al.*, 2002
Shidasterone (353)	*V. canescens*	Root bark	Suksamrarn *et al.*, 1997
Scabrasterone (354)	*V. scabra*	Stem bark	Suksamrarn *et al.*, 2002
Pterosterone (355)	*V. scabra*	Stem bark	Suksamrarn *et al.*, 2002
Polypodine B (356)	*V. scabra*	Stem bark	Suksamrarn *et al.*, 2002
Deoxycrustecdysterone (358)	*V. leptobotrys*	Stem bark	Thuy *et al.*, 1998
Iridoids			
Mussaenosidic (359)	*V agnus-castus*	Root bark	Kuruuzum-Uz *et al.*, 2003
6-*O*-p-hydroxybenzomussaenosidic acid (360)	*V agnus-castus*	Root bark	Kuruuzum-Uz *et al.*, 2003
Agnucastoside A (361)	*V agnus-castus*	Root bark	Kuruuzum-Uz *et al.*, 2003
Agnucastoside B (362)	*V agnus-castus*	Root bark	Kuruuzum-Uz *et al.*, 2003
Agnucastoside C (363)	*V agnus-castus*	Root bark	Kuruuzum-Uz *et al.*, 2003
Aucubin (364)	*V agnus-castus*	Root bark	Kuruuzum-Uz *et al.*, 2003
Agnuside (365)	*V agnus-castus*	Root bark	Kuruuzum-Uz *et al.*, 2003
Negundoside (366)	*V. negundo*	Leaves	Gautum, 2008
Flavonoids			
Apigenin (318)	*V. agnus-castus*	Fruits	Jarry *et al.*, 2006
Pachypodol (367)	*V. penduncularis*	Leaves	Meena *et al.*, 2010
Casticin (368)	V. agnus-castus	Fruits	Jarry *et al.*, 2006
5-Hydroxy-3,6,7,4-tetramethoxyflavone (369)	*V. agnus-castus*	Fruits	Jarry *et al.*, 2006
5-Hydroxy-3,6,7,-trimethoxy-(3,4-dimethoxyphenyl)-4H-chrome-4-one (370)	*V. negundo*	Leaves	Maurya *et al.*, 2007
5,7-dihydroxy-2-(3,4-dihydroxyphenyl)-4H-chromen-4-one (371)	*V. negundo*	Leaves	Maurya *et al.*, 2007
Vitexin (372)	*V. peduncularis*	Leaves	Meena *et al.*, 2010
Isovitexin (373)	*V. peduncularis*	Leaves	Meena *et al.*, 2010
Orientin (374)	*V. pinnata*	Flowers	Sharma & Aithal, 1990
Isoorietin (375)	*V. pinnata*	Flowers	Sharma & Aithal, 1990
Vitetrifolin A (376)	*V. trifolia*	Stem bark	Ono *et al.*, 2000
Vitetrifolins C (377)	*V. trifolia*	Stem bark	Ono *et al.*, 2000
Rotunndifuran (378)	*V. trifolia*	Stem bark	Ono *et al.*, 2000
	V. agnus castus	fruits	Stiche *et al.*, 1999
6β,7β-diacetoxy-13-hydroxylabda-8,14-diene (379)	*V. agnus-castus*	Fruits	Jarry *et al.*, 2006
Cleroda-1,3,14-triene-13-ol (380)	*V. agnus-castus*	Fruits	Jarry *et al.*, 2006
Cleroda-7,14-dien-13-ol (381)	V. agnus-castus	fruits	Jarry *et al.*, 2006
8,13-dihydroxy-14-labdene (382)	V. agnus-castus	Fruits	Jarry *et al.*, 2006
Vitexilactone (383)	V. agnus-castus	Fruits	Jarry *et al.*, 2006
Vitexlactam A (384)	V. agnus-castus	Fruits	Jarry *et al.*, 2006
Dihydrosolidagenone (385)	*V. trifolia*	Stem bark	Ono *et al.*, 2000
Abietatriene 3B (386)	*V. trifolia*	Stem bark	Ono *et al.*, 2000
3-Acetoxy-14,15,16-trinor-13,9-labdanolide (387)	*V. negundo*	Seeds	Ono *et al.*, 2004
Vitedoamine A (388)	*V. negundo*	Seeds	Chawla *et al.*, 1992b
Detetrahydroconidendrin (389)	*V. negundo*	Seeds	Ono *et al.*, 2004
Vitedoin A (390)	*V. negundo*	Seeds	Ono *et al.*, 2004
Vitrofolal A (391)	*V. rotundifolia*	Subterranean	Kawazoe *et al.*, 2001
Vitrofolal B (392)	*V. rotundifolia*	Subterranean	Kawazoe *et al.*, 2001
Vitrofolal E (393)	*V. rotundifolia*	Subterranean	Kawazoe *et al.*, 2001
Vitrofolal F (394)	*V. rotundifolia*	Subterranean	Kawazoe *et al.*, 2001
Vitrofolal C (395)	*V. rotundifolia*	Subterranean	Kawazoe *et al.*, 2001
Vitrofolal D (396)	*V. rotundifolia*	Subterranean	Kawazoe *et al.*, 2001
2α,3β-7-O-methylcedrusin (397)	*V. negundo*	Seeds	Ono *et al.*, 2004

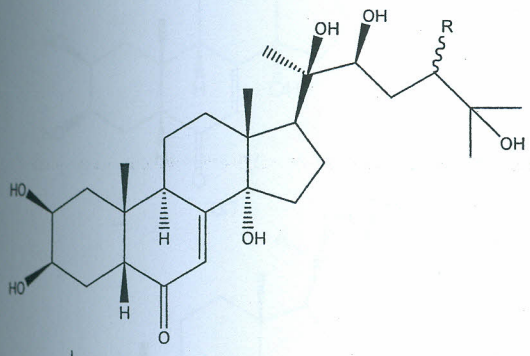

	R
334	H
338	OH_α
339	OH_β
340	Me_β
341	Me_α

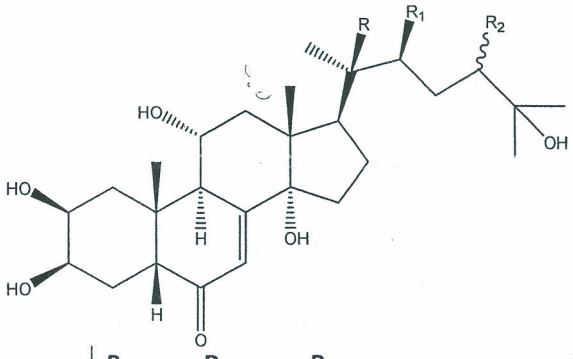

	R	R_1	R_2
335	H	OH	H
336	OH	OH	OH_β
349	OH	OH	H
354	OH	H	H

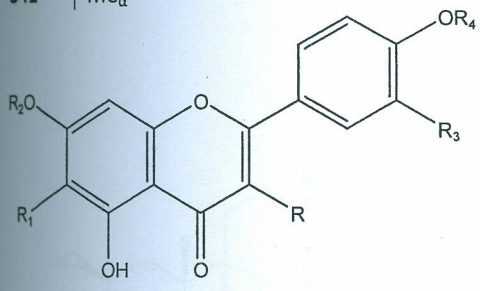

	R	R_1	R_2	R_3	R_4
318	H	H	H	H	H
365	OMe	H	Me	OMe	H
368	H	OMe	Me	OH	Me
369	OMe	OMe	Me	H	Me
370	OMe	OMe	Me	OMe	Me
371	H	H	H	OH	H

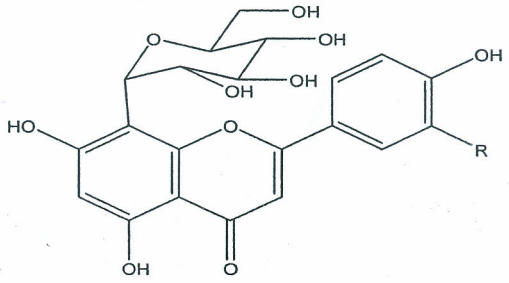

372: R = H
374: R = OH

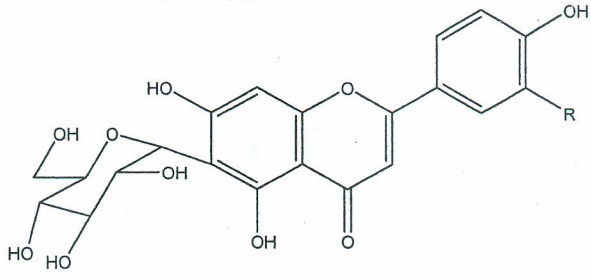

373: R = H
375: R = OH

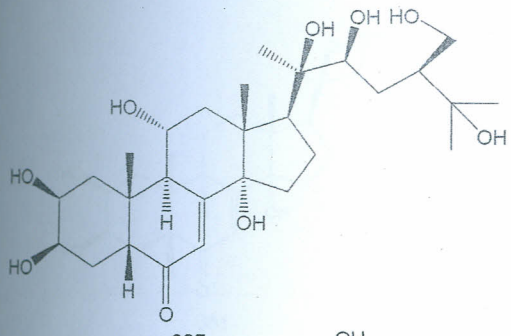

337

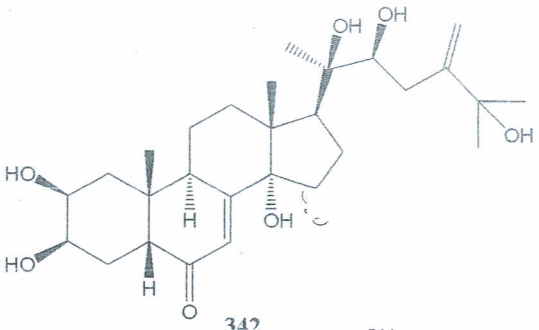

342

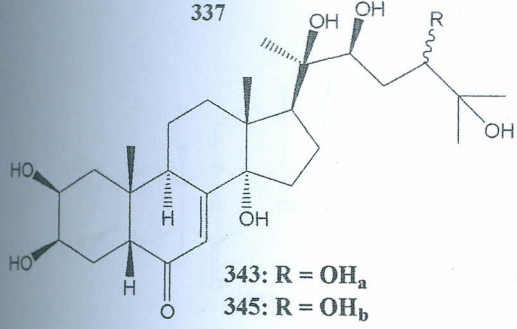

343: R = OH_a
345: R = OH_b

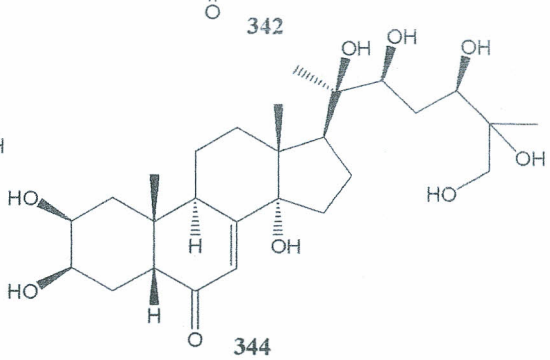

344

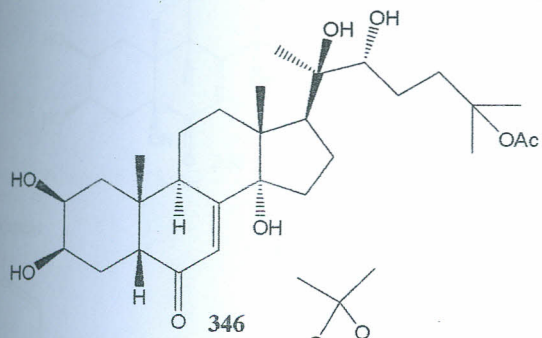

346

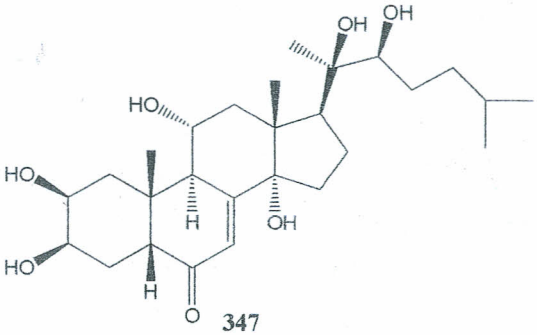

347

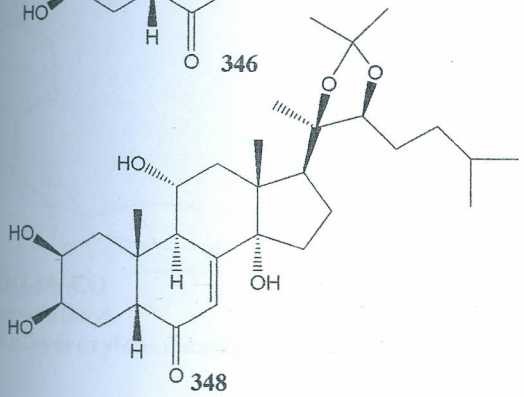

348

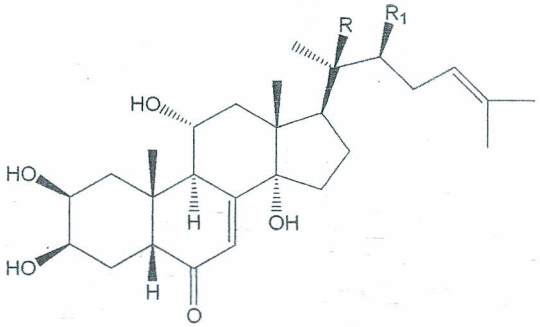

350

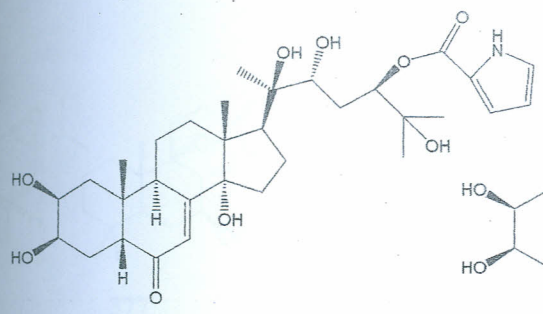

351

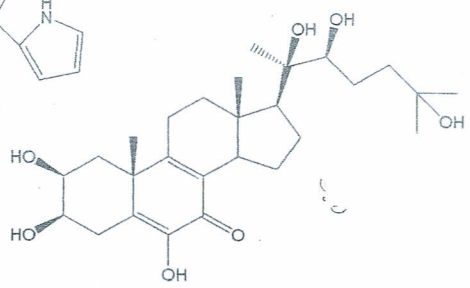

352

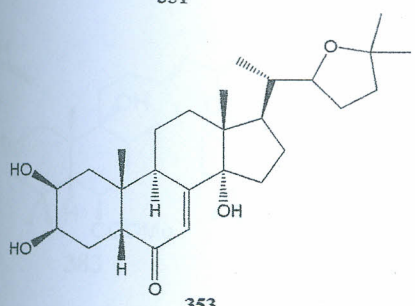

353

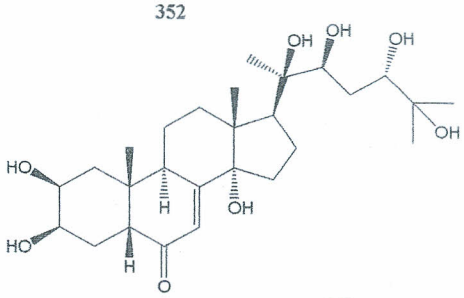

355

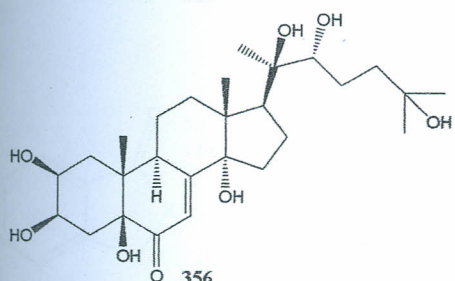

356

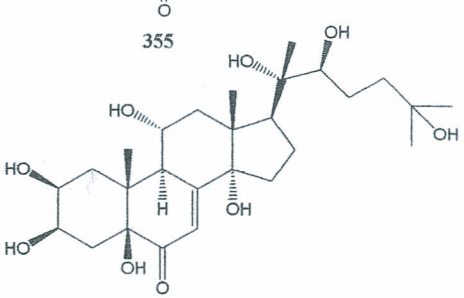

357

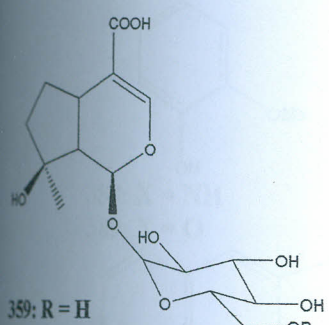

359: R = H
360: R = *p*-OH-Ph-CO
361: R = foliamenthoyl
362: R = 6,7-dihydroxyfoliamenthoyl

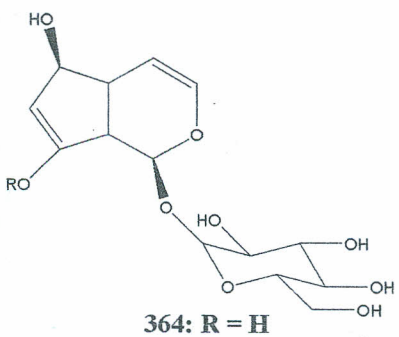

364: R = H
365: R = *p*-OH-Ph-CO

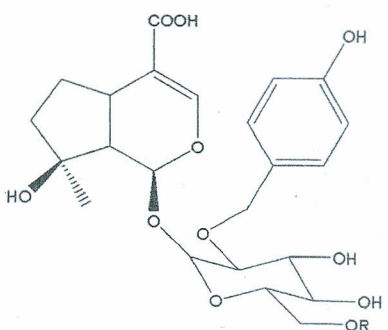

366

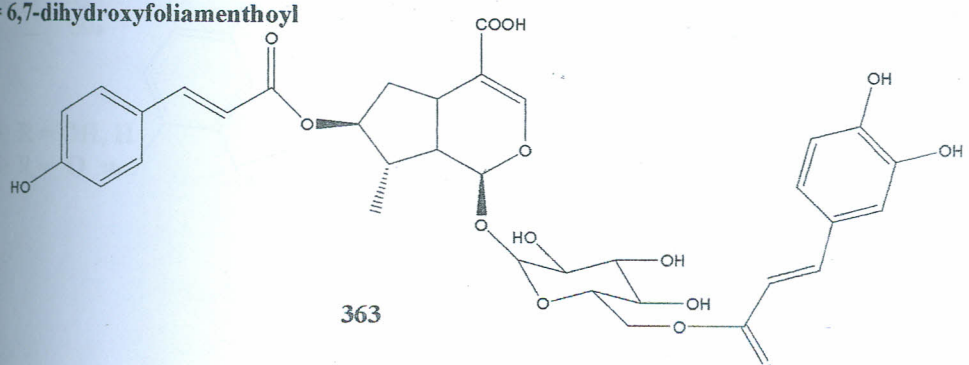

363

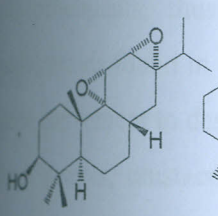

376

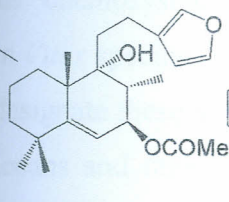

377

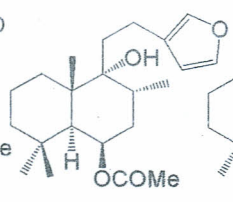

378

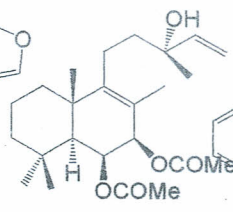

379

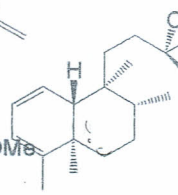

380

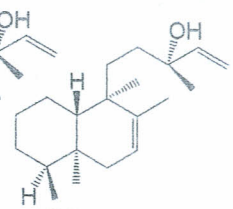

381

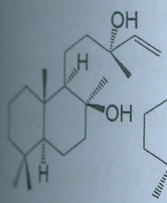

382

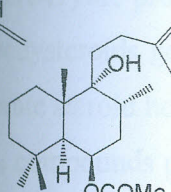

383

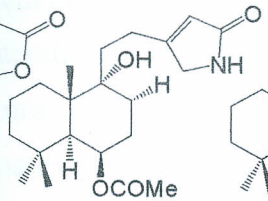

384

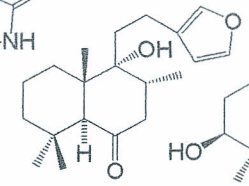

385

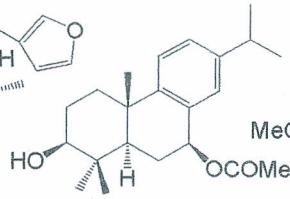

386

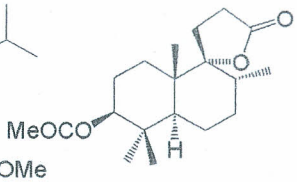

387

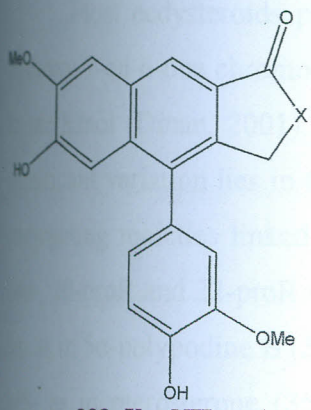

388: X = NH
389: X = O

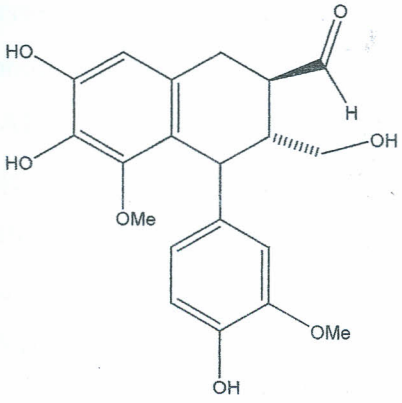

390

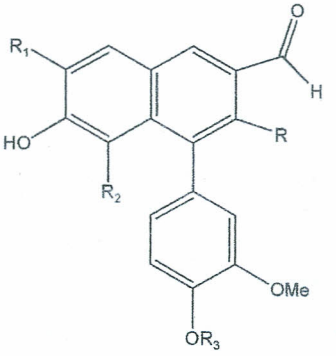

	R	R_1	R_2	R_3
391:	H	H	OMe	Me
392:	OH	H	OMe	Me
393:	H	OMe	H	H
394:	OH	OMe	H	H

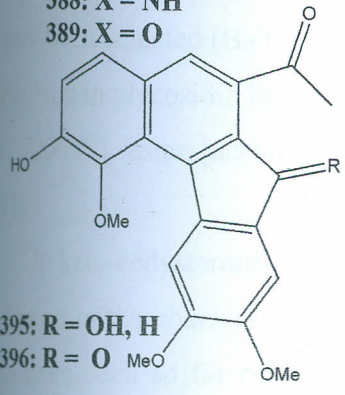

395: R = OH, H
396: R = O

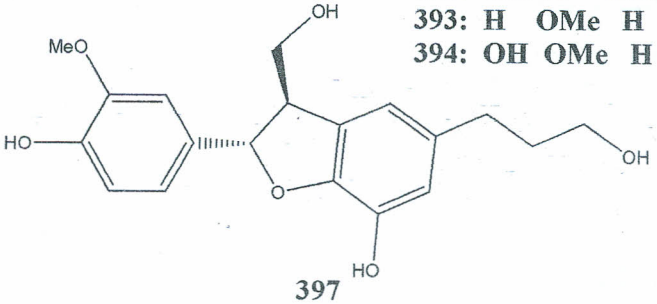

397

As shown in Table 4 it is clear that *Vitex* species elaborate ecdysteroids more than other phytochemicals, thus chemosystematics relationship can be studied from the pattern of ecdysteroids found in *Vitex* species. Since the discovery of ecdysteroid analogues in plants, it has been convenient to designate these as phytoecdysteroids to differentiate them from those isolated from insects, crustaceans and other animal sources (zooecdysteroids). However, this division must be regarded as non-exclusive, since many ecdysteroids (20E-makisterone (**340**), ajugasterone C (**347**) are present in both animals and plants (Dinan, 2001).

Phytoecdysteroids generally are a family of about 200 plant steroids related in structure to the invertebrate steroid hormone 20-hydroxyecdysone (**334**) (Dinan, 2001). Typically, they are C_{27}, C_{28} or C_{29} compounds possessing a 14α-hydroxy-7-en-6-one chromophore and A/B-*cis* ring fusion (5β-H) and rarely *trans* (5β-H) (Dinan, 2001). However, some are derived from phytosterols with C_{28} or C_{29} skeleton, with an alkyl group at C-24. Naturally, phytoecdysteroids have β-configured methyl groups at C-10 and C-13 with a *trans* B/C- and C/D- ring junctions.

Most ecdysteroids possess a hydroxyl group at the 2α-, 3α-, 14α-positions. The 14α-hydroxy-7-en-6-one chromophore exhibits characteristic UV-Vis absorption with λ_{max} at 242 nm in methanol (Dinan, 2001). Although variation in the steroid ring structure is not substantial, significant variation lies in the number, position and orientation of the hydroxyl groups and the conjugating moieties linked through these. The commonly hydroxylated sites are the 2β-, 3β-, 14α-, 20-proR and 22-proR carbons of ecdysteroids. Hydroxyl groups may also be present at the 5α- as in 5α-polypodine B (**356**), 11α- as in [**335**, **336**, **354** and **347-350**] (Calcagno *et al.*, 1996), 24S- as in pterosterone (**355**) (Ba'thori *et al.*, 1998), and 21-hydroxyecdysteroids have only recently been detected (Ba'thori *et al.*, 1999; Dinan *et al.*, 1999). The hydroxyl group(s) may also be involved in glycosidic linkages [galactoside, glucoside and xyloside (Baltayev, 1998; Sadikov *et al.*, 2000),], ester [acetate, benzoate, cinnamate, 3-p-coumarate, crotonate (Ba'thori *et al.*, 1997)].

In keto-ecdysteroids, an oxo-group may be relocated at the 2-, 3-, 12-, 17, 20, and/or 22 in addition to the characteristic C-6 oxo group as in calonysterone (**352**). The olefinic position bonds have been so far reported at 4(5), 8(8), 9(11), 12(13), 14(15), 24(25) and/or 24(28) as exhibited by 24(28)-dehydromakisterone A (**342**), vitexirone (**350**) with 24(25) unsaturation, and calonysterone (**352**) with 8(9), 14(15) and 5(6) sp^2 carbons. Phytoecdysteroid with one- or two – alkyl group may be present at C-24, resulting in a C_{28} [24*R*-makisterone A (**340**), 24*S*-epi-

makisterone A (**341**)]. An extension of the C_{27} skeleton provides a basis for the classification of these compounds into C_{28}, C_{29} or C_{30} (suppose 4-methyl group is also present) phytoecdysteroids (Dinan, 2001). The alkyl groups may be unsaturated (methenyl or ethenyl [24(28)-dehydromakisterone A (**342**)) (Baltayev *et al.*, 1997). A furan ring may be generated in some cases by cyclization of a parent C_{27} skeleton side-chain through dehydration of C-22 and C-25 hydroxyls [shidasterone (**353**) (Suksamrarn *et al.*, 1997). Phytoecdysteroids lacking either a complete or a partial side chain of C_{19}, C_{21} or C_{24} parent skeleton, have been isolated from several plants and are regarded as ecdysteroid metabolites (Dinan *et al.*, 1999).

Current knowledge of the biosynthetic pathways for ecdysteroids have relied mostly on synthesis in invertebrates, for which more is known. A review by Adler & Grebenok (1995) highlighted biosynthesis of phytoecdysteroids. However, the presence of phytoecdysteroids in various plant parts at different concentrations could not allow any conclusion about the tissues or organ in which these compounds are primarily produced. Plants (unlike insects) are capable of biosynthesizing phytoecdysteroids from mevalonic acid, and it has been demonstrated to proceed via cholesterol and/or lanosterol (Alder & Grebenok, 1995). Through application of [4-^{14}C, 7α-$^{3}H_1$] and [4-^{13}C, 7β-$^{3}H_1$] cholesterols to *Taxus baccata* and *Polypodium vulgare*, it was shown that the *cis* 7β- and 8β-hydrogens of cholesterol are removed during the biosynthesis of ecdysteroids (Cook *et al.*, 1973).

From other studies involving specifically-labeled cholesterols, the location of the radiolabel "H" in biosynthesized 20 ecdysteroid indicated that hydrogen migration occur from the 3α- and 4β- positions to C-4 and C-5, respectively, whereas 4α-H is retained at C-4. Such rearrangement results in formation of the A/B *cis*-ring junction which is explained by concomitant 1,2-Wagner-Meerwein hydride shift from the 4β- to the 5β- and from the 3α- to the 4α- position with the implicit displacement of the 4α-hydrogen of cholesterol to the 4β- position in the ecdysteroid (Davies *et al.*, 1980). This study indicates the involvement of a 3-oxo-4-ene intermediate, however, a study by Nomura *et al.*, (2000) demonstrated a contrasting result that showed the involvement of cholesterol as a precursor phytosterol of the C_{28} and C_{29} ecdysteroids. The study noted the conversion of cholesterol to 20-ecdysteroid with retention of labels without migration from [3β-^{2}H]-, [4α-^{2}H]-, and [4β-^{2}H]- cholesterols and [3α-^{2}H] and [5-^{2}H]-3β-hydroxy-5β-cholest-7-en-6-ones are all compatible with 3β-hydroxy-5β-cholest-7-en-6-one

being an intermediate in the biosynthesis of 20 ecdysteroids. Furthermore, [5-^{2}H] 3β-hydroxy-5α-cholest-7-en-6-one was not converted to 20-ecdysteroid (Nagakari *et al.*, 1994).

Application of [6-^{2}H] cholesterol to *Ajuga reptans* hairy roots revealed that 6-H largely become the 5β-H (compatible with the intermediacy of a 5α, 6α-epoxide) but one third of the 5β-H derives from other sources, indicating that the route (s) to the A/B *cis*-ring junction are more complex (Fujimoto *et al.*, 1997). Using the root hairy system, Nakagawa *et al.*, (1997) investigated the stereochemistry of hydroxylation at C-25, which was found to proceed with a mixture of retention and inversion of configuration. Hydroxylation at C-2 proceeds with retention of configuration (Nomura & Fujimoto, 2000). *Ajuga reptans* hairy roots convert 3β-hydroxy-5β-cholestan-6-one and 2β,3β-dihydroxy-5β-cholestan-6-one to 20-ecdysteroid, demonstrating that the 7-ene is introduced at a later stage in the biosynthetic pathway and that 7-dehydrocholesterol is not an obligatory intermediate (Hyodo & Fujimoto, 2000). A possible composite scheme of ecdysteroids biosynthesis based on result obtained with several species is given in Scheme 6. Because of this information, the category of ecdysteroids from *Vitex doniana* may be expected to fall in any of the above biosynthetic structures.

Considering the structural diversity of known phytoecdysteroids, it is possible to estimate that over 1000 possible structures might occur in nature (Dinan, 2001), and more could be detected in future from other *Vitex* plants not yet investigated like *V. doniana*. It has also been noted that most of the structural modifications are found only in minor ecdysteroids and the available biological evidence suggests that most of these modifications result in compounds with remarkable changes in activity compared to 20-ecdysteroid (Dinan *et al.*, 1999). This raises the possibility that different compounds may be isolated from *V. doniana* with different biological potentials.

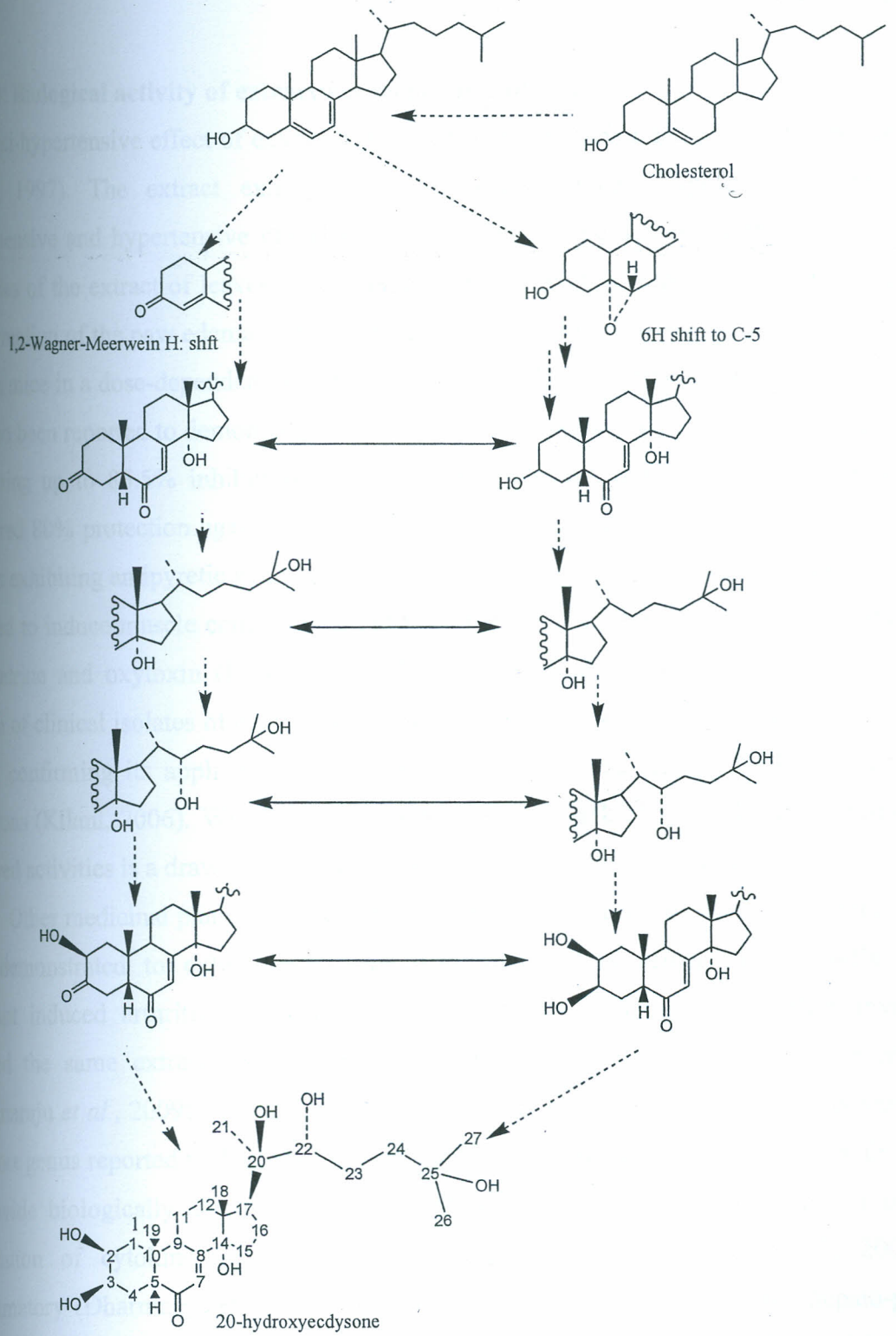

Scheme 5: Possible composite scheme of diverging pathways of ecdysteroid biosynthesis (Rees, 1995)

2.6.1.4. Biological activity of extractives from *Vitex* plants

The anti-hypertensive effect of extract of the stem bark of *V. doniana* has been reported (Ladeji *et al.*, 1997). The extract exhibited a marked dose-related hypotensive effect in both normatensive and hypertensive rats (Ladeji *et al.*, 1997). The anti-inflammatory and analgesic activities of the extract of leaves of *V. doniana* sweet has also been reported with inhibition of the formation of the paw edema induced by agar in rats and increased reaction latency to thermal pain in mice in a dose-dependent manner (Iwueke *et al.*, 2006). Ethanol extracts of the stem bark has also been reported to demonstrate dose-dependent reduction of egg albumen induced oedema conferring up to 86.5% inhibition of inflammation (Tijjani *et al.*, 2012). The same extracts conferred 80% protection against convulsive dose of penetylene tetrazole (PTZ) treated rats as well as exhibiting antipyretic activities (Tijjani *et al.*, 2012). The stem bark of *Vitex doniana* was reported to induce muscle contractions and potentiated the contractile effects of prostaglandins, ergometrine and oxytoxin (Ladeji *et al.*, 2005). Stem bark extracts were able to inhibit the growth of clinical isolates of *Salmonella typhi, Shigella dysnteriae* and *Escherichia coli* (Kilani, 2006), confirming its application in the management of dysentery and other gastroenterictic infections (Kilani, 2006). With such biological activities, lack of phytochemical account of the observed activities is a draw back to the result reported by different authors.

Other medicinal plants of the genus *Vitex* include *Vitex leucoxylon* whose stem bark have been demonstrated to exhibit significant anti-inflammatory effects on Freund's complete adjuvant induced arthritis in Sprague rats (Krishnaraju *et al.*, 2009). Further investigation realized the same extract reduced circulating proinflammatory cytokine TNF-α and 1L-1β (Krishnaraju *et al.*, 2009). The major biological activities and the phytochemical composition of the *Vitex* genus reported to date have demonstrated that the plants of this genus have the potential to provide biologically active compounds that act as antioxidants (Sarikurkcu *et al.*, 2009), modulation of cytokines and mediators of inflammation (Paulillac *et al.*, 2009), anti-inflammatory (Dharmasiri *et al.*, 2003), antimicrobial (Rahman *et al*, 2001), hepato-protective activity (Tandon, 2008), analgesic and anti-histamine (Sharma & Aithal, 1990), anti-implantation (Banerjee *et al.*, 2007). Regarding the foregoing potentials, the *Vitex* species are great natural sources necessary for the development of new drugs to meet the current need for availability of new plant-derived bioactive molecules.

CHAPTER THREE

3.0. MATERIALS AND METHODS

3.1. Plant materials

The roots of *Senna didymobotrya* Fresen were collected from Bondo constituency in Siaya County, Kenya. The plant material was identified by Mr. V. Okello (Taxonomist, Department of Botany, Maseno University) and the voucher specimen (COO-SD-2009-02) was deposited at the Herbarium of Department of Botany, Maseno University, Kenya.

The root bark and stem bark of *Caesalpinia volkensii* Harms were collected from Gatamaiyo Forest's edge (O° 55′18.34′′S; 36°42′45.66′′E) in Kiambu County of Kenya. A voucher specimen (COO-CV- 2010-01) was deposited at the Herbarium, School of Biological Science, University of Nairobi. Identification was done by Mr. Patrick Mutiso (Taxonomist) of the School of Biological Science, University of Nairobi.

The stem bark and root bark of *Vitex doniana* Sweet were collected from the Mau Forest, Kenya (0°29'07.70"S; 34°44' 02.28"E; elevation 4815 m a.s.l). A voucher specimen (COO-VD-2010-02) was deposited at the Herbarium, School of Biological Science, University of Nairobi. Identification was done by Mr. Patrick Mutiso (Taxonomist) of the School of Biological Science, University of Nairobi.

3.2. General instrumentation

Melting points were determined using a Koffler melting point apparatus and are uncorrected. Optical rotations were recorded on Perkin-Elmer 341 polarimeter in $CHCl_3$ or MeOH solutions. ^{1}H-NMR (300 MHz) and ^{13}C-NMR (75 MHz) were recorded in $CDCl_3$ using Varian Mercury 300 MHz (Varian, U.S.A) with TMS as internal standard. Some NMR spectra were measured on Bruker Avance-500 FT 500 MHz NMR spectrometer using TMS as internal standard. ESIMS: direct inlet, (70 eV) was recorded using MAT 8200A Varian Bremen instrument. HRESIMS were measured with an AccuTOFCS JMS-T100CS mass spectrometer (JEOL). IR was performed using Perkin Elmer FTIR 600 series. UV-Vis spectra were recorded on a Shimadzu UV-1650 PC (Shimadzu Corporation, Kyoto Japan). Kiesalgel 60 F_{254} (Merck) TLC plates were used and *p*-anisaldehyde was employed as visualizing agent. Silica gel (Merck 60-120 mesh ASTM) and Sephadex LH-20 (Amersham Pharmacia Biotech) were used in column

chromatographic separation. Acetic acid (May & Baker Ltd., Dagenham, England); Ibuprofen (Total Healthcare, Parwanoo, India); morphine (Martindale Pharma®, Essex, United Kingdom), hot plate (Electrothermal Eng. Ltd, MH8514B) were used for antinociceptive activity. Beckman Coulter Biomek 2000 automated laboratory workstation (Beckman coulter, Inc., Fullerton U.S.A) and Tecan Genios Plus (Tecan US, Inc., Durham, U.S.A) were used in antiplasmodial activity assay. UV spectrophotometer Microplate reader (Bio-Rad, U.S.A) was used in quantification of the adipocytes cell viability. All fine chemicals were purchased from Sigma Aldrich (St. Louis, MO), otherwise sources stated in parenthesis where applicable.

3.3. Extraction, Isolation and Identification of Isolates

3.3.1 Extraction and isolation of compounds from the *Caesalpinia volkensii* root bark

Ground-dried root bark (1.2 kg) of *C. volkensii* was extracted with cold methanol for 5 days, solvent evaporated under vacuum at 45°C to afford a brownish crude (25.4 g) extract. The extract was suspended in distilled water and then partitioned successively with *n*-hexane (CVR-1), chloroform (CVR-2), ethyl acetate (CVR-3), and *n*-butanol (CVR-4). Each fraction was evaporated under reduced pressure to afford 2.1 g, 9.2 g, 7.6 g, and 3.3 g extracts, respectively. The *n*-hexane and *n*-butanol extracts were not purified further due to low yields. The chloroform extract was purified by column chromatography (CC) on silica gel (280 g) using *n*-hexane as starting eluent and increasing polarity with chloroform to give six major fractions (C1-C6). Fraction C2 (2.2 g) eluted with 20% chloroform in *n*-hexane was recrystallized from MeOH to give voucapane (**398**) (64 mg) and the mother liquor (1.6 g) was further subjected to CC on silica gel (48 g) eluting with chloroform/*n*-hexane (3/7 v/v) to afford four fractions (C2a-C2d). Sub-fraction C2c (0.82 g) was purified by preparative TLC using $CHCl_3$-hexane, with careful spraying and heating of the TLC plate edges; two compounds, voucapan-5α-ol (**19**) (21 mg) and caesaldekarin C (**38**) (34 mg) were obtained as white amorphous solids. Fraction C3 (3.4 g) was recrystallized from MeOH to give colourless crystals of deoxycaesaldekarin (**95**) (2.4 g). Its mother liquor (0.7 g) upon fractionation over Sephadex-LH20 (50 g) column eluted with $CHCl_3$ afforded 5-hydroxy vinhaticoic acid (**399**) (58 mg) and a mixture of **38** (15 mg) and **95** (41 mg) that was separated using prep TLC (2% MeOH in $CHCl_3$). Colourless crystalline solid of compound **95** (1.5 g) was obtained from C4 (2.4 g) after crystallization from MeOH while 1α,5α-

dihydroxyvoucapane (**400**) (36 mg) was obtained from prep TLC of the mother liquor of C4 using $CHCl_3$ as eluent. Fractions C5 (0.5 g) and C6 (0.4 g) were combined, then subjected to CC with EtOAc/*n*-hexane (1/4, v/v) followed by prep TLC with 2% MeOH in $CHCl_3$ to afford 1α,6β-dihydroxyvoucapane-19β-methyl ester (**401**) (43 mg) and triacontanyl ferrulate (**402**) (57 mg).

The ethyl acetate extract (7 g) was fractionated by CC silica gel (210 g) with *n*-hexane-EtOAc gradient to give six fractions (E1-E6). Fraction E2 afforded **19** (60 mg) after crystallization in MeOH. Crystallization in MeOH of E3 (2.4 g) afforded **401** (134 mg). The mother liquor upon passing through a small CC on silica gel yielded more of **19** (20 mg) and **402** (67 mg). Fractions E4 (1.02 g) and F5 (0.74 g) were combined and passed through Sephadex LH-20 (100 g, MeOH/$CHCl_3$, 1:1) to afford two fractions. The first sub-fraction afforded **401** (43 mg) while the second sub-fraction yielded **399** (65 mg) upon crystallization from *n*-hexane/dichloromethane as white amorphous solid. Fraction E6 (210 mg) consisted of two compounds on TLC under 254 nm UV light which upon fractional crystallization afforded triacontanyl-(*E*)-caffaete (**403**) (106 mg) as brown amorphous compound. Preparative TLC of the mother liquor yielded 30′-hydroxytriacontanyl-(*E*)-ferrulate (**404**) (54 mg) as pale yellow solid.

3.3.2. Physical and spectroscopic data of compounds isolated from *Caesalpinia volkensii* root bark

Compound **19** (Voucapan-5α-ol): white amorphous solid, m.pt 98-100°C. IR (KBr) ν cm^{-1}: 706, 1509, 1648 (furan C=C), 3592 (OH). ^1H NMR and ^{13}C NMR ($CDCl_3$, 300 MHz and 75 MHz): See Tables 5 and 6. HRESIMS *m/z* 303.3139 $[M^+]$ (calcd. for $C_{20}H_{30}O_2$, 303.3157).

Compound **38** (Caesaldekarin C): colourless needles, m.pt 137-138°C. $[\alpha]_D^{25}$ =+37° (c =2.8, $CHCl_3$ at 20°C). IR (KBr) ν cm^{-1}: 3564, 1722, 1465, 705. ^1H NMR and ^{13}C NMR ($CDCl_3$, 300 MHz and 75 MHz): See Tables 5 and 6. HRESIMS *m/z* 346.1403 $[M + H]^+$ (calcd. for $C_{21}H_{30}O_4$, 346.1423).

Compound **95** (Deoxycaesaldekarin C) colourless crystals, m.p 104-105°C. uncorrected. $[\alpha]_D^{25}$ = +56.3° (c = 0.0005, $CHCl_3$). UV (MeOH) λ_{max}: 220 nm. IR (KBr) ν cm^{-1}: 726, 1509,

1652, 1710. ^{1}H NMR and ^{13}C NMR ($CDCl_3$, 300 MHz and 75 MHz): See Tables 5 and 6. ESIMS *m/z* 331 $[M+H]^+$.

Compound **398** (Voucapane): white needles, m.p 84-85°C. IR (KBr) *v* cm^{-1}: 1676, 1512, 706. ^{1}H NMR and ^{13}C NMR ($CDCl_3$, 300 MHz and 75 MHz): See Tables 5 and 6. HRESIMS 286.1851 $[M+H]^+$ (calcd. for $C_{20}H_{30}O_3$, 286.1887).

Compound **399** (5-Hydroxyvinhaticoic acid): white amorphous solid, m.pt 161-162°. $[\alpha]_D^{20}$ = +73° (c = 0.003, $CHCl_3$ at 20°C). IR (KBr) *v* cm^{-1}: 925, 1710, 3418. ^{1}H NMR and ^{13}C NMR ($CDCl_3$, 300 MHz and 75 MHz): See Table 5 and 6. ESIMS *m/z* 333 $[M+H]^+$.

Compound **400** (1α,5α-Dihydroxyvoucapane): colourless crystals, m.pt 104-105°C. $[\alpha]_D^{20}$ = +39° (c = 2.8, $CHCl_3$ at 20°C). IR (KBr) *v* cm^{-1}: 706, 1509 (C=C), 1648 (C=C), 3592 (OH). ^{1}H and ^{13}C NMR data ($CDCl_3$, 300 MHz and 75 MHz): See Tables 5 and 6. ESIMS 70 eV, *m/z* (rel. int.): 319.0 $[M+H]^+$ (100). HRESIMS *m/z*: 318.4615 $[M]^+$ (calcd. for $C_{20}H_{30}O_3$, 318.4687).

Compound **401** (1α,6β-Dihydroxyvoucapane-19β-methyl ester): colourless crystals, m.p 131-133°C. $[\alpha]_D^{25}$ = +58.3° (c = 0.0005, $CHCl_3$). IR (KBr) *v* cm^{-1}: 1509 (C=C), 1652 (C=C), 1710 (C=O), 3493 (OH). ^{1}H and ^{13}C NMR data ($CDCl_3$, 300 MHz and 75 MHz): See Table 5 and 6. ESIMS 70 eV, *m/z* (rel. int.): 363.2$[M + H]^+$, 344 $[(M + H)-H_2O]$ (70), 318 [(M + H) - CO] (60), 300 $[(M + H) - H_2O - CO]$ (55). HRESIMS *m/z*: 362.2390 $[M + H]^+$ (calcd. for $C_{21}H_{18}O_5$, 362.2321).

Compound **402** (Triacontanyl-(*E*)-ferrulate): brown amorphous solid, m.p 93-94°C. IR (KBr) *v* cm^{-1}: 934, 1461 (aromatic C=C), 1653 (C=C), 1730 (C=O), 3428 (OH). ^{1}H NMR and ^{13}C NMR ($CDCl_3$, 300 MHz and 75 MHz): See Table 7. ESIMS 613.2 $[M + H]^+$ (65) $C_{40}H_{70}O_4$, 437.0 (15), 192 (10).

Compound **403** (Triacontanyl-(*E*)-caffeate): brown amorphous solid m.p 113-115°C. IR (KBr) *v* cm^{-1}: 962, 1264 (C-O), 1513 (aromatic C=C), 1731 (C=O), 1625 (C=C), 3443, 3381 (OH). ^{1}H NMR and ^{13}C NMR ($CDCl_3$, 300 MHz and 75 MHz): See Table 7. HRESIMS, *m/z* (rel. int. %) 601.5118 $[M+H^+]$, ESIMS *m/z* 601.4 $[M + H]^+$ (40), $C_{40}H_{70}O_5$, 194.9 (40), 176.9 (20).

Compound **404** (30′-Hydroxytriacontanyl-(*E*)-ferrulate): pale yellow solid, m.p 97-99°C. IR (KBr) ν cm^{-1}: 3440, 2910, 1712, 1687, 1500, 960. ^{1}H NMR and ^{13}C NMR ($CDCl_3$, 300 MHz and 75 MHz): See Table 7. HRESIMS *m/z* (rel. int. %) 631.5223 [M+H^+]. ESIMS *m/z* 631.9 [M +$H]^+$ (69); $C_{39}H_{68}O_4$, 435.3 (20), 192.2 (68), 176.5 (32), 162.2 [caffeoyl]$^+$ (15).

3.3.3. Extraction and isolation of compounds from *Caesalpinia volkensii* stem bark

The air-dried stem bark (1.5 kg) of *C. volkensii* was extracted with methanol (2 x 5 L) for 5 days at room temperature. The crude extract was evaporated under reduced pressure to afford greenish substances (48.2 g). The extract was suspended in distilled water and then partitioned successively with *n*-hexane (CVS-1), chloroform (CVS-2), ethyl acetate (CVS-3), and *n*-butanol (CVS-4). Each fraction was evaporated under reduced pressure to afford 2.6 g, 15.5 g, 17.6 g, and 9.3 g, respectively. The crude $CHCl_3$ extract was separated by column chromatography (CC), eluting with *n*-hexane as the starting eluent increasing polarity with $CHCl_3$ and then MeOH to give ten fractions (F1-F10, each 250 ml). Fraction F3 (3.42 g) was subjected to CC on silica gel eluting with EtOAc/*n*-hexane (1:19) to afford four sub fractions (F3a-F3d, each 150 ml). Sub fraction F3b (921 mg) was crystallized from MeOH to give stigmasterol (**176**) (337 mg). The mother liquor (580 mg) was further subjected to CC using $CHCl_3$-hexane (1:4) to give voucapan-5α-ol (**19**) (102 mg) and 3-β-acetoxyolean-12-en-28-methyl ester (**405**) (43 mg). Sub fraction F3c was separated by silica gel CC eluting with $CHCl_3$/*n*-hexane (3:7) to give β-sitosterol (**177**) (23.7 mg) and **19** (35 mg). Fraction F5 (7.43 g) was subjected to CC on silica gel using *n*-hexane as the starting eluent and increasing polarity with $CHCl_3$ to afford five sub fractions (F5a-F5e, each 200 ml). Sub fraction F5c (754.3 mg) was separated by CC on Sephadex LH-20 eluting with MeOH/$CHCl_3$ (1:1) to afford three sub fractions, the first fraction consisted of chlorophyll and thus was discarded, the subsequent fractions afforded voulkensin C (**406**) (32 mg) and deoxycaesaldekarin (**95**) (53 mg) upon crystallization from MeOH, respectively. Sub fraction F5e (802.5 mg) was purified by CC on silica gel with $CHCl_3$/*n*-hexane (2:3 v/v) to give more of **406** (79.4 mg) after crystallization in MeOH. Fraction F7 (1.7 g) was subjected to CC on silica gel eluting with $CHCl_3$/*n*-hexane (2:3) to afford four sub fractions (F7a-F7d, each 150 ml). Sub fraction F7b (353.6 mg) was purified by CC on silica gel with EtOAc/*n*-hexane (1:19) to give **406** (34 mg) and voulkensin B (**407**) (42.4 mg). Sub fraction F7d (210.5 mg) was separated by CC on silica gel with EtOAc/*n*-hexane (1:1) to give more of **407**

(45 mg) and oleanolic acid (**185**) (42 mg). Fractions F1 and F2 were not purified further due the complexity of the non polar stuff while F4 and F6 were interface fractions between fractions that showed distinct spots on TLC. The last three fractions F8, F9 and F10 showed intractable spots thus were not followed further.

The crude ethyl acetate (15 g) extract was fractionated by CC on silica gel (450 g) eluting with *n*-hexane as the starting eluent and increasing polarity with $CHCl_3$ and MeOH successively to give eight fractions (E1-E8, each 250 ml). Fraction E3 (1.6 g) was subjected to CC on silica gel (48 g) eluting with EtOAc/*n*-hexane (1:4) to give **176** (143 mg) and **405** (63 mg). Fraction E5 (1.78 g) was separated by CC on silica gel (50 g) eluting with $CHCl_3$/*n*-hexane (1:1) to afford six fractions (E5a-E5f, each 150 ml). Sub fraction E5c (98.3 mg) was cystallized with CH_2Cl_2/*n*-hexane to give **407** (25 mg). Sub fraction E5e (321 mg) was purified by CC on silica gel (10 g) eluting with $CHCl_3$ (100%) to afford **185** (70.4 mg) and voulkensin A (**408**) (51.4 mg). Additional crystals of **408** (157 mg) was obtained from the subsequent sub fraction E5f after recrystallization in CH_2Cl_2/*n*-hexane.

The *n*-butanol crude (7 g) extract was subjected to CC on silica gel (200 g), eluting with $CHCl_3$-MeOH (19:1, 9:1, 4:1, and 7:3) collecting 250 ml per fraction. The first fractions (1.02 g) eluting with $CHCl_3$-MeOH, 19:1 afforded a mixture of **408** and **185** as could be evidenced by TLC upon spraying with *p*-anisaldehyde reagent. The second fractions eluted with $CHCl_3$-MeOH, 9:1 afforded caffeic acid (36 mg) which was considered as column metabolite emanating from **408**. The third fractions (1.5 g) eluted with $CHCl_3$-MeOH, 4:1 afforded 3-*O*-[β-glucopyranosyl(1→2)-*O*-β-xylopyranosyl]-stigmasterol (**409**) (124.3 mg) from $CHCl_3$-MeOH mixture (3:2). The compound showed a homogeneous spot on silica gel TLC using EtOAc/*n*-butanol/acetic acid (9:2:1) as solvent and I_2 vapour as visualizing agent. The last fraction eluted with $CHCl_3$-MeOH, 7:3 showed no distinct spot on TLC, thus was not pursued further.

A portion of **409** (50 mg) was dissolved in MeOH (10 ml) containing 2N HCl (10 ml) and refluxed on an oil bath for 6 h at 80°C. The reaction mixture was evaporated and the hydrolysate after dilution with H_2O (10 ml) was extracted with $CHCl_3$ (3 x 10 ml). The $CHCl_3$ extracts were evaporated to afford the aglycone which was identified as stigmasterol (*m/z* 413 by ESIMS and its NMR spectral data). The aqueous phase was neutralized with Na_2CO_3, filtered and evaporated in *vacuo* to give a whitish residue. The residue was compared with standard sugars by silica gel co-TLC with an authenticated sample (*n*-BuOH-EtOAc-H_2O; 5:4:1) and

visualizing the spots with aniline phthalate reagent, which indicated the sugars to be glucose and xylose.

3.3.4. Physical and spectroscopic data on compounds isolated from *Caesalpinia volkensii* stem bark

Compound **176** (Stigmasterol): white powder, m.pt 167-169°C. ^{1}H NMR and ^{13}C NMR ($CDCl_3$, 300 MHz and 75 MHz): See Table 11. ESIMS *m/z* (rel. int.): 413 $[M + H]^+$ ($C_{29}H_{48}O$).

Compound **177** (β-Sitosterol): colourless needles, m.pt 138-139°C. IR (KBr) ν cm^{-1}: 3429, 3373, 2959, 2866, 1463, 1367. ^{1}H NMR and ^{13}C NMR ($CDCl_3$, 300 MHz and 75 MHz): See Table 11. ESIMS *m/z* (rel. int): 414 $[M]^+$ ($C_{29}H_{50}O$).

Compound **185** (Oleanolic acid): white amorphous solid, m.pt 305-306°C; IR (KBr) ν cm^{-1}: 1450, 1697, 2945, 3123 and 3482. ^{1}H NMR and ^{13}C NMR ($CDCl_3$, 300 MHz and 75 MHz): See Table 10. ESIMS *m/z* (rel. int): 457 $[M + H]^+$ ($C_{30}H_{48}O$), 439 $[M\text{-}H_2O]^+$, 237 $[C_{15}H_{24}O]^+$, 221 $[C_{15}H_{28}O]^+$.

Compound **405** (3-β-Acetoxyolean-12-en-28-methyl ester): white amorphous solid, m.pt 298-300°C; IR (KBr) ν cm^{-1}: 1702 (ester) and 1675 (C=O); ^{1}H NMR and ^{13}C NMR ($CDCl_3$, 300 MHz and 75 MHz): See Table 10. ESIMS *m/z* (rel. int): 512.7 $[M + H]^+$.

Compound **406** (Voulkensin C; 16-hydroxy-11-oxocass-12-ene): white amorphous solid, m.pt 149-151°C. $[\alpha]_D^{27}$ = -36.5° (c = 0.08, $CDCl_3$). IR (KBr) ν cm^{-1}: 3385, 2958, 1610, 1523, 1450, 1376, 1284, 1164, 1105, 1070, 1048. UV (MeOH) λ_{max} (log ε): 216 (2.86). ^{1}H NMR and ^{13}C NMR ($CDCl_3$, 500 MHz and 125 MHz): See Table 8. HRESIMS *m/z* (ToF): 327.2051 (calcd. For $C_{20}H_{32}O_2Na$, 327.2052 $[M + Na]^+$).

Compound **407** (Volkensin B; 16-hydroxy-11-oxocass-12,14-diene): white crystals, m.pt 143-145°C. $[\alpha]_D^{27}$ = -18.5° (c = 0.05, $CDCl_3$). IR (KBr) ν cm^{-1}: 3423 (O-H), 2959 (C-H), 1707 (C=O), 1629 (C=C-C=C-C=O), 1457, 1376, 1370 (C=C), 1038 (C-O). UV (MeOH) λ_{max} (log ε): 227 (2.48) and 339 (3.83). ^{1}H NMR and ^{13}C NMR ($CDCl_3$, 500 MHz and 125 MHz): See Table 8. ESIMS *m/z* (rel. int): 303.1 $[M + H]^+$. HRESIMS *m/z* (ToF): 325.2134 (calcd. For $C_{20}H_{30}O_2Na$, 325.2144$[M + Na]^+$).

Compound **408** (Voulkensin A; 16-*O*-caffeoyl-11-oxocassa-12,14-diene): pale yellow solid, mp 129-131°C. $[\alpha]_D^{27}$ = -21.7° (c = 0.05, MeOH). IR (KBr) ν cm^{-1}: 3407 (O-H), 2956 and 2923 (C-H stretching), 1710 (ester), 1604 (C=O), 1517 (C=C aromatic), 1456 (C=C). UV

(MeOH) λ_{max} (log ε): 207 (2.53), 222 (4.81), 283 (3.98), 309 (2.32) and 318 (3.85) nm. ^{1}H NMR and ^{13}C NMR ($CDCl_3$, 500 MHz and 125 MHz): See Table 8. HRESIMS *m/z* (ToF): 465.2636 (calcd. For $C_{29}H_{26}O_5$, 465.2651[M + H]$^+$), 482.2901 (calcd. For $C_{29}H_{26}O_5NH_4$, 482.2899 [M + NH_4]$^+$), 487.2455 (calcd. For $C_{29}H_{26}O_5Na$, 487.2455 [M + Na]$^+$).

Compound **409** {3-*O*-[β-glucopyranosyl(1→2)-*O*-β-xylopyranosyl]-stigmasterol}: white amorphous solid, m.p 231-233°C. $[\alpha]_D^{25}$ + 51.2° (c = 0.1, MeOH). IR (KBr) ν cm^{-1}: 3517 and 3452 (O-H), 2925 and 2856 (C-H stretching), and 1647 (C=C). ^{1}H NMR and ^{13}C NMR (CD_3OD, 500 MHz and 125 MHz): See Table 9. HRESIMS *m/z* (rel. int): 707.4450 (cald. For $C_{40}H_{66}O_{10}$, 707.4448 [M + H]$^+$).

3.3.5. Extraction and isolation of compounds from *Senna didymobotyra* roots

Air dried and ground roots of *S. didymobotrya* (approximately 2 kg) were extracted using methanol at room temperature for 5 days. The solvent was evaporated in *vacuo* and a dark red residue obtained (58 g) which was suspended in distilled water (1 L) and partitioned between *n*-hexane (SD-F1), ethyl acetate (SD-F2), *n*-butanol (SD-F3) and water residue (SD-4F). The yields of the partitioned extracts yielded 4.3, 24.5, 16.5 and 9.6% of the crude extract, respectively. Portions (5 g) of each fraction were used for bioassays. Preliminary bioassay screening of the fractions were performed and the results indicated SD-F3 as the most active, a portion (20 g) of which was subjected to column chromatography (CC) over silica gel eluting with *n*-hexane followed by stepwise gradient of *n*-hexane-$CHCl_3$ to pure $CHCl_3$ and finally 5% MeOH in $CHCl_3$. Seventy fractions of 100 ml each were collected and combined on the basis of TLC analysis to afford six main fractions (Fr. 1-6). Fraction 1 and 2 (8.6 g) eluted with *n*-hexane-$CHCl_3$ (9:1, 8:2, 7:3, 3:2) were purified by CC over silica gel (300 g) using *n*-hexane-$CHCl_3$ to yield chrysophanol (**269**) (4.3 g). Chrysophanol-10,10′-bianthrone (**295**) (3.7 g) crystallized out in $CHCl_3$-MeOH from fraction 3 (6 g) after elution with *n*-hexane-$CHCl_3$ (1:1 and 2:3). Further purification of the mother liquor on Sephadex LH-20 CC resulted to isolation of physcion (**273**) (67 mg), stigmasterol (**176**) (47 mg) and physcion-10,10'-bianthrone (**299**) (25 mg). Fraction 4 (2.3 g) eluted with *n*-hexane-$CHCl_3$ (3:7) was subjected to CC on Sephadex LH-20 (100 g) eluting with MeOH/$CHCl_3$ (1:1) to yield two fractions; the first fraction afforded obtusifolin (**285**) (52 mg) and nataloemodin-8-methyl ether (**279**) (54 mg) after further preparative TLC. Fraction 5 (3 g) eluted with *n*-hexane-$CHCl_3$ (1:4, 1:9, and 0:1) was

rechromatographed over silica gel using *n*-hexane-EtOAc with an increasing amount of EtOAc to afford compounds; **279** (32 mg), **285** (69 mg) and 1,6-di-*O*-methylemodin, **410** (21 mg).

3.3.6. Physical and spectroscopic data on compounds isolated from *Senna didymobotrya* roots

Compound **269** (Chrysophanol; 1,8-dihydroxy-3-methylanthracene-9,10-dione): orange needles, m.pt 194-196°C. IR (KBr) ν cm^{-1}: 3469 (OH), 1719 C=O and 1633 (chelated C=O). ^1H NMR and ^{13}C NMR ($CDCl_3$, 300 MHz and 75 MHz): See Tables 12 and 13. ESIMS positive mode, 255.08 $[M+H]^+$. UV (MeOH) λ_{max} nm (log ε): 213 (2.07), 253 (3.32), 302 (3.21) and 432 (3.99)

Compound **273** (Physcion; 1,8-dihydroxy-6-methoxy-3-methylanthracene-9,10-dione): brick red needles (MeOH), m.pt 204-206°C. ^1H NMR and ^{13}C NMR ($CDCl_3$, 300 MHz and 75 MHz): See Tables 12 and 13. ESIMS positive mode, *m/z* 285.3 $[M+H]^+$. UV (MeOH) λ_{max} nm (log ε): 225 (3.97), 246 (3.42), 280 (2.75), 302 (3.21) and 430 (4.21).

Compound **279** (Nataloemodin-8-methyl ether; 1,7-hydroxy-8-methoxy-3-methylanthracene-9,10-dione), yellow crystals, m.p 235-236°C. ^1H NMR and ^{13}C NMR ($CDCl_3$, 300 MHz and 75 MHz): See Tables 12 and 13. ESIMS positive mode, *m/z* 285.2 $[M+H]^+$. UV (MeOH) λ_{max} nm (log ε): 217 (4.02), 265 (3.87), 286 (3.67) and 433 (4.03). IR (KBr) ν cm^{-1}: 3468, 3095, 1675, 1626, 1583.

Compound **285,** (Obtusifolin; 2,8-dihydroxy-1-methoxy-3-methylanthracene-9,10-dione), yellow crystals (MeOH), m.pt 202-204°C. ^1H NMR and ^{13}C NMR ($CDCl_3$, 300 MHz and 75 MHz): See Tables 12 and 13. ESIMS positive mode, *m/z* 285.3 $[M+H]^+$. UV (MeOH) λ_{max} nm (log ε): 232 (3.7), 252 (4.01), 281 (3.65) and 403 (3.02).

Compound **295** (Chrysophanol-10,10'-bianthrone): brown amorphous solid, m.p 210-212°C. $[\alpha]_D^{27} = 0°$ (c = 0.05, $CDCl_3$). IR (KBr) ν cm^{-1}: 1575, 1580 (aromatic), 1610 (chelated C=O), 3401 (OH). ^1H NMR and ^{13}C NMR ($CDCl_3$, 300 MHz and 75 MHz): See Table 14. ESIMS positive mode, 479.2 $[M+H]^+$, 239.10$[M^+/2 + H]^+$.

Compound **299** (Physcion-10,10'-bianthrone): light yellow crystals, m.p 273-274.5°C: $[\alpha]_D^{25} = 0°$ (c = 0.05, $CDCl_3$). IR (KBr) cm^{-1}: 1585, 1600 (chelated C=O), 1630 (C=O) and 3502 (OH). ^1H NMR and ^{13}C NMR ($CDCl_3$, 300 MHz and 75 MHz): See Table 14. ESIMS positive mode, 539.5 $[M + H]^+$. 270 $[M^+/2]$ 241 $[M/2\text{-}CO]^+$.

Compound **410**, (1,6-di-*O*-methylemodin; 2,8-dihydroxy-1,6-dimethoxy-3-methylanthracene-9,10-dione): red-orange crystals, m.p 216-218°C. ^{1}H NMR and ^{13}C NMR ($CDCl_3$, 300 MHz and 75 MHz): See Table 12 and 13. ESIMS positive mode *m/z*: 315.0 $[M+H]^+$. UV (MeOH) λ_{max} nm (log ε): 254 (3.2), 268 (3.71), 289 (3.02) and 436 (4.01).

3.3.7. Extraction and isolation of compounds from *V. doniana* root bark

Pulverized, dry root bark *V. doniana* (5 kg) was extracted successively with *n*-hexane and MeOH in a soxhlet extraction apparatus. The concentrated MeOH extract was diluted with H_2O and the filtered dark brownish solution extracted successively with $CHCl_3$, EtOAc and *n*-BuOH, using a continuous liquid-liquid extraction apparatus. The $CHCl_3$ extract (120 g) was chromatographed on silica gel (Merck silica gel 70-230 mesh) using $CHCl_3$-MeOH as eluent, with increasing MeOH content and two main fractions were selected by TLC examination of the eluates. The first fraction was repeatedly chromatographed to afford 70 mg of 2,3-acetonide-24-hydroxyecdysone (**411**). The second fraction was rechromatographed and crystallized from MeOH-CH_2Cl_2 to give 11-hydroxy-20-deoxyshidasterone (**412**) (64 mg).

The EtOAc extract (47 g) was subjected to CC on silica gel (Merck silica gel 70-230 mesh), using a similar eluting solvent as that employed for the $CHCl_3$ extract and three fractions were subjected to further separation. Fraction 1 eluted with $CHCl_3$-MeOH (19:1 to 9:1) was rechromatographed to afford a fraction containing an ecdysteroid according to TLC colour reactions with *p*-anisaldehyde-sulphuric acid. The impure ecdysteroid fraction (150 mg) was further purified by MPLC [column: Spherisorb ODS 2-5 pm, 250 x 4.6 mm; mobile phase: MeOH-H_2O (1:1); flow rate: 1.0 ml/min; detector: 254 nm] to furnish 32 mg of 21-hydroxyshidasterone (**413**). Fraction 2 (432 mg) eluted with $CHCl_3$-MeOH (17:3 to 4:1) crystallized in MeOH-EtOAc to afford 102 mg of 24-hydroxyecdysone (**414**) as a colourless needle-like crystals, which was identified by TLC and spectroscopic (IR and ^{1}H NMR) comparison with those of authentic sample (Lafont *et al.*, 2002). The mother liquor afforded 61 mg of **414** after MPLC (same conditions as described earlier) purification and crystallization in MeOH-EtOAc. A white amorphous solid precipitated from fraction three eluted with $CHCl_3$-MeOH (4:1 to 7:3) from the EtOAc extract, which was then triturated using hot MeOH several times to afford 43 mg a mixture of **414** and unidentified component.

The *n*-BuOH extract (34 g) was chromatographed on silica gel (Merck SilGel 70-230 mesh) using $CHCl_3$-MeOH as eluent, adjusting the polarity using MeOH and three major fractions were obtained. The first fractions contained the previously isolated compounds from the EtOAc extracts (fraction 2) while the second fractions (361 mg) gave a positive colouration of ecdysteroids with *p*-anilashyde reagent on TLC and was subjected to reverse-phase MPLC separation resulting into isolation of 2,3-acetonide-22-*O*-β-D-glucosyl-20-hydroxyecdysone (**415**) (40 mg). Much of the compound (119 mg) was obtained by precipitation of the fractions after repeated CC on silica gel. A portion of **415** (50 mg) was dissolved in MeOH (10 ml) containing 2N HCl (10 ml) and refluxed on boiling water bath for 6 h. After concentration at reduced pressure, the reaction product was diluted with water and extracted with ethyl acetate. The aqueous phase was neutralized with Na_2CO_3, filtered and evaporated in *vacuo* to give a whitish residue. It was identified as glucose by co-TLC with an authenticated sample (*n*-BuOH-EtOAc-H_2O; 5:4:1) and visualizing the spots with aniline phthalate reagent. The observed optical rotation of the glycone (sugar) $[\alpha]_D$ = +41.6° (c 0.5 in H_2O, 26°C) revealed that it was D-glucose. The identity of the aglycone moiety of this compound was made by analysis of the ^1H and ^{13}C NMR with reference to reported data (Lafont *et al.*, 2002).

3.3.8. Physical and spectroscopic data on compounds isolated from *Vitex doniana* root bark

Compound **411** (2,3-Acetonide-24-hydroxyecdysone; 2β,3β-acetonide-14α,22R,24R,25-tetrahydroxy-cholest-7-en-6-one): white needles crystals, m.pt 158-160°C. $[\alpha]_D^{25}$= + 56.4° (c = 0.9 MeOH). UV (MeOH) λ_{max} nm (log ε): 244 (3.95). IR ν_{max}^{KBr} cm^{-1}: 1050, 1376, 1462, 1653, 2937 and 3423. ^1H NMR and ^{13}C NMR (CD_3OD, 300 MHz, 75 MHz): See Tables 15 and 16. ESI-MS *m/z*: 520.7 (20) $[M]^+$, 502 (5) $[M - H_2O]^+$, 484 (25) $[M - 2H_2O]^+$, 466 (5) $[M - 3H_2O]^+$, 448 (20) $[M - 4H_2O]^+$, 396 (20), 360 (50) $[M+H - C_{20}\text{-}C_{29}\ C_8H_{17}O_3]^+$, 342 (80) $[M+H\text{-}(C_8H_{17}O_3 + H_2O)]^+$, 300 (100) $[M+H\text{-}(C_8H_{17}O_3 + CH_3C\text{-} + H_2O)]^+$, 282 (20) $[M+H - (C_8H_{17}O_3 + CH_3C\text{-} + 2H_2O)]^+$, 161 (40) $[C_8H_{17}O_3]^+$, 125 (30) $[C_8H_{17}O_3 - 2H_2O]^+$.

Compound **412** (11-hydroxy-20-deoxyshidasterone; {(2β,3β,5β,11β,22R) 22, 25-Epoxy-2,3,11,14-tetrahydroycholest-7-en-6-one}): white powder, m.p 258-262°C. $[\alpha]_D^{25}$ = +7° (c = 0.01, MeOH). UV (MeOH) λ_{max} nm (log ε): 249 (3.54). IR ν_{max}^{KBr} cm^{-1}: 1059, 1654, 2832 and 3427. ^1H NMR and ^{13}C NMR (CD_3OD, 500 MHz, 125 MHz): See Tables 15 and 16. ESI-MS (rel. int) 463

(60) $[M + H]^+$, 445 (100) $[M + H - H_2O]^+$, 427 (30) $[M + H - 2H_2O]^+$, 407 (60) $[M + H - 3H_2O]^+$.

Compound **413** (21-hydroxyshidasterone; {(2β,3β,5β,22R)-22,25-epoxy-2,3,14,20,21-pentahydroxycholest-7-en-6-one}): m.p. 232-234°C. $[\alpha]_D^{25}$ = +13° (c = 0.1, MeOH). UV (MeOH) λ_{max} nm (log ε): 249 (2.34). IR ν_{max}^{KBr} cm^{-1}: 1057, 1514, 1652, 2968, 3448. ^1H NMR and ^{13}C NMR (CD_3OD, 300 MHz, 75 MHz): See Tables 15 and 16. ESI-MS *m/z*: 479 (50) $[M + H]^+$, 461 (40) $[M + H - H_2O]^+$, 443 (40) $[M + H - 2H_2O]^+$, 425 (35) $[M + H - 3H_2O]^+$, 407 (100) $[M + H - 4H_2O]^+$, 380 (60) $[M + H - C_6H_{11}O,C_{20}/C_{22}]^+$, 362 (30) $[M + H - C_6H_{11}O - H_2O]^+$, 344 (65) $[M + H - C_6H_{11}O - 2H_2O]^+$, 326 (35) $[M + H - C_6H_{11}O - 3H_2O]^+$, 308 (30) $[M + H - C_6H_{11}O - 4H_2O]^+$.

Compound **414** (24-hydroxyecdysone): white crystals, m.p 244-246°C. IR ν_{max}^{KBr} cm^{-1}: 1039, 1693, 2933, and 3424. ^1H NMR and ^{13}C NMR (CD_3OD, 300 MHz, 75 MHz): See Tables 15 and 16. UV (MeOH) λ_{max} nm (log ε): 299 (3.07). ESI-MS *m/z*: 481(65) $[M + H]^+$, 463 (35), $[M + H - H_2O]^+$, 445 (20) $[M + H - 2H_2O]^+$, 427 (20) $[M + H - 3H_2O]^+$, 348 (40), $[M + H - C_8H_{13}O_3]^+$, 330 (30), $[M + H - C_6H_{13}O_3 - H_2O]^+$, 320 (20), $[M + H - C_8H_{17}O_3]^+$, 162 (10), $[C_8H_{17}O_3 + H]^+$.

Compound **415** (2,3-acetonide-22-*O*-β-glucosyl-20-hydroxyecdysone); white powder, m.p 262-264°C. UV (MeOH) λ_{max} nm (log ε): 242 nm (4.01). IR ν_{max}^{KBr} cm^{-1}: 1072, 1375, 1465, 1642, 2822, 2922 and 3367. ^1H NMR and ^{13}C NMR (CD_3OD, 500 MHz, 125 MHz): See Table 15 and 16. ESIMS *m/z*: 683 (70) $[M + H]^+$, 665 (60) $[M + H - H_2O]^+$, 647 (40) $[M + H - 2H_2O]^+$, 502 (60), $[M + H - \text{hexose}]^+$, 484 (40) $[M + H - (\text{hexose} + H_2O)]^+$, 466 (30) $[M + H - (\text{hexose} + 2H_2O)]^+$, 448 (50) $[M + H - (\text{hexose} + 3H_2O)]^+$, 388 (40), $[M + H - (C_{22}\text{-}C_{27}, C_6H_{13}O_2 + \text{hexose})]^+$), 360 (100) $[M + H - (C_{20}\text{-}C_{27}, C_8H_{16}O_2 + \text{hexose})]^+$.

3.4. Bioassay studies

3.4.1. *In vitro* antiplasmodial activity assay

The crude extract and pure compounds were assayed using a non-radioactive assay technique (Smilkstein *et al.*, 2004) to determine 50% growth inhibition on cultured parasites. An *in vitro* drug susceptibility assay using the fluorochrome called "SYBR Green", a non-radioactive intercalating DNA marker that accurately depicts *in vitro* parasite replication. Two parasitic strains, chloroquine-sensitive Seirra Leone I (D6) and chloroquine resistant Indochina I (W2), of *Plasmodium falciparum* were grown as described by Johnson *et al.*, (2007). The culture-adapted *P. falciparum* were added on to the plate containing dose range of drugs (5×10^{-4} ng/ml) and incubated in a gas mixture (5% CO_2, 5% O_2, and 90% N_2) at 37°C for 72 h and frozen at -80°C. After thawing, lysis buffer containing SYBR green I (1 x final concentration) was added directly to the plates and gently mixed using the Beckman Coulter Biomek 2000 automated laboratory workstation.

The plates were incubated for 10-15 min at room temperatures in the dark. Parasite growth inhibitions were quantified by measuring the per-well relative fluorescence units (RFU) of "SYBR green 1" dye using the Tecan Genios Plus with excitation and emission wavelengths of 485 nm and 535 nm, respectively. Differential counts of relative fluorescence units (RFU) were used in calculating IC_{50} for each drug using Prism 4.0 software for windows (Graphpad Software, San Diego, USA). Three separate determinations were carried out for each sample. Replicates had narrow data ranges hence presented as mean ± SD.

3.4.2. *In vivo* antinociceptive assays

3.4.2.1. Laboratory animals

Swiss albino mice (20 – 25 g) of either sex used in this study were in-bred and obtained from the Division of Laboratory Animals, Central Drug Research Institute, Lucknow, India. The experimental procedures were in accordance with the guidelines for Care and Use of Laboratory animals of the Institute provided by the Animal Care Committee of Division of Laboratory Animals. The guidelines conformed to United States National Institutes of Health Guidelines for Care and Use of Laboratory Animals in Biomedical Research (NIH, 1985). The animals were

kept in well-ventilated and hygienic atmosphere maintained under standard environmental conditions and fed with standard rodent pellet diet (Liptan India Ltd) and water *ad libitum*.

3.4.2.2. Acute toxicity test

Acute toxicity to mice was performed according to the method of Lorke, (1983). Mice were divided into control and test groups (n = 6). First group served as normal control. Crude methanol extract of *Caesalpinia volkensii, Senna didymobotyra* and *Vitex doniana* were administered intraperitoneal (i.p) to different groups at the increasing doses of 200, 400, 500, 1000 and 2000 mg/kg. After injections of extracts, mice were allowed food and water *ad libitum*. All the animals were observed for possible mortality cases and behavioral changes for 72 h.

3.4.2.3. Analgesic effect on the hot plate test

The modified method of Eddy & Leimbach (1953) was used. Groups of mice (5 per group) of either sex (17-30 g) were used.

Figure 3: A hot plate analgesic meter with a mouse (Electrothermal Eng. Ltd, MH8514B) used for antinociceptive activity

The mice were initially screened by placing the animals in turn on a hot plate set at 55 ± 1°C (Fig. 3) and the animals which failed to lick the hind paw or jump (nociceptive response) within 15 seconds were discarded. Eligible animals were divided into five groups of five mice each and pre-treatment reaction time for each mouse was determined before drug treatment so that each

animal serves as it is own control. The time until the animal licked the paw, flutter any of the paws or jump was taken as reaction time and were recorded with aid of an inbuilt stopwatch. Mice in the different groups were then treated with normal saline water [10 ml/kg, per oral (p.o)], test samples (crude extracts or pure isolates, 100 mg/kg) and morphine [10 mg/kg, subcutaneous injection (*s.c*)]. The latency was recorded after 30 and 60 minutes following oral administration of extracts (100 mg/kg), normal Saline (10 ml/kg) and subcutaneous administration of morphine (10 mg/kg). A post-treatment cut-off time of 30 seconds was used to avoid paw tissue damage (Omisore *et al.*, 2004). Percentage analgesic activity was estimated using the formula I.

$$\text{Inhibition (\%)} = \frac{[\text{Post-treatment Latency}] - [\text{Pre-treatment Latency}]}{(\text{Cut-off Time}) - (\text{Pre-treatment Latency})} \text{ X } 100 \qquad \text{(Formula I)}$$

3.4.2.4. Acetic acid (chemical-induced) writhing method

Abdominal writhes consist of contraction of the abdominal muscle together with a stretching of the hind limbs, induced by i.p injection in mice of acetic acid (0.8% solution in normal saline, 0.1 ml/10 kg), the nociceptive agent (Koster *et al.*, 1959). The test samples (crudes extracts and/or pure samples, 100 mg/kg) or Ibuprofen (10 mg/kg, p.o) was administered to mice (animals fasted overnight and divided into five groups of six animals each) 60 min before intraperitoneal injection of acetic acid (0.6%, v/v in normal saline, 10 ml/kg, i.p). Normal saline was used as the control. The number of writhes (characterized by contraction of the abdominal musculature and extension of the hind limbs) was counted for 30 min at 5 min interval of intraperitoneal injection of acetic acid (Adeyemi *et al.*, 2004). Percentage writhing inhibition was calculated using formula II.

$$\text{Inhibition (\%)} = \frac{\text{Number of writhes [control]} - \text{Number of writhes [Treatment]}}{\text{Number of Writhes [Control]}} \text{ X } 100 \text{ (Formula II)}$$

3.4.2.5. Anti-inflammatory activity

Carrageenan-induced rat paw oedema method described by Adeyemi *et al.*, (2004) was adopted. Sprague Dawley rats (140 - 170 g) of either sex were randomly divided into groups of 5 animals each, and were used after a 12 h fast but allowed free access to water except during the experiment. *Vitex doniana* extracts and compounds (100 mg/kg/bw. p.o.), diclofenac 50 mg/kg, p.o. (reference drug) and 0.05% DMSO in normal saline 10 ml/kg, p.o. (Control) were administered one hour before subcutaneous injection of 100 µl of carrageenan ($1\%^{w}/_{v}$ in 0.9 %

normal saline) into the callus of the right hind paw of the animal. Paw volume was measured by means of a volume displacement method using a plethysmometer (Ugo-Basile, Varese, Italy) prior to the injection of carrageenan and thereafter at 1, 2, 3, 4, 5, 6 and 24 h. Oedema was expressed as the increase in paw volume (mL) after carrageenan injection relative to the pre-injection value for each animal. The data obtained for the various groups were reported as mean ± S.E.M. and percentage inhibition of oedema were calculated with the formula III.

$$\text{Inhibition (\%)} = \frac{\text{Increase in paw oedema [Control]} - \text{Increase in paw oedema [treated]}}{\text{Increase in paw oedema [control]}} \text{ X } 100 \text{ (formula III)}$$

3.4.2.6. Statistical analysis

Results obtained were expressed as mean ± standard error of mean (SEM) or standard deviation (SD). The data were analyzed using one way ANOVA followed by Bonferroni posttests and Dunnett's multiple comparison tests. Values were considered significant when $P \leq 0.05$.

3.4.3. Lipid lowering *in vivo* assays

3.4.3.1. Laboratory animals

Animals study was performed with the approval of Animal Care Committee of Division of Laboratory Animal, Central Drug Research Institute, Lucknow, India and conformed to the guidelines for Care and Use of Laboratory Animals of the United States National Institutes of Health Guidelines for Care and Use of Laboratory Animals in Biomedical Research (NIH, 1985). Male rats of *Charles Foster* strains (100-150g) were used. Six animals in each group were kept in controlled conditions, temperature 25-26°C, relative humidity 60-80% and 12/12h light/dark cycles (light from 8.00 a.m to 8.00 p.m) under hygienic conditions. They were kept on a standard pellet diet (Liptan India Ltd) and water *ad libitum*.

3.4.3.2. Acute toxicity test in rats

Five groups of 5 rats each fasted for 12 h prior to the experiment were administered sample crude extracts at doses of 1, 2, 4, 8 and 10 g/kg. Animals in the different groups were observed for 12 h post-treatment for immediate signs of toxicity. Mortality observed in each group within 24 h was recorded. Animals that survived were observed for signs of delayed toxicity for a further 7 days. The LD_{50} were estimated by the log dose-probit analysis method where applicable (Litchfield & Wilcoxon, 1949).

3.4.3.3. Triton induced hyperlipidaemia

Triton induced hyperlipidaemia was performed following the procedures described by Wing & Robinson (1968). Rats were divided into twelve groups; control, triton induced and triton plus test samples (crudes extracts, 250 mg/kg and pure isolates, 100 mg/kg b.w) treated groups containing six animals per group. One group was treated with triton plus standard drug (Gemfibrozil). Hyperlipidaemia was induced by administration of triton WR-1339 at a dose of 400 mg/kg intraperitoneally (i.p) to animals of all the groups except the control. The test samples were macerated with gum acacia (0.2 mg), suspended in distilled water (2 ml) and fed simultaneously with triton at a dose of 250 mg/kg (crude samples) or 100 mg/kg (compounds) per oral administration (p.o).

Animals of control and triton treated groups were given the same amount of gum acacia (10% w/v) suspension in distilled water (vehicle). After 18 hours, the animals were anaesthetized with thiopentene solution (50 mg/kg b.w) prepared in normal saline and 1 ml blood was withdrawn from retro-orbital sinus using glass capillary in EDTA coated Eppendorf tubes. The blood was centrifuged (2500 rpm) at 4°C for 10 min and plasma was separated. Plasma was diluted with normal saline (ratio 1:3) and used for analysis of total cholesterol (Tc), triglycerides (Tg), phospholipids (Pl) and protein (Pr) by standard methods (Appendix 2). Post heparin lipolytic activity (PHLA) and lecithin cholesterol acyltransferase activity (LCAT) were assayed by method of Wing & Robinson (1968) (Appendix 2) using spectrophotometer and Bechmann auto-analyzer and standard kits.

3.4.3.4. Statistical analysis

All experiments were done in triplicate and results are reported as means ± standard deviation (SD) (n = 6). One way analysis of variance (ANOVA) was performed by comparison of result from triton treated group with control, triton and test samples with triton only. Significant differences were determined at $P \leq 0.01$.

3.4.4. Cell culture and adipocytes differentiation assay

Adipocytes differentiation assay was performed as described by Gregoire *et al.*, (1998). The 3T3-L1 cell line and supplements were obtained from Invetrogen (Carlsbad, Califonia, U.S.A). All other fine chemicals were purchased from Sigma Aldrich (St. Louis, MO). The cells were maintained in 5% CO_2 at 37°C in Dulbecco's-modified Eagle medium (DMEM) containing 10%

calf serum and 1% penicillin-streptomycin. The cells were cultured in 100 mm diameter culture dishes at a density of 2 x 104 cells per well, the medium was changed after every 2 days and cells were seeded into 96-well culture plates.

When the cells reached confluence (day 0) after 5 days of incubation, the medium was exchanged for fresh medium containing 0.5 mm 3-isobutyl-1-methylxanthine (IBMX), 1 µg/ml insulin and 1µM dexamethasone (DEX) for 48 h, and the samples dissolved in dimethyl sulfoxide were added. The samples extracts and pure isolates from *S. didymobotrya* and *V. doniana* and insulin were added to the medium at the time of every medium change during the 8 days of incubation. To test the effect of the compounds (**273, 279, 299, 411, 413, 414** and **415**) on the differentiation of 3T3-L1 preadipocytes to adipocytes, they were used at different concentrations (0.1 µM, 10 µM and 50 µM) throughout differentiation. For assessment of adipogenesis the differentiated cells were fixed in 4% paraformaldehyde w/v for 20 min, washed with phosphate buffered saline (PBS) and stained with 0.34% Oil Red O in 60% isopropanol for 15 minutes (Gong *et al.*, 2004). The unbound stain was washed with PBS thrice and stain was extracted with 80% isopropanol by keeping it at room temperature for 30 minutes on an orbital shaker. Fat accumulation was examined under a Nikon Eclipse TS 100 microscope (X 400) equipped with a Nikon Coolpix camera (Nikon Corporation, Japan). The bound dye was eluted with 80% isopropanol at room temperature for 30 min, and the optical density (OD) was read at 550 nm using a microplate reader (Bio-Rad, U.S.A). Percent inhibition of adipogenesis in test samples treated culture cells was calculated in comparison with the OD in vehicle control treated cultures.

3.7.4.1. 3-(4,5-dimethylthiazol-2-yl)-2,5-diphenyltetrazolium bromide (MTT) cell viability assay

Cell viability was assessed using 3-(4,5-dimethylthiazol-2-yl)-2,5-diphenyltetrazolium bromide (MTT) assay (Denizot & Lang, 1986). The cells were seeded in 96-well plates. Equal number of 3T3-L1 preadipocytes (5000 cells/well) was plated in 96-well bottom plates and differentiated as above. Vehicle (dissolution medium) control culture wells received only a maximum of 0.1% DMSO. Matured adipocytes were incubated in 5% CO_2 at 37°C mixed with serum-free DMEM with test samples at various concentrations for a period 24 h. Thereafter, 0.5 mg/ml of MTT reagent was added to each well and the microplate was incubated further for 4 h at 37°C in the presence of 5% CO_2. Finally, the cells were solubilised and the extent of MTT reduction to

formazon within cells was quantified by measuring the absorbance at 540 nm using a microplate reader (BioRad, U.S.A). The cell proliferation index of the samples treated wells were calculated from the mean absorbance (from quadruplicate wells) considering that of the vehicle treated culture as 100% using Formular III.

$$\% \text{ cell proliferation index: } \frac{\text{Absorbance of control} - \text{absorbance of treated sample x 100}}{\text{absorbance of control}} \qquad \text{Formular III}$$

3.4.5. Antioxidant activity assays

3.4.5.1. Superoxide radical inhibition

The effect of crude extracts and compounds on generation of superoxide anions in enzymatic system of xanthine-xanthine oxidase was investigated as described by Bindoli *et al.*, (1985). Xanthine oxidase inhibition activity was measured in a solution containing 0.1 ml of 80 µM xanthine in 2.4 ml phosphate buffer (0.1 M, pH 7.4) and 0.1 ml of 0.03 units/ml of xanthine oxidase, were mixed with known concentrations of samples extracts and fractions (100 µg/ml), compounds (5-100 µM) and standard drug (Allopurinol, 20 µg/ml, 10-50 µM) to a final volume of 2.5 ml. The change in optical density/min measured at 295 nm was compared with the change in reaction mixture without any test sample. The results for test samples were expressed as mean ± SD of three determinations (µmol uric acid formed/min).

The effects of test samples on nitroblue tetrazolium (NBT) reduction by $O_2^{\cdot-}$ anions were measured (Leong *et al.*, 2008) with slight modification. A reaction mixture containing 0.03 units/ml of xanthine oxidase, 0.1 ml of 160 µM xanthine and 0.1 ml of 160 µM NBT in a 2.4 ml of phosphate buffer (1 M, pH 7.4) was incubated at room temperature (25-27°C) for 30 min in the presence of crude samples (5-200 µg/ml) or pure compounds (5-100 µM) followed by addition of 1 ml glacial acetic acid to terminate the reaction. Absorbance was read at 560 nm. Water was used as a blank while (Allopurinol, 20 µg/ml, 10-50 µM) was used as a reference compound.

The effect of test samples on generation of $O_2^{\cdot-}$ anions in a nonenzymic system was performed according to Bindoli *et al.*, (1985). The reaction mixtures comprising of 0.1 ml of 320 µM NBT, 0.2 ml of 160 µM NADH and 0.2 ml of 10 µM phenozine methosulphate in 2.0 ml of pyrophosphate buffer (0.1 M, pH 9.2) were incubated for 90 seconds at 37°C in the presence of various concentrations of crude extracts (5 - 200 µg/ml), compounds (5 - 100 µM) and

Allopurinol (50 µM). The reaction was terminated by adding 1 ml glacial acetic acid and the optical density was read at 560 nm against water blank. The results for crude extracts and pure compounds were expressed as mean ± SD of three determinations (nmol formazon formed/min) in the two later assays.

The activity of the pure compounds from the three assays were further transformed to percentage inhibitory activity (IA%), which was calculated using the following formula IV: IA (%) =1- $\frac{As)}{Ao}$ x 100 (Formula IV), where A_S is the absorbance of the sample and A_0 is the absorbance of the blank. The IC_{50} value of each sample was determined from the linear regression of probit-percentage curves against samples concentrations.

3.4.5.2. Hydroxyl radical inhibition

Hydroxyl radical inhibition was assayed as described by Halliwell *et al.* (1987) with a slight modification. The assay was based on quantification of the degradation product of 2-deoxyribose by condensation with thiobarbituric acid (TBA). Hydroxyl radical is generated by the Fe^{3+}-ascorbate-EDTA-H_2O_2 system (the Fenton reaction). The reaction mixture contained, in a volume of 1 ml, 2-deoxy-2-ribose (2.8 µM); KH_2PO_4-KOH buffer (20 µM, pH 7.4); $Fe_2SO_4.7H_2O$ (100M); EDTA (100M); H_2O_2 (1.0M); ascorbic acid (100M) and various concentrations of the test samples (100 and 200 mg/ml) or standard drug (mannitol, 100 mg.ml). After incubation for 1 h at 37°C, 0.5 ml of the reaction mixture was added to 1 ml 2.8% trichloroacetic acid (TCA), followed by 1 ml 1% aqueous TBA and the mixture incubated at 90°C for 15 min to develop colour. After cooling to 20°C, the absorbance was measured at 532 nm against the control (reaction mixture without test sample). Percentage inhibition was evaluated based on the difference between the test sample and control.

IA (%) =1- $\frac{As)}{Ao}$ x 100 (Formula IV), where A_S is the absorbance of the sample and A_0 is the absorbance of the blank. The IC_{50} value of each sample was determined from the linear regression of probit-percentage curves against samples concentrations.

3.4.5.3. Microsomol lipid peroxidation assay

The crude samples and pure isolates were tested for their inhibitory action against microsomol lipid peroxidation *in vitro* by nonenzymatic inducers using TBA method (Okhawa *et al.*, 1979). Different samples concentrations (100 and 200 µg/ml) and standard drug (α-tocopherol, 100 µg/ml) was added to the liver homogenate. Lipid peroxidation was initiated by addition of 1.5 ml of 20% aqueous acetic acid, 0.2 g of sodium dodecyl sulphate and 1.5 ml TBA (1% in acetic acid). The volume of the mixture was made up to 4.0 ml with distilled water, followed by 95°C incubation in a water bath for 60 min. After incubation the tubes were cooled to room temperature (25-27°C) and final volume adjusted to 5 ml with distilled water in each tube. Five (5.0) ml *n*-butanol-pyridine (15:1) mixture was added and the content vortexed thoroughly for 2 min. After centrifugation at 3000 rpm for 10 min, the organic upper layer was taken and optical density (O.D) of test sample tubes and control (reaction mixture without test samples) were read at 532 nm spectrophotometrically.

IA (%) =1- $\frac{As)}{Ao}$ x 100 (Formula IV), where A_S is the absorbance of the sample and A_0 is the absorbance of the blank. The IC_{50} value of each sample was determined from the linear regression of probit-percentage curves against samples concentrations.

CHAPTER FOUR

4.0. RESULTS AND DISCUSSION

4.1. Phytochemical analysis

4.1.1. Structural elucidation of compounds from *Caesalpinia volkensii* root bark

Antinociceptive assay of the partitioned fractions revealed that both chloroform and ethyl acetate extracts had relatively ($P \leq 0.01$) higher activity compared to the *n*-hexane and *n*-butanol extracts. This impelled the bioassay guided fractionation of chloroform and ethyl acetate extracts by various chromatographic techniques leading to isolation of 1α,5α-dihydroxyvoucapane (**400**) and 1α,6β-dihydroxyvoucapane-19β-methyl ester (**401**) alongside known compounds voucapan-5α-ol (**19**), voucapane (**398**) (Cheenpracha *et al.*, 2006), caesaldekarin C (**38**) (Kitagawa *et al.*, 1996), deoxycaesaldekarin C (**95**) (Dickson *et al.*, 2007), 5-hydroxyvinhaticoic acid (**399**) (Vieira *et al.*, 2007) and triacontanyl-(*E*)-ferrulate (**402**), triacontanyl-(*E*)-caffaete (**403**) (Saha *et al.*, 1991) and 30′-hydroxytriacontanyl-(*E*)-ferrulate (**404**) (Doghal *et al.*, 1999). Analysis of ESIMS, ^{1}H (Table 5) and ^{13}C (Table 6) NMR spectral data indicated that compounds **19**, **400**, **398** and **399** had 20 carbon atoms while **38, 95,** and **401** had 21 carbon atoms. On the basis of comparison spectral data with those previously isolated from related *Caesalpinia* species, the molecular skeleton implied furanoditerpenoids.

4.1.1.1. Voucapane (398)

Compound **398** was isolated from *C. volkensii* from the chloroform extract of the roots as the least polar component as white crystalline solids with m.p 84-85°C. The IR spectrum showed no hydroxyl absorption bands instead had prominent peaks for a furan ring at 1678 and 1509 cm^{-1} (C=C) absorption. The ^{1}H NMR (Table 5) spectrum showed signals for three tertiary methyl groups at δ_H 0.92 (3H, s), δ_H 1.04 (3H, s), δ_H 1.06 (3H, s) and a secondary methyl signal δ_H 0.99 (3H, d, J = 7.0 Hz). Two low field adjacent olefinic protons observed at δ_H 6.15 and 7.19 (each 1H, d, J = 1.7 Hz) were typical of a 1,2-disubstituted furan ring. On the other hand, methylenic protons showing J_{gem}, *trans* $J_{ax/ax}$ and gauche $J_{ax/eq}$ coupling [δ_H 2.41 (dd, J = 14.0, 8.3 Hz, H-11α) and δ_H 2.32 (dd, J = 14.0, 10.5 Hz, H-11β] and a mutliplet at δ_H 2.56 (1H, H-14) confirmed a cassane diterpene skeleton. This fact was unambiguously supported by ^{13}C NMR and DEPT

spectra which exhibited 20 carbon atoms (Table 6). In fact, four olefinic carbon atoms of the furan ring (δ_C 109.6, 122.6, 140.3, 149.8), four methyl groups, six methylene carbons, four aliphatic methine carbons and two quaternary aliphatic carbon atoms suggested the structure to be voucapane **398** (Cheenpracha *et al.*, 2006, Godoy *et al.*, 1989), a fact that was confirmed by the ESIMS molecular weight *m/z* 286 corresponding to $C_{20}H_{30}O$.

4.1.1.2. Voucapan-5α-ol (19)

Compound **19**, isolated as white crystals with m.pt 98-100°C exhibited molecular ion at *m/z* 303.3139 from HRESIMS corresponding to $C_{20}H_{30}O_2$ molecular formula. The IR (KBr) showed bands at 3592 cm^{-1} (free OH absorption) and 1648 and 1509 cm^{-1} furan (C=C) stretching frequencies and 706 cm^{-1} indicating presence aromatic system. The ^1H NMR spectrum (Table 5) had resonances due to three tertiary methyls at δ_H 0.97 (s), 1.08 (s), 1.11 (s) and a secondary methyl at δ_H 1.04 (d, J = 9 Hz) same as **398**. The presence of a 1, 2-disubstituted furan was also evident from signals at δ_H 6.20 and 7.24 (each 1H, d, J = 1.7 Hz,). The ^{13}C NMR and DEPT spectra were similar to those of **398** except for the presence of five quaternary carbons of which one was oxygenated at δ 76.9 (C-5) (Table 6) and the disappearance of an up field double doublet at δ_H 1.17 (dd, J = 10, 3 Hz, H-5). The compound was identified as voucapan-5α-ol (**19**) by comparison of the spectral information (Tables 5 and 6) with the literature data (McPherson *et al.*, 1986; Roengsumran *et al.*, 2000).

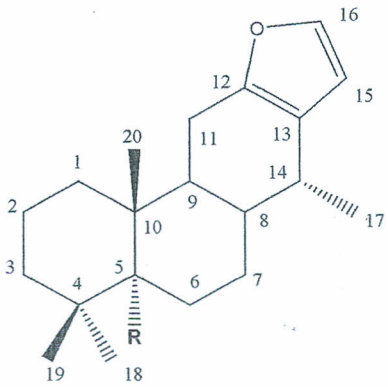

19: R = OH
398: R = H

4.1.1.3. Caesaldekarin C (38)

Caesaldekarin C (**38**) was isolated as colourless needles with m.pt 137-138°C. The IR spectrum had absorbance characteristic of hydroxyl (3564 cm^{-1}), ester (1722 cm^{-1}) and furan ring (1525, cm^{-1}) groups. The HRESIMS data indicated molecular ion of *m/z* 346.1403 corresponding to $C_{21}H_{30}O_4$. The ^1H NMR spectrum had resonances assignable to two tertiary methyl groups δ_H 0.98 and 1.34 (both s), one secondary methyl (δ_H 1.18, d, J = 7 Hz) and one methyl ester (δ_H 3.84, s) together with α, β-disubstituted furan ring (δ_H 6.34 and 7.25, both br s) groups. The ^{13}C NMR spectrum (Table 6) showed 21 carbon signals attributable to the presence of one methyl ester (δ_C 52.5), three methyl [δ_C 18.3 (C-17), 23.3 (C-18), and 15.8 (C-20)], six methylene [δ_C 33.3 (C-1), 19.5 (C-2), 35.5 (C-3), 25.7 (C-6), 28.8 (C-7) and 24.6 (C-11)], three methine [δ_C 32.8 (C-8), 32.1 (C-9) and 49.8 (C-14)] and two quaternary [δ_C 42.7 (C-4) and 38.5 (C-10)] carbons together with four sp^2 [δ_C 110.6 (C-15), 123.6 (C-13), 141.3 (C-16) and 150. 6 (C-12)], a carbinyl carbon [δ_C 77.3 (C-5)] and one carboxyl ester at δ_C 178.3. The carbinyl carbon was attributed to C-5, corroborated by the IR spectrum at 3564 cm^{-1} stretching frequency and by HMBC correlation of δ_H 1.34 (s) for Me-18 and δ_H 0.98 (s) for Me-20 protons to δ_C 77.3 (C-5) (Fig. 4). The 2D (HMBC and COSY), ^1H and ^{13}C NMR spectra of compound **38** and compounds **95** were comparable except for the oxygenated carbon C-5 in **38** resulting in a down-field shift of signals for H-3β, H-6α, and 18-Me by 0.33, 0.45 and 0.13 ppm, respectively. These proton and carbon chemical shift values of compound **38** agreed with those reported for caesaldekarin C (Kitagawa *et al.*, 1996).

4.1.1.4. Deoxycaesaldekarin C (95)

Deoxycaesaldekarin C (**95**) was isolated as colourless crystalline solids with m.pt 104-105°C from methanol had molecular formula $C_{20}H_{30}O_3$, deduced from ESIMS molecular ion at *m/z* 331 $[M + H]^+$ and NMR (Tables 5 and 6) spectral evidence. The presence of ester and furan functional groups was evident from the IR spectrum absorptions at 1710 and 1509 cm^{-1}, respectively. The ^1H and ^{13}C NMR spectra of compound **95** showed the presence of two tertiary methyl groups [δ_H 0.83 and 1.21 (both s)], one secondary methyl group [δ_H 1.03 (d, J = 6.0 Hz)], one methyl ester group [δ_H 3.69 (s)] and α,β-disubstituted furan ring [δ_H 7.22 and 6.19 (each d, J = 1.7 Hz)] (Table 5). The ^{13}C NMR spectrum (Table 6) indicated the presence of sixteen sp^3

carbons [4 methyls, 6 methylenes, 3 methines, and 3 quaternary carbons], four sp^2 carbons [2 methine and 2 quaternary carbons] and one carboxyl group with comparable values as **38**, except that of carbinol carbon is replaced with a methine carbon. The HMBC spetrum (Fig. 4) indicated correlation of a proton at δ_H 6.19 with carbons at δ_C 122.4 (C-13), 140.4 (C-16) and 149.6 (C-12) while the proton at δ_H 7.22 was correlated to carbons at δ_C 109.5 (C-15), 122.4 (C-13) and 149.6 (C-12). A proton at δ_H 2.64 (H-14) connected to carbon at δ_C 49.1 (C-14) showed cross peaks with carbons at δ_C 18.7 (C-17), 31.6 (C-9), 122.4 (C-13) and 149.6 (C-12), suggesting the proximity of C-14 to the furan moiety. On the same note, the HMBC data revealed a correlation between H-11 and δ_C 122.4 (C-13) indicating the methylene carbons were connected to the furan ring. On the basis of NOESY analysis, the two methyl groups at C-18 and C-20 were shown to be in α-equatorial and β-axial orientations, respectively, due to spartial correlation between methoxy (δ 3.69) and C-20 methyl protons (δ 0.83) (Fig. 4). Compound **95** was identified as deoxycaesaldekarin C due to identical spectral data with the literature data (Dickson *et al.*, 2007; Peter *et al.*, 1998).

4.1.1.5. 5-Hydroxy vinhaticoic acid (399)

Compound **399** isolated as white crystalline solid m.pt. 162-163°C showed a molecular ion $[M+H^+]$ at *m/z* 334 in the ESIMS spectrum, which together ^{13}C NMR and DEPT data (Table 6) conferred a molecular formula of $C_{20}H_{28}O_4$. The presence of carboxyl functionality was evident from IR absorptions [925 (C-O-H out of plane bending), 1710 (C=O stretching) and 3418 (O-H stretching)] cm^{-1}. The ^1H and ^{13}C NMR spectral data (Tables 5 and 6) of compound **399** were similar to those of **38** except for the absence of the OMe signal, thus indicating the presence of a free carboxylic acid instead of the methyl ester at C-19. A fact further supported by HMBC spectrum, in which the methyl protons at δ_H 1.36 (Me-18) correlated with the carbons at δ_C 36.5 (C-3), δ 77.5 (C-5), δ 41.5 (C-4), and δ 184.5 (C-19). The spectral data (Table 5 and 6) were comparable to those of vinhaticoic acid except for the presence of hydroxyl group at C-5 (Vieira *et al.*, 2007). Therefore, compound **399** was characterized as 5-hydroxy vinhaticoic acid a derivative of vinhaticoic acid reported from *Caesalpinia crista* stem bark (Cheenpracha *et al.*, 2005).

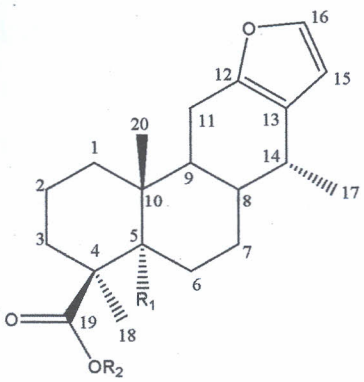

38: R_1 = OH; R_2 = Me
95: R_1 = H; R_2 = Me
399: R_1 = OH; R_2 = H

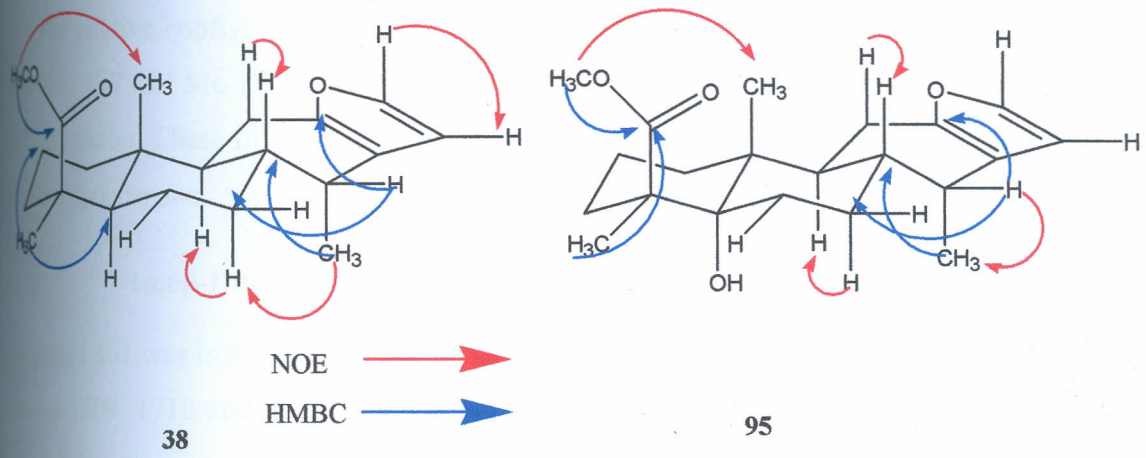

38 **95**

Figure 4: NOE and HMBC correlations for compound **38** and **95**

4.1.1.6. 1α,5α-Dihydroxyvoucapane (400)

Compound **400** was obtained as colourless needle-like crystals with m.p 104-105°C. Assignment of the molecular formula $C_{20}H_{18}O_3$ was based on ^1H and ^{13}C NMR data (Table 5 and 6) and ESI mass peak at *m/z* at 318.9, confirmed by HRESIMS (318.4615 $[M]^+$, calcd. 318.4687). Its IR (KBr) spectrum showed bands at 3592 (OH), 1648 and 1509 cm^{-1} (furan ring absorptions) (Cheenpracha *et al.*, 2006). The ^1H NMR spectrum showed characteristic peaks of a 2,3-furanocassane framework (Cheenpracha *et al.*, 2006). The presence of α, β-disubstituted furan ring was deduced from the ^1H NMR resonances at δ_H 6.22 and 7.25 (each 1H, d, J = 1.7 Hz). The ^1H NMR spectrum showed the presence of three methyl groups attached to quaternary carbon at δ_H 0.98 (3H, s, Me-20), 1.10 (3H, s, Me-19), 1.12 (3H, s, Me-18), a secondary methyl at δ_H 1.06 (3H, d, J = 7 Hz, Me-17) and a low field proton attached to carbon bearing an oxygen

functionality at δ_H 3.51 (1H, d, J = 3.8 Hz). The ^{13}C NMR (Table 6) and DEPT spectra displayed 20 carbons including a sp^3 quaternary carbon at δ_C 77.1 (C-5), sp^3 methine carbon at δ_C 72.6 (C-1), five methylenes, four olefinic, four methyls, three methines and two quarternary carbons. Heteronuclear Multiple Bond Coherence (HMBC) (Fig. 5) correlations between the oxymethine proton at δ_H 3.51 and the carbons at δ_C 77.1 (C-5), 36.5 (C-3) and 32.7 (C-9) together with the correlations of the methyl proton at δ_H 0.98 (s) and the carbons at δ_C 72.6 (C-1), 77.1 (C-5) and 32.7 (C-9) established the location of the two hydroxyl groups at C-1 and C-5. On the basis of the *trans/anti/trans* ring junction (A/B/C) spatial orientation of cassane framework and the $^3J_{1,2}$ = 3.8 Hz, H-1 is in β-*equatorial* position exhibiting a dihedral angle *ca.* 60°C to H-2eq and H-2ax. The relative configuration was confirmed by NOE correlations between Me-18 and Me-20 as well as H-7 and Me-17. Lack of NOE correlation on H-1 to H-9 implied β-orientation for the carbinol proton. These observations allowed establishment of the new compound **400** as 1α,5α-dihydroxyvoucapane.

4.1.1.7. 1α,6β-Dihydroxyvoucapane-19β-methyl ester (401)

Compound **401** was isolated as colourless crystals, with m.pt 131-133°C. Its IR (KBr) absorption bands at 1509, 1710 and 3493 cm^{-1} indicated the presence of a furan sp^2 bonds, a carbonyl and hydroxyl groups, respectively. The molecular formula of compound **401** was established as $C_{21}H_{18}O_5$ 363.2390 $[M+H]^+$ (calcd. for $C_{21}H_{18}O_5$, 363.2393) based on HR-ESI mass spectrum while ESI Mass spectrum showed $[M+H]^+$ peak at *m/z* 363.2. The presence of 2,3-disubstituted furan ring was deduced from ^1H NMR signals (Table 5) for a pair of aromatic protons [δ_H 6.20 and 7.22, (each 1H, br s)] and four sp^2 carbon signals [δc 110.8 (C-15), 122.9 (C-13), 141.4 (C-16) and 150.7 (C-12)]. The ^1H NMR spectrum also had resonances for four methyl groups; two of these were quaternary methyl at δ_H 0.83 (3H, s, Me-20) and 1.21 (3H, s, Me-18), while the third was a secondary methyl at δ_H 1.04 (3H, d, J = 7 Hz, Me-17) and the fourth methyl ester at δ_H 3.70 (3H, s). The presence of two carbinol protons was evident from signals at δ_H 3.52 (1H, br t, $W_{h/2}$ = 7 Hz) and 3.92 (1H, br t, $W_{h/2}$ = 16 Hz). The HSQC spectrum of compound **401** revealed that the two carbinol protons were directly attached to carbons at δ_C 75.6 and δ_C 71.9, respectively. Moreover, ^{13}C NMR (Table 6), DEPT spectra indicated the presence of 12 sp^3 carbons (4 methyl carbons, 4 methylenes carbons, 2 methines, 2 quaternary carbons) alongside the four furan sp^2 carbons, two oxygenated carbons and one carbonyl carbon (δ_C 179.1). The

location of the carbinol proton at δ_H 3.52 was established to be on C-1 on the basis of its HMBC correlations with C-2 (δ_C 20.2), C-5 (δ_C 39.2), C-20 (δ_C 16.0) and C-9 (δ_C 28.3) (Fig. 5). Long range HMBC correlation observed between proton signal at δ_H 3.92 and δ_C 49.8 (C-4) which in turn correlated with δ_C 32.5 (C-8) and 42.6 (C-10) indicated that the second hydroxyl group was at C-6 (δ_C 71.9). In addition, the HMBC correlation of methyl proton at δ_H 1.21 (Me-18) with the ester carbonyl carbon at δ_C 179.1 (C-19) indicated connection of the carboxymethyl group to C-4 (δ_C 49.7). The spartial orientation of cassane-type framework indicated that the methyl ester is on the β-face due to the NOE correlation between Me-20 protons and methyl ester protons (Fig. 5). The cross peak observed between Me-18 and H-6, indicated that H-6 was α-equatorial and the hydroxyl moiety being β-axial. This justified the assignment of substituents on ring A and B. A proton at δ_H 2.62 (m, H-14) which correlated with a carbon at δ_C 36.2 (C-14) in the HSQC spectrum was observed to show cross peaks with carbons at δ_C 18.2 (Me-17), 28.3 (C-9), 31.3 (C-7), 110.8 (C-15) and 150.7 (C-12) in the HMBC spectrum, suggesting that C-14 must be connected to the furan ring. The appearance of 17-methyl as a doublet in the ^{1}H NMR indicated that C-14 was not oxygenated. The NOE correlation between Me-17 and H-7 established the configuration at C-14 orienting the Me-17 as α-*axial* while the H-7 on the β-*equatorial* face.

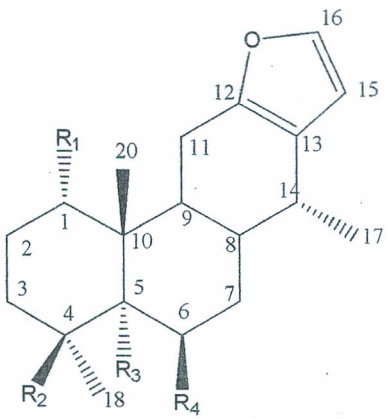

	R_1	R_2	R_3	R_4
400:	**OH**	**Me**	**OH**	**H**
401:	**OH**	**CO_2Me**	**H**	**OH**

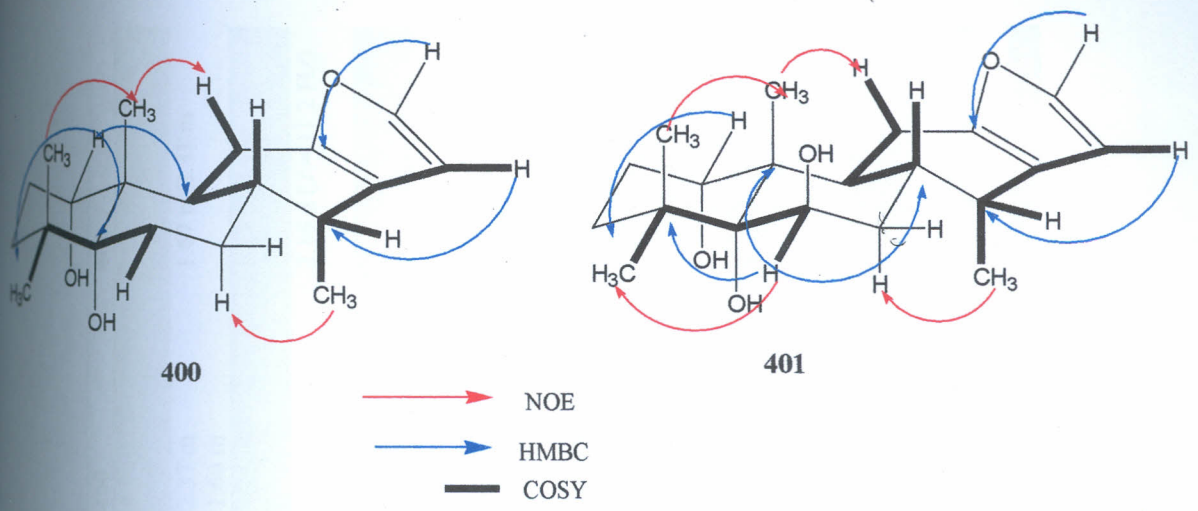

Figure 5: HMBC, NOESY and COSY correlation on compound **400** and **401**

The HMBC spectrum indicated that the carbon signal at δ_C 23.2 (C-11) could be assigned as the methylene carbon connected to furan ring based on $^3J_{HC}$ correlations between germinal protons [δ_H2.75 (1H, dd, J = 16.8, 6.4 Hz); 2.47 (1H, dd, J = 16.4, 10 Hz)] and δ_C 122.9 (C-13). Complete bond connectivity was determined using ^{1}H-^{1}H COSY and HMBC correlations (Fig. 5) thus, characterizing the compound **401** as 1α,6β-dihydroxyvoucapane-19β-methyl ester. Although several cassane furanoditerpenoids have been isolated from the genus *Caesalpinia*, compound **400** and **401** are reported for the first time as new natural products.

Table 5: ^{1}H NMR spectral data for compound **19, 38, 95, 398-401** ($CDCl_3$, 300 MHz)

Atom	19	38	95	398	399	400	401
1α	1.39 m	2.38 m	2.48 m	1.32 m	2.76 m	3.51 d (J = 3.8 Hz)	3.52 br s ($W½$ = 7.0 Hz)
1β	1.65 m	1.73 m	1.76 m	1.60 m	1.61 m		
2α	1.22 m	1.67 m	1.50 m	1.18 m	1.89 m	2.37 m	1.67 m/2.31 m
2β	1.64 m	1.78 m	1.63 m	1.59 m	1.66 m	1.66 m	
3α	1.46 m	1.57 m	1.45 m	1.35 m	1.87 m	1.23 m	1.71 m/2.48 m
3β	1.51 m	2.14 m	1.81 m	1.46 m	1.65 m	1.72 m	
5	-------		1.86 m	1.17 dd (J = 10, 3 Hz)		------	2.16 d (J = 11.2 Hz)
6α	1.27 m	1.96 m	1.51 m	1.23 m	1.92 m	1.69 m	3.92 t ($W½$ = 16.0 Hz)
6β	1.65 m	1.77 m	1.77 m	1.57 m	1.78 m	1.72m	
7α	1.52 m	2.76 m	1.52 m	1.56 m	2.76 m	1.56 m	1.61 m
7β	1.83 m	1.66 m	2.72 m	1.79 m	1.67 m	2.39 m	2.27 m
8	1.87 m	2.01 m	1.81 m	1.82 m	1.96 m	1.88 m	2.21 m
9	1.66 m	1.91 m	1.58 m	1.64 m	1.87 m	1.58 m	1.98 dt (J = 11.1, 6.6 Hz)
11α	2.46 dd (J = 14.0, 8.3 Hz)	2.65 dd J = 16.1, 6.6 Hz)	2.50 dd (J = 16.4, 7.0 Hz)	2.41 dd (J = 14.0, 8.0 Hz)	2.66 dd (J = 16.1, 6.6 Hz)	2.45 dd (J = 14.3, 10.6 Hz)	2.75 dd (J = 16.8, 6.4 Hz)
11β	2.37 dd (J = 14.0, 8.4 Hz)	2.49 dd (J = 16.1, 10.3 Hz)	2.35 dd (J = 16.4,10.3 Hz)	2.32 dd (J = 14.0, 10.5 Hz)	2.50 dd (J = 16.5, 10.3 Hz)	2.36 dd (J = 14.3, 3 Hz)	2.47 dd (J = 16.4, 10.5 Hz)
14	2.60 m	2.77 m	2.64 m	2.56 (m)	2.79 m	2.62 m	2.62 m
15	6.20 d (J = 1.7 Hz)	6.34 br s	6.19 d (J = 1.7 Hz)	6.15 (d, J = 1.7 Hz)	6.22 d (J = 1.7 Hz)	6.22 d (J = 1.7 Hz)	6.20 br s
16	7.23 d J = 1.7 Hz)	7.25 br s	7.22 d (J = 1.7 Hz)	7.19 (d, J = 1.7 Hz)	7.23 d (J = 1.7 Hz)	7.25 d (J = 1.7 Hz)	7.22 br s
17	1.04 d (J = 7.0 Hz)	1.18 d (J = 7.0 Hz)	1.03 d (J = 6.6 Hz)	0.99 (d, J = 7.0 Hz)	1.17 d J = 7.0 Hz)	1.06 d (J = 7.0 Hz)	1.04 d (J = 6.6 Hz)
18	1.11(s)	1.34 s	1.21 s	1.06 (s)	1.36 s	1.12 s	1.21 s
19	1.08(s)			1.04 (s)		1.10 s	-----
20	0.97(s)	0.98 s	0.83 s	0.92 (s)	0.98 s	0.98 s	0.83 s
OCH_3		3.84 s	3.69 s				3.70 s

Table 6: ^{13}C NMR spectral data of compounds **19**, **38**, **95**, **398-401** ($CDCl_3$, 75 MHz)

Atom	19	38	95	398	399	400	401
1	32.7	33.3	32.3	32.5	38.8	72.6	75.6
2	22.6	19.5	17.4	18.2	22.7	22.5	20.2
3	36.5	35.5	34.7	36.4	36.5	36.5	33.7
4	41.4	42.7	41.7	41.2	41.5	41.5	49.8
5	76.9	77.3	37.6	34.5	77.5	77.1	39.2
6	34.9	25.7	27.9	24.4	24.7	34.8	71.9
7	24.9	28.8	24.8	22.3	28.2	23.9	31.3
8	31.7	32.8	31.6	31.5	32.8	28.3	32.5
9	28.3	32.1	31.6	28.0	31.7	32.7	28.5
10	38.6	38.5	32.1	38.4	38.5	38.6	42.6
11	25.9	24.6	23.9	25.7	24.9	25.8	23.2
12	150.2	150.6	149.6	149.8	149.8	149.9	150.7
13	122.7	123.6	122.4	122.6	122.6	122.6	122.9
14	37.8	49.8	49.1	37.6	38.0	37.8	36.2
15	109.4	110.6	109.5	109.6	109.9	109.6	110.8
16	140.1	141.3	140.4	140.3	140.3	140.3	141.4
17	18.4	18.4	18.7	17.5	18.3	17.7	18.2
18	24.6	23.3	22.5	24.7	24.7	25.0	25.9
19	17.8	178.3	177.5	17.1	184.5	18.5	179.1
20	17.4	15.8	15.0	17.0	17.3	17.3	16.0
21		52.5	51.6				52.2

4.1.1.8. Triacontanyl-(*E*)-ferrulate (402)

Compound **402** was obtained from ethyl acetate extract of *C. volkensii* root bark as a brown amorphous solid, m.pt. 93-94°C. The ESIMS indicated a molecular ion of $[M]^+$ *m/z* 613.2. The IR spectrum of the compound indicated the presence of hydroxyl and ester groups at 3428 and 1730 cm^{-1}, respectively in addition to absorption bands for aromatic and vinylic moieties at 1653 and 1464 cm^{-1}, respectively. The ^1H NMR spectrum (Table 7) exhibited characteristic aromatic proton signals with an ABX (δ_H 6.93, dd, J = 8.1, 1.2 Hz, H-6; 7.05 d, J = 8.1 Hz, H-5 and 7.08, d, J = 1.2 Hz, H-2) spin system alongside a pair of downfield shifted doublets for *trans* vinylic protons (δ_H 6.31, d, J = 15 Hz, H-8 and 7.63, d, J = 16 Hz) typical of ferrulic acid moiety. In the aliphatic region, a singlet observed at δ_H 5.87 was assigned to phenolic hydroxyl proton while methoxyl protons appeared as a singlet at δ_H 3.95. Signals for a deshielded methylene (δ_H 4.21, t, J = 6.7 Hz), a methylene envelope (δ_H 1.27, s) and a methyl triplet (δ_H 0.90, s), indicated the presence of a long alkyl chain. The ^{13}C NMR (Table 7) confirmed the presence of a 4-hydroxy-3-methoxy cinnamic acid derivative with resonance attributable to a carbonyl group (δ_C 167.9), two deshielded oxygen bearing quaternary carbons, five sp^2 hybridized methine carbons, quaternary carbon, a methoxyl carbon and an oxymethylene carbon. The difference in mass

between 4-hydroxy-3-methoxy cinnamic moiety ($C_{10}H_9O_4$) and the molecular ion the *m/z* 613 will leave an alkyl chain of mass 421 a.m.u equivalents to the C_{30} *n*-alkyl. Therefore, the structure of compound **402** was established as triacontanyl ferrulate, reported as new natural product.

4.1.1.9. Triacontanyl-(*E*)-caffaete (403)

Compound **403** isolated as a brown amorphous solid m.pt 113-115°C showed $[M+H]^+$ ion at *m/z* 600.5 on ESIMS, suggesting a molecular mass of 600 equivalent to $C_{39}H_{68}O_4$ and consistent with the structure of triacontanyl-(*E*)-caffeate confirmed by NMR data. In spite of the apparent difference between **402** and **403**, the ^1H and ^{13}C NMR spectra (Table 7) were similar except for the absence of methoxyl group in **403**. The ^1H NMR spectrum of compound **403** showed signals characteristic for 3,4-dihydroxy-*trans*-cinnamic moiety [δ_H 6.26 (d, J = 16 Hz); δ_H 6.99 (d, J = 8 Hz); δ_H 6.87 (d, J = 8 Hz); δ_H 7.10 (s); δ_H 7.57 (d, J = 16 Hz)] and triacontanyl unit [δ_H 0.89 (t, J = 6.8 Hz); δ_H 1.27 (br, s); δ_H 1.72 (quin, J = 6.7 Hz); δ_H 4.20 (t, J = 6.7 Hz)]. The deshielded nature of the oxymethylene signal (δ_H 4.20) confirmed its link to the carbonyl of the 3,4-dihydroxy cinnamic moiety and thus provided evidence for ester formation. The spectroscopic data were in good agreement with those published data for triacontanyl-(*E*)-caffaete **403** (Saha *et al*., 1991).

4.1.1.10. 30′-Hydroxytriacontanyl-(*E*)-ferrulate (404)

Compound **404** isolated as pale yellow solid with m.pt 97-99°C was identified from the ESIMS spectrum as *m/z* 630.5, which was 16 a.m.u higher than the mass for **402**, this suggested an additional O to the skeleton of **402**. The ^1H NMR (Table 7) data for **404** were comparable to that of **402** except absence of the up field triplet for the terminal methyl and presence of two triplets of almost equal intensity and coupling constants at δ_H 4.21 and 3.66 (2H, J = 6.6 Hz each) indicating two oxymethylene groups, ascribed to a methylene attached to ester linkage (Ar-OC-CH_2-R) and a methylene protons attached to hydroxyl groups (-CH_2OH), respectively. The signal for -OH group appeared at δ_H 3.51 (*s*) and a broad singlet at δ_H 1.16 showed the presence of the remaining 56H for the $(CH_2)_{28}$ groups. The ^1H and ^{13}C NMR were comparable to the data for 34-hydroxytetratriacontanyl ferrulate isolated from Plumeria bicolor (Doghal *et al*., 1999) except for

the difference in mass. Therefore, the new compound was named 30′-hydroxytriacontanyl-(*E*)-ferrulate.

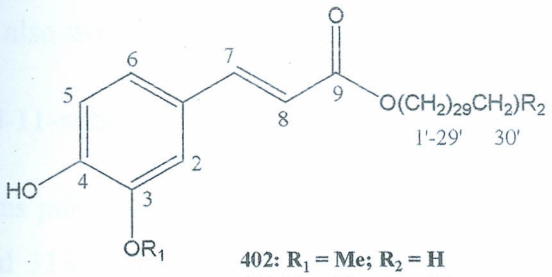

402: R_1 = Me; R_2 = H
403: R_1 = H; R_2 = H
404: R_1 = Me; R_2 = OH

Table 7: ^{1}H (300 MHz) and ^{13}C (75 MHz) NMR spectral data for compounds **402-404** ($CDCl_3$)

Atom	402		403		404	
	^{1}H NMR	^{13}C NMR	^{1}H NMR	^{13}C NMR	^{1}H NMR	^{13}C NMR
1	------	129.9	------	127.4	-----	129.3
2	7.08 (d, 1.2 Hz)	114.3	7.10 (br s)	100.9	7.05 (s)	114.3
3	-------	144.9	------	145.4	-----	148.6
4	-------	148.6	------	146.4	----	146.4
5	7.05 (d, J = 8.1 Hz)	115.5	6.87 (d, J = 8 Hz)	114.0	7.09 (d, J = 7.7 Hz)	115.5
6	6.93 (d, J = 8.1, 1.2 Hz)	122.3	6.99 (d, J = 8 Hz)	122.4	6.93 (d, J = 8.1 Hz)	122.3
7	7.63 (d, J = 16 Hz)	144.1	7.57 (d, J = 16 Hz)	144.1	7.63 (d, J = 15.8 Hz)	144.1
8	6.31 (d, J = 16 Hz)	115.4	6.26 (d, J = 16 Hz)	115.6	6.31 (d, J = 15.7 Hz)	115.8
9	-------	167.9	-------	167.9	-----	169.9
1′	4.21 (2H, t, J = 6.7 Hz)	64.8	4.20 (2H, t, J = 6.7 Hz)	65.2	4.21(t, J = 6.6 Hz)	64.8
2′			1.72 (2H, quin J = 6.7 Hz)	31.9		
$(CH_2)_n$	1.27 (56H, s, $28CH_2$)	22.7-31.9	1.27 (54H, s, $27CH_2$)	22.6-30.1	1.16 (56H, s, $28CH_2$)	22.7-31.9
CH_3 CH_2OH	0.90 (3H, t, J = 6.8 Hz)	14.1	0.89 (3H, t, J = 6.8 Hz)	14.5	3.66 (t, J = 6.6 Hz)	63.1
OCH_3	3.95 (s)	56.1			3.96 (s)	56.8
@OH	5.87 (s)		5.48 (s)		5.88 3.51	

4.1.2: Structural elucidations of compounds from *Caesalpinia volkensii* stem bark

The air-dried ground stem bark of *C. volkensii* was extracted with methanol, and then the extract partioned into *n*-hexane, $CHCl_3$, ethyl acetate and *n*-butanol, successively. Separation and purification of the three later extracts led to the isolation of three new cassane diterpenes [voulkensin A, (**408**), voulkensin B, (**407**), and voulkensin C, (**406**)] and one new steroidal glycoside [3-*O*-[β-glucopyranosyl(1→2)-*O*-β-xylopyranosyl]-stigmasterol (**409**)] together with

two known triterpenes [oleanolic acid (**185**) and 3-β-acetoxyolean-12-en-28-methyl ester (**405**)] and two common steroids [stigmasterol (**176**) and β-sitosterol (**177**)]. Some cassane furanoditerpene isolated [(voucapan-5-ol (**19**), caesaldekarin C (**38**) and deoxycaesaldekarin C (**65**)] from the root bark were also isolated from the stem bark extracts (Section 4.1.1).

4.1.2.1. 16-*O*-Caffeoyl-11-oxocassa-12,14-diene (Voulkensin A) (408)

Compound 408 was isolated as pale yellow solid with m.pt 129-130°C. The UV spectrum (λ_{max} 207, 222, 283, 253, 293, and 318 nm) suggested the presence of conjugated system. The IR absorption at 3407, 1710, 1604, 1456 cm^{-1} in association with the ^{13}C NMR spectroscopic data suggested the presence of hydroxyl, carbonyl, ester carbonyl, and aromatic functionalities. It showed pseudo-molecular ion $[M + Na]^+$ at *m/z* 487.2429 ($C_{29}H_{36}O_5$) in the HRESIMS spectrum predicting 12 degrees of unsaturation.

The ^1H NMR spectrum indicated resonances for three methyl groups [δ_H 1.06, 1.11 and 1.12 (each s)], an exocyclic methylene protons [δ_H 4.75 and 4.84 (br s each)], and an oxymethylene protons [δ_H 4.20 (2H, $W_{h/2}$ = 11 Hz)] alongside characteristic peaks for a caffeoyl group evidenced by the presence of two vinylic protons with an AB spin system at δ_H 6.30 (1H, d, J = 16.4 Hz) and 7.61 (1H, d, J = 16.4 Hz) for an *E*-geometry of the vinyl group and a *pseudo*-ABX spin system at δ_H 6.90 (1H, d, J = 7.7 Hz), 7.02 (1H, d, J = 7.7 Hz) and 7.12 (br s) for a 1,3,4-trisubstituted aromatic ring. With establishment of the caffeoyl moiety constituting six degrees of unsaturation, it implied the remaining six degrees of unsaturation could be attributed to a tricyclic system and three double bond moieties. A tricyclic system was possible, considering the cassane-type diterpenoids elaborated by *Caesalpinia* species. The presence of three tertiary methyl proton (δ_H 1.06, 1.11 and 1.12, each s) and exocyclic vinyls protons (δ_H 4.75 and 4.84 each s) suggested a cassane-type deterpene skeleton with methyl group at C-14 unsaturated and an additional endocyclic vinylic moiety (δ_H 5.49, s).

^{13}C NMR and DEPT spectra (Table 8) showed 29 carbon signals, nine of which were due to a caffeoyl ester and twenty for a diterpenoid moiety confirmed by HMQC spectrum. A long-range correlation between downfield shifted oxymethylene proton [δ_H 4.20 (2H, $W_{h/2}$ = 11 Hz)] to the carbonyl carbon at δ_C 167.3 on HMBC spectrum (Fig 6) suggested an ester linkage of the caffeoyl group to the diterpenoids group. The signals of terminal methylene protons [δ_H 4.75 and

4 (br s)] which showed HMBC correlations with the carbons at δ_C 41.6 (C-8), 146.4 (C-13), and 144.0 (C-14) confirmed the location of the exocyclic double bond at C-14. The connectivity of ring B and C of the diterpenoids moiety was secured through HMBC correlation of methine proton at δ_H 2.50 (d, J = 10.2 Hz, H-9) with the carbons at δ_C 17.5 (C-20), 122.3 (C-12), 25.4 (C-7), 144 (C-14), and 198.2 (C-11). The observed HMBC correlation also confirmed the location of an endocyclic double bond between C_{12}-C_{13} and a keto group at C_{11} through HMBC long-range correlation between the vinyl proton at δ_H 5.49 (br s, H-11) and carbon signals at δ_C 144.0 (C-14), 54.5 (C-9), and 34.2 (C-15). An extended conjugated system (H_2C=C(C)-C(C)=CH-C=O) and a trisubstituted vinyl moiety connected to the ring side chain (HC=C-CH_2-CH_2-OH) was therefore noted. Another key HMBC correlation was observed between the oxymethylene protons (δ_H 4.20 t, H-16) and the carbon resonances at δ_C 146.4 (C-14), 34.2 (C-15) and 167.3 (C-1') confirmed the connection of the ring side chain at C-14 and the caffeoyloxy group at C-16. All other long-range HMBC (Fig 6) correlations supported the proposed structure for **408**.

With reference to elaboration of cassane furanoditerpene, the compound was plausibly derived furanoditerpenoid with 16-caffeoyloxyl ester linkage. The COSY spectrum of **408** showed five spin systems for H_2-1/H_2-2/H_2-3, H-5/H_2-6/H_2-7/H-8/H-9, and H_2-15/H_2-16, the exocyclic methylene protons (Fig 6), plus the *trans* vinylic protons and a trisubstituted aromatic ring of the caffeoyl moiety. The relative stereochemistry of **408** was determined by an analysis of coupling constants and NOE data (Fig 6). Both the H-8 and H-9 signals, although not completely first-order, H-8 had half-height widths of > 25 Hz, while H-9 exhibited doublet (J = 10.2 Hz) consistent with a *trans*-diaxial orientation. The NOE correlations of H-8 with the Me-18 and Me-20 and in turn with the H-12 (vinyl protons) placed H-8 on the same face as the β-methyls (Me-20 and Me-18) groups. These data supported β-orientations of H-8, Me-18, Me-20 and α-orientation of H-9. The up-field exocyclic methylene proton (δ_H 4.75) showed a NOE with the H-7 protons, while the downfield proton (δ_H 4.84) showed a NOE with H-15. These data were consistent with the stereochemistry proposed for the new compound **408,** structurally elucidated as 16-*O*-caffeoyl-11-oxocassa-12,14-diene and named as Voulkensin A.

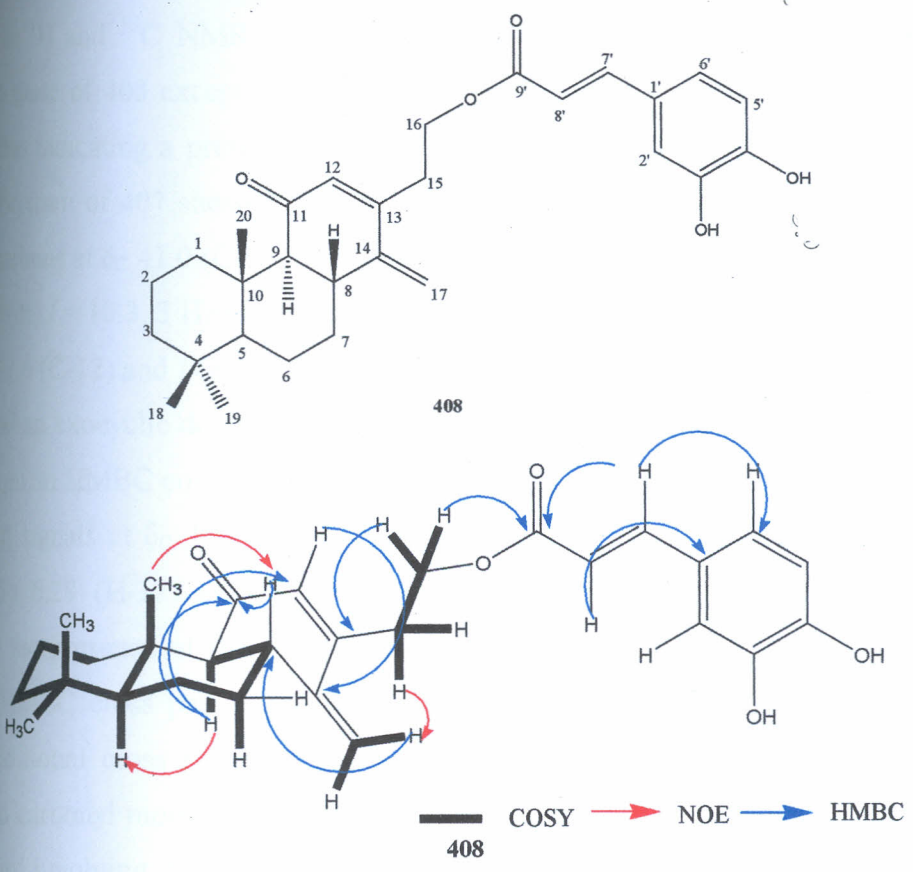

Figure 6: COSY, HMBC and NOE correlations for compound **408**

4.1.2.2. 16-Hydroxy-11-oxocass-12,14-diene (voulkensin B, 407)

Compound **407** was isolated as a white crystals with m.pt of 143-145°C and a molecular formula $C_{20}H_{30}O_2$, established from HRESIMS *pseudo*-molecular ion peak at *m/z* 325.2134 $[M + Na]^+$ and ESIMS molecular ion at *m/z* 303 $[M + H]^+$, indicating six degrees of unsaturation. The IR spectrum exhibited absorption typical of hydroxyl group (3423 cm^{-1}), α,β-unsaturated carbonyl (1629 cm^{-1}) and vinyl (1457 and 1370 cm^{-1}) functionalities. The UV spectrum had absorption bands at λ_{max} 257 and 339 nm for α,β-unsaturated carbonyl chromophore. The ^1H NMR spectrum had oxymethylene resonances associated with a primary hydroxyl group at δ_H 3.52 dt (2H, J = 11.5, 6 Hz), a vinylic proton at δ_H 6.29 (br s) and two terminal exocyclic methylenic protons at δ_H 4.66 and 4.87 (both br s). The ^{13}C NMR/DEPT and HMQC spectra revealed the presence of 20 nonequivalent carbon signals including three methyl groups, one sp^3 carbon bearing oxygen, eight methylenes, three methines, four quaternary carbons, and a ketonic carbonyl carbon.

The ^{1}H and ^{13}C NMR spectral data (Table 8) of **407** showed characteristic features similar to those of **408** except for the absence of the aromatic signals associated with caffeoyl moiety, thus indicating a presence of a free hydroxyl group at C-16 of a cassane diterpenoid.. HMBC spectrum of **407** showed that the oxymethylene protons at δ_H 3.52 (δ_C 61.3) correlated with the carbons at δ_C 41.0 (C-15), 149.9 (C-13). Similarly, the signals for the methylene protons at δ_H 2.08 (dt, J = 10.3, 3 Hz) and 2.32 (dt, J = 11.5, 4 Hz) correlated with the carbons at δ_C 61.3 (C-16), 122.6 (C-12) and 148.6 (C-14), which suggested the presence of $-CH_2CH_2OH$ substituent at C-13 and an exocyclic double bond at C-14. A ketone as part of an extended conjugation was evident from an HMBC correlation (Fig. 7) observed between signals at δ_H 4.66 and 4.87 (H-17) and carbon signals at δ_C 149.9 (C-13), 148.6 (C-14) and 28.5 (C-8) together with correlation between δ_H 6.29 (H-12) and δ_C 149.9 (C-13), 148.6 (C-14), 54.4 (C-9) and 41.0 (C-15) confirmed the presence of the vinylic proton at C-12. Furthermore, a signal at δ_H 2.17 (H-8) exhibited HMBC cross peaks to keto carbon signal at δ_C 200.9 (C-11) and δ_C 149.9 (C-13) besides additional cross peaks to δ_C 23.3 (C-6) and δ_C 113.6 (C-17) confirmed an α,β,γ,δ-unsaturated carbonyl moiety across C_{17}=C_{14}-C_{13}=C_{12}-C=O. The COSY spectrum established the spin system involving H-6/H-7/H-8/H-9; H-17/H-17 and H-15/H-16 (Fig. 7). The relative stereochemistry of **407** was similar to the configuration established for the cassane moiety of **408** as determined by NOE (Fig. 7). In particular, H-8 had cross-peaks with Me-20 which in turn showed NOE correlation to Me-18, which indicated that they were β-oriented, while the orientation of H-9 followed from its cross-peaks with H-7_{axial} and H-5, and from the *trans*-diaxial vicinal coupling with H-8 indicated an α-orientation. These results as summarized in Table 8, led to the structural assignment the new compound **407** as 16-hydroxy-11-oxocass-12,14-diene and named voulkensin B.

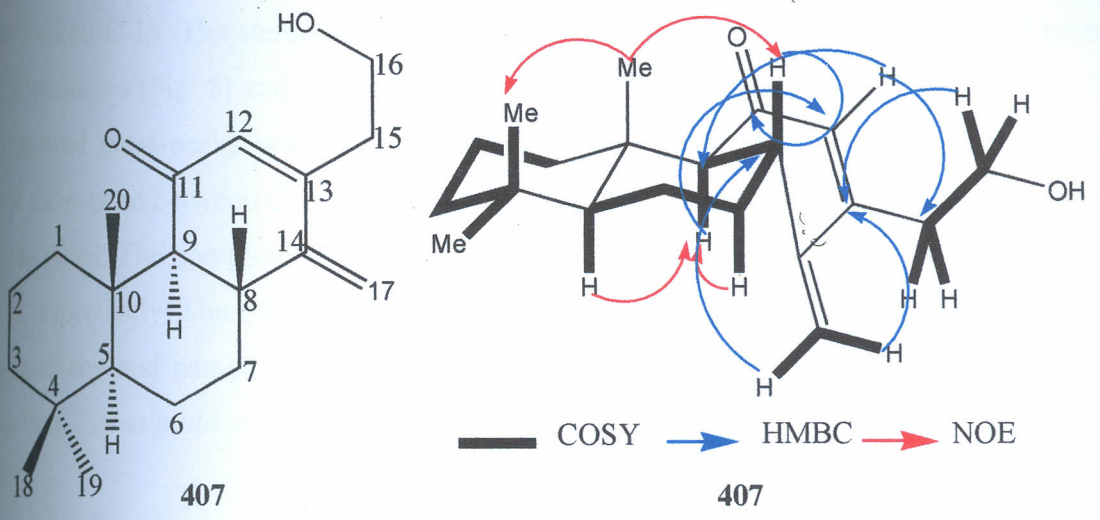

407 **407**

Figure 7: COSY, HMBC and NOE correlation of compound **407**

4.1.2.3. 16-Hydroxy-11-oxocass-12-ene (voulkensin C, 406)

The compound was isolated as white needlelike crystals with m.pt of 149-153°C and the molecular formula $C_{20}H_{32}O_2$, based on *pseudo*-molecular ion *m/z* 327.2051 (calcd. 327.2052 $[C_{20}H_{32}O_2Na]^+$) from HR-ESI mass spectral analysis. The IR spectrum had absorptions at 3385, 1610 and 1523 cm^{-1} due to hydroxyl, α, β-unsaturated carbonyl and vinyl functionalities, respectively. The ^1H NMR (Table 8) spectrum had resonances due to three quaternary methyls at δ_H 0.71, 0.73 and 1.07, a secondary methyl at δ_H 1.22 (d, J = 7.0 Hz) and a typical vinyl proton at δ_H 5.41 (s). The presence of a primary hydroxyl group was revealed by a resonance at δ_H 3.79 (2H, t, $W_{h/2}$ = 13.6 Hz) connected to a carbon at δ_C 62.9 on HMQC spectrum and showed COSY cross-peaks to methylene protons at δ_H 2.19 (dt, J = 13.6, 5.6 Hz) and 2.06 (dt, J = 13.6, 4.5 Hz). The ^{13}C NMR spectrum (Table 8) along with DEPT experiment displayed 20 carbons typical of a diterpenoids, three of these were for α,β-unsaturated carbonyl moiety [attributable to two quaternary carbons (δ_C 199.2 and 161.2) and one methine carbon (δ_C 125.2)]. In the HMBC experiment (Fig. 8), the ethylenic proton at δ_H 5.41 showed long-range correlations to the two secondary carbon resonances at δ_C 54.2 (C-9) and 41.0 (C-14) and in turn correlated to a primary carbon at δ_C 43.4 (C-15). The C-8 proton also showed long-range correlations to the unsaturated ketone at δ_C 210.9 which was located at C-11. The oxymethylene protons at δ_H 3.79 also displayed long-range correlations to the quaternary carbons at δ_C 161.2 indicating an ethyl alcohol side chain attached to the unsaturated carbonyl moiety. This result suggested that the unsaturated carbonyl moiety was on ring-C of cassane diterpene as C_{13}=C_{12}-C_{11}=O and the side

chain attached on C-13. The stereochemical conformation of ring A and B were assigned based on NOE correlations (Fig. 8) and biogenetic consideration in which the methyl group at δ_H 0.73 (Me-20) showed cross-peaks with a methine proton at δ_H 2.06 (H-8). However, due to free rotation of the σ-bond between C15-C16, no observable NOE correlation with the oxymethylene protons was noted. The complete ^1H and ^{13}C NMR assignments for compound **406** are reported in Table 8, respectively. Thus, the relative stereo structure of **406** was confirmed as 16-hydroxy-11-oxocass-12-ene and named volkensin C, reported as a new cassane diterpene with cleaved furan ring from *Caesalpinia volkensii.*

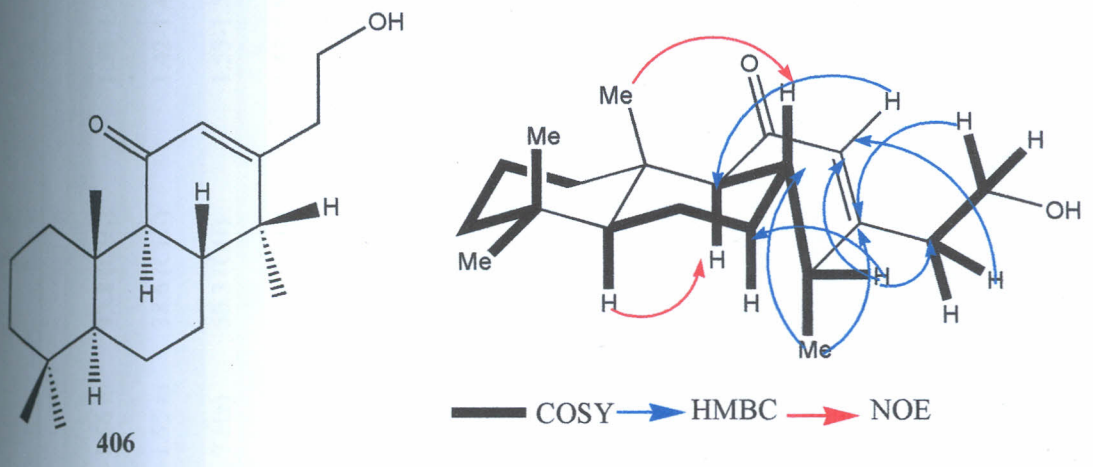

Figure 8: Significant COSY, HMBC and NOE correlation of compound **406**.

Table 8: ^{1}H (500 MHz) and ^{13}C (125 MHz) NMR spectral data for compounds **406-408** ($CDCl_3$)

Atom	406		407		408	
	^{1}H NMR	^{13}C NMR (DEPT)	^{1}H NMR	^{13}C NMR(DEPT)	^{1}H NMR	^{13}C NMR (DEPT)
1	1.33-1.35 m/1.52-1.61 m	36.4 (CH_2)	1.08-1.17 m/1.52-1.56 m	33.8 (CH_2)	1.33-1.40 m/1.40-1.42 m	39.3 (CH_2)
2	1.42-1.47 m/1.43-1.49 m	18.8 (CH_2)	1.27-1.32 m/1.75-1.78 m	21.7 (CH_2)	1.47-1.49 m/1.50-1.52 m	17.1 (CH_2)
3	1.54-1.61 m/1.56-1.64 m	38.6 (CH_2)	1.42-1.44 m/1.52-1.55 m	38.6 (CH_2)	1.42-1.47 m/1.52-1.55 m	38.1 (CH_2)
4	-------	49.0	------	48.5	-------	47.3
5	1.50-1.57 m	53.5 (CH)	1.18 dd (J = 15.8, 7 Hz)	50.3 (CH)	1.53-1.55 m	48.9
6	1.55-1.61 m/1.56-1.64 m	19.2 (CH_2)	1.60-1.62 m/1.42-1.44 m	23.3 (CH_2)	1.52-1.55 m/1.61-1.63 m	20.4 (CH_2)
7	1.74-1.78 m/1.27-1.33 m	25.2 (CH_2)	1.71-1.75 m/1.67-1.72 m	27.1 (CH_2)	1.63-1.66 m/1.70-1.75 m	25.3 (CH_2)
8	2.05 dd (J = 12.2, 9 Hz)	29.6 (CH)	2.17 m	28.5 (CH)	2.62 m	41.6 (CH)
9	2.70 d (J = 12.2 Hz)	54.2 (CH)	1.98 d (J = 12.1 Hz)	54.4 (CH)	2.50 d (J = 10.2 Hz)	54.4 (CH)
10	------	45.5	--------	43.7	-------	38.7
11	------	199.2	-------	200.9	-------	198.2
12	5.41 s	125.2 (CH)	6.29 br s	122.6 (CH)	5.49 s	122.3
13	------	161.2	-------	149.9	------	146.4
14	2.60 m	41.0 (CH)	-------	148.6	------	144.0
15	2.19 dt (J = 13.6, 5.6 Hz) 2.06 t (J = 13.6, 4.5 Hz)	43.4 (CH_2)	2.08 dt (J = 10.3, 3 Hz) 2.32 dt (J = 11.5, 4 Hz)	41.0 (CH_2)	2.11 dt (J = 12.2, 1.8 Hz) 2.08 dt (J = 12.2, 1.8 Hz)	34.2 (CH_2)
16	3.79 br t ($W_{h/2}$ = 13.6 Hz)	62.9 (CH_2)	3.52 dt (J = 11.5, 6Hz)	61.3 (CH_2)	4.20 t ($W_{h/2}$ = 12 Hz)	62.4 (CH_2)
17	1.22 d (J = 7 Hz)	16.4 (CH_3)	4.66 br s 4.87 br s	113.6 (CH_2)	4.84 br s 4.75 br s	114.3 (CH_2)
18	0.71 s	21.0 (CH_3)	0.90 s	25.3 (CH_3)	1.06 s	27.1 (CH_3)
19	0.73 s	23.4 (CH_3)	1.02 s	25.2 (CH_3)	1.11 s	21.0 (CH_3)
20	1.07 s	18.7 (CH_3)	1.04 s	18.7 (CH_3)	1.12 s	17.5 (CH_3)
1'					-------	127.6
2'					7.12 br s	119.1 (CH)
3'					--------	159.9
4'					--------	158.2
5'					6.90 d (J = 7.7 Hz)	115.5 (CH)
6'					7.02 d (J = 7.7 Hz)	122.4 (CH)
7'					7.61 d (J = 16.4 Hz)	145.0 (CH)
8'					6.30 d (J = 16.4 Hz)	115.4 (CH)
9'					--------	167.3

4.12.4. 3-*O*-[β-Glucopyranosyl(1-2)-*O*-β-xylopyranosyl]-stigmasterol (409)

Compound **409** was isolated as white amorphous solid from the *n*-butanol extract with m.pt of 231-233°C. The molecular formula of was established as $C_{40}H_{66}O_{10}$ by a quasi-molecular ion peak in the HRESIMS at *m/z* 707.4450 $[M+H]^+$. The IR spectrum showed characteristic absorption bands for hydroxyl (3452 cm^{-1}), olefinic (1647 cm^{-1}) groups and absorption at 2925 and 2856 cm^{-1} were due to aliphatic C-H stretching.

The ^1H and ^{13}C NMR (Table 9) spectra of **409** displayed signals for C-29 sterol and one hexose and one pentose units, confirmed by a fragment ions at *m/z* 544.4 and 413.7, due to loses of terminal hexose unit followed by lose of a pentose unit from stigmasterol. Compound **409** exhibited six methyl signals in the ^1H NMR spectrum; two were singlets at δ_H 0.65 (H-18) and 0.96 (H-19), three were doublets at δ_H 0.77 (J = 7.0 Hz, H-27), 0.79 (J = 7.0 Hz, H-26) and 0.90 (J = 6.5 Hz, H-21), and one was a triplet at δ_H 0.83 (J = 7.0 Hz, H-29). An ethylenic proton at δ_H 5.33 coupled to up field protons in the COSY spectrum revealed presence of a trisubstituted double bond (C5/C6); a *trans*-disubstituted double bond was also present with two double doublets at δ_H 5.25 and 5.13 (each, J = 18.0 and 8.1 Hz, H-22/23). These signals belonged to stigmasterol, confirmed by the ^{13}C NMR assignments of **409** that were in agreement with those described in the literature (Siddiqui *et al.*, 2007).

Analysis of the ^{13}C and DEPT-135 NMR (Table 9) spectra showed the presence of signals for three quaternary, twenty methine, eleven methylene and six methyl carbon. Resonances of C atoms bearing hydrogen included two anomeric carbons (δ_C 101.3 and 106.4), ten oxymethine carbons (δ_C 63.8, 65.3, 68.0, 69.6, 70.3, 73.4, 74.9, 76.6, 77.7 and 82.3), and four sp^2 carbons (δ_C 121.1, 128.2, 137.9 and 140.3) that were identified in the HSQC spectrum. The one hexose and one pentose units were determined as β-glucose and β-xylose (pyranose forms) according to analysis of the thirteen protons spin systems.

The ^1H and ^{13}C NMR spectra (Table 9), clearly indicated the presence of two anomeric protons [δ_H 4.49 (d, J = 8.0 Hz) and 4.89 (d, J = 8.0 Hz)] and two anomeric carbons (δ_C 101.4 and 106.4). The anomeric configurations for the sugar moieties were fully defined from their chemical shifts and $^3J_{diax}$ coupling constants. Accordingly, both the xylose and the glucose were established to have β-configuration, conversely α-configuration would have been J = 2.5-4.0 Hz

(Altona & Haasnoot, 1980). The ^{13}C NMR showed a C-3 signal at 82.3 shifted downfield by +5.3 ppm as compared to stigmasterol (**176**), due to glycosylation shift, suggesting that the sugar moieties are linked to the oxygen at C-3 of the aglycone. Upon acid hydrolysis, compound **409** afforded stigmasterol (**176**) identified by comparison of the NMR data with literature values (Jamal *et al.*, 2009; Alam *et al.*, 1996; Reginatto *et al.*, 2001), and glucose and xylose identified on TLC (silica gel, *n*-BuOH-EtOAc-H_2O, 5:4:1) by comparison with authentic samples. The sequence and interglycosidic linkage of the sugar chain could be established by HMBC experiment (Fig. 9). Long-range correlations were observed between H-1 of xylose [δ_H 4.49 d (J = 8.8 Hz)] and C-3 of aglycone (δ_C 82.3), and H-1 of glucose [δ_H 4.89 d (J = 8.8 Hz)] and C-2 of xylose (δ_C 74.9) were observed with and a reverse correlation between H-2 of xylose and C-1 of terminal glucose. Thus, the structure of **409** was established to be 3-*O*-[β-glucopyranosyl-(1→2)-(β-xylopyranosyl]-stigmasterol isolated as new compound.

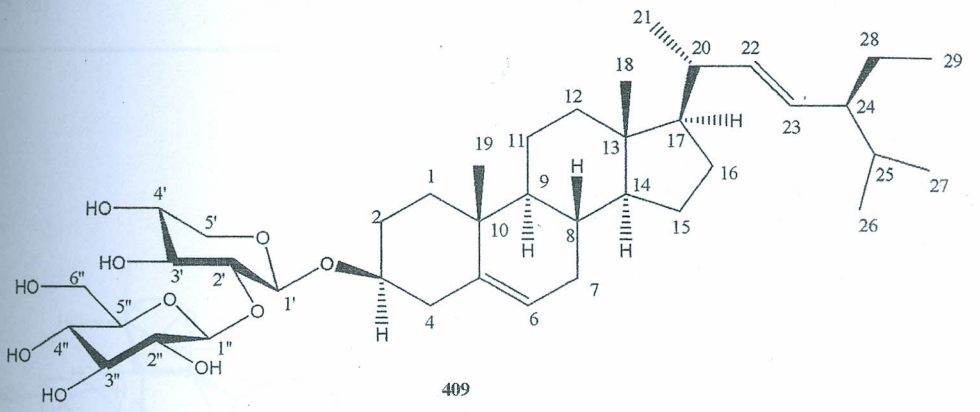

409

Table 9: (^{1}H 500 MHz)and ^{13}C (125 MHz) NMR spectral data of compounds **409** (CD_3OD)

Atom	^{1}H NMR	^{13}C NMR	Atom	^{1}H NMR	^{13}C NMR
1	1.14-1.20 (2H, m)	38.2	21	0.90 (1H, d, J = 6.5 Hz)	20.8
2	1.80/1.78 (2H, m)	31.3	22	5.25 (1H, dd, J = 18.0, 4.2 Hz)	137.9
3	3.92 (1H, m)	82.3	23	5.13 (1H, dd, J = 18.0, 8.1 Hz)	128.2
4	2.92 (2H, m)	42.7	24	1.45 (1H, m)	55.3
5		140.3	25	1.43 (1H, m)	29.2
6	5.33 (1H, m)	121.1	26	0.79 (3H, d, J = 7.0 Hz)	21.0
7	1.47/1.67 (2H, m)	35.4	27	0.77 (3H, d, J = 7.0 Hz)	20.2
8	2.50 (1H, m)	31.7	28	1.23-1.34 (2H, m)	27.7
9	2.38 (1H, m)	49.4	29	0.83 (3H, t, J = 7.0 Hz)	18.7
10		38.3	1'	4.49 (1H, d, J = 8.8 Hz)	106.4
11	1.49/1.74 (2H, m)	22.5	2'	3.83 (1H, t, J = 8.8 Hz)	74.9
12	2.10/1.96 (2H, m)	39.7	3'	3.62 (1H, m)	77.7
13		41.6	4'	3.40 (1H, m)	69.6
14	1.23 (1H, m)	56.1	5'	4.46 (1H, dd, J = 12.3, 5.5 Hz) 3.13 (1H, m)	65.3
15	1.15/2.23 (2H, m)	25.3	1''	4.89 (1H, d, J = 8.8 Hz)	101.3
16	1.02/2.20 (2H, m)	28.6	2''	4.22 (1H, d, J = 8.8 Hz)	70.3
17	0.98(1H, m)	50.4	3''	4.05 (1H, d, J = 8.8 Hz)	76.6
18	0.65 (3H, s)	20.3	4''	4.78 (1H, d, J = 8.8 Hz)	73.4
19	0.96 (3H, s)	20.5	5''	3.48 (1H, m)	68.0
20	1.51 (1H, m)	40.0	6''	4.46 (1H, dd, J = 12.3, 3.0 Hz) 4.49 (1H, dd, J = 12.3, 3.0 Hz)	63.8

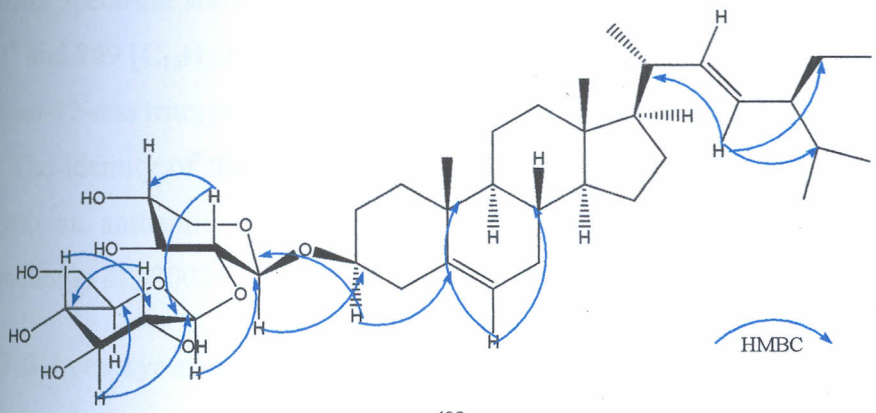

409

Figure 9: Significant HMBC correlation of compound **409**

4.1.2.5. Oleanolic acid (185)

The compound was isolated from the ethyl acetate extract of *C. volkensii* stem bark, as a white solid with m.pt 305-306°C. The IR spectrum exhibited characteristic absorption band for hydroxyl group (3482 cm^{-1}), carboxylic hydroxyl functionality (3123 cm^{-1}), C-H aliphatic stretching (2945 cm^{-1}), carboxylic functionality (1697 cm^{-1}) and ethylenic absorption at 1450 cm^{-1}. The ^1H NMR (Table 10) spectrum indicated the presence of seven quaternary methyl groups (δ_H 0.72, 0.77, 0.80, 0.84, 0.92, 1.00 and 1.04) and a characteristic olefinic proton for pentacyclic triterpenoid at δ_H 5.24 (1H, t, J = 4 Hz) (Seebacher *et al.*, 2003). Another definitive proton signal was for an oxygenated methine proton at δ_H 3.14 (1H, dd, J = 11.0, 5.1 Hz), which was assigned to H-3.

The ^{13}C NMR spectrum (Table 10) revealed presence of signals due to an oxygenated carbon at δ_C 77.6 (C-3), one tri-substituted double bond at δ_C 121.4 (C-12) and 142.9 (C-13), and one carboxyl group at δ_C 179.8 among other aliphatic carbons which were identified by DEPT and HMQC data, typical of an olean-12-en derivatives (Seebacher *et al.*, 2003).

The ESIMS spectrum showed molecular ion at *m/z* 457 $[M + H]^+$ and fragment ion *m/z* 249 $[C_{15}H_{24}O_2]^+$ and 209 $[C_{15}H_{28}O]^+$ characteristics of *Retro*-Diels Alder cleavage of ring-B and C typical for olean-12-ene triterpene. Based on above evidence, compound **185** was identified as oleanolic acid. The identity of the compound was further confirmed by comparison (TLC and mixed m.pt) with an authentic sample and by comparison of ^{13}C-chemical shifts with the literature (Seebacher *et al.*, 2003).

4.1.2.6. 3-β-Acetoxyolean-12-en-28-methyl ester (405)

Compound **405** was isolated as white crystals with m.pt 298-300°C, R_f value 0.63 (silica gel, *n*-hexane/ethyl acetate, 4:1) which was higher than the R_f for **185** (0.23, silica gel, *n*-hexane/ethyl acetate, 4:1). The compound displayed ^1H and ^{13}C NMR spectral features characteristic of acetylated olean-12-en-28-oic acid as evidenced by δ_H 4.49 (1H, t, J = 4 Hz, H-12); 3.75 (1H, dd, J = 11, 4.3 Hz, H-3); 2.04 (3H, s, H-Ac); δ_C 115.9 (C-12), 145.1 (C-13), 22.9 (C-OC<u>C</u>H$_3$) and signals due to seven tertiary methyl groups, which were also reminiscent of olean-12-en-28-oic acid type triterpene (Seebacher *et al.*, 2003). The ^1H NMR further showed a down field broad singlet integrating for three protons at δ_H 3.48, indicative of methyl esterification of the C-28

carboxyl unit. The structure was confirmed by it mass (ESI) spectrum, which displayed molecular ion *m/z* 512.7. The compound was thus identified as acetate of an esterified **185**, a fact further corroborated by the IR spectrum which showed no absorption band for hydroxyl group, but indicated the presence of carbonyl esters 1702 and 1675 cm^{-1} for carboxyl group. Compound **405** was thus identified as 3-β-acetoxyolean-12-en-28-methyl ester.

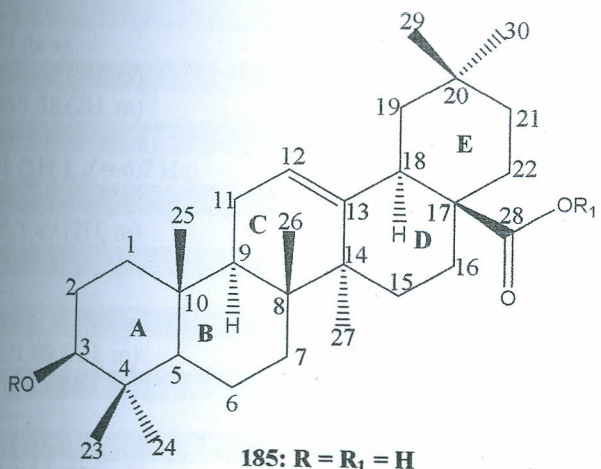

185: R = R_1 = H
405: R = OAc; R_1 = Me

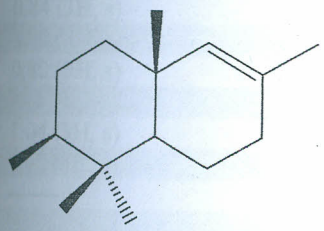

185a: $C_{14}H_{24}O$ *m/z* 209

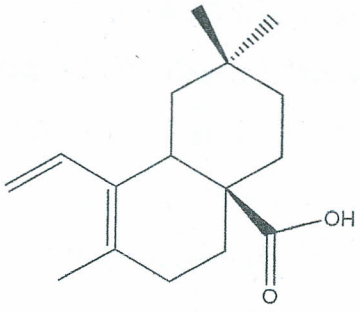

185b: $C_{16}H_{25}O_2$ *m/z* 249

Table 10: ^{1}H (300 MHz) and ^{13}C (75 MHz) NMR spectral data for compounds **185 and 405** ($CDCl_3$)

	Oleanolic acid (185)		3-β-acetoxyolean-12-en-28-methyl ester (405)	
Atom	^{1}H NMR	^{13}C NMR	^{1}H NMR	^{13}C NMR
1	1.55/1.73 (2H, m)	32.0	1.46/1.72 (2H, m)	38.9
2	1.58/1.63 (2H, m)	25.8	1.60/1.62 (2H, m)	25.6
3	3.14 (1H, dd, J = 8.4, 5.1 Hz)	77.6	3.75 (1H, dd, J = 11, 4.3 Hz)	76.5
4	------	38.5	--------	41.1
5	0.71 (br s)	54.7	0.90 (br s)	47.3
6	1.52/1.57 (2H, m)	17.5	1.42/1.83 (2H, m)	16.8
7	1.26/1.38 (2H, m)	31.8	1.25/1.38 (2H, m)	29.7
8	--------	40.7	---------	43.4
9	1.58 (1H, t, J = 6.7 Hz)	47.0	1.70 (1H, m)	48.1
10	------	36.2		37.8
11	1.85/1.89 (2H, m)	22.6	1.90/1.81 (2H, m)	22.4
12	5.24 (br s)	121.4	4.49 (1H, t, J = 4 Hz)	115.9
13	------	142.9	---------	145.1
14	------	38.3	--------	41.7
15	1.03/1.09 (2H, m)	26.8	0.93/1.08 (2H, m)	27.8
16	1.53/1.61 (2H, m)	22.1	1.42/1.62 (2H, m)	22.2
17	-------	45.6	------	45.3
18	2.85 (1H, dd, J = 13.6, 3.6 Hz)	40.6	2.83 (1H, br d, J = 12 Hz)	36.4
19	1.21/1.36 (2H, m)	37.8	1.76/1.81 (2H, m)	37.1
20	-------	32.9	------	35.4
21	1.21/1.36 (2H, m)	29.7	1.19/1.35 (2H, m)	29.1
22	1.95/1.58 (2H, m)	45.3	1.88/1.83 (2H, m)	47.3
23	0.72 (3H, s)	14.3	0.75 (3H, s)	12.6
24	0.92 (3H, s)	26.9	1.06 (3H, s)	25.3
25	0.84 (3H, s)	13.9	0.92 (3H, s)	16.0
26	1.00 (3H, s)	15.8	1.13 (3H, s)	20.0
27	0.80 (3H, s)	24.7	0.85 (3H, s)	23.8
28	-------	179.8	------	174.8
29	1.04 (3H, s)	22.2	1.07 (3H, s)	22.6
30	0.77 (3H, s)	32.2	0.84 (3H, s)	32.8
$OCCH_3$	-------		2.04 (3H, s)	169. 9, 22.9
$OOCH_3$			3.48 (3H, s)	52.5

4.1.2.7. Stigmasterol (176)

The compound was isolated as white crystals, m.pt 167-169°C. The mass spectral data gave molecular a molecular ion at *m/z* 413 $[M + H]^+$. ^{13}C NMR and DEPT spectra (Table 11) which showed the presence of 29 carbon atoms including six methyls, nine methylenes, eleven methines and three quaternary carbon atoms. The ^{1}H NMR (Table 11) spectrum showed the presence of six methyls that appeared at δ_H 0.68, 0.79, 0.84, 0.86, 0.93 and 1.02 together with a multiplet at δ 3.53 for an oxymethine proton and olefinic protons at δ_H 5.36 (d, J = 4.5 Hz), 5.17 (dd, J = 14.8, 5.5 Hz) and 5.01 (dd, J = 15.2, 6.6 Hz). The ^{13}C NMR olefinic peaks at δ_C 141.2, 138.7, 129.4 and 121.9 confirmed the presence of two carbon-carbon double bonds (tri- and di-

substituted) at C-5 and C-22 while a signal at δ_C 71.9 confirmed the presence of oxymethine carbon atom at C-3 (Reginatto *et al.*, 2001; Alam *et al.*, 1996). Other peaks in the ^{13}C NMR spectrum were at δ_C 12.2, 14.3, 19.4, 21.0, 21.3, and 23.1 which confirmed the presence of six methyl groups. Based on the spectral data as well as literature (Reginatto *et al.*, 2001; Alam *et al.*, 1996), compound **176** was identified as stigmasterol.

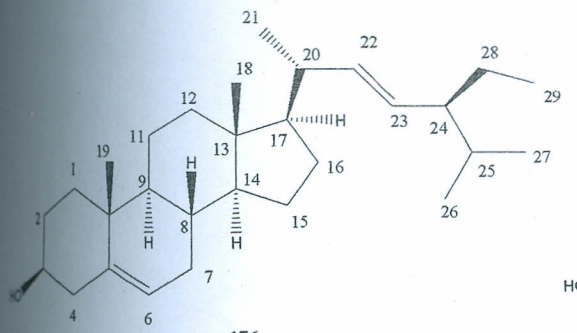

176

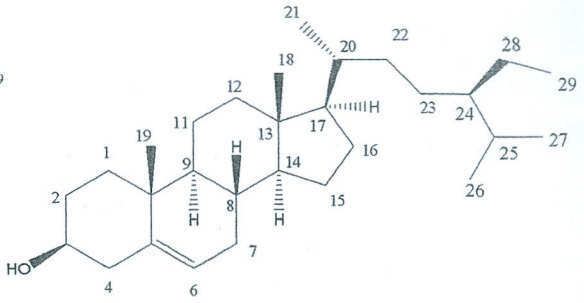

177

4.1.2.8. β-sitosterol (177)

Compound **177** was isolated as white flaky crystals with m.pt 138-139°C. The spectral data for compound **177** were almost similar to that of **176** except for the absence of one olefinic moiety and the ESIMS spectrum that showed a molecular ion at *m/z* 414, which is higher by 2 a.m.u higher than for **176**, indicating a molecular formula of $C_{29}H_{50}O$. ^1H NMR (Table 11) spectrum showed the presence of six methyls at δ_H 0.69 (d, J = 6 Hz), 0.79 (d, J = 6 Hz), 0.83 (t, J = 6 Hz), 0.87 (s), 0.91 (d, J = 6 Hz), and 0.93 (s) together with a multiplet signal at δ 3.48 due to the oxymethine proton on C-3 and an olefinic proton at δ 5.36 (m) which was ascribed for a proton on C-5. ^{13}C NMR showed twenty nine carbon signal including six methyls, eleven methylenes, ten methine and three quaternary carbons. The sp^2 carbons appeared at δ_C 140.8 and 121.7 justifying the structure to be β-sitosterol (Jamal *et. al.*, 2009).

Table 11: ^{1}H (300 MHz) and ^{13}C (75 MHz) NMR spectral data of compounds **176** and **177** ($CDCl_3$)

Atom	Stigmasterol (176)		β-sitosterol (177)	
	^{1}H-NMR	^{13}C-NMR	^{1}H-NMR	^{13}C-NMR
1		37.3		37.3
2		31.8		31.6
3	3.53m	71.9	3.48 m	71.8
4		42.1		42.3
5		141.2		140.8
6	5.36 d (J = 4.5 Hz),	121.9	5.36 m	121.7
7		29.8		31.7
8		34.1		36.1
9		49.9		56.1
10		36.8		36.5
11		24.4		23.1
12		39.8		39.8
13		48.2		45.9
14		57.0		56.8
15		26.5		26.1
16		28.1		29.1
17		56.1		50.2
18	1.02 s	21.3	0.87 (s)	18.8
19	0.68 s	14.3	0.93 (s)	19.2
20		40.1		33.9
21	0.93 d	23.1	0.91 d (J = 6 Hz)	19.0
22	5.17 dd (J = 14.8, 5.5 Hz)	138.7		31.9
23	5.01dd (J = 15.2, 6.6 Hz)	129.4		28.2
24		51.1		19.8
25		25.3		29.5
26	0.84 d	21.0	0.79 d (J = 6 Hz)	21.1
27	0.79 d	12.2	0.69 d (J = 6 Hz)	19.8
28		35.1		24.3
29	0.86 t (J = 6 Hz)	19.4	0.83 t (J = 6 Hz)	11.9

4.1.3. Structural elucidation of compounds from *Senna didymobotrya* roots

Fractionation of the ethyl acetate extract of the roots of *S. didymobotyra* led to the isolation of three rare anthraquinones; obtusifolin (**285**), nataloemodin-8-methyl ether (**279**) and 1,6-di-*O*-methylemodin (**410**) together with five other common compounds namely, chrysophanol (**269**), physcion (**273**), chrysophanol-10,10′-biathrone (**295**) (Alemayehu *et al.*, 1993), physcion-10,10′-bianthrone (**299**) (Kitanaka & Takido, 1982) and stigmasterol (**176**) (Jamal *et al.*, 2009). Structures of the isolates were established based on spectral data and comparison with literature report.

4.3.1. Chrysophanol (269)

Compound **269** was isolated from the first eluent of the ethyl acetate extract as yellow needle-like crystals from MeOH with a melting point of 180-182°C. The IR spectrum of the compound showed a strong absorption band at 3469 cm^{-1}, together with two carbonyl absorption bands at 1719 and 1633 cm^{-1}, for free and chelated keto groups, respectively. The ^{1}H NMR spectrum (Table 12) showed two sharp down-field singlets at δ_H 12.01 and 12.11, characteristic of two chelated hydroxyl groups, and signals for five aromatic protons [7.11 (1H, br s, H-2); 7.30 (1H, d, J = 8 Hz, H-7); δ_H 7.66 (1H, br s, H-4); 7.69 (1H, t, J = 8 Hz, H-6) and 7.83 (1H, d, J = 7 Hz, H-5)] and for an aromatic methyl [δ_H 2.48 (s)]. These data were supported by the ^{13}C NMR spectral data (Table 13) and the ESIMS spectrum that showed molecular ion peak at *m/z* 255.1 $[M+H]^+$. On the basis of its spectroscopic data, and by comparing with those reported in the literature (Garcia-Sosa *et al.*, 2006), the compound was identified as chrysophanol (1,8-dihydroxy-3-methylanthracene-9,10-dione, **269**), an anthraquinone derivative reportedly known to posses antibacterial and antifungal activity (Suresh *et al.*, 2003).

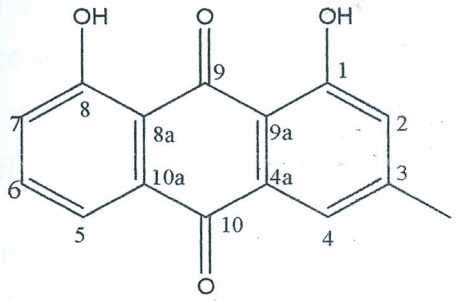

269

4.3.2. Physcion (273)

Compound **273** was isolated as orange needles, m.pt 204-205°C. The molecular formula $C_{16}H_{12}O_5$ followed from ESIMS molecular ion at *m/z* 285. Its UV-Visible absorption maxima in $CHCl_3$ at λ_{max} 225 246 280 302 and 430 nm coupled with IR absorption at 1681 and 1628 cm^{-1} which suggested an anthraquinone skeleton (Thomson, 1971). The ^{1}H and ^{13}C NMR (Table 12 and 13) revealed the presence of C-methyl [δ_H 2.45 (3H, s)] and *O*-methyl groups [δ_H 3.94 (3H, s)], two sets of *meta*-oriented aromatic protons [δ_H 7.62 (1H, br s, H-2), 7.26 (1H, br, s, H-4), 6.69 (1H, d, J = 3 Hz, H-5) and 7.37 (1H, d J = 3 Hz, H-7)], and the protons of two hydrogen bonded phenolic hydroxyl groups (δ_H 12.11 and 12.31, both br s). The ^{13}C NMR spectrum (Table 13) revealed the presence twelve aromatic carbons including four methines and eight quaternary

carbons of which five bore oxygen, two carbonyls, and one bonded to methyl carbon. These data identified the orange compound to be physcion (1,8-dihydroxy-6-methoxy-3-methylanthracene-9,10-dione, **273**) a conclusion that was confirmed by direct comparison with an authentic sample. Physcion (**273**) is wide spread among higher plants and ubiquitous within the genus *Senna*.

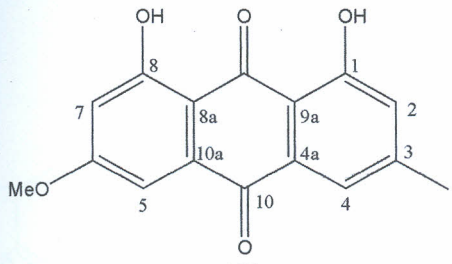

273

4.3.3. Obtusifolin (285)

Compound **285** was isolated as yellow needles, m.pt 227-229°C from methanol. It ESIMS showed molecular ion peak at *m/z* 285 $[M + H]^+$. The IR (KBr) spectrum showed absorption bands characteristics of hydroxyl (3083 cm^{-1}), free carbonyl stretching vibration (1674 cm^{-1}), chelated carbonyl (1635 cm^{-1}), and benzene skeleton vibration (1403 cm^{-1}). The UV spectrum ($CHCl_3$) indicated absorbance at λ_{max} (log ε) 232 (3.7), 252 (4.01), 281 (3.65) and 403 (3.02) nm typical of an anthraquinone with a characteristic red shift at suggesting presence of additional proton donor subsituents (OH) to the ring systems.

The ^1H (Table 12) and ^{13}C NMR (Table 13) indicated 12 proton signals and 16 carbon signals, respectively. The ^1H NMR spectrum (Table 12) revealed the presence of two pairs of *ortho*-coupled protons [δ_H 7.62 and 7.78 (each d, J = 7.0 Hz)], a triplet aromatic proton [δ_H 7.62 (t, J = 7.0 Hz)] and a singlet aromatic proton (δ_H 7.77). These spectral data suggested a 1,2,3,8 tetra-substituted anthraquinone derivative. Moreover, the ^1H and ^{13}C NMR spectra revealed the presence of one chelated hydroxyl group [δ_H 12.92 (s)], another hydroxyl group [δ_H 10.40, s], one aromatic methyls group [δ_H 2.27 (s), δ_C 22.6] and one methoxy group [δ_H 4.06 (s), δ_C 62.1].

In the ^1H NMR spectrum of **285**, the presence of a 1,2,3- mutually coupled protons located at C-5, C-6 and C-7 was supported by their mutual HMBC correlation (Fig. 2) experiments. On the other hand, the position of methoxyl group could be assigned C-1 on the basis of the ^{13}C chemical signal shifted downfield (δ_C 62.1) which indicated di-*ortho* subsititution and the existence of an OH group possibly on C-2, which also indicated an ^{13}C upfield shift (δ_C 155.5) and such premises were supported by the HMBC correlation between

OMe/C-1. Similarly the placement of an OH group at C-2 was due to HMBC cross peak between δH 2.27 (s, 3-Me) and C-2 and C-4 confirmed the placement of the free OH group on C-2. On the basis of the spectroscopic data compound **285** was deduced as 2,8-dihydroxy-1-methoxy-3-methyl-anthracene-9,10-dione previously isolated from *Cassia obtusifolia* named as obtusifolin (Li *et al.*, 2004).

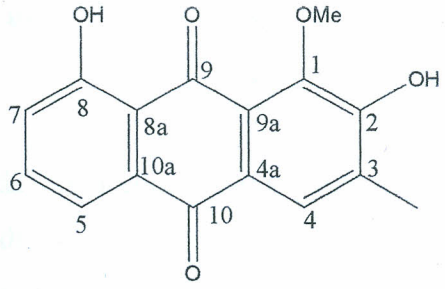

285

4.1.3.4. 1,6-di-*O*-methylemodin (410)

Compound **410** was obtained as red-orange crystals with m.pt 216-218°C and its UV spectrum in MeOH showed maxima at λ_{max} 254, 268 289 and 436 nm. The ESIMS gave a positive molecular ion at *m/z* at 315.7 precdicted for molecular formular of $C_{17}H_{14}O_6$ confirmed by the ^{13}C NMR spectrum (Table 13) which displayed seventeen non-equivalent signals. The compound displayed *meta* coupled protons [δ_H 7.03 and 7.69 (each d, J = 3.0 Hz)] and a singlet at δ_H 7.36 (H-5) together with signals due to two OMe groups (δ_H 3.93 and 4.04, each s) a *peri*-hydroxyl (δ_H 12.83, br s) and an aromatic methyl (δ_H 2.44, s) in the ^1H NMR spectrum (Table 12). Compound 410 was proposed to bear structural similarity with **285** except for the presence of methoxyl group at C-6.

Presence of the methyl group at C-3 was indicated by the HMBC cross peak between C_3-Me and H-4 (δ_H 7.35, s) which in turn correlated to carbonyl signal (δ_C 186.2, C-10) and a oxygenated carbon (δ_C 152.7, C-2). The aromatic methyl on the other hand showed HMBC cross peak with δ_C 152.7 (C-2) and 118.6 (C-4). This was confirmed by ^1H-^1H COSY correlations observed between H-4/Me-3 (Fig 10). The chemical shifts from both ^1H and ^{13}C NMR, indicated one OMe group was within a di-*ortho* position C-1/C-2 (δ_H 4.04 and δ_C 60.3) and the other (δ_H 3.93, δ_C 56.4) at C-6 between the *meta*-coupled protons. The exact placement of downfield OMe

was evidenced by HMBC (Fig 10) cross peaks observed between δ_H 4.04 and δ_C 135.5 ascribed for C-1.

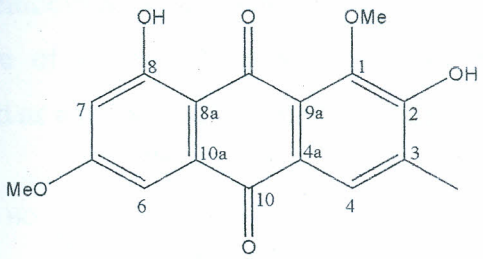

410

Based on the spectroscopic data and comparison of the same to literature, compound 410 was concluded to 2,8-dihydroxy-1,6-dimethoxy-3-methylanthracene-9,10-dione (1,6-di-*O*-methylemodin, **410**) whose constitutional isomer have been isolated from *Melanoxylon braunia* named 6,8-di-*O*-methylemodin (Gottlieb *et al.*, 1971).

4.1.3.5. Nataloemodin-8-methyl ether (279)

Compound **279** was isolated as yellow crystals with m.p 235-236°C and molecular formula $C_{16}H_{12}O_5$ as deduced from ESI-MS (observed *m/z* 285.2, $[M + H]^+$) and NMR spectral data. The IR spectrum showed characteristic absorption bands of hydroxyl group at 3468 cm^{-1}, a chelated carbonyl at 1626 cm^{-1}, an unchelated carbonyl at 1675 cm^{-1} and aromatic ring at 2583 cm^{-1}. Its UV spectrum (MeOH) absorption maxima were observed at λ_{max} 221, 252 and 420 nm characteristics of hydroxylated anthraquinone.

The ^1H and ^{13}C NMR (Table 12 and 13) depicted signals corresponding to an anthraquinone skeleton with a di-*ortho* substituted OMe group (δ_H 4.02, δ_C 60.1). The ^1H NMR spectrum showed a singlet at 12.72 assigned to a chelated hydroxyl proton at C-1, three aromatic protons appearing as a pair of doublets (both J = 9.0 Hz) at δ_H 8.11 (H-5) and 7.35 (H-6) and another pair of meta-coupled aromatic signals (both J = 1.2 Hz) at 7.07 (H-2) and 7.60 (H-4) revealing the substitution on the aromatic rings based on biogenetic possibility.

Unequivocal information on the substitution mode of **279** was established from HSQC, HMBC and ^1H-^1H COSY (Fig 10). In fact comparison of compound **279** data with those of **285** and **410** suggested that position C-6 in the former compound was unsubstituted, an interpretation that was supported by ^1H-^1H COSY cross peak between H-5/H-6 and further confirmed by

HMBC (Fig. 10) correlations between H-6/C-8, implying the positions of OH and OMe were basically C-7 and C-8, respectively. Furthermore, detailed comparison of spectroscopic data of compound **279** with nataloemodin-8-methyl ether (Delle-Monache *et al.*, 1991), previously obtained from tissue culture of *Cassia didymobotrya* were in complete agreement. Thus, compound **279** was confirmed as nataloemodin-8-methyl ether

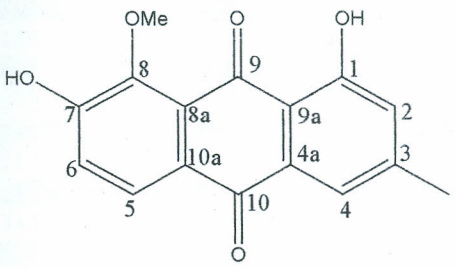

279

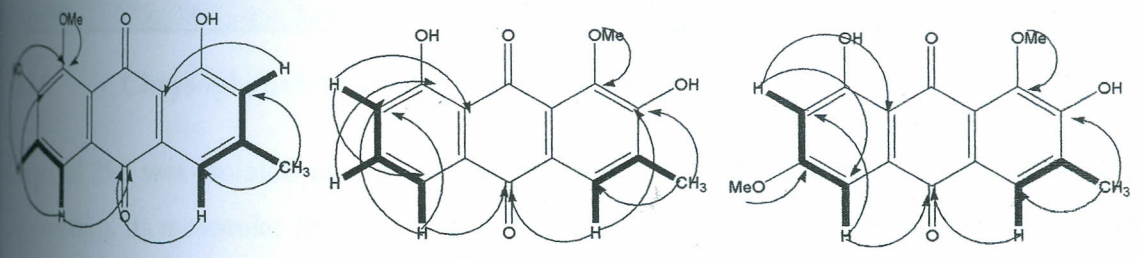

279 **285** **410**

HMBC COSY

Figure 10: Significant HMBC and COSY correlations for compounds **279, 285** and **410**

Table 12: ^{1}H NMR spectral data for compounds **269, 273, 279, 285, 410** ($CDCl_3$, 300 MHz)

Atom	269	273	279	285	410
2	7.11 br s	7.26 br s	7.07 (J = 1.2 Hz)	-----	-----
4	7.66 br s	7.62 br s	7.60 (J = 1.2 Hz)	7.77 s	7.35 s
5	7.83 d (J = 7 Hz)	7.37 d (J = 3 Hz)	8.11 d (J = 9 Hz)	7.31 d (J = 7 Hz)	7.69 d (J = 3 Hz)
6	7.69 t (J = 8 Hz)	-----	7.35 d (J = 9 Hz)	7.62 t (J = 7 Hz)	------
7	7.30 d (J = 8 Hz)	6.69 d (J = 3 Hz)	------	7.78 d (J = 7 Hz)	7.03 d (J = 3 Hz)
6-OCH_3	-----	3.94 s	------	------	3.93 s
8-OCH_3	-----		4.02 s	4.06 s	4.04 s
CH_3	2.48 s	2.45 s	2.44 s	2.27 s	2.44 s
1-OH	12.01 s	12.11	12.72 s	12.92 s	12.83 s
8-OH	12.11 s	12.31	------	------	------

Table 13: ^{13}C NMR spectral data for compounds **269**, **273**, **279**, **285** and **410** ($CDCl_3$, 75 MHz)

Atom	269	273	279	285	410
1	162.4	162.4	165.3	149.1	135.5
2	124.3	124.3	124.5	155.5	152.7
3	149.3	148.3	148.5	148.1	148.2
4	121.3	121.1	121.3	118.7	121.4
4a	133.2	135.2	133.2	133.0	129.6
5	119.9	108.1	126.8	112.4	106.6
6	124.5	166.2	108.0	136.2	166.7
7	133.6	106.7	157.1	124.6	124.6
8	162.7	165.1	166.5	167.4	165.5
8a	115.8	110.2	107.1	117.2	110.8
9	192.5	190.7	194.4	190.1	194.3
9a	113.7	113.6	110.8	137.5	108.6
10	181.9	181.9	186.7	181.1	186.1
10a	136.9	133.2	135.5	130.2	133.2
6-OMe	------	55.9	-----	------	56.4
8-OMe	------		60.1	62.1	60.3
3-CH_3	22.2	22.0	22.4	22.6	21.9

4.1.3.6. Chrysophanol-10,10'-bianthrone (295)

Compound **295** was isolated as a brown amorphous solid from the ethyl acetate extract of *S. dichlymobotrya*. Its molecular formula $C_{30}H_{22}O_6$ was established by HRESIMS (*m/z* 479.2463 [M + H]$^+$. The IR spectrum showed a broad band at 3401 cm^{-1} OH group, aromatic system at 1610 and 1580 cm^{-1} and a sharp (C=O stretch) bond at 1620 cm^{-1}. The structure was deduced from detailed analyses of ^1H and ^{13}C NMR (Table 14) data together with 2D NMR experiments (^1H-^1H COSY, HSQC and HMBC). The compound was suggested to be a bianthrone due to the presence of duplicate signals observed in the ^1H and ^{13}C NMR spectra. Ten signals in the region of δ_H 5.73-7.48 indicated the presence of aromatic system and were confirmed by the aromatic carbons signals in the region of δ_H 135.3-191.6, of which four were oxygenated and two carbonyl carbons. Such data provided evidence for 1,8-dihydroxyl dimeric anthrone moiety.

The ^1H NMR signal observed at δ_H 4.46 (2H, br s) showing HSQC correlation to δ_C 56.3 characteristically signified the presence of a 10,10'-dianthrone (Alemayehu *et al.*, 1993). Similarly, the presence of two methyl groups were evidenced by the proton signals at δ_H 2.22 and 2.32 which showed HSQC correlations to δ_C 21.9 and 22.1, respectively. Compound **295** was a product of oxidative coupling of two molecules of chrysophanol anthrone C-units, evidence by the both the NMR data and the molecular ion peak at *m/z* 478 in the ESIMS, which is in accordance with the total mass of two chrysophanol anthrone derivatives. The HMBC contours confirmed the assignments cited above, with apparent long range correlations observed between

8/2' to C-1/1', H-4/4' to C-3/3', H-6/6' to C-8/8', H-7/7' to C-6/6' and H-7/7' to C8/8' confirming the chrysophanol bianthrone skeleton for this compound. The data were thus consistent with the structure of chrysopahnol-10,10'-bianthrone (**295**), which had been reported from *Senna longiracemosa* (Alemayehu *et al.*, 1993), *and Cassia torosa* (Kitanaka & Takido 1982).

4.3.3.7. Physcion-10,10'-bianthrone (299)

The IR spectrum of compound **299** indicated similar functional group entities as **295**, except for the ^{1}H-NMR which indicated the presence of two methyls, two methoxy groups, eight *meta* coupled protons, four chelated hydroxyl groups and two benzylic methine protons (Table 14). The ^{1}H NMR spectrum indicated methoxylation of **299** at positions C-6/6' based on the HMBC correlation between the OMe protons at δ_H 3.81/3.83 and δ_H 152.7/152.6, consistent with the structure of physcion-10,10'-bianthrone (Kinanaka & Takido, 1982). A fact corroborated by the ESIMS spectrum which showed a peak at *m/z* 538 for $[M+H]^+$ which was 62 a.m.u higher than molecular mass of **295** and 270 for $[M/2 + H]^+$ fragment ions ($C_{16}H_{14}O_4$) due to symmetrical bianthrone cleavage to anthrones. The two compounds **295** and **299** exhibited no optical activity, which indicated both to be *meso* stereoisomers (Alemayehu *et al.*, 1993). From literature point of view, it was noted that isolation of physion-10,10'-bianthrone (**299**) from natural plants is rare as opposed to **295**. Never-the-less, it is reported to have been isolated from *Cassia torosa* (Kitanaka & Takido, 1982) and *Rumex japonicus* exhibiting strong activity against A549, PC-3, VO-31 and HCT-15 human cancer cell lines (Hwang *et al.*, 2004).

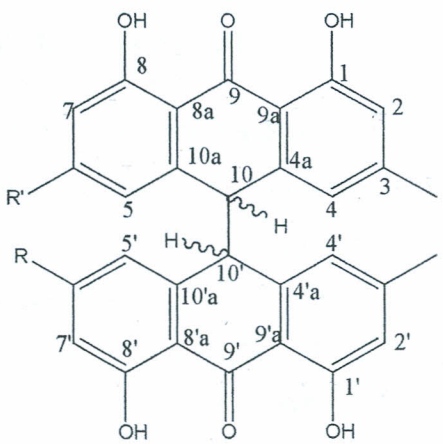

295: R = R' = H
299: R = R' = OMe

Table 14: ^{1}H (300 MHz) and ^{13}C (75 MHz) NMR spectral data for compound **295** and **299**

Atom	295		299	
	^{1}H NMR	^{13}C NMR	^{1}H NMR	^{13}C NMR
1/1'	----	162.3/162.1		162.8/162.5
2/2'	6.65/6.67 (br s)	121.2/121.0	6.33/6.36 (d, J = 2.5)	121.7/121.4
3/3'	----	147.5/147.3	----	148.0/147.7
4/4'	5.73/6.16 (br s)	116.8/116.6	5.97/6.04 (d, J = 2.4Hz)	117.3/117.1
4a/4a'	----	135.7/135.3	----	136.1/135.8
5/5'	6.34/6.37 (d, J = 9Hz)	119.3/119.3	6.10/6.12 (br s)	119.7/119.5
6/6'	7.35/7.48 (t, J = 8.1Hz)	135.7/135.3	----	152.7/152.6
7/7'	6.94/6.87 (d, J = 8.1Hz)	117.2/117.0	6.68/6.70 (br s)	117.5/117.3
8/8'	----	161.9/161.8	----	162.4/162.2
8a/8a'	----	113.9/114.5	----	114.8/114.4
9/9	----	191.7/191.6	----	192.2/192.1
9a/9a'	----	140.8/140.9	----	141.4/141.3
10/10'	4.46 (br s)	56.3	4.35 (br s)	56.9
10a/10a'	----	139.6/142.1	----	142.5/140.1
3/3'-Me	2.22/2.32 (s)	21.9/22.1	2.31/2.91(s)	22.5/22.3
6/6'-OMe	----	-----	3.81/3.83 (s)	58.36/58.44
1,8/1',8'-OH	11.88,11.96,12.15,12.13 (s)		11.81,11.87,12.12,12.17 (s)	

4.1.4. Structural elucidation of compounds from *Vitex doniana* stem-bark

A number of *Vitex* species have been investigated for ecdysteroids (Suksmararn *et al.*, 2000). Ecdysteroids analysis of *Vitex* has shown the occurrence of the three common (C-27, C-28 and C-29) ecdysteroids skeletal types (Filho *et al.*, 2008). In the course of this study, isolation of four new ecdysteroids, 2,3-acetonide-24-hydroxyecdysone (**411**), 11-hydroxy-20-deoxyshidasterone (**412**), 21-hydroxyshidasterone (**413**) 2,3-acetonide-22-*O*-β-glucosyl-20-hydroxyecdysone (**415**) together with one known 24-hydroxyecdysone (**414**) (Coll *et al.*, 1994) was achieved.

4.1.4.1. 21-Hydroxyshidasterone (413)

Compound **413** was obtained as colourless needles m.pt 232-234°C. Its ESI-MS molecular ion peak at *m/z* 479 with the formula $C_{27}H_{42}O_7$, as shown by HRESIMS molecular ion *m/z* 478.6182 [M$^+$] (calculated 478.6131 [M$^+$] $C_{27}H_{42}O_7$). The characteristic fragment ions were formed from the intact parent ion by the loss of four molecules of water: *m/z* 461 $[M + H - H_2O]^+$, 443 $[M + H - 2H_2O]^+$, and 425 $[M + H - 3H_2O]^+$, 407 $[M + H - 4H_2O]^+$ which is a common feature in ecdysteroids mass spectra (Suksamrarn *et al.*, 1995) and signified the presence of at least four OH groups. The IR spectrum showed strong absorption of hydroxyl groups at 3448 and characteristic absorption of α, β- unsaturated carbonyl moiety at 1652 cm^{-1}.

The ^{1}H and ^{13}C NMR chemical shifts data of this compound are summarized in tables 15 and 16. For the signal assignments, four methyl signals appearing as singlets were indentified in the ^{1}H NMR spectrum contrary to the expected five methyl groups for majority of the ecdysteroids. Such an observation implied an oxidation of one methyl groups (C-26/C-27 or C-21). The characteristic HMBC correlations (Fig. 11) of the methyl groups through two and three bonds were utilized in the assignments of the germinal Me-26 (δ_H 1.28, 2H, s) and Me-27 (δ_H 1.28, 2H, s) groups owing to their mutual HMBC correlation, indicating lack of oxygenation on C-26/C-27. The differentiation between Me-19 (δ_H 1.05, 3H, s) and Me-18 (δ_H 0.98, 3H, s) groups of the angular methyl groups was achieved by considering the ^{3}J correlation of the latter with C-17. Appearance of a doublet signal at δ_H 3.54 (1H, J = 12 Hz) coupling to another doublet overlapping with solvent signal at δ_H 3.41 (1H, d, J = 12 Hz) in the ^{1}H NMR spectrum and HMBC cross peaks between the same signals and δ_C 50.8 ascribed for C-17 suggested an oxymethylene protons on C-21.

The ^{13}C NMR chemical shift values (Table 16) of C-22 (84.0) and C-25 (82.5) and the H-22/Me-26 NOE correlation (Fig. 11) proved the presence of OR (R≠H) and a five membered-ring unit in the side chain (Simon *et al.*, 2008). Further support for this structure was achieved from the comparison of its spectral data with those of shidasterone (**353**) (Lafont *et al.*, 2002), except for one methyl Me-21 replaced by instead the oxymethylene signals in **413**. The chemical shift δ_C 85.3 for C-14 established an OH substitution, which is in accordance with a 7-en-6-one moiety, which showed HMBC cross-peak with the olefinic H-7 (5.90, 1H, d J = 2.2 Hz) and in turn correlated with two CH units [δ_C 52.2, C-5) and 42.4, C-9)]. The HMBC ^{2}J coupling of the latter methine H-atoms with the C-atom of the oxo group (207.0) and the quaternary C-atom in the sp^2 hybrid state (122.6) justified their assignments.

The H_α-9/H_α-2 and Me-19/H_β-5 correlations in the NOE spectrum of **413** established a *cis*-type junction of rings A and B (Fig. 11). Moreover, the presence of Hβ-12/Me-18, Hβ-12/CH_2OH-21 and Hα-12/Hα-17 cross peaks and the absence of Hα-9/Hα-15 correlations verified the *trans*-type junction of rings C and D. The NOESY plots were sufficient to identify the configuration at C-20, but insufficient to identify the configuration at C-22. Fortunately, the absolute configuration (22R) of shidasterone (**353**) has been established (Roussel *et al.*, 1995). Based on the biogenetic considerations, the intramolecular closure of the furanyl ring from the known precursor 20-hydroxecdysone followed by oxidation of Me-21 further implied the

stereochemical arrangement of compound **413** must be similar to **353**. It was thus concluded that compound **413** was 22,25-epoxy-2,3,14,20,21-pentahydroxycholest-7-en-6-one named 21-hydroxyshidasterone which is a new compound.

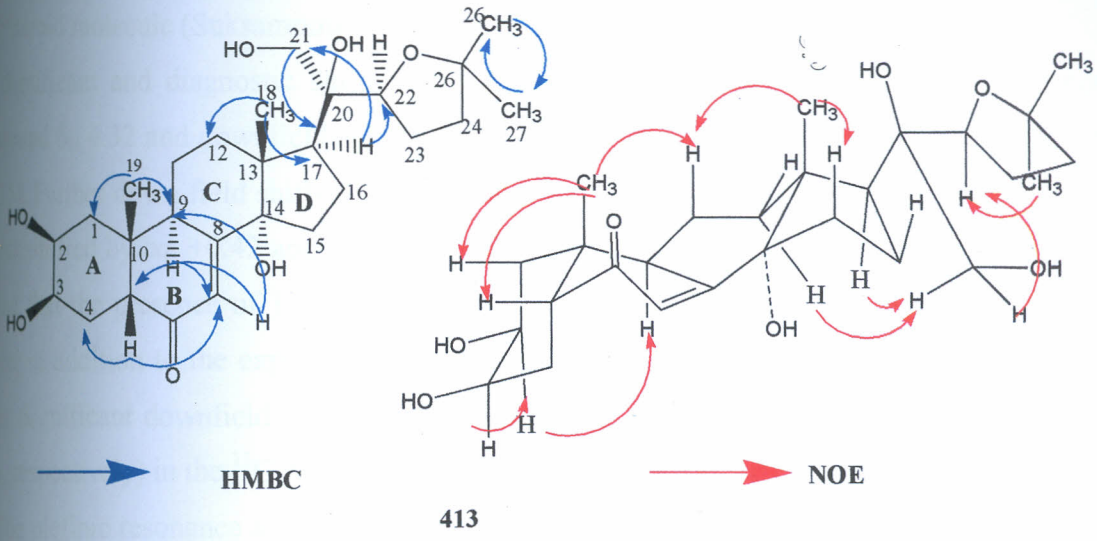

413

Figure 11: Significant HMBC correlations and NOE correlations for compound **413**

4.1.4.2. 11-Hydroxy-20-deoxyshidasterone (412)

Compound **412** was isolated as minor component from the methanol extract of *V. doniana* root bark as white crystalline solid with m.pt 258-262°C showing greenish grey spot upon spraying with *p*-anisaldehyde on TLC plate (Rf, 0.23, silica gel, 3% MeOH in $CHCl_3$). A molecular-ion peak at *m/z* 463.6188 ($[M + H]^+$, calculated for 463. 6081 $[M + H]^+$) suggested a formula $C_{27}H_{42}O_6$, and was in accordance with the ^1H- and ^{13}C-NMR data (Table 15 and 16). The IR spectrum showed strong absorptions of hydroxyl at 3427 and 1059 cm^{-1} and characteristic peak of α,β-unsaturated keto group at 1654 cm^{-1}.

The ^1H NMR spectral features and relative positions of H-2, H-3, H-5, H-7, H-9 and H-17 as well as those of Me-18 and Me-19 of this compound were almost identical to those of **415**, thus suggesting presence of the ecdysteroid nuclei. However, a notable difference was the presence of a methyl doublet [δ_H 0.92 d (3H, J = 6.5 Hz, H-21)] and an additional oxymethine proton [δ_H 4.32 m (1H, d, J = 5 Hz, H-11)] in the ^1H NMR spectrum. In reference to compound **413**, the methyl doublet could possibly exist at C-21, implying 20-deoxyshidasterone. C-11 has been identified as a biosynthetically labile hydroxylation point in ecdysteroids (Simon *et al.*, 2008; Dinan, 2001; Ba'thori & Pongraczi, 2005), with cyclization of the side chain to the

tetrahydrofuran, attachment of a hydroxyl group at C-11 was the other possible difference between the compounds **412** and **413**. Furthermore, the downfield shift observed for many signals in the ^{1}H NMR spectrum were attributed to the introduction of an 11-hydroxyl group to the ecdysteroid molecule (Suksamrarn *et al.*, 2000).

Significant and diagnostic shifts were observed by the presence of a carbinol proton signal around δ_H 4.32 and downfield shifts of H-9 and H-12$_{ax}$ of *ca.* 0.10 and 0.22, respectively (Table 15). Further down-field shifts of the remote protons were also observed, for H-1$_{eq}$ and H-12$_{eq}$ which shifted by *ca.* +0.42 and +0.47, respectively as compared those of compound **413**. It was noted that the presence of 11-hydroxyl group caused a + 2.1 ppm downfield shift of C-1 resonance, in addition to the expected down-field shift of the C-11 resonance in the ^{13}C NMR spectrum. Significant downfield signals were also observed for C-9 and C-12 signal (*Ca.* +3.3 and 10.6, respectively) in the ^{13}C NMR spectrum as compared to those of compound **413**.

The olefinic resonance at 5.62 (d, J = 1.5 Hz) showed HMBC correlations (Fig. 12) with C-5 (51.9), C-6 (206.9), C-8 (168.9), C-14 (85.3) and C-9 (42.5), which confirmed the presence of α,β-unsaturated carbonyl at C-6, one of the diagnostic features of ecdysteroids. The position of the carbinol proton at δ_H 3.76 (m, H-11) was defined by its correlations with C-8, C-10 (δ_C 34.5) and C-13 (δ_C 37.5), taken with H-12 (δ_H 2.25/2.23) correlating to C-9, C-13 and C-14. Ring C connectivity to the ring B was established by the correlations of H-7 to C-14, while the ring D connection was based on correlation of H-15 to C-14.

Positions of the angular methyl groups C-18 (δ_H 0.80, s) and C-19 (δ_H 0.83, s) were both secured by correlations of their respective protons to their α and β carbons. The doublet Me-21 (δ_H 0.92, J = 6.5 Hz) signals showed HMBC correlation with C-17 (δ_C 50.6), C-20 (δ_C 35.2) and C-22 (δ_C 85.0), considered together with H-17 (δ_H 2.52, dd, J = 9.6, 8.5 Hz) correlation to C-20, C-21 and C-22 confirmed the connectivity of ring D to the side chain. A carbinol proton signal at δ_H 3.95 (H-22) showing ^{3}J correlation to C-25 (δ_C 79.5), which in turn showed ^{3}J correlation with two geminal methyl protons Me-26 (1.05, s) and Me-27 (1.01, s) (reciprocally correlated in HMBC) confirmed the presence of tetrahydrofuran moiety.

The coupling patterns found for H-2 and H-3 of **412** were in close agreements with those of **413** indicating the two compounds had the same relative configuration at C-2 and C-3 (Fig. 12). The configuration at C-2/C-3 relative to the rest of the ring system was determined based on NOE data. NOE correlations between H-9 and H-11 established H-11 as axial whereas a

correlation between H-17 and Me-21 which in turn correlated with H-22 established the relative configuration at C-11 as β-OH and α-H_{17}; consequently compound **412** was thus characterized as 22,25-epoxy-2,3,11,14-tetrahydroycholest-7-en-6-one assuming the stereochemical characteristic of compound **413** except at C-11 (Fig. 12).

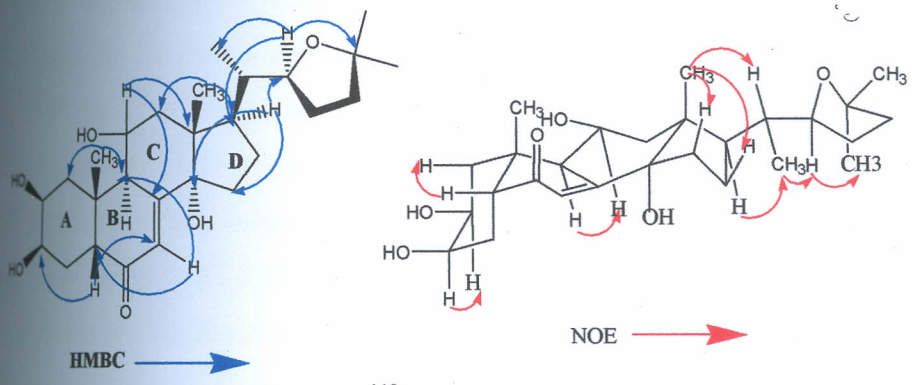

412

Figure 12: Significant HMBC correlation and NOE correlations for compound **412**

4.4.3. 24-Hydroxyecdysone (414)

Compound **414** was obtained as an amorphous solid with m.pt 244-246°C. The IR absorption bands at 3424 and 1693 cm^{-1} indicated the presence of hydroxyl and α,β-unsaturated keto groups. The ESIMS showed molecular ion *m/z* 481.0 (positive ion mode $[M+H]^+$) and the common ecdysteroid characteristic fragment ions formed from the successive loss of five water molecules (*m/z* 463 $[M + H - H_2O]^+$, 445 $[M + H - 2H_2O]^+$, 427 $[M + H - 3H_2O]^+$, 409 $[M + H - 4H_2O]^+$ and 391 $[M + H - 5H_2O]^+$) indicative of the presence of at least five OH groups.

The colour reactions to *p*-anisaldehyde reagent as well as the ^1H and ^{13}C NMR (Tables 15 and 16) indicated that the isolate was an ecdysteroid. The ^1H NMR spectral features and the splitting patterns of the key resonances δ_H 3.99 (1H, m, $J_{W½}$= 2.5 Hz, H-2), 3.89 (1H, m, $J_{W½}$= 7Hz, H-3), 2.44 (1H, dd, J = 10, 4.5 Hz, H-5), 5.86 (1H, s, H-7), 3.19 (1H, m $J_{W½}$= 9 Hz, H-9), 2.41 (1H, m, H-17), 0.93 (3H, s, Me-18) and 1.01 (3H, s, Me-19) were in support of an ecdysteroid, however, a number of ^1H NMR signals revealed some significant differences in both the splitting patterns and chemical shift as compared with those of 20-hydroxyecdysone (Budensinsky *et al.*, 2008). The doublet signals at δ_H 1.08 (3H, d, J = 6.8Hz), 3.54 (1H, m) and 4.59 (1H, t, $J_{W½}$= 22Hz) indicated the presence of a secondary methyl group and two side-chain secondary hydroxyl groups, respectively. One side-chain hydroxyl group was suggested to be

located at C-25, since the C-26 and C-27 methyl protons resonances appeared as two singlet signals at δ_H 1.13 (3H, s) and 1.19 (3H, s).

It was also evident that C-20 was not oxygenated, since the secondary methyl (Me-21) coupled with a proton at δ_H 2.15 (1H, m, H-20) which in turn coupled to H-22 according to ^{1}H-^{1}H COSY spectrum. Consequently, the three side-chain hydroxyl functionalities could be located at C-22, C-24 and C-25. The structure of **414** was further confirmed by ^{13}C NMR spectral data comparison with that of ecdysone (Budensinsky *et al.*, 2008). The only significant difference between the chemical shift values of the ^{13}C NMR resonances of these two compounds was that of oxygenated C-24 at δ_C 83.7 (Table 16). The structure of compound **414** was established as 24-hydroxyecdysone on the basis of spectral similarity with those of 24-hydroxyecdysone isolated from *Polypodium vulgare* (Fern) (Coll *et al.*, 1994).

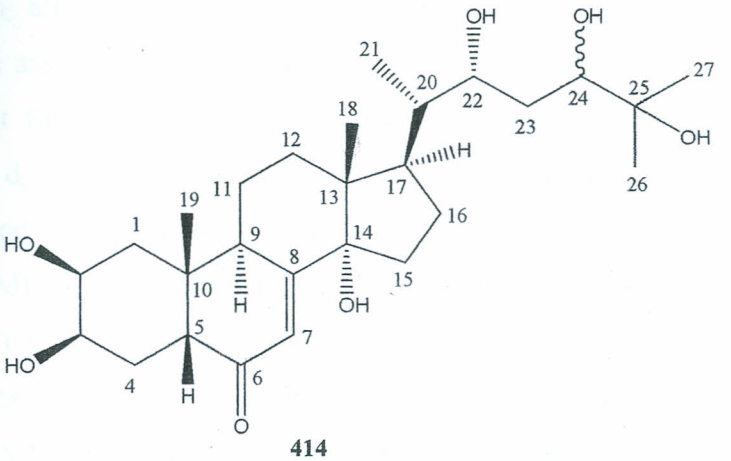

414

4.1.4.4. 2,3-Acetonide-24-hydroxyecdysone (411)

Compound **411** was isolated as white needles with m.p 158-160°C. The IR spectrum of the compound contained absorption bands of hydroxyl groups (3423 cm^{-1}) and a keto group conjugated with a double bond (1653 cm^{-1}). Its UV spectrum (λ_{max}^{MeOH} 244 nm) further confirmed the presence of a 7-en-6-keto group in the steroid nucleus. The ESIMS showed molecular ion base peak *m/z* 520 $[M]^+$ along with fragment ions at *m/z* 502, 484, 466, 448 corresponding to successive loss of four water molecules from the parent ion. The ^{13}C NMR spectrum of **411** (Table 16) displayed six signals for oxygenated carbons, besides that of the unsaturated ketone.

Analysis of mass fragmentation and ^{13}C NMR data of **411** suggested the location of three hydroxyl groups at the side chain of this ecdysteroid. The peak at *m/z* 360 in the mass spectrum corresponded to the loss of side chain moiety to give a fragment ion bearing the ecdysteroid rings

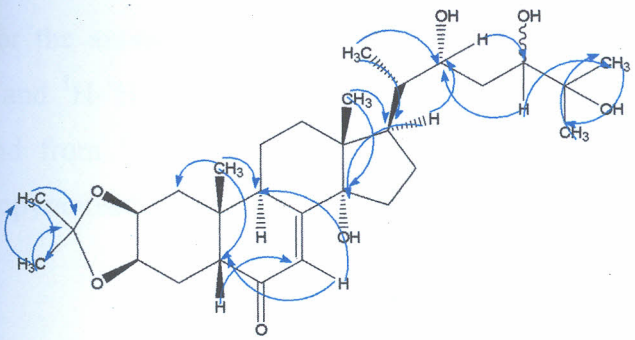

411

Figure 13: Significant HMBC correlations for compound **411**

4.1.4.5. 2,3-Acetonide-22-*O*-β-glucosyl-20-hydroxyecdysone (415)

Compound **415** was isolated as a white powder with m.pt of 262-264°C. The ESIMS showed molecular ion base peak at *m/z* 683 and fragment ion peak at *m/z* 521 representing [M + H - 162], which suggested the presence of a hexose unit in the molecule. The ^{1}H NMR (Table 15) spectrum showed seven methyl signals (one doublet and six singlets) indicating the compound belonged to the ecdysone series with a ketal moiety due to the signals for two pairs of methyl singlets [Me 26/27 (δ_H 1.43/1.43) and $Me_2C=(O)_2$ (δ_H 1.09/1.23)] which presented correlations in the COSY spectrum and auto-correlations in HMBC spectrum (Fig. 14). The other pair of methyl singlets were thus for the C-18 and C-19 typical of a steroid molecular skeleton. The compound was envisaged to be a derivative of compound **414**, with modified side chain and alkylated hydroxyl groups.

The ^{1}H-^{1}H COSY correlations between 22-H (3.68 m $J_{W½}$= 9.7 Hz) and 20-H (2.19, m), and between 17-H (2.40, t, J = 6.5 Hz) with the methyl doublet (1.28, d, J = 8 Hz, 21-H) implied 20-deoxyecdysteroid skeleton. The presence of the sugar moiety was evident by the additional peaks in the ^{1}H NMR spectrum in the region of the hydrogen attached to oxygenated carbons (δ_H 3.3-4.9) and from the ^{13}C NMR (Table 16) spectrum, where six additional oxygenated carbon signals were observed (δ_C 64.7.8-97.7). This was in agreement with the link of the ecdysteroids with a glycoside group (Maria *et al.*, 2005). The C-22 signal (δ_C 90.4) was more deshielded (*ca.* +12 compared to other 20-hydroxyecdysones) (Ba'thori *et al.*, 1998; Snogan *et al.*, 2007) and thus suggested the attachment of the sugar unit at C-22, a conclusion confirmed from the ^{1}H-^{13}C long range (^{3}J) correlations of H-1′ to C-22 and H-22 to C-1′ observed in the HMBC spectrum (Fig. 14). The identity of the sugar moiety as β-glucopyranose was concluded from the

characteristic signal for the anomeric proton at δ_H 4.90 (d, J = 4.5Hz) (Jones *et al.*, 1993; Snogan *et al.*, 2007), and ^{1}H-^{1}H coupling patterns observed for H-3′ and H-5′; H-2' and H-4' (COSY spectrum), and from ^{13}C-NMR C-2′, C-3′, C-4′ and C-5′ chemical shifts were in agreement with β-glucopyranoside (Breitmaier & Voelter, 1987).

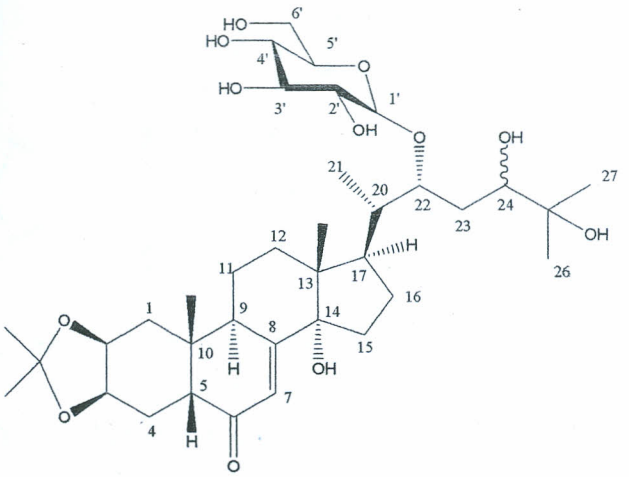

415

The ^{13}C NMR spectrum (Table 16) showed that the compound was similar to 22-*O*-β-glucosylecdysone except for the presence of three more peaks corresponding to the ketal group (δ_C 108.61, 26.12, and 26.1) and the signal for C-2 and C-3 were shifted downfield δ_C 72.7 and 72.3. The mass spectrum of compound **415** showed the molecular ion peak at *m/z* 683.8. This is 42 a.m.u higher than the molecular weight of 22-*O*-β-glucosyl-20-hydroxyecdysone. Accordingly the structure of compound **415** was characterized as 2,3-acetonide-22-*O*-β-glucosyl-20-hydroxyecdysone, on the basis comparison with published data for related compounds (Sadikov *et al.*, 2000; Snogan *et al.*, 2007). Since acetone was not used in the extraction and subsequent treatment of the extractive substance, the compound was a real natural product from the stem bark of *Vitex doniana*.

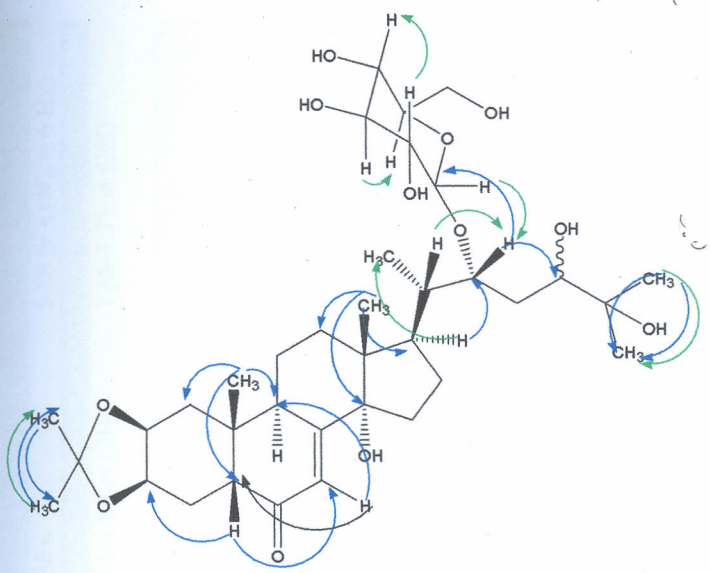

415

Figure 14: HMBC and COSY correlations for compound **415**

Although 20-deoxyecdysteroids (11α-hydroxyecdysone, **335**) derivatives similar to **411-415** have previously been reported from *V. scabra,* and *V. strickeri* (Suksamrarn *et al.*, 2002; Zhang *et al.*, 1992), the co-occurence of a series of such compounds with tetrahydrofuran cyclized side chain, acetonides and/or glycosidated metabolites like compounds **411-415** is unprecedented among the *Vitex* species. Compound **412** and **413** merits special attention as regards the C-11 and C-21 oxygenation, respectively in addition to a five-membered ether ring in the steroid skeleton. Such ecdysteroids derivatives are rather unusual, but it is noteworthy that they are characteristic for *V. doniana.* Ecdysteroids influence many physiological activities in a positive way and show no toxicity to mammals (Simon *et al.*, 2008). The most pronounced effect on mammals is stimulation of protein synthesis without adverse androgenic, antigonadotropic or thymolytic side effects (Ba'thori & Pongraczi, 2005).

Table 15: ^{1}H NMR (300 MHz) spectral data for ecdysteroids [411-415] isolated from *V. doniana* stem bark

Atom	411 (CD_3OD)	412 (CD_3OD)	413 (CD_3OD)	414 (CD_3OD)	415 (DMSO-d_6)
1	1.99-2.00 m H_{eq} 1.77-1.80 m H_{ax}	2.49 m H_{eq} 1.25-1.34 m H_{ax}	2.07 m H_{eq} 1.99 m H_{ax}	1.81 m H_{eq} 1.43-1.51 m H_{ax}	1.96-2.00 m H_{eq} 1.86-1.88 m H_{ax}
2	4.18 m ($W_{½}$ = 18.6 Hz)	4.44 m ($W_{½}$ = 5.5 Hz)	4.62 br s	3.99 m ($W_{½}$ = 12.5 Hz)	4.28 m ($W_{½}$ = 7.5 Hz)
3	3.94 m ($W_{½}$ = 3 Hz)	4.35 m ($W_{½}$ = 2.5 Hz)	4.04 d (J = 1.1H z)	3.89 m ($W_{½}$ = 11 Hz)	4.46 m
4	1.95-1.98 m H_{eq} 1.74-1.77 m H_{ax}	1.70-1.72 m (2H)	2.04 m H_{eq} 2.14 m H_{ax}	1.71-1.76 m H_{eq} 1.63-1.68 m H_{ax}	1.83-1.84 m H_{eq} 1.68-1.76 m H_{ax}
5	2.45 dd (J = 11.1, 3.6 Hz)	2.26 dd (J = 13.1, 3.5 Hz)	2.49 d (J = 5Hz)	2.44 dd (J = 10, 5 Hz)	2.44 dd (J = 10, 5 Hz)
7	5.80 d (J = 2.7 Hz)	5.62 d (J = 1.5 Hz)	5.90 d (J = 2.2 Hz)	5.86 s	5.88 br s ($W_{½}$ = 6 Hz)
9	3.13 t (J = 7 Hz)	3.14 m ($W_{½}$ = 10 Hz)	3.24 m ($W_{½}$ = 6 Hz)	3.19 m ($W_{½}$ = 9 Hz)	3.02 m ($W_{½}$ = 26 Hz)
11	1.71-1.75 m H_{eq} 1.77-1.81 m H_{ax}	4.76 d (J = 5 Hz)	1.89 m H_{eq} 1.71 m H_{ax}	1.71-1.87 m (2H)	1.68-1.73 m (2H)
12	1.95-1.97 m H_{eq} 2.10 dd (J = 12.9, 5 Hz)	2.25 dd (J = 12.5, 10.4 Hz) 2.23 dd (J = 12.4, 6.0 Hz)	2.03 m H_{eq} 1.76 m H_{ax}	2.15 m H_{eq} 1.86 m H_{ax}	1.86-1.96 m (2H)
15	1.64-1.67 m H_{α} 1.77-1.80 m H_{β}	1.47-1.49 m H_{α} 1.90-2.00 m H_{β}	1.86-1.88 m (2H)	1.57-1.64 m H_{α} 1.98-2.04 m H_{β}	2.01-2.18 m H_{α} 1.63-1.66 m H_{β}
16	1.69-1.73 m H_{α} 2.36 m ($W_{½}$ = 5.4 Hz)	1.58-160 m H_{α} 1.49-1.50 m H_{β}	2.04-2.06 m (2H)	1.90-1.98 m H_{α} 1.71-1.76 m H_{β}	1.88-1.95 m H_{α} 1.52-1.63 m H_{β}
17	2.50 m ($W_{½}$ = 13 Hz)	2.52 dd (J = 9.6, 8.5 Hz)	2.47 dd (J = 12.8, 4.6 Hz)	2.41 m ($W_{½}$ = 9.7 Hz)	2.40 t ($W_{½}$ = 6.5 Hz)
18	0.90 s	0.80 s	0.98 s	0.93 s	0.95 s
19	0.96 s	0.83 s	1.05 s	1.01 s	1.36 s
20	1.99 m	2.44 m		2.15 m ($W_{½}$ = 5 Hz)	2.19 m
21	1.41 d (J = 6 Hz)	0.92 d (J = 6.5 Hz)	3.54 d (J = 12 Hz) 3.41 d (J = 12 Hz)	1.08 d (J = 6.8 Hz)	1.28 d (J = 8 Hz)
22	3.82 dt (J = 15, 4 Hz)	3.95 m	3.90 m ($W_{½}$ = 11.3 Hz)	3.54 m ($W_{½}$ = 11 Hz)	3.68 m ($W_{½}$ = 9.7 Hz)
23	2.07-2.12 m (2H)	1.70-1.72 m, H_{α}/ 1.97-2.00 m, H_{β}	2.03 m H_{eq}/ 1.81 m H_{ax}	1.98-2.05 m (2H)	1.47-1.66 m (2H)[a]
24	3.52 t ($W_{½}$ = 10.5 Hz)	1.72 -1.74 m (2H)	1.68-1.70 m (2H)[a]	4.59 t ($W_{½}$ = 22 Hz)	3.65 t ($W_{½}$ = 9 Hz)
26	1.31 s	1.05 s	1.28 s	1.13 s	1.43 s
27	1.29 s	1.01 s	1.28 s	1.19 s	1.43 s
Me_2C=	1.19 s/ 1.45 s				1.09 s /1.23 s
1'					4.90 d (J = 4.5Hz)
2'					3.99 d (J = 8 Hz)
3'					3.82 m
4'					4.08 d (J = 8 Hz)
5'					3.77 dd (J = 11.7, 5 Hz)
6'					3.87 dd (J = 11.7,5 Hz) 3.86 dd (11.7, 6Hz)

Table 16: ^{13}C NMR (75 MHz) spectral data for ecdysteroids [**411-415**] isolated from *V. doniana* stem bark

Atom	411 (CD_3OD)	412 (CD_3OD)	413 (CD_3OD)	414 (CD_3OD)	415 (DMSO-d_6)
1	45.0	39.4	37.3	38.2	46.3
2	75.1	71.4	68.7	68.7	72.7
3	73.6	68.8	68.0	67.2	72.3
4	25.7	33.1	35.1	32.3	32.8
5	54.9	51.9	52.2	51.9	48.0
6	205.9	206.9	207.0	203.7	203.6
7	122.4	121.7	122.6	124.1	123.9
8	155.4	168.6	168.5	152.7	170.2
9	35.2	42.5	39.2	36.2	36.00
10	39.2	34.5	41.5	39.7	40.7
11	21.2	76.3	22.7	21.2	22.0
12	33.7	43.5	32.9	30.5	31.8
13	44.6	37.5	39.4	46.5	45.0
14	85.7	85.3	85.3	86.2	85.8
15	31.8	32.4	31.6	29.3	31.6
16	22.2	21.7	21.4	22.7	22.4
17	51.5	50.6	50.8	50.6	50.5
18	17.0	18.2	18.5	18.3	18.5
19	24.1	24.5	23.6	23.6	21.9
20	40.4	35.2	76.3	41.9	45.4
21	18.5	21.2	71.9	17.5	22.1
22	77.8	85.0	84.0	78.1	90.4
23	27.0	29.7	26.1	30.5	29.3
24	79.1	37.3	42.4	83.7	85.7
25	68.7	79.5	82.5	70.7	76.3
26	29.8	27.5	28.9	28.2	26.7
27	28.6	27.3	28.1	26.1	26.7
$Me_2C=$	28.6/27.1				24.4/25.6
OCO	108.6				108.6
1'					97.8
2'					73.2
3'					69.9
4'					70.7
5'					74.4
6'					64.7

4.2. Biological activity studies

In the course of this study, a bioassay guided isolation of the active components of the three plants (*Caesalpinia volkensii, Senna didymobotrya* and *Vitex doniana*) was envisaged and the structural elucidation of the pure compounds is discussed in section 4.1. The biological activities carried out on the crude methanol extracts of *C. Volkensii* root and stem bark, *S. didymobotrya* roots and *V. doniana* followed by screening of the partitioned fractions. The bioassay experiment carried included antiplasmodial, antinociceptive, anti-inflammatory antidyslipidemic, antiadipogenesis and antioxidant activities. Further purification of the active fractions and the choice biological evaluation for the pure isolates was based on the performance of the crude extracts at the initial biological screening. The relative activities of the compounds reported herein have been studied relative to respective relevant standards drugs.

4.2.1. Antiplasmodial activities

4.2.1.1. Antiplasmodial activity of the crude extracts from *Caesalpinia volkensii, Senna didymobotrya and Vitex doniana*

In the preliminary studies, all the five methanol extracts from the three plants were screened using a non-radioactive assay technique (Smilkstein *et al.*, 2004) to determine 50% growth inhibition of the cultured chloroquine-sensitive (D6) and resistant-strains (W2) of *Plasmodium falciparum*. From the results presented in table 17, at least two extracts exhibited antiplasmodial activity, with IC_{50} values ranging from 10.47 to 20.97 µg/ml. The most active crude extracts was that of the root bark extract of *Caesalpinia volkensii*, with an IC_{50} of 12.26 and 13.87 µg/ml against D6 and W2, respectively while the stem bark was IC_{50} 15.28 /19.98 µg/ml. Such activity of *C. volkensii* root-bark and stem-bark could be rated as limited or moderate antiplasmodial activities on scale described by Basco *et al.*, (1994). *S. didymobotrya* root extract showed IC_{50} of 21.23 /18.38 µg/ml against D6 and W2, respectively (Table 17) and this was within low activity ranges on scale described by Basco *et al.*, (1994). The activity for *Vitex doniana* stem-bark and root-bark were with $IC_{50} > 50$ (Table 17) were considered inactive.

Table 17: *In vitro* antiplasmodial activity (50% growth inhibition) of MeOH extract of *C. volkensii* root and stem-bark, *S. didymobotrya* roots and *V. doniana* stem and root-bark against D6 and W2 strains of *Plasmodium falciparum*.

Experimental schedule	D6 Clone IC_{50} (µg/ml ± SD)	W2 Clone IC_{50} (µg/ml ± SD)
C. volkensii root-bark	12.26 ±2.44[a]	13.87 ± 2.6
C. volkensii stem-bark	15.28 ± 2.10[a]	19.98 ± 1.71[a]
S. didymobotrya roots	21.23 ± 0.09	18.38 ± 0.47[a]
V. doniana stem-bark	NA	NA
V.doniana root-bark	NA	NA
Chloroquine	0.008 ± 0.004	0.05 ± 0.01

Values with same superscript in the same column are significantly the same at $P \leq 0.05$ (one-way ANOVA followed by Bonferroni posttests). Samples with NA did not show activity in tested range (50 µg/ml).

Following the screening result, the most active crude extract (CVR and CVS) were further partitioned using different solvents, which were tested for antiplasmodial activity before isolation of the pure compounds from the active fractions (Section 4.2.1-2).

4.2.1.2. Antiplasmodial activities of *Caesalpinia volkensii* root bark extracts and pure isolates

The ethyl acetate extract of *C. volkensii* showed significantly ($P \leq 0.05$) moderate antiplasmodial activity against D6 and W2 strains of *Plasmodium falciparum* with IC_{50} values of 0.23 ± 0.09 and 4.38 ± 0.47 µg/ml, respectively, compared to standard drug chloroquine (Table 18). In spite of the low antiplasmodial activity observed with most of the pure compounds isolated from this fraction (Table 18), moderate ($P \leq 0.05$) activity exhibited by the methyl ester voucapane derivatives could be attributed to the activity of ethyl acetate extracts that was most active fractions.

Antiplasmodial activity of furanoditerpenes (caesalpinins and norcaesalpinin) with IC_{50} ranges of 90 nM to 6.5 µM from *Caesalpinia crista* seed kernels has been reported against *Plasmodium falciparum* FCR-3/42 *in vitro* (Linn *et al.*, 2005). It was noted that furanoditerpenes from the root bark of *C. volkensii* exhibited lower antiplasmodial activities compared to those reported by Linn *et al.*, (2005) and this could be attributed to the molecular structural difference between cassane-type diterpenes and norcassane-type diterpenes. Such differences can justified by the notable potent activity of norcaesalpinin E (**163**) at IC_{50} 90 nM higher than that of chloroquine (IC_{50} 283- 291 nM) against FCR-3/42 strains (Linn *et al.*, 2005)

Table 18: *In vitro* antiplasmodial activity (IC_{50}) of a fractionated MeOH extract of *C. volkensii* root bark (CVR) and some isolates against D6 and W2 strains of *Plasmodium falciparum*.

Experimental schedule	D6 Clone IC_{50} (µg/ml ± SD)	W2 Clone IC_{50} (µg/ml ± SD)
n-hexane extract	16.59 ± 1.44[a]	10.87 ± 1.65[a]
CH_2Cl_2 extract	15.28 ± 2.10[a]	13.98 ± 1.71[a]
EtOAc extract	0.23 ± 0.09[b*]	4.38 ± 0.47
n-BuOH extract	NA	NA
Chloroquine	0.007 ± 0.001[b*]	0.027 ± 0.004
	IC_{50}(µM ± SD)	**IC_{50} (µM ± SD)**
1α,5α-dihydroxyvoucapane (**400**)	NA	NA
Voucapan-5-ol (**22**)	NA	NA
1α,6β-dihydroxyvoucapane-19β-methyl ester (**401**)	46.13 ± 1.95[a]	34.43 ± 1.39[a]
Deoxycaesaldekarin C (**95**)	25.67 ± 1.93	30.33 ± 0.92[a]
Caesaldekarin C (**38**)	34.44 ± 3.33	30.69 ± 2.35[a]
5-hydroxyvinhaticoic acid (**399**)	46.14 ± 3.37[a]	47.54 ± 2.10
Triacontanyl-(*E*)-ferrulate (**402**)	NA	NA
Triacontanyl-(*E*)-caffaete (**403**)	NA	NA
Chloroquine	0.017 ± 0.008	---
Mefloquine		0.040 ± 0.007

Values with same superscript in the same column are significantly the same at $P \leq 0.05$ (one-way ANOVA followed by Bonferroni posttests). Significant activities [b*]$P \leq 0.05$ comparable to control chloroquine or mefloquine). Samples with NA were not active at the tested range (50 µg/ml and/or 50 µM).

4.2.1.3. Antiplasmodial activities of *Caesalpinia volkensii* stem bark extracts and pure isolates

The partitioned fractions of the methanol extract from *C. volkensii* stem bark all showed significantly moderate activities against both chloroquine sensitive and resistant strains of *P. falciparum* (IC_{50} range from 1.35 ± 0.54 to 14.32 ± 3.23 µg/ml) except *n*-hexane fraction that was inactive at 50 µg/ml (Table 19). The active fractions were realized to be generally more active against the chloroquine resistant strain than the sensitive strain of *P. falciparum*, with *n*-butanol exhibiting the highest activity comparable to mefloquine ($P \leq 0.05$). Although these result were not significantly different between the strains, the activities of the stem extracts were better than the activities of the water and petroleum ethers leave extracts at IC_{50} 404 µg/ml and 250 µg/ml, respectively (Kuria *et al.*, 2001) against FCA: 20GHA chloroquine sensitive and W2, chloroquine resistant strains of *P. falciparum*. This implied *C. volkensii* elaborate more active components against malarial parasites than the root bark and the leaves.

Table 19: *In vitro* antiplasmodial activity (IC_{50}) of a fractionated MeOH extract of *C. volkensii* stem-bark and some isolates against D6 and W2 strains of *Plasmodium falciparum*.

Experimental schedule	D6 Clone IC_{50} (µg/ml ± SD)	W2 Clone IC_{50} (µg/ml ± SD)
n-hexane extract	NA	NA
CH_2Cl_2 extract	14.32 ± 3.23^{a}	11.30 ± 1.94^{a}
EtOAc extract	10.43 ± 1.85^{a}	8.75 ± 1.21^{b}
n-BuOH extract	4.54 ± 0.86^{b}	$1.35 \pm 0.54^{c*}$
Chloroquine	$0.007 \pm 0.001^{c*}$	0.027 ± 0.004^{c}
	IC_{50}(µM ± SD)	**IC_{50} (µM ± SD)**
Voulkensin A (**408**)	11.63 ± 1.05^{d}	16.53 ± 1.08^{d}
Voulkensin B (**407**)	17.26 ± 1.58^{d}	22.79 ± 1.34^{d}
Voulkensin C (**406**)	18.69 ± 1.22^{d}	15.57 ± 1.01^{d}
3-β-Glu-3-xyl-stigmasterol (**409**)	4.44 ± 0.88^{e}	2.74 ± 1.10^{e}
Oleanolic acid (**185**)	23.81 ± 2.57^{d}	26.24 ± 1.50^{d}
3-β-acetylolean-12-en-28-methyl ester (**405**)	18.69 ± 1.11^{d}	24.44 ± 1.25^{d}
stigmasterol (**176**),	NA	NA
β-sitosterol (**177**)	NA	NA
Chloroquine	0.017 ± 0.01^{f}	-------
Mefloquine	---------	0.04 ± 0.01^{f}

Values with same superscript in the same column are significantly the same at $P \leq 0.05$ (one-way ANOVA followed by Bonferroni posttests). Significant activities $^{b*}P \leq 0.05$ comparable to control (chloroquine or mefloquine). Samples with NA were not active at the tested range (50 µg/ml and/or 50 µM).

Following the moderate activities exhibited by the three fractions (Table 19), chromatographic separation and purification of the possible active compounds ensued and eight compounds were isolated [voulkensin A, (**408**), voulkensin B, (**407**), and voulkensin C (**406**), voucapan-5-ol (**19**), caesaldekarin C (**38**), deoxycaesaldekarin C (**95**), oleanolic acid (**185**), 3-β-acetoxyolean-12-en-28-methyl ester (**405**), stigmasterol (**176**), β-sitosterol (**177**) and 3-*O*-[β-glucopyranosyl(1→2)-*O*-β-xylopyranosyl]-stigmasterol (**409**)]. The antiplasmodial activities of the compounds unique to the stem bark of *C. volkensii* are summarized in Table 19. Compound 409 exhibited the highest antiplasmodial activity with IC_{50} values of 4.44 ± 0.88 and 2.74 ± 1.10 µM against D6 and W2 strains, respectively. Although this activity was inferior to chloroquine and mefloquine, it was remarkable within the range of moderate activity according to Muriithi *et al.*, (2002). The other compounds showed activities within the range of IC_{50} values 11 to 26 µM which fall between moderate to low activity (Muriithi *et al.*, 2002). Considering the activities of the crude fractions (Table 19), the IC_{50} were ranging between good activity and moderate activity on scale adopted from Basco *et al.*, (1994).

4.2.2. *In vivo* antinociceptive and anti-inflammatory assays

4.2.2.1. Acute toxicity of the root bark of *C. volkensii*, roots of *S. didymobotrya* and stem bark of *V. doniana* methanol extracts to mice

Prior to administration of the plant extracts on mice, acute toxicity experiment was performed on the crude extracts of *C. volkensii, S. didymobotrya* and *V. doniana* in order to determine the toxicity levels (NIH, 1985). The methanol extract of *C. volkensii* root bark at doses of 200, 500 and 1000 mg/kg i.p given to mice, had no effect on their behavioural responses and no mortality during the observation period of 72 h after administration. The extract from *V. doniana* showed no mortality cases up to dose of 1500 mg/kg i.p given to mice and no adverse behavioural responses were observed. Based on low toxicity profile observed, *in vivo* pharmacological assay using the extracts from *V. doniana* stem bark was warranted. The animals treated with *S. didymobotrya* extract at doses above 1000 mg/kg exhibited decreased motor activity and calmness, followed by severe passing out of watery stool. This showed the laxative effect of the *S. didymobotrya* components.

4.2.2.2. Antinociceptive activities of crude extracts of *C. volkensii, S. didymobotrya* and *V. doniana*

The methanol extracts of *C. volkensii* root (CVR) and stem bark (CVS), *S. didymobotrya* root bark (SDR) and *V. doniana* root (VDR) and stem bark (VDS) given by intraperitoneal injection in mice showed a significant analgesic activity ($P \leq 0.05$) in the two antinociceptive test models at a doses of 100 mg/kg (Fig 15 and 16). Two extracts (CVR and VDS) were more active showing significant activities ($P \leq 0.05$) comparable to ibuprofen and morphine however the activities of SDR and VDR were significantly ($P \leq 0.05$) low in the thermal induced nociception (hot plate test) whereas CVS showed moderate activity upto138.09% inhibition at 100 mg/kg (Fig. 15). *S. didymobotrya* extract (SDR) showed no analgesic activity. These preliminary antinociceptive activities results of the crude extracts indicated that *C. volkensii* and *V. doniana* root bark extracts possess antinociceptive principles which warranted further investigations.

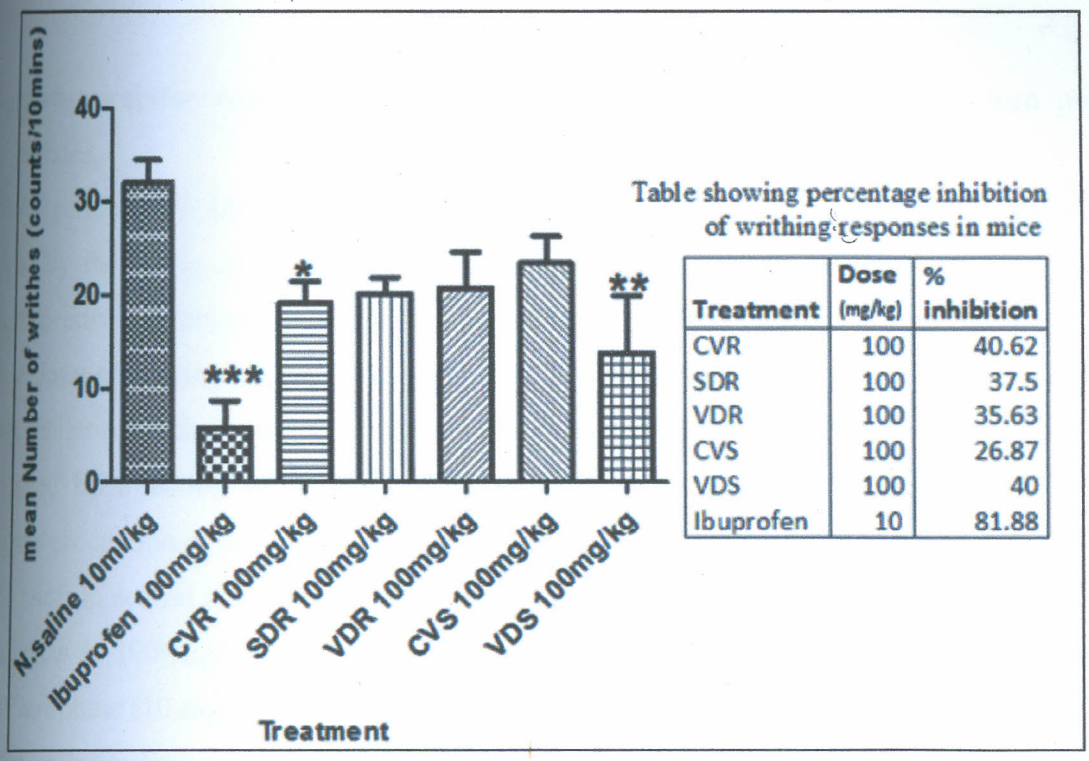

Table showing percentage inhibition of writhing responses in mice

Treatment	Dose (mg/kg)	% inhibition
CVR	100	40.62
SDR	100	37.5
VDR	100	35.63
CVS	100	26.87
VDS	100	40
Ibuprofen	10	81.88

Figure 15: Antinociceptive effects of crude methanol extracts of *C. volkensii* root (CVR) and stem bark (CVS); *S. didymobotrya* root bark (SDR); *V. doniana* root (VDR) and stem bark (VDS) on acetic acid writhing test. *P ≤ 0.05, **P ≤ 0.01, ***P ≤ 0.001 vs. control (one-way ANOVA followed by Bonferroni posttests). % inhibition calculated against normal saline water (vehicle).

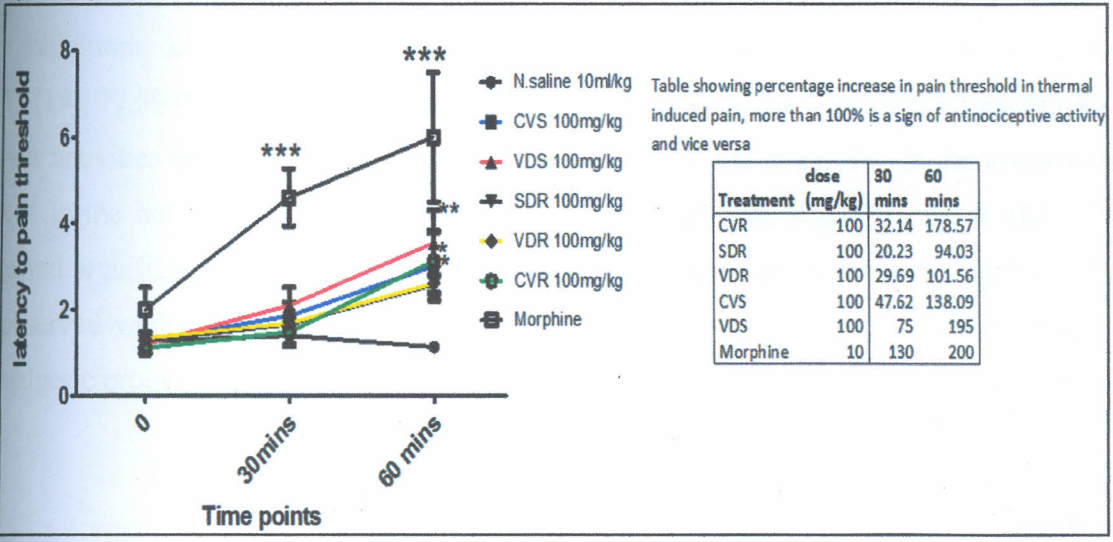

Table showing percentage increase in pain threshold in thermal induced pain, more than 100% is a sign of antinociceptive activity and vice versa

Treatment	dose (mg/kg)	30 mins	60 mins
CVR	100	32.14	178.57
SDR	100	20.23	94.03
VDR	100	29.69	101.56
CVS	100	47.62	138.09
VDS	100	75	195
Morphine	10	130	200

Figure 16: Antinociceptive effects of crude methanol extracts of *C. volkensii* root (CVR) and stem bark (CVS); *S. didymobotrya* root bark (SDR); *V. doniana* root (VDR) and stem bark (VDS) on hot plate nociceptive test. *P ≤ 0.05, **P ≤ 0.01, ***P ≤ 0.001 vs. control (one-way ANOVA followed by Bonferroni posttests). % inhibition calculated against normal saline water (vehicle).

4.2.3. Antinociceptive Activities of *Caesalpinia volkensii* root bark extracts and pure isolates

Both peripherally and centrally mediated effects of the extracts and isolates were investigated by the acetic acid induced abdominal constriction test and hot plate analgesics methods, respectively (Vongtau *et al.*, 2004). On enteral administration of different extracts of *C. volkensii* at doses of 100 mg/kg, only two extracts ($CHCl_3$ and EtOAc extracts) produced 40.6% and 44.4% inhibition of the writhing process in mice ($P \leq 0.05$, Table 20), which is an algogenic state triggered by injection of acetic acid (Deraedt *et al.*, 1980). These extracts could be inhibiting the production of such mediators hence the antinociceptive property.

To confirm central analgesic activity, the hot plate test showed that *n*-hexane, $CHCl_3$ and EtOAc extracts at 100 mg/kg had significant effect ($P \leq 0.05$) comparable to the inhibitory activity of morphine (10 mg/kg) (Table 20). This implied no opioid-like receptors were involved and may be linked to lipoxygenase inhibition (Duarte *et al.*, 1992). These results suggest that *C. volkensii* extracts have analgesic metabolites extracted by the medium polar solvents. The administration of **19**, **38**, **95**, **398** and **403** (100 mg/kg) caused a significant ($P \leq 0.01$) reduction in the number of writhing episodes induced by acetic acid compared to the control (Fig 17). The percentage inhibitions of abdominal constrictions were calculated as 81.88 (ibuprofen), 65.62 (**398**), 68.75 (**19**), 77.59 (**95**), 67.19 (**38**), and 40.01 % (**403**). All the test compounds except **403** showed lower activities but insignificant ($P \leq 0.01$) difference to the ibuprofen in the acetic acid writhing test. In the hot plate method, the same compounds **19**, **38**, **95**, **398** except **403** (100 mg/kg) showed significant ($P \leq 0.01$) activity at 60 minutes relative to control (Fig 18). The activities observed were associated with the presence of the furanoditerpenes in line with the previous analgesic properties reported for cassane-type furanoditerpenes (Nunan *et al.*, 1982).

Table.20: Effects of *Caesalpinia volkensii* root bark extracts on hot plate-induced pain and acetic acid-induced writhing in mice

Dose Treatment (mg/kg)	Pain threshold (Hot plate induced)					Writhing response	
	Pre-treatment latency (s)	**Post-treatment latency (s)**		% Inhibition		Total No. of writhes	% Inhibition
		30 min	**60 min**	**30 min**	**60 min**		
n-Hex ext	1.12 ± 0.37	1.48 ± 0.45	3.12 ± 0.59*	1.25	6.92	20 ± 3.06	37.5
$CHCl_3$ ext	1.26 ± 0.15	1.86 ± 0.69	3 ± 0.42*	2.09	6.05	19 ± 3.34*[a]	40.62
EtOAc ext	1.2 ± 0.45	2.1 ± 0.22	3.54 ± 0.39**	3.13	8.13	17.8 ± 2.27**[a]	44.38
n-BuOH ext	1.34 ± 0.19	1.68 ± 0.41	2.6 ± 0.38	1.19	4.40	20.6 ± 8.96	35.63
Morphine (10 mg/kg)	1.9 ± 0.1	4.73±0.32***	6.03 ± 0.15***	10.07	14.70	NT	NT
Ibuprofen (10 mg/kg)	NT	NT	NT	NT	NT	3.2 ± 1.10***[a]	81.88
N.saline water	1.27 ± 0.16	1.4 ± 0.42	1.3 ± 0.15	0.45	0.10	32 ± 5.52	0.0

Values are mean ± SEM (n = 6). Significant activities *P ≤ 0.05, **P ≤ 0.01, ***P ≤ 0.001 vs. control (one-way ANOVA followed by Bonferroni posttests). [a] P<0.05 vs control (one way ANOVA followed by Dunnet's Multiple Comparison test). NT = not tested. *n*-Hex ext, hexane extract, $CHCl_3$ extract, EtOAc extract and *n*-BuOH, *n*-butanol extracts at 100 mg/kg.

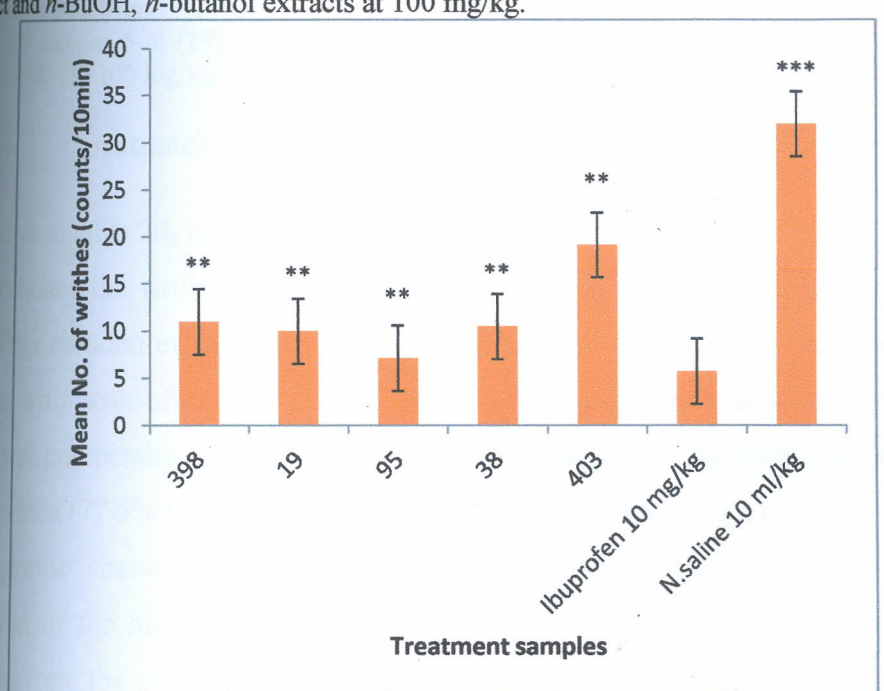

Figure 17: The antinociceptive effect of the compounds of *C. volkensii* root-bark, ibobrufen, and 0.8% saline water as observed in acetic acid-induced writhing test. Values are presented as the mean ± SEM (n = 6). ***P ≤ 0.001, and **P ≤ 0.01 significant difference compared to control (10 ml/kg). Voucapane (**398**); Voucapan-5-ol (**19**); Deoxycaesaldekarin C (**95**); Caesaldekarin C (**38**); Triacontanyl-E-caffaete (**403**) at 100 mg/kg each.

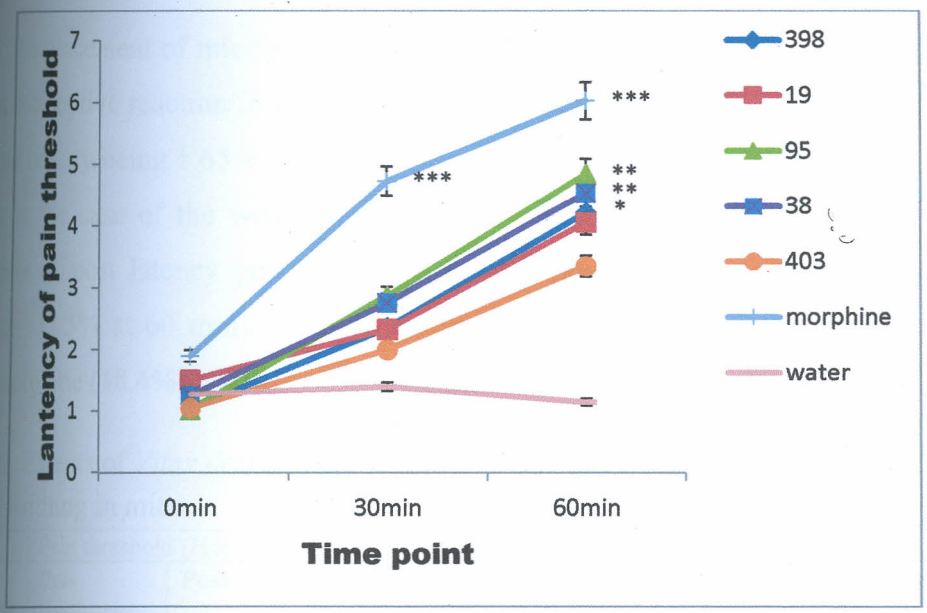

Figure 18: The antinociceptive effect of compounds from *C. volkensii*, morphine and 0.8% saline water as observed in hot-plate test. Values were presented as the mean ± SEM (n = 6). *** P≤0.001, **P≤0.01 and *P≤0.05, significant difference from control (10 ml/kg). Voucapane (**398**); Voucapan-5-ol (**19**); Deoxycaesaldekarin C (**95**); Caesaldekarin C (**38**); Triacontanyl-E-caffaete (**403**) at 100 mg/kg each; Morphine 10 mg/kg.

4.2.2.4. Antinociceptive activities of *Vitex doniana* stem bark extracts

As shown in table 20, intraperitoneal injection of acetic acid (Koster *et al.*, 1959; Vongtau *et al.*, 2004) elicited the writhing syndrome in control mice with 40.90 ± 3.59 writhes counted in 20 min. *Vitex doniana* extracts exhibited a significant ($P \leq 0.05, 0.01$) reductions in the number of writhes with peak effect (52.2% inhibition) produced by *n*-butanol extract (100 mg/kg). This effect was comparable and not significantly different ($P \leq 0.05$) from that produced by 10 mg/kg of ibuprofen (77.5% inhibition). The intraperitoneal injection (i.p) of acetic acid elicited writhing (a syndrome characterized by a wave of abdominal musculature contraction followed by extension of the hind limbs). The induction of writhing by chemical substances injected i.p resulting from the sensitization of nociceptors by prostaglandins (Nunez-Guillen *et al.*, 1997) and the test is useful for evaluation of mild analgesic non-steroidal anti-inflammatory drugs (NSAID) (Berkenkopf & Weichmann, 1988). The inhibition of writhing induced by acetic acid in this study by the *V. doniana* extracts suggest a peripherally mediated analgesic activity based on the association of the model with stimulation of peripheral receptors especially the local peritoneal receptors at the surface of cells lining the peritoneal cavity (Bentley *et al.*, 1983)

The placement of mice on the hot plate (Eddy & Leimbach, 1953; Vongtau *et al.*, 2004) elicited nociceptive reaction in the control group (normal saline water injections) with the post-treatment latency being 1.65 ± 0.22 s compared to pre-treatment latency of 1.30 ± 0.16 s (Table 21). As in the case of the writhing test, *V. doniana* extracts produced significant ($P \leq 0.05$) increments of post latency period with *n*-butanol extract (100 mg/kg) exhibiting the highest inhibition (32.5% at 60 min). This effect was comparable ($P \leq 0.05$) to that produced by 10 mg/kg morphine (48.4%).

Table 21: Effects of *Vitex doniana* stem bark extracts on hot plate-induced pain and acetic acid-induced writhing in mice

	Pain threshold (Hot plate induced)					Writhing response	
Dose Treatment (mg/kg)	**Pre-treatment latency (s)**	**Post-treatment latency (s)**		% Inhibition		Total No. of writhes	% Inhibition
		30 min	**60 min**	**30 min**	**60 min**		
n-Hex ext (100)	1.62 ± 0.37	3.44 ± 0.81	5.18 ± 0.63*	6.41	12.54	30.89 ± 2.12*	24.48
$CHCl_3$ ext (100)	1.56 ± 0.15	4.36± 0.61	7.72 ± 0.98*	9.85	21.66	26.40 ± 1.59**[a]	35.46
EtOAc ext (100)	1.49 ± 0.45	5.17 ± 0.24	8.75 ± 0.79**	12.90	25.46	22.72 ± 1.78**[a]	44.45
n-BuOH ext (100)	1.67 ± 0.19	6.45 ± 0.87	10.88 ± 1.02**	16.87	32.51	19.55± 2.00	52.20
Morphine (10ml/kg)	2.11 ± 0.1	8.83 ± 0.32***	15.16 ± 1.21***	23.28	48.40	NT	NT
Ibuprofen (10)	NT	NT	NT	NT	NT	9.18 ± 0.85***[a]	77.55
N.saline H_2O	1.30 ± 0.16	1.65 ± 0.22	1.53 ± 0.32	1.22	0.80	40.90 ± 3.59	0.0

Values are mean ± SEM (n = 6). Significant activities *$P \leq 0.05$, **$P \leq 0.01$, ***$P \leq 0.001$ vs. control (one-way ANOVA followed by Bonferroni posttests). [a] $P \leq 0.05$ vs control (one way ANOVA followed by Dunnet's Multiple Comparison test). NT = not tested

The thermally induced pain is widely used for assessing central antinociceptive activities, which involves supraspinally-organized response to pain (Morales *et al.*, 2001). Such pain stimuli are detected through neuronal pathways and are normally palliated by opioid-like analgesic agents exhibiting their analgesic effects both through supraspinal and spinal receptors (Ismaa *et al.*, 2005). In this study, the *V. doniana* extracts exhibited statistically significant ($P \leq$ 05), but lesser antinociceptive activity relative to morphine in the hot plate tests. It seems quite ossible that as in the acetic acid writhing test, *n*-butanol also have more potent central tinociceptive effect and opioid mechanism mediated antinociceptive effects was likely. The

results, concurred with the previously reported activities of *V. doniana* antidepressant effects on both peripheral and central nervous system by inducing sleep at dose 400 mg/kg, potentiating sodium thiopental sleeping time, showing significant muscle relaxation activities and producing analgesic effects (Abdulrahman *et al.*, 2007).

4.2.5. Anti-inflammatory activities of *Vitex doniana* stem bark extracts

Injection of carrageenan into the sub-plantar tissue of the right hind paw of rats in the control group caused oedema development which peaked (1.04 ± 0 cm, increase in paw circumference) at 5 h post-phlogistic injection (Table 22). The effect of *Vitex doniana* extracts (100 mg/kg) was observed from 3rd to the 6th h with peak effect (68.06, 70.83, and 72.22% inhibition) produced by three chloroform, ethyl acetate and *n*-butanol, respectively at the 6th hour. These effects were less but was not significantly different ($P \leq 0.05$) from that produced by 20 mg/kg diclofenac (81.94%). All the tested fractions of *V. doniana* presented a significant reduction in carrageenan-induced paw oedema formation, where the *n*-butanol fraction presented the most potent inhibitory effect. These findings were indicative of the fact that compounds involved in the inhibition of the neutrophil migration are in higher concentrations in the *n*-butanol fractions. The leaf extract of *V. doniana* have also been shown to inhibit the formation of paw oedema inflammation induced by agar in rats and increased reaction latency to thermal pain in mice (Iwueke *et al.*, 2006). Besides, the extracts inhibited the activities of phospholipase-A_2 and prostaglandins synthase (Iwueke *et al.*, 2006). The stem bark extracts have now demonstrated anti-inflammatory activities on carregeenan induced paw oedema indicating *V. doniana* has analgesic and anti-inflammatory compounds.

substances (histamine, serotonin and kinins) and prostaglandins (Vineger *et al.*, 1969). However, doubts exist unto the structural requirement for ecdysteroids anti-inflammatory actions, since ecdysteroids with furan ring side chain (**411** and **412**) used in this study showed comparable ($p \leq 0.05$) peak effects to ecdysteroids with non cyclized side chain (**413-415**).

These results differ with anti-inflammatory result reported previously, where ecdysteroids with cyclized side chain (polypodine B, **356**) exhibited low anti-inflammatory activity while ecdysteroids with OH group on the side chain had potent anti-inflammatory actions on TPA-induced inflammation (Sun & Yasukawa, 2008) while non specified ecdysteroids from *Pfaffia resinoids* roots did not show appreciable anti-inflammatory activities (Taniguchi *et al.*, 1997). A series of ecdysteroids including ajugasterone (**347**) studied against production of nitric oxide by immune-activated mammalian macrophages showed lack of interference to the immunobiological activities of the cells (Harmatha *et al.*, 2008). Such discrepancies in biological activities can be attributed to the fact that minor structural difference could result into major changes biological activities. Different assays models with different limitations may also cause different trends in bioactivities. Data indicating the effect of these ecdysteroids on prostaglandins release could be valuable in future studies to indicate their bioactivities against inflammation mediators.

4.2.3. Antioxidant activities

4.2.3.1. Antioxidant activity of the compounds from *C. volkensii* root bark

Antioxidant activities of the fractions from the root bark extracts of *C. volkensii* were performed using different enzymatic and nonezymatic assays. The effects of the test samples on superoxide anion ($O_2^{\bullet -}$) concentration was performed against xanthine-xanthine oxidase (XO) activity (enzymatic) which catalyses the generation of $O_2^{\bullet -}$ and uric acid from hypoxanthine and xanthine (Salaris *et al.*, 1991; Cos *et al.*, 1998). The extent of XO activity is determined by the amount of uric acid formed per minute. The $O_2^{\bullet -}$ scavenging activity was measured both enzymatically and nonenzymatically by observing the amount of formazon formed per minute (Leong *et al.*, 2008; Bindoli *et al.*, 1985). Inhibition of the activities of XO implies no or less $O_2^{\bullet -}$ accumulation, consequently less uric acid generated. Suppose the rate of uric acid reduction equals the rate of superoxide reduction then it implies that the test samples inhibit the actions of XO without any

additional $O_2^{\bullet-}$ scavenging activity (Salaris *et al.*, 1991; Cos *et al.*, 1998). In case $O_2^{\bullet-}$ scavenging activities predominates over inhibition of XO, then less formazon chromophores are formed ($O_2^{\bullet-}$ anions are reduced) but less inhibition of uric acid (relatively high concentration) is observed.

The result for XO inhibition and $O_2^{\bullet-}$ scavenging activities by *C. volkensii* extracts are summarized in table 24. *n*-Hexane and chloroform extracts exhibited significant ($P \leq 0.05$) reduction in uric acid production with an almost equivalent reduction in superoxide anion generation, though to a lesser extent compared to the ethyl acetate and *n*-butanol extracts. EtOAc and *n*-BuOH extracts displayed significant ($P \leq 0.05$) inhibition of XO activity and $O_2^{\bullet-}$ anion scavenging in the enzymatic and nonenzymatic systems, since an additional reduction of $O_2^{\bullet-}$ concentration was observed from the fact that less formazon was formed in the presence of the two extracts i.e. the corresponding scavenging percentage was high for the two extracts (EtOAc and n-BuOH).

The extracts of *C. volkensii* were examined for their ability to act as hydroxyl radical scavenging agent. Ferric-EDTA was incubated with H_2O_2 and ascorbic acid at pH 7.4; hydroxyl radicals ($^{\bullet}OH$) were generated in free solution and detected by their ability to degrade 2-deoxy-2-ribose into metabolites that on heating with TBA and at low pH forms a pink chromogen (Halliwell *et al.*, 1987). The extracts exhibited significant ($P \leq 0.05$) moderate to strong scavenging activity of hydroxyl radical except *n*-hexane extract (Table 24). The polar extracts (EtOAc and *n*-BuOH) showed the highest percent (45 and 21%, respectively) scavenging activity.

Lipid peroxidation is a complex process and occurs in multiple stages. Antioxidants retard lipid peroxidation in foods and biological systems. In the course of this investigation, TBA assay method (Okhawa *et al.*, 1979) was used to detect lipid oxidation by measuring the extent of malondialdehyde (MDA) formation as the split product of an endoperoxide of unsaturated fatty acids resulting from oxidation of a lipid substrate. The results for lipid peroxidation inhibition of liver tissue (measured by the colour intensity of MDA-TBA complex), were excellent and in the order of EtOAc>*n*-BuOH>$CHCl_3$>*n*-hexane extracts, although *n*-hexane showed insignificant ($P \leq 0.05$) reduction in MDA formed per hour per mg protein (Table 24).

The result indicated that the polar extracts had better antioxidant activities due to the presence of triacontanyl-*E*-ferrulate **(402),** triacontanyl-*E*-caffeate (**403**), 30′-hydroxytricontanyl-*E*-ferrulate (**404**), caesaldekarin C (**38**), and 5-hydroxyvinhaticoic acid (**399**). Compounds **402**,

Table 24). These results indicate that triacontanyl-*E*-cinnamoates from *C. volkensii* are the primary antioxidants compounds, which react aggressively with free radicals, particularly ($^{\bullet}$OH), thereby terminating the radical-chain reactions and retard the formation of hydroperoxides (Frankel, 1991).

The triacontanyl-*E*-cinnamoates [**402**, **403** and **404**] isolated from EtOAc and *n*-BuOH extracts showed inhibition of lipid peroxidation evidenced by significant ($P \leq 0.05$) reduction of MDA/h/mg protein formation on the liver homogenate reaction mixture (Table 24). The compounds [**402**, **403** and **404**] and α-tocopherol can transfer their phenolic hydrogen to a peroxy free radical of a peroxidized polyunsaturated fatty acid (PUFA), thereby breaking the radical chain reaction and preventing further peroxidation of PUFA in cellular and subcellular membrane phospholipids (Lampi *et al.*, 1999)

The antioxidant activity of these tricontanyl-*E*-cinnamoates can be attributed to the formation of stable antioxidation product from the caffeic acid moiety possessing an *ortho*-dihydroxy and α, β-unsaturated carbonyl that can form stabilized quinonoid intermediates (Masuda *et al.*, 2001). The structural features of the *C. volkensii* phenolics are therefore excellent antioxidants constituents as radical scavengers via hydrogen donation to lipid peroxyl radicals. Ferrulic acid esters **402** and **404** have been noted to undergo hydrogen donation to a radical and produce ferrulate radicals that couple to produce stable dihydrobenzofuran product (Masuda *et al.*, 2006).

The antioxidant mechanisms for ferrulate and caffeate moieties are considered to be based on the phenolic hydroxyl groups. Whereas ferrulate has one phenolic hydroxyl group, which undergoes hydrogen donation to a lipid peroxyl radical (Masuda *et al.*, 2006) to produce a ferrulate radical, the caffeate has *ortho*-phenolic hydroxyl groups which can donate hydrogen to a radical followed by resonance stabilization in the same way as a catechol moiety (Scheme 6). Two ferrulate radicals can couple at the 5-position of the aromatic part of one of the ferrulate radicals and the 2-position of the alkyl part of another ferrulate radical. The produced coupling intermediate dimer is not very stable because its two aromatic moieties have an unstable quinoid structures. These facts are thus considered as the major contributors to the observed activities. However, the fatty alcohol chain effects to the polarity of the compounds might have imposed a negative influence on the activities of these compounds tested in aqueous conditions. The antioxidant property of this plant has not been previously reported but the antioxidant activities

related species *Caesalpinia sappan, Caesalpinia benthamannia*, have been documented. This study is the first report of the presence of triacontanyl-*E*-cinnamoates in this plant alongside known cassane-type diterpenoids, which are phytochemically elaborated by several species of *Caesalpinia* genus.

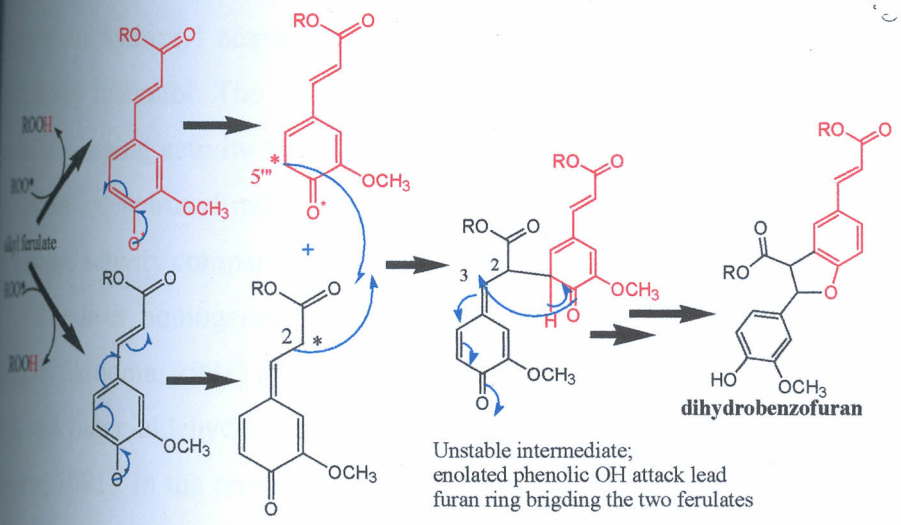

Scheme 6: Proposed radical scavenging antioxidation mechanism of alkyl ferrulate (ROOH and ROO* denote lipid hydroperoxide and lipid peroxyl radical, respectively) (Masuda *et al.*, 2007).

4.2.3.2. Antioxidant activity of the compounds from *S. didymobotrya* roots

The xanthine oxidase (XO) inhibiting and $O_2^{\bullet -}$ anion scavenging activities by the *S. didymobotrya* extracts and compounds are shown in Table 25. The results show that all the *S. didymobotrya* extracts (100 µg/ml) exhibited significant ($P \leq 0.05$) inhibition of XO activity comparable to allopurinol (20 µg/ml). All the tested fractions showed high inhibition percentage of the XO, with values ranging from 40 to 70%. The activities were 2 to 3 times greater than the inhibition or scavenging activities of the same fractions against $O_2^{\bullet -}$ anion both in enzymatic and nonenzymatic systems. The most active of all the fractions was ethyl acetate with 68, 33 and 38% percentage inhibition of XO, $O_2^{\bullet -}$ anions in enzymatic and nonenzymatic systems, respectively. In contrast, the anthraquinones (**269**, **273**, **279**, **285**, **295** and **299**) isolated from the EtOAc extract all showed weak to moderate activities comparing their IC_{50} values to that of standard control. Although XO inhibition was notably higher than the effect on $O_2^{\bullet -}$ scavenging, which implied the components of *S. didymobotrya* could be having inhibitory actions against XO and not able to scavenge the radical anion.

When *S. didymobotrya* extracts and the standard drug (mannitol) were added to the reaction mixture, removal of hydroxyl radicals and/or inhibition of deoxyribose degradation was observed (Table 25). All the *S. didymobotrya* extracts except *n*-hexane extract showed significant ($P \leq 0.05$) reduction in the amount of MDA formed. n-Butanol extract showed the highest inhibition of hydroxyl scavenging by up to 39% comparable ($P \leq 0.05$) to 50% inhibition exhibited by mannitol. The pure compounds exhibited significantly ($P \leq 0.05$) better hydroxyl radical scavenging activity than $O_2^{\bullet -}$ anion scavenging activity. This was evidenced by the low IC_{50} values for hydroxyl radical scavenging (Table 25), although the values could be considered as moderate activity compared to the IC_{50} for the reference drug (mannitol).

The liver homogenate undergo peroxidation when incubated with $FeSO_4$ and produce peroxides (Aruoma, 1991) and they attack the biological system. This leads to the formation of MDA and other aldehydes, which form a pink chromogen with TBA, absorbing at 535 nm (Aruoma, 1991). In the presence of antioxidants, this process can be retarded, as it was observed with the extracts of *S. didymobotrya* that displayed moderate ($P \leq 0.05$) reduction in MDA formation (Table 25).

All the extracts showed inhibition of peroxidation effect although the extent was inferior to α-tocopherol. The highest anti-lipid peroxidation activity was observed from EtOAc extract at 35% followed by n-BuOH extract at 33% (Table 25) whereas α-tocopherol exhibited 53% inhibition of lipid peroxidation. In an attempt to determine the most potent compounds, the 6-methoxylated anthraquinones with physcion (**273**) and physcion10,10′-bianthrone (**299**)] exhibiting the highest anti-lipid peroxidation (Table 25).

The observed antioxidant activities of these compounds are due to the presence of phenolic functionality in their structures. The difference in activities of the compounds may be attributed to the extent of unpaired π-electron delocalization in each compound. Although the pattern is the same in all the structures, the role of methoxyl group in stabilization of phenolic radical formed after hydrogen donation to the reactive free radical species may have led to the better scavenging activity observed from **273** and **299**.

Table 25: Effects of the *S. didymobotrya* root bark extracts and compounds on the generation of superoxide anions, hydroxyl radicals and lipid peroxidation in microsomes

Sample	Xanthine-oxidase inhibition[a] (100 µg/ml)	Superoxide anion scavenging ($O_2^{\bullet -}$)		Hydroxyl radicals ($^{\bullet}OH$)[c]	Microsomal lipid peroxidation[c]
		Enzymatic system[b] (100 µg/ml)	Nonenzymatic system[b] (100 µg/ml)		
Control	184.87 ± 7.4 (0)	92.68 ± 6.1 (0)	76.41 ± 5.6 (0)	81.92 ± 6.94	90.39 ± 6.48
n-hexane ext	76.31 ± 4.8 (59)*	71.77 ± 3.6 (23)*	61.78 ± 3.1 (19)^{NS}	75.90 ± 6.11 (-7)^{NS}	76.96 ± 4.80 (-15)*
EtOAc ext	59.32 ± 5.5 (68)*	62.52 ± 3.1 (33)*	47.24 ± 5.0 (38)*	62.22 ± 4.11 (-24)*	58.48 ± 3.97 (-35)*
n-BuOH	107.11 ± 4.7 (42)*	72.48 ± 2.2 (23)*	63.01 ± 2.9 (18)^{NS}	57.77 ± 4.30 (-29)*	60.23 ± 5.00 (-33) *
Water ext	110.48 ± 6.4 (40)*	78.53 ± 4.5 (15)^{NS}	65.23 ± 3.5 (15)^{NS}	50.18 ± 3.14 (-39)*	70.37 ± 5.22 (-22)*
Standard drugs	55.76± 5.1 (70)*[d]	27.70 ± 3.8 (70)*[d]	21.08 ± 4.7 (72)*[d]	40.66 ± 2.64 (-50) *[e]	42.29±2.84 (-53)*[f]
Compounds	**IC_{50} (µM)**	**IC_{50} (µM)**	**IC_{50} (µM)**	**IC_{50}(µM)**	**100 µM**
269	17.54	25.54	33.86	23.75	74.63 ± 4.71 (-17) *
273	13.43	34.68	32.53	15.21	68.22 ± 3.28 (-25) *
279	13.42	45.25	30.33	19.32	76.65 ± 3.74 (-15) *
285	39.60	54.36	41.75	21.43	72.77 ± 5.44 (-19) *
295	9.46	28.55	30.69	17.48	70.54 ± 5.37 (-22) *
299	9.14	21.62	25.71	12.04	69.29 ± 3.62 (-23) *
Standard drugs	0.24[d]	0.23[d]	0.19[d]	4.86[e]	42.29 ± 2.84 (-53) *[f]

Values for activities are mean ± SD of three determinations. [a]µmol uric acid formed/min, [b]nmol formazon formed/min), [d, e,] and [f] are Standard drug sample Allopurinol (20 µg/ml), mannitol (100 g/ml), α-tocopherol (100 g/ml), respectively. *values are significantly different, ^{NS} not significant at $P \leq 0.05$ compared to the control.

4.4. Antidyslipidemic activities

4.4.1. Acute toxicity of the extracts from *S. didymobotyra*, *C. volkensii* and *V.doniana* extracts

No death was recorded at dose of 1-4 g/kg of *S. didymobotrya* within seven days. The animals were calm, hypoactive and passed watery stools. The same observations, but with greater intensity, were made at the higher doses of 8 and 10 g/kg, with the animals also exhibiting increased breathing frequency. Such result demonstrated that *S. didymobotrya* root bark extract were not toxic, only exhibited laxative effects. Since no death was observed within 7 days the LD_{50} as a measure of lethality was not established. On the other hand, both *C. volkensii* root bark extract and *V. doniana* stem bark extracts at the doses of 0.5 – 8 g/kg i.p given to the rats, had no effect on their behavioural responses and mortality during the observation period of 7 days after administration. Therefore, it can be suggested that *C. volkensii* and *V. doniana* have no toxicity profiles against Charles Foster rats and could be used on the animals for antidyslipidaemic assays.

4.4.2. Effects of crude extracts from *S. didymobotrya* against triton induced hyperlipidaemia in rats

The intraperitoneally (i.p) administration of triton WR-1339 into the rats caused marked increase in the serum levels of total cholesterol (Tc), phospholipids (Pl), total glycerides (Tg) and proteins (Pr) (Table 26). Triton treatment inhibited plasma post heparin lipolytic activity (PHLA) by 40% and lecithin cholesterol acyltransferase activity (LCAT) by 42%. After treatment with *n*-hexane (SD-F1), ethyl acetate (SD-F2), *n*-butanol (SD-F3), and water residue (SD-F4) fractions of methanol extract at 250 mg/kg (p.o), SD-F2 reversed the plasma levels of lipids significantly ($P < 0.01$) followed by SD-F1 on the triton induced hyperlipidaemic rats (Table 26) while SD-F3 and the aqueous extract (SD-F4) showed mild activity.

4.2.3. Effects of isolated compounds from *S. didymobotrya* against triton induced hyperlipidaemia in rats

Treatment of hyperlipidaemic rats with the anthraquinones at a dose of 100 mg/kg (p.o) reversed the plasma levels of total lipid cholesterol (Tc), total triglyceride (Tg), phospholipids (Pl) and proteins (Pr) to varying extents (Table 27). Compounds **269** and **285** showed insignificant ($P \leq 0.05$) low activity while **295** showed mild ($P \leq 0.05$) antidyslipidaemic activities compared to standard drug Gemibrozil (100 mg/kg). The active samples inhibited cholesterol biosynthesis and potentiated the activities of lipolytic enzymes to early clearance of lipids from circulation in triton induced hyperlipidaemia. This was demonstrated by the effect of triton induced hyperlipidaemia in rats inhibiting the PHLA and LCAT activity by 42 and 40%, respectively (Table 27) while in case of triton plus samples (**273**, **279** and **299**) activities of PHLA and LCAT were reversed in the range of 10-32% in the treated rats. The most active compound was **299**, which reactivated the enzymatic activities by 32 and 26%, respectively the extent was less than but not significantly ($P \leq 0.05$) different to the activities of the gemfibrozil (standard drug), which showed 42 and 39% reversal, respectively (Table 27).

Triton WR-1339 is non-ionic detergent that prevents catabolism of triacylglycerol and secretion or clearance rate of very low density lipoprotein (Hayashi *et al.*, 1981), increases hepatic cholesterol biosynthesis by interfering with the tissues uptake of plasma lipids (Holmes, 1964), and interfering with the cholesterol excretion and metabolism (Vogel & Vogel, 1997). Thus reductions in the serum lipid contents (Tc, Tg, Pl and Pr) of triton treated rats as observed with SD-F2 treatment and the compounds in this study suggested that *S. didymobotrya* root extracts could be inhibiting cholesterol biosynthesis and potentiated the activity of lipolytic enzymes to early clearance of lipids from circulation in triton induced hyperlipidaemia. The biological activity observed for the anthraquinone **299**, indicated that it is an effective antidyslipidaemia and antioxidant agent in addition to the previously reported strong activity against A549, PC-3, HCT-15 and VO-31 human cancer cell lines (Hwang *et al.*, 2004).